Vol. 56 NOVEMBER, 1952 No. 8

THE JOURNAL OF PHYSICAL CHEMISTRY

(Registered in U. S. Patent Office)

Founded by Wilder D. Bancroft

Founded by Wilder D. Bancroft

THE JOURNAL OF PHYSICAL CHEMISTRY

(Registered in U. S. Patent Office)

Published monthly (except July, August and September) by the American Chemical Society at 20th and Northampton Sts., Easton, Pa.

Entered as second-class matter at the Post Office at Easton, Pennsylvania.

The *Journal of Physical Chemistry* is devoted to the publication of selected symposia in the broad field of physical chemistry and to other contributed papers.

Manuscripts originating in the British Isles, Europe and Africa should be sent to F. C. Tompkins, The Faraday Society, 6 Gray's Inn Square, London W. C. 1, England.

Manuscripts originating elsewhere should be sent to W. Albert Noyes, Jr., Department of Chemistry, University of Rochester, Rochester 3, N. Y.

Correspondence regarding accepted copy, proofs and reprints should be directed to Assistant Editor, Allen D. Bliss, Department of Chemistry, Simmons College, 300 The Fenway, Boston 15, Mass.

Business Office: American Chemical Society, 1155 Sixteenth St., N. W., Washington 6, D. C.

Advertising Office: American Chemical Society, 332 West 42nd St., New York 18, N. Y.

Articles must be submitted in duplicate, typed and double spaced. They should have at the beginning a brief Abstract, in no case exceeding 300 words. Original drawings should accompany the manuscript. Lettering at the sides of graphs (black on white or blue) may be pencilled in, and will be typeset. Figures and tables should be held to a minimum consistent with adequate presentation of information. Photographs will not be printed on glossy paper except by special arrangement. All footnotes and references to the literature should be numbered consecutively and placed on the manuscript at the proper places. Initials of authors referred to in citations should be given. Nomenclature should conform to that used in *Chemical Abstracts*, mathematical characters marked for italic, Greek letters carefully made or annotated, and subscripts and superscripts clearly shown. Articles should be written as briefly as possible consistent with clarity and should avoid historical background unnecessary for specialists.

Symposium papers should be sent in all cases to Secretaries of Divisions sponsoring the symposium, who will be responsible for their transmittal to the Editor. The Secretary of the Division by agreement with the Editor will specify a time after which symposium papers cannot be accepted. The Editor reserves the right to refuse to publish symposium articles, for valid scientific reasons. Each symposium paper may not exceed four printed pages (about sixteen double spaced typewritten pages) in length except by prior arrangement with the Editor.

Remittances and orders for subscriptions and for single copies, notices of changes of address and new professional connections, and claims for missing numbers should be sent to the American Chemical Society, 1155 Sixteenth St., N. W., Washington 6, D. C. Changes of address for the *Journal of Physical Chemistry* must be received on or before the 30th of the preceding month.

Claims for missing numbers will not be allowed (1) if received more than sixty days from date of issue (because of delivery hazards, no claims can be honored from subscribers in Central Europe, Asia, or Pacific Islands other than Hawaii) (2) if loss was due to failure of notice of change of address to be received before the date specified in the preceding paragraph, or (3) if the reason for the claim is "missing from files."

Annual Subscription: $8.00 to members of the American Chemical Society, $10.00 to non-members. Postage free to countries in the Pan American Union; Canada, $0.40; all other countries, $1.20. Single copies, $1.25; foreign postage, $0.15; Canadian postage $0.05.

The American Chemical Society and the Editors of the *Journal of Physical Chemistry* assume no responsibility for the statements and opinions advanced by contributors to THIS JOURNAL.

The American Chemical Society also publishes *Journal of the American Chemical Society*, *Chemical Abstracts*, *Industrial and Engineering Chemistry*, *Chemical and Engineering News* and *Analytical Chemistry*. Rates on request.

THE JOURNAL OF PHYSICAL CHEMISTRY

Founded by Wilder D. Bancroft

VOLUME 56 NOVEMBER 15, 1952 NUMBER 8

THE STRUCTURE OF GRAPHITE OXIDE

BY R. J. BECKETT AND R. C. CROFT

Division of Industrial Chemistry, Commonwealth, Scientific and Industrial Research Organization, Melbourne, Australia

Received July 31, 1951

Difficulties relating to the determination of the structure of graphite oxide have been reviewed. Fresh evidence indicating the structural nature of this compound is presented. This was obtained from electron microscope studies of small particles of South Australian graphite and the oxide prepared from it. The latter exhibits considerable folding but the former does not. This difference is attributed to the redistribution of valency linkages between carbon atoms in the layer planes of graphite occurring when the latter is converted to graphite oxide.

Introduction

Most of the lamellar compounds of graphite have been shown by means of chemical and X-ray methods to consist of the original aromatic carbon layer planes of the graphite crystal separated by intercalated ions, atoms or molecules, which are regularly arranged both relative to each other and to the carbon atoms in the layer planes above and below them. The many attempts, however, which have been made to obtain similar data for graphite oxide have met with little success. The application of chemical methods,[1-4] has failed to establish a definite empirical formula for this substance. Examination of the oxide by the X-ray diffraction method[5] only shows that it is composed of parallel lamellae spaced at greater distances than the carbon layer planes in pure graphite. Failure of both methods to elucidate the structure of graphite oxide appears to be due to the ease with which this substance absorbs water and other liquids. Since the complete removal of these absorbed liquids is virtually impossible,[6] chemical analysis of oxides prepared in different ways yields variable results. Furthermore, because liquid absorption increases the interlamellar spacing in graphite oxide until the lamellae are ultimately dispersed as two-dimensional sheets, it evidently weakens those interlamellar forces which might preserve a regular structure, as in graphite, and therefore permits relative displacement of the oxide lamellae. The extinction of all lines in the X-ray diffraction powder pattern of graphite oxide other than those of (000*l*) and (*hki*0) planes is further evidence of this effect.

Of the few structures suggested[5,7] for graphite oxide, that proposed by Hofmann appears to be best supported by experimental data. He obtained evidence from X-ray measurements that the oxygen in graphite oxide is bonded to the carbon atoms of the hexagon layer planes by an epoxy linkage (see Fig. 1). He was unable, however, either to measure changes in the C–C distances or to confirm buckling of the carbon layer planes, both of which would be caused by a redistribution of carbon valencies. There is some chemical evidence that the graphite oxide structure can also contain hydroxyl ions.[5,7] Ruess[3] has confirmed this and has in addition obtained results which show that graphite oxide is capable of being hydrated to various extents. Hofmann and Holst[2] showed also that it is possible to prepare graphite oxide in which the atomic ratio of carbon to oxygen approaches 2.

The carbon atoms in the layer planes of which graphite is composed are linked by strongly directional bonds of the order 1.5. If, however, oxygen is linked in a covalent manner to these atoms, this bond system is broken down. Taking epoxy group

(1) U. Hofmann, *Kolloid Z.*, **104**, 112 (1943).

(2) Zusammengefasst bei U. Hofmann, *Erg. exakt. Naturwiss.*, **18**, 229 (1939).

(3) G. Ruess, *Kolloid Z.*, **110**, 17 (1945).

(4) H. Thiele, *Z. anorg. allgem. Chem.*, **190**, 145 (1930); *Kolloid Z.*, **56**, 129 (1931).

(5) U. Hofmann and R. Holst, *Ber.*, **72**, 754 (1939).

(6) U. Hofmann, A. Frenzel and E. Csalan, *Ann.*, **510**, 1 (1934).

(7) J. Weiss, *Nature*, **114**, 744 (1940).

Table I

Details of Preparation of Colloidal Graphite and Graphite Oxide Suspensions

Sample	Obtained from	Oxidation treatment	Method of preparing suspension
1 (Graphite oxide)	−325 mesh purified South Australian graphite	Staudenmaier	Oxide shaken with dilute (1:3) ammonia for 24 hr., then agitated by ultrasonics for 12 hr.
2 (Graphite oxide)	Same	Brodie	Same
3 (Graphite)	Pipetted from water suspension of homogenized −325 mesh graphite, at 28 cm. after 32 hr. settling	....	Pipet sample diluted with 1:3 ammonia subjected to ultrasonic agitation for 8 hr.
4 (Graphite oxide)	Graphite pipetted from water suspension of homogenized −325 mesh graphite, at 2 cm. after 2 weeks settling	Three Brodie oxidations	Shaken with dilute (1:3) ammonia for 6 hr.
5 (Graphite oxide)	Same graphite as used to prepare sample 3	Same	Same

formation as an example of how oxygen may become attached to the carbon layer planes when graphite is converted to graphite oxide, it is apparent from Fig. 1 that the epoxy group, if itself rigid, only confers structural rigidity on every second C–C linkage. Also, formation of this group results in the bond order of the other C–C linkage being reduced from 1.5 in graphite to 1 in graphite oxide. Whether saturation of carbon valencies in the graphite layer planes is achieved by formation of epoxy groups or other types of covalent groups, *viz.*, peroxide, the redistribution of C–C valency bonds must be the same as described above. This view is supported by results of chemical analysis performed on graphite oxide by Hofmann and Holst.[2] Their results indicate that the oxygen in this compound is attached only to adjacent carbon atoms.

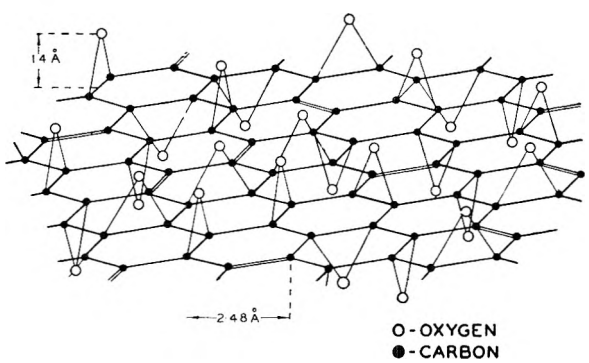

Fig. 1.—Layer-plane of graphite oxide according to U. Hofmann.

If it is presumed that the rigidity of layer planes decreases as the bond order of linkages between carbon atoms composing them is reduced, then, according to the arguments set out above, thin lamellae of graphite oxide should show a greater tendency to bend than graphite particles of the same dimensions. Confirmation of this theory was sought by examining dispersions of each of these materials under the electron microscope.

Experimental

Coarsely crystalline graphite from Uley, South Australia, was purified by alternate treatments with hydrochloric and hydrofluoric acids until impurities were reduced to less than 0.5% and was finally ground to minus 325 mesh (Tyler). The purified graphite was shown by X-ray powder photographs[8] to contain 95% of the Bernal structure, the remaining graphite being in the Lipson and Stokes form.

Suspensions of colloidal graphite were obtained by homogenizing a mixture of the graphite with tannic acid and water in the ratio 100:5:120 by weight. After homogenizing the paste was agitated with water and allowed to settle. Pipet samples were removed from this suspension at depths and after settling periods shown in Table I. Some of the pipet samples were subjected to agitation by ultrasonic waves (500 kc./s.) with the object of further reducing the size of particles suspended in them.

Graphite oxide samples were prepared by Brodie's[9] method both from the sized fractions and from the original purified graphite. This was done by warming graphite with a mixture of fuming nitric acid and potassium chlorate. Some samples, however, were prepared by Staudenmaier's[10] method. In this case oxidation is effected by agitation with a cold mixture of concentrated nitric and sulfuric acids (2:1 by volume) containing potassium chlorate. After washing, the partially oxidized graphite is heated with acid permanganate solution. Various methods were employed to disperse the oxides to the extent necessary for inspection under the electron microscope. Some samples were shaken with either water or dilute ammonia. In the case of the oxide prepared from the original purified graphite, large particles were separated by decantation. Some of the oxide suspensions were subjected to ultrasonic treatment. The methods of preparation of colloidal graphite and graphite oxide suspensions are summarized in Table I.

Suitably diluted suspensions were mounted on specimen screens in the usual manner for electron microscopy and the specimens shadow-cast with 10 Å. thickness of uranium before examination in the electron microscope, the shadowing ratio being 4:1.

The microscope used was an R.C.A. model E.M.U. instrument fitted with a self-biased gun and having the objective lens asymmetry corrected. An adjustable objective aperture was employed[11] and the magnification was calibrated by the method of Farrant and Hodge.[12]

Interpretation of Micrographs

The main feature of graphite oxide evident from electron-micrographs in Figs. 2, 3, 5 and 6 is the folding which occurs in particles of this substance. Fully oxidized samples of the oxide (containing 30% oxygen) whether prepared by Staudenmaier's method (Fig. 2) or by Brodie's method (Fig. 3)

(8) These were taken by A. McL. Mathieson of this Division.

(9) B. C. Brodie, *Phil. Trans.*, **149**, 249 (1859).

(10) L. Staudenmaier, *Ber.*, **31**, 1481 (1898); **32**, 1394 (1899); **33**, 2824 (1899).

(11) J. L. Farrant and A. J. Hodge, *J. Sci. Instruments*, **27**, 77 (1950).

(12) J. L. Farrant and A. J. Hodge, *J. Applied Phys.*, **19**, 840 (1948).

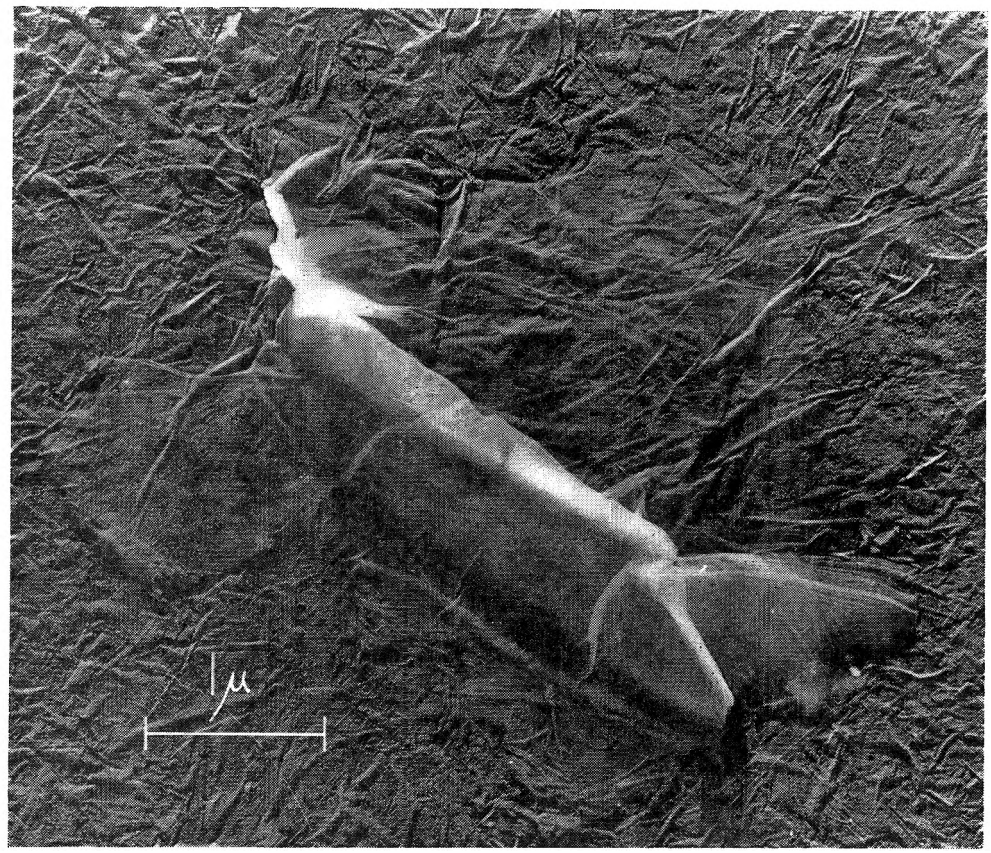

Fig. 2.—Graphite oxide (Sample 1).

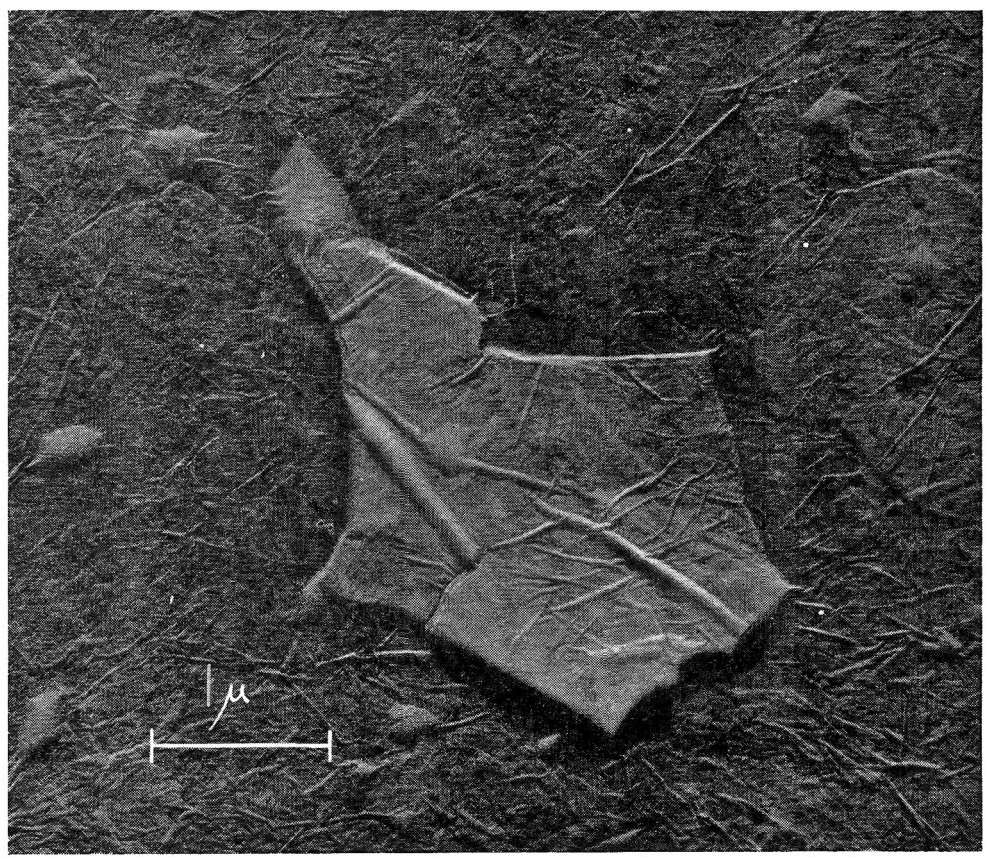

Fig. 3.—Graphite oxide (Sample 2).

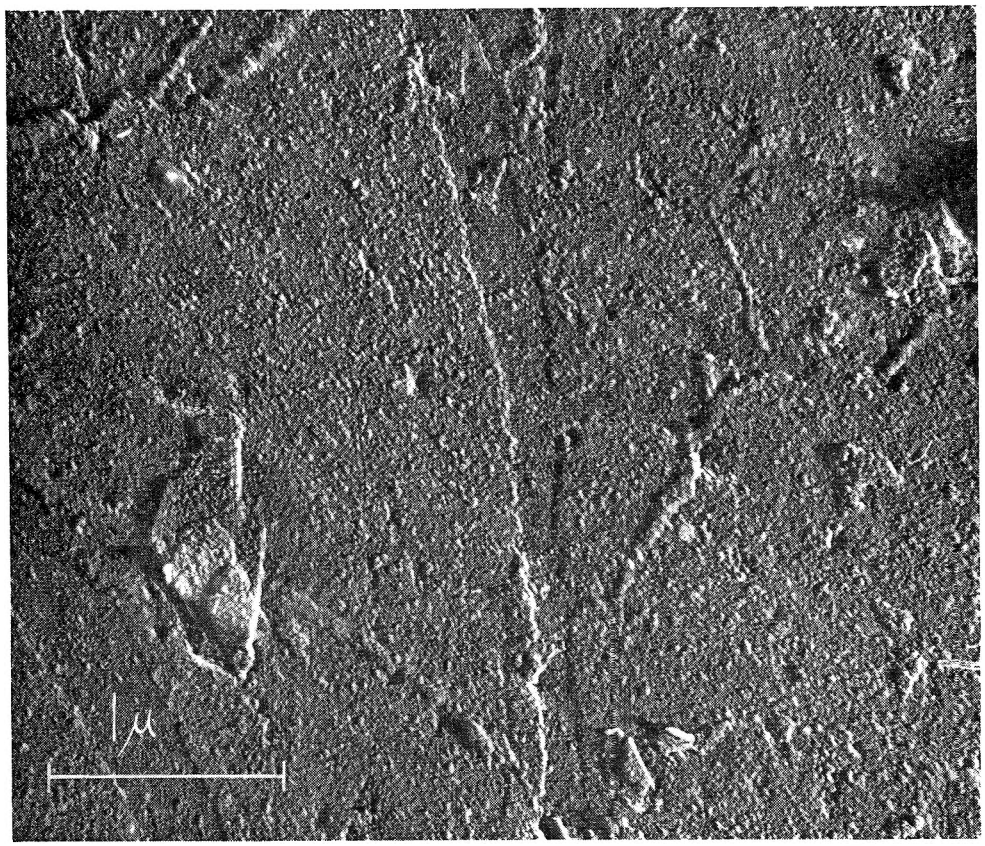

Fig. 4(a).—Colloidal graphite (Sample 3); average thickness of particles 70 Å.

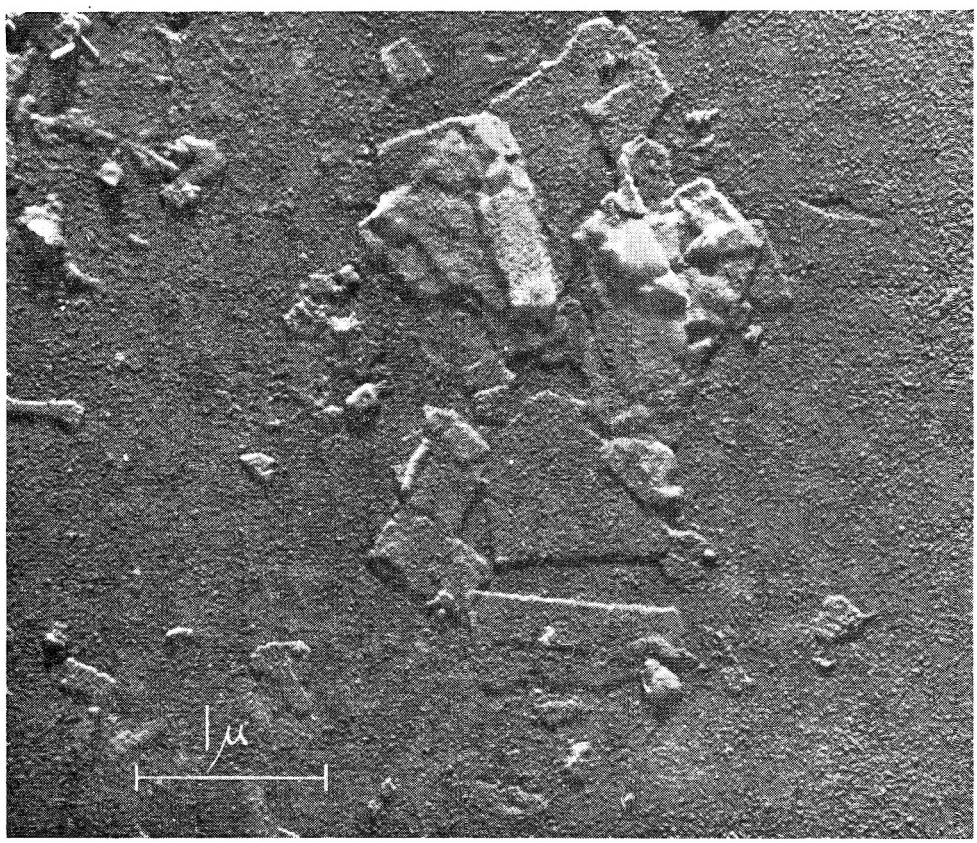

Fig. 4(b).—Colloidal graphite (Sample 3); average thickness of particles 130 Å.

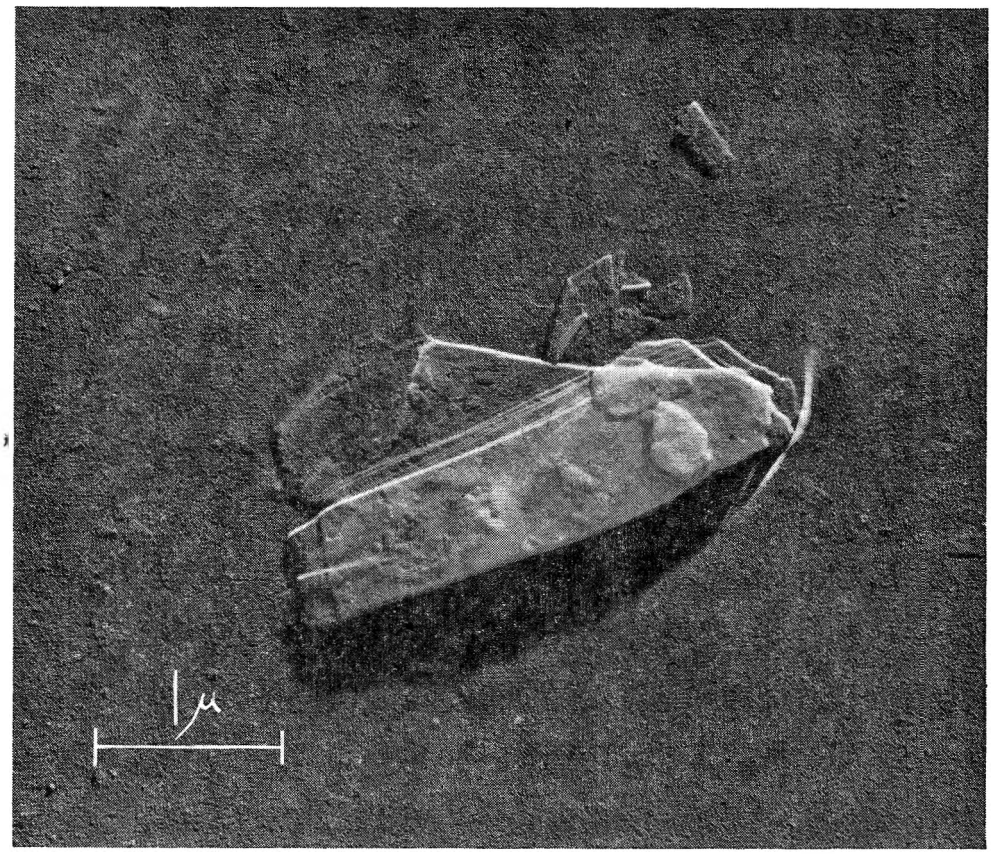

Fig. 5(a).—Graphite oxide (Sample 4); thickness of particles 1500 Å.

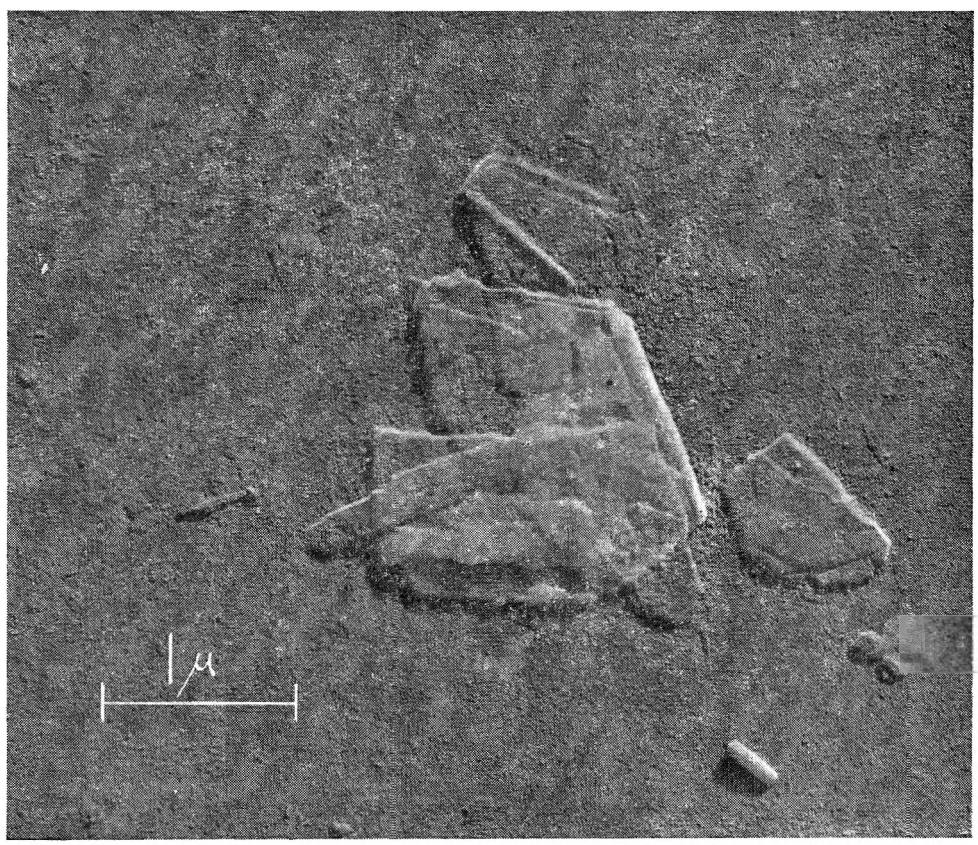

Fig. 5(b).—Graphite oxide (Sample 4); thickness of particles 150 Å.

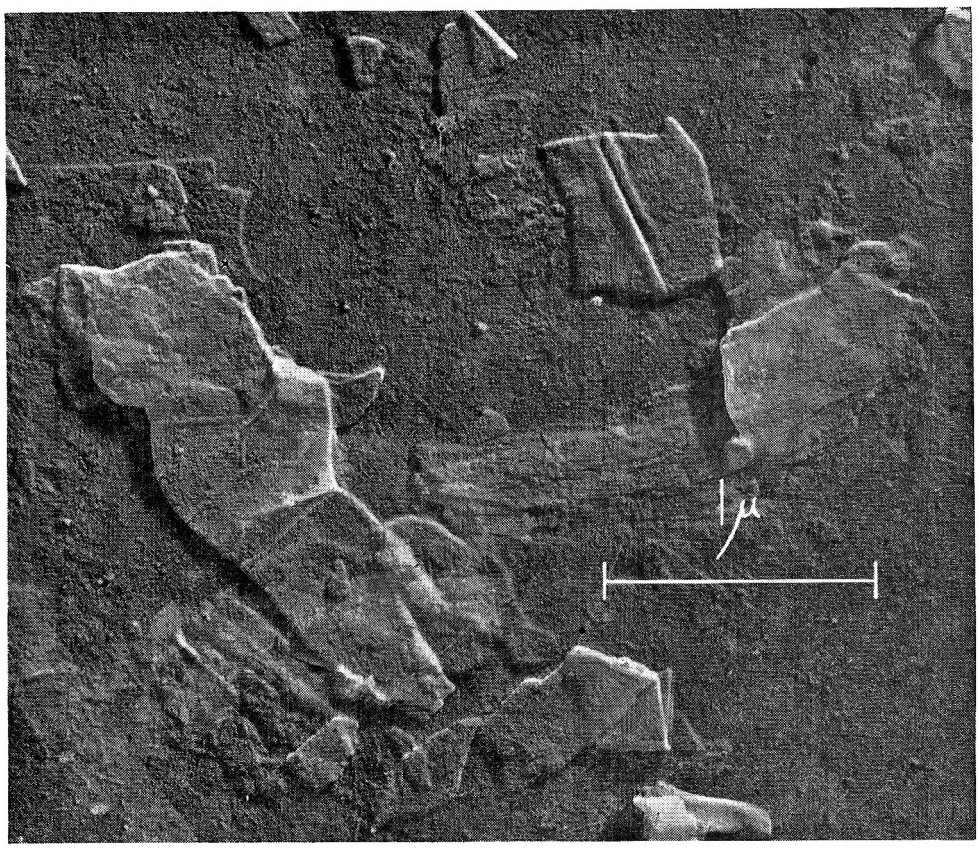

Fig. 6.—Graphite oxide (Sample 5); thickness of particles 50–200 Å.

show extensive folding which is general and not confined to any particular area. Other samples containing smaller amounts of oxygen exhibit less folding. In all cases, however, folds extend right through even the thickest oxide particles and appear also to be predominantly about straight lines. The latter have no obvious preferred direction. Although Figs. 5(a) and 6 show that it is possible for sheets of oxide to be folded back on themselves, this was seldom observed. Further evidence of the readiness of the oxide lamellae to bend is shown in Fig. 5(b), in which a long narrow sheet of oxide is seen to conform to the contour of an underlying particle like a carpet on stairs. It was mentioned earlier that the powder diffraction pattern of graphite oxide contains only ($hki\bar{0}$) and ($000l$) reflections. This implies that, although parallel, the oxide lamellae are not orientated in a particular manner relative to each other. Figure 5(a) suggests that slipping has caused relative displacement of the lamellae in a composite particle of graphite oxide. It shows a number of almost parallel lines at one edge of a relatively thick plate of oxide. Since all of these lines are the same shape and show the same irregularities, they presumably originate from the same graphite flake.

Micrographs of graphite show that, although some of the particles photographed are thinner than those of graphite oxide, they do not exhibit the folding which may possibly be expected of thin flexible sheets. Comparison of Figs. 4(a) and 4(b) with Figs. 5 and 6 illustrates this.

Discussion

The conclusion that the above results support the theory that valence linkages between carbon atoms in graphite are redistributed when the latter is converted to graphite oxide, is based on the assumption that the aromatic structure of graphite layer planes originally proposed by Debye and Scherrer[13] is valid. This assumption, however, is justified by data obtained by more recent investigators, among whom Bernal,[14] Laidler and Taylor,[15] Lipson and Stokes,[16] are notable. These data all confirm that carbon atoms in the layer planes of graphite are disposed hexagonally and linked, each with its three neighbors, by 1.5 order valency bonds as in aromatic compounds. It is suggested, therefore, that oxygen intercalated in graphite forms covalent linkages with carbon atoms in the layer planes by saturating the free valencies which, in graphite, these atoms share by resonance.

The difference in the rigidities of layer planes of graphite and its oxide is demonstrated by folding of lamellae which occurs only in the case of the oxide and is believed to be due, as explained earlier, to modification of strongly directional 1:5 order C–C linkages in graphite layer planes by covalent linking of oxygen to adjacent pairs of carbon atoms in these planes with consequent reduction of the order of bonds between remaining carbon atoms. This interpretation is in agreement with Hofmann's[5]

(13) P. Debye and P. Scherrer, *Physik. Z.*, **18**, 291 (1917).
(14) J. D. Bernal, *Proc. Roy. Soc. (London)*, **A106**, 749 (1924).
(15) D. S. Laidler and A. Taylor, *Nature*, **146**, 130 (1940).
(16) H. Lipson and A. R. Stokes, *ibid.*, **149**, 328 (1942).

proposed graphite oxide structure which, because of the relative disorder of the oxide lamellae, would be difficult to confirm by X-ray measurements.

Although sheets of graphite oxide appear folded in electron micrographs, it is probable that, when suspended in a suitable liquid, they are extended and flat. The possibility that the folding just referred to was due entirely to the method of mounting specimens and not to structural weakness in the oxide lamellae is discounted because the same method of mounting did not produce similar effects in graphite lamellae.

APPLICATION OF THE CATHODE-RAY OSCILLOSCOPE TO POLAROGRAPHIC PHENOMENA. III. POTENTIALS OF ADSORPTION-DESORPTION CAPACITY PEAKS AND SURFACE CHARGE DENSITY RELATIONSHIPS EXHIBITED BY ALCOHOLS AT AQUEOUS SALINE SOLUTION-MERCURY INTERFACES

BY J. WEST LOVELAND[1a] AND PHILIP J. ELVING[1b]

The Pennsylvania State College, State College, Pennsylvania

Received August 22, 1951

Differential capacity oscillograms for the saturated solutions of *n*-octyl and *n*-heptyl alcohols show four capacity peaks on each of the cathodic and anodic sweeps rather than the expected two peaks, indicating double film formation. The patterns for a saturated *n*-hexyl alcohol solution are characterized by two and sometimes three capacity peaks on the charging and discharging curves. A saturated solution of *n*-amyl alcohol gives only two adsorption-desorption capacity peaks in each trace, indicating the formation of a mono film layer. The lower the molecular weight of the alcohol, the greater is the potential span between capacity peaks for the saturated solutions. For undegassed supersaturated solutions of the four normal alcohols, only two peaks per branch were observed. This picture reverts to that of the saturated solution upon degassing. The potentials of the reversible capacity peaks are given for both saturated and supersaturated solutions. In general, the desorption processes were found to proceed at the same or at a faster rate than the adsorption process as indicated by the sharpness of the corresponding capacity peak heights. Calculations of surface charge density according to the capacity peak potentials for the saturated solutions indicate that adsorption processes depend directly on the surface charge existing at the mercury surface.

In previous papers[2] experimental arrangements were described which were capable of producing differential capacity and surface charge density patterns on the face of an oscilloscope. The application of these techniques to the observation of film formation at the dropping mercury electrode, D.M.E., was indicated. The present paper is concerned with the results obtained from a systematic study based on oscilloscopic observation of the adsorption-desorption phenomena exhibited by various alcohols at the D.M.E., *i.e.*, at the interface between the mercury and aqueous salt solutions.

Heretofore, the study of the effect of non-electrolytes on the surface properties of a mercury electrode have been carried out for the most part by the determination of the surface tension which exists between a mercury drop surface and an electrolyte solution to which has been added some organic material. The usual procedure is to determine the surface tension over a selected applied voltage range and to plot the values of surface tension as a function of the applied voltage to give what is commonly called an electrocapillary curve. Gouy[3,4] published the most extensive surface tension data available for electrolytic solutions, both with and without the addition of non-electrolytes. The shape of the electrocapillary curve for a pure electrolyte is parabolic in form with a maximum coming at the potential of zero charge on the surface of the mercury. In the presence of slightly soluble organic compounds the maximum is either flattened or shifted to a potential different from that of the original electrocapillary maximum.

Frumkin,[5] likewise, found that the presence of adsorbable organic substances in solution modified the shape of the electrocapillary curve from that of the pure solution. Frumkin, *et al.*,[6] determined the influence of capronic (caproic?) acid and phenol on the surface tension of a mercury-sodium sulfate solution boundary by a capillary-electrometer method and found that in the neighborhood of the saturated solutions the two organic compounds are adsorbed as multilayers. Alternating current measurements by Proskurnin and Frumkin[7] of the capacity at a mercury surface in contact with a solution of sodium sulfate and octyl alcohol, showed abrupt increases in the capacity of the electrical double layer at potentials at which the adsorption and desorption processes of the alcohol took place, and a decreased capacity at intermediate potentials.

Grahame[8] studied the capacity and resistance at a mercury electrode in contact with solutions of potassium nitrate, sodium chloride and hydrochloric acid, all saturated with octyl alcohol, as a function

(1) (a) Sun Oil Co., Norwood, Pennsylvania. (b) University of Michigan, Ann Arbor, Michigan.

(2) (a) J. W. Loveland and P. J. Elving, THIS JOURNAL, **56**, 250 (1952); (b) J. W. Loveland and P. J. Elving, *ibid.*, **56**, 255 (1952).

(3) G. Gouy, *Ann. chim. phys.*, [8] **9**, 291 (1906).

(4) G. Gouy, *ibid.*, [8] **9**, 75 (1906).

(5) A. Frumkin, *Z. Physik*, **35**, 792 (1926).

(6) A. Frumkin, A. Gorodetskaya and P. Chugunov, *Acta Physicochim. U.R.S.S.*, **1**, 12 (1934); *C. A.*, **29**, 2046 (1935).

(7) A. Proskurnin and A. Frumkin, *Trans. Faraday Soc.*, **31**, 110 (1935).

(8) D. C. Grahame, *J. Am. Chem. Soc.*, **68**, 301 (1946).

of frequency and potential. Capacity peaks were observed at potentials corresponding to the adsorption and desorption processes of the alcohol at the mercury surface. Similar effects were produced on the differential capacity between mercury and an aqueous sodium sulfate solution by the addition of *n*-heptyl alcohol.[9]

Oscilloscopic observations of charging current curves were used by Barclay and Butler[10] for studying the adsorption effects of *t*-amyl alcohol at a mercury electrode. The curves showed discontinuities over the potential range in which the alcohol was adsorbed.

Brdicka[11] has discussed the adsorption theory in view of anomalous polarograms obtained with certain reversible organic oxidation–reduction systems. The polarographic wave is shifted to more negative potentials if the oxidized form is adsorbed, and to more positive potentials if the reduced form is adsorbed. Current–time oscillograms were used to study adsorption effects. For diffusion controlled processes, the current–time patterns showed a $^1/_6$ order parabola, while for adsorption processes definite maxima distorted the parabola.

Others[12–18] have determined the influence of slightly soluble organic compounds on the polarographic diffusion currents of electroactive metals and their ions. Invariably, the measured diffusion current is decreased at potentials over which adsorption takes place. When the applied potential is sufficiently negative that desorption occurs, the diffusion current becomes normal. As the concentration of the surface-active species is decreased, the diffusion currents increase toward their limiting value in "pure" solution, *i.e.*, in the absence of surface-active material.

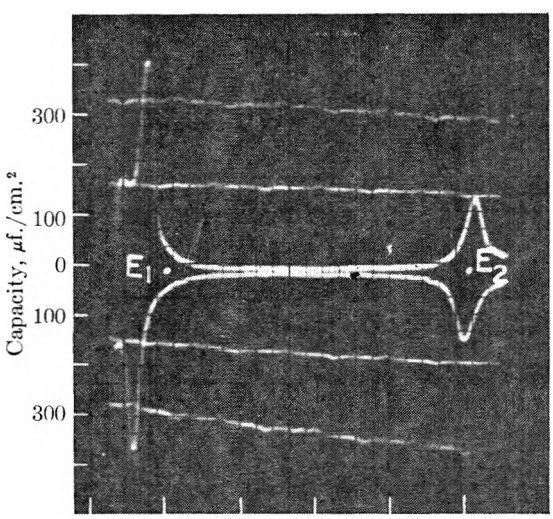

Fig. 1.—Differential capacity relation for 1 *N* KBr solution saturated with *n*-$C_6H_{13}OH$; E_1 = −0.202 v., E_2 = −1.017 v.; exposure time, 14.2 seconds; mass per second, 0.291 mg.; sensitivity resistance for curve, 12 ohms; for calibration, 150, 300 ohms.

Thus far, the majority of data concerning electrocapillary-active phenomena at a polarized mercury surface has been obtained as a result of the measurement of either surface tension or capacity at definite applied potentials. The data available is too meager to make any correlations regarding the general behavior of a given series of adsorbable compounds. To this end, the present authors have studied a series of alcohols under various conditions at the D.M.E. by the oscillographic techniques described previously.[1,2]

There are several advantages in using the oscilloscopic approach to the study of film formations. The method is rapid; a complete capacity or surface charge density spectrum may be obtained in a fraction of a second. The entire history for a single drop of mercury may be observed. Oscillograms for a given set of conditions are reproducible. Both charging and discharging curves are produced, the comparison of which serves to indicate the reversibility of the adsorption–desorption processes. The influence of film formation on the oxidation–reduction patterns of electroactive species can be studied. The method has the disadvantage of not being able to differentiate between polarization resistance and time-lag. In the present work, resistance has been calculated on the assumption that time-lag, as shown by Grahame,[9] is negligible. If this assumption is invalid, the resistance values will be in error. Nevertheless, whether resistance or time-lag or the sum of the two is measured, the calculated capacity values would be the same.

Method of Measurement

Photographic Technique.—Photographs of the differential capacity and surface charge density (S.C.D.) oscillograms for the D.M.E. in contact with an electrolyte solution containing alcohol were obtained in a manner analogous to that outlined previously.[1,2] For all alcohol solutions investigated, the capacity peaks of the adsorption and desorption processes on the charging cycle (cathodic—top curve) occurred at a more negative potential than those for the corresponding reverse process on the discharging cycle (anodic—bottom curve) (Fig. 1). Where the capacities of the peaks were approximately equal on the two branches, the adsorption and desorption processes were considered to be reversible, and the potential corresponding to the reversible process was taken as the average of the potentials of each of the peaks (anodic and cathodic). The reason for the difference of the cathodic and anodic capacity peak potentials is undoubtedly due to the larger iR drops associated with the very high peak currents (50 to 300 μa.) and the solution resistance and possibly polarization resistance[8] than with pure electrolytes; these large iR drops across the cell cause the cathodic capacity peaks to be shifted to more negative potentials than usual and the anodic capacity peaks to be shifted to more positive potentials. The average of the two potentials corresponds to the value which is obtained when no current is drawn by the cell. This is the point mid-way between the charging and discharging curves.

(9) D. C. Grahame, *Chem. Revs.*, **41**, 441 (1947).

(10) I. M. Barclay and J. A. V. Butler, *Trans. Faraday Soc.*, **36**, 128 (1940).

(11) R. Brdicka, *Collection Czechoslov. Chem. Comms.*, **12**, 522 (1947).

(12) B. Keilin, *J. Am. Chem. Soc.*, **70**, 1984 (1948).

(13) A. Kryukova, *J. Phys. Chem.* (*U.S.S.R.*), **20**, 1179 (1946); *C. A.*, **41**, 3004 (1947).

(14) A. Kryukova and A. Frumkin, *Zhur. Fiz. Khim.*, **23**, 819 (1949); *C. A.*, **43**, 8911 (1949).

(15) M. Loshkarev and A. Kryukova, *Doklady Akad. Nauk S.S.S.R.*, **62**, 97 (1948); *C. A.*, **43**, 503 (1949).

(16) M. Loshkarev and A. Kryukova, *Zhur. Fiz. Khim.*, **22**, 805 (1948); *C. A.*, **43**, 1269 (1949).

(17) M. Loshkarev and A. Kryukova, *Doklady Akad. Nauk S.S.S.R.*, **72**, 919 (1950); *C. A.*, **44**, 9827 (1950).

(18) L. Meites and T. Meites, *J. Am. Chem. Soc.*, **73**, 177 (1951).

The S.C.D. oscillograms for solutions which were saturated with alcohol were S-shaped (Fig. 2) and the exact points to be chosen as representing the surface charge density differences (S.C.D.D.) were not distinct; hence, these records were not used for calculation. The more precise procedure for the determination of S.C.D.D. values involved applying the capacity peak potential data obtained from the differential capacity oscillograms of the alcohol solutions to the smooth S.C.D. patterns of the pure electrolyte solution.

The sweep frequency used was 7.5 c.p.s. unless otherwise specified.

Direct Measurement of Potential.—The potentials at which the adsorption and desorption peaks occurred can be measured directly without the use of the photographic procedure. A point on the grid of the oscilloscope is chosen, and the cathodic and anodic peaks aligned with respect to this point. The voltage sweep is turned off and the spot remaining on the screen of the oscilloscope adjusted to the selected point by means of the potentiometer (R_a, Fig. 2, ref. 2) in series with the polarographic cell. The e.m.f. is then measured on a student type potentiometer. This method of measuring reversible peak potentials is rapid and results are reproducible to within ±4 millivolts.

Experimental

Preparation of Solutions.—The *n*-octyl, *n*-heptyl, *n*-hexyl and *n*-amyl alcohols were investigated in 1 *N* potassium chloride as the supporting electrolyte. The *n*-octyl and *n*-hexyl alcohols were also studied in 1 *N* potassium bromide and 1 *N* potassium iodide solutions. The alcohols were either Eastman Kodak Co. purest grade or stockroom grade which had been purified by distillation. Only the middle portions of the distillate which boiled in a 2° range were used.

Saturated solutions of the alcohols were made by titrating the alcohol from a microburet into a known volume of the electrolyte solution and shaking the solution several minutes after each small addition of alcohol until a few very small globules of alcohol were visible on the surface of the aqueous solution. This end-point could be reproduced with fair accuracy to within 5%. The molarity of the saturated alcohol solution is given in Table I.

TABLE I

MOLARITY OF SATURATED ALCOHOL SOLUTIONS

Alcohol	1 *N* KCl	1 *N* KBr	1 *N* KI
n-C_8	0.0017	0.0022	0.0028
n-C_7	.0071		
n-C_6	.028	0.031	0.039
n-C_5	.15		

Supersaturated solutions were made by adding a slight excess of the alcohol to the corresponding saturated solution and shaking vigorously until the solution was colloidal and turbid in appearance. The authors use the term "supersaturated" in the sense that an excess of alcohol is present in dispersed form in the aqueous phase over the amount required for saturation.

For preparing alcohol solutions other than the saturated and supersaturated, the appropriate volume of alcohol was measured from a microburet and sufficient 1 *N* salt solution added to bring the concentration of the alcohol to the desired molarity.

All solutions were investigated at room temperature, which remained constant at 24 ± 1°.

D.M.E. and Cell.—The low resistance dropping mercury electrode and cell arrangement used have been described elsewhere.[1] All potential values are reported against the mercury pool with the 1 *N* electrolyte indicated.

The usual procedure for cleaning the cell after each run was as follows: After removal of the test solution by suction, the cell was washed twice with distilled water and once with acetone. It was again washed with water and then rinsed twice with the alcohol solution to be investigated.

Reproducibility of Curves.—Although the oscillographic patterns for a given set of conditions were easily reproduced with respect to potential and capacity measurements of the peak capacities for the adsorption-desorption processes, it should be pointed out that on observation of alcohol concentrations in the vicinity of saturation, the shape of the capacity oscillograms would sometimes undergo changes during the lifetime of the drop. For example, two capacity peaks would appear close together at the early stages of drop growth, but these would merge into one peak after a few seconds. This was more true of the higher molecular weight alcohols than of the lower molecular weight alcohols.

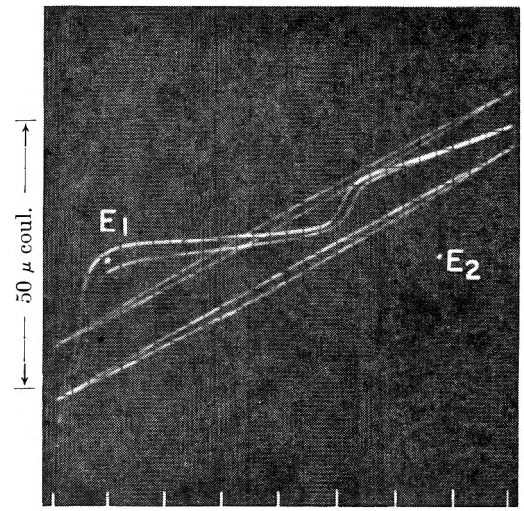

Fig. 2.—Surface charge density pattern for 1 *N* KBr solution saturated with *n*-$C_6H_{13}OH$; E_1 = −0.199 v., E_2 = −1.326 v., exposure time, 11.6 seconds; mass per second, 0.291 mg.; sensitivity resistance for curve, 50 ohms; for calibration, 120 ohms.

Variations as great as 40 millivolts for the reversible peak potentials were recorded in a few instances when degassing was carried out over different time intervals. The majority of the deviations was of the order of 20 millivolts. In general, for saturated solutions the potential of the more positive peaks became more negative while that of the more negative peaks shifted to a more positive potential. This change in peak potentials with degassing time has been correlated with a change in concentration of the alcohol. Such peak potential variations were not effectively reduced by first passing the nitrogen stream through a bubbler containing the pure alcohol, whose saturated aqueous solution was under investigation. It was, therefore, necessary to standardize degassing methods to permit correlation of the data obtained.

The data given in the subsequent discussion have been obtained with solutions that were either degassed for 5 minutes or not degassed at all, as indicated. The presence of oxygen did not affect the shape of any of the oscillograms observed. The potential values given are a composite of those obtained by direct measurements and those from photographs. A sufficient number of readings were made on different cell solutions of the same solution so that for any given alcohol solution, the average deviation of the potential measurements by the two methods did not vary by more than ±10 millivolts.

Discussion of Observed Behavior

Saturated Solutions.—Probably the most outstanding feature shown by the capacity oscillograms for saturated solutions of the *n*-heptyl and *n*-octyl alcohols was that more than the two expected capacity peaks were observed on both the charging and the discharging curves. Both degassed and undegassed saturated solutions of *n*-octyl alcohol gave two adsorption and two desorption peaks in both the charging and discharging curves for all three potassium halide solutions (Fig. 3). In Fig. 3 the peaks (labeled A_1 and A_2, and B_1 and B_2) correspond to the adsorption processes on the charging and discharging branches of the oscillogram, respectively. The peaks (labeled A_3 and

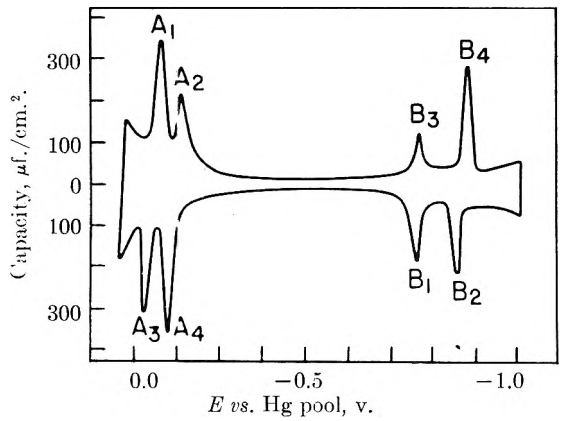

Fig. 3.—Differential capacity relation of 1 *N* KI solution saturated with n-$C_8H_{18}OH$.

A_4, and B_3 and B_4) indicate the desorption processes taking place at the mercury-solution interface. If degassing of the saturated *n*-octyl solution is continued for several minutes beyond the first five minutes, the peaks corresponding to B_2 disappear, and, in the place of B_1, a more rounded peak occurs than was originally present. At the same time, the peaks of A_1 and A_2 appear to decrease in size. In the case of the iodide solution, after a total of 15 minutes of degassing, the peaks of A_1 and A_2 completely disappeared. Instances where a small pip was superimposed on the rounded wave at B_1 while all the other peaks were present, were recorded. These same general phenomena also occurred with saturated solutions of *n*-heptyl alcohol. The disappearance or reduction of wave height is due to the decrease in the concentration of the alcohol in solution. The disappearance of peaks due to solubility and concentration effects may be more fully realized by comparison of the oscillograms observed for 1 millimolar alcohol solution which are reported in a subsequent section.

Saturated *n*-hexyl alcohol solutions did not manifest four peaks in each branch as were observed for saturated solutions of the two higher molecular weight alcohols (Fig. 1). Occasionally, pips which correspond to peaks B_2 and B_4 of Fig. 3 would appear under either degassed or undegassed conditions. These pips were superimposed on the negative potential sides of the peaks of B_1 and B_3 close to the apex of the latter peaks. The heights of the pips B_2 and B_4 depended to a great degree on the voltage range and starting potential of the applied voltage sweep. The variation of the peak heights with the potential range of the voltage sweep will be discussed subsequently. At the more positively applied potentials, only one peak on each of the traces was observed.

The saturated *n*-amyl alcohol solution showed only one adsorption and one desorption peak in both the charging and discharging curves. The reversible peak potentials for the degassed saturated solutions of the four alcohols are tabulated in Table II as V_2 and V_3, where V_2 corresponds to the capacity peaks appearing at the lower negative potential.

To simplify discussion, the average potentials corresponding to the "reversible" peaks (A_1, A_3), (A_2, A_4), (B_1, B_3) and (B_2, B_4) of Fig. 3 shall hence-

TABLE II

POTENTIALS OF CAPACITY PEAKS FOR DEGASSED SATURATED ALCOHOL SOLUTIONS

Alcohol	Solution	V_2, v.	V_3, v.	$V_3 - V_2$, v.
n-Amyl	1 *N* KCl	0.079	1.213	1.134
n-Hexyl	1 *N* KCl	.099	1.167	1.068
	1 *N* KBr	.123	1.020	0.897
	1 *N* KI	.160	0.789	0.629
n-Heptyl	1 *N* KCl	.126	1.146	1.020
n-Octyl	1 *N* KCl	.130	1.139	1.009
	1 *N* KBr	.152	0.967	0.815
	1 *N* KI	.184	0.735	0.551

forth be designated as V_1, V_2, V_3 and V_4, respectively.

Supersaturated Solutions.—The undegassed supersaturated solutions in the form of colloidal dispersions of the four alcohols always gave one adsorption and one desorption peak on each of the anodic and cathodic traces for all of the halide solutions studied (Fig. 4). A five-minute degassing period usually converted the shape of the oscillograms of these solutions to those obtained for the saturated solution. The *n*-octyl and *n*-heptyl alcohol solutions would correspond to Fig. 3, while *n*-hexyl and *n*-amyl would appear as in Fig. 1.

Table III contains the peak capacity potential values obtained with supersaturated solutions which have been degassed for 5 minutes. The potentials,

TABLE III

POTENTIAL VALUES OF CAPACITY PEAKS FOR SUPERSATURATED SOLUTIONS

Alcohol	Solution	V_1, v.	V_2, v.	V_3, v.	V_4, v.	$V_4 - V_1$, v.
n-Amyl	1 *N* KCl	0.047	...	...	1.250	1.203
n-Hexyl	1 *N* KCl	.056	0.118[a]	1.213	1.241	1.185
	1 *N* KBr	.079	.105	1.077	1.101	1.022
	1 *N* KI	.132	.132[b]	0.825	0.857	0.725
n-Heptyl	1 *N* KCl	.056	.126	1.164	1.249	1.193
n-Octyl	1 *N* KCl	.051	.125	1.131	1.243	1.192
	1 *N* KBr	.088	.149	0.970	1.092	1.004
	1 *N* KI	.138	.186	0.737	0 863	0.725

[a] Peak potential of cathodic wave only. [b] V_1 and V_2 are the same, since one peak was observed.

V_1 and V_4, apply as well to undegassed supersaturated solutions which give only one adsorption and one desorption peak for each trace as in Fig. 4. This is true because the values of V_1 and V_4 were the same within the experimental error

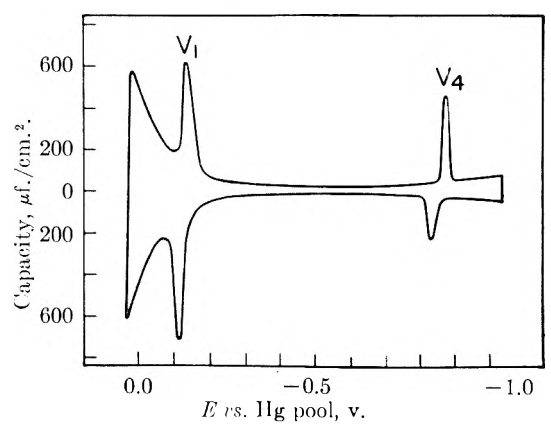

Fig. 4.—Capacity oscillogram for *N* KI solution supersaturated with n-$C_8H_{17}OH$ (no degassing).

whether only two, three or four peaks were observed on either the cathodic or anodic branches.

The following facts may be derived from the data of Tables II and III: (1) The difference ($V_3 - V_2$) between the potentials of the capacity peaks under saturated solution conditions decreases as the molecular weight of the alcohol increases. This is seen best by comparison of the data for potassium chloride solution. (2) The difference between the most positive (V_1) and the most negative (V_4) capacity peak potentials for supersaturated solutions is practically independent of the molecular weight of the alcohol for a given halide solution. (3) The difference between the potentials of the adsorption and desorption peaks for both *n*-hexyl and *n*-octyl alcohol solutions decreases, going from the chloride to the bromide to the iodide solution. (4) The potential difference between V_1 (Table III) and V_2 (Table II) is less than the potential difference between V_3 (Table II) and V_4 (Table III) for all solutions investigated. (5) Comparison of the values of V_2 and V_3 of Tables II and III shows that for *n*-octyl alcohol the values agree well within the experimental error of the measurements for both the saturated (Table II) and supersaturated solutions (Table III). However, as the molecular weight of the alcohol decreases, the variation of these values increases. This is best realized by inspection of the V_2 and V_3 values for *n*-hexyl alcohol.

Other facts pertinent to the study of alcohol film formations which were observed are: (1) At certain stages of degassing of the supersaturated solutions, the capacity current peaks corresponding to V_2 and V_3 appeared at the early stages of the mercury drop but soon disappeared as the drop continued to increase in area. (2) The rate of potential variation had no discernible effect on the reversible peak capacity potentials. (3) Whenever the peaks of V_3 and V_4 occurred simultaneously, the peaks of V_4 disappeared on both the anodic and cathodic curves when the voltage sweep was started at a potential between that of V_3 and V_4. When the voltage sweep ended between V_3 and V_4, the peaks of V_3 were always present. The same experiment could not be performed on the peaks of V_1 and V_2 since the oxidation of mercury occurred at such positive potentials. (4) The heights of the capacity peaks of V_4 on the discharging (adsorption) and the charging (desorption) branches decreased as the voltage sweep of constant magnitude was moved to more negative potentials until the starting potential of the sweep reached the potential of V_3 at which time the capacity peaks of V_4 disappeared. The adsorption peak of V_4 disappeared before the desorption peak of V_4. (5) The capacity peaks of V_4 on both the charging and discharging curves covered a much narrower potential band (more peaked) than the corresponding capacity peaks of V_3 (Fig. 5) and in many cases consisted of single lines, especially when the voltage sweep ended a few millivolts beyond the peak potential, V_4. (6) For supersaturated solutions, the peak capacity of the desorption process on the charging cycle (V_4) is greater than the peak capacity for the corresponding adsorption process (Fig. 4, compare

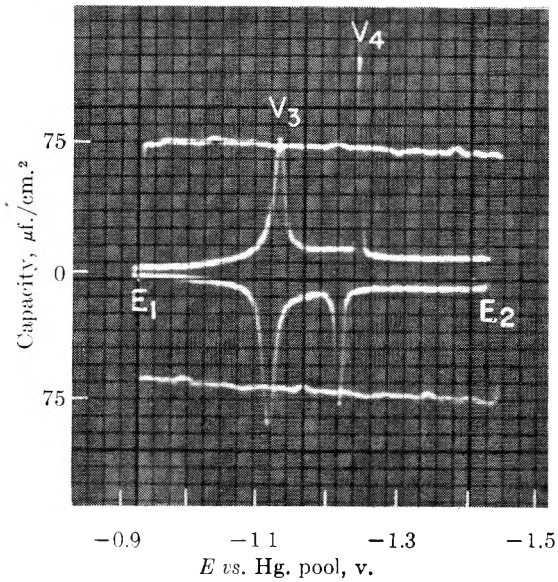

Fig. 5.—Comparison of capacity peak widths for 1 *N* KCl solution saturated with *n*-$C_8H_{17}OH$; $E_1 = -0.927$ v., $E_2 = -1.427$ v.; exposure time, 14.0 seconds; mass per second, 0.280 mg.; sensitivity resistance for curve, 25 ohms; for calibration, 325 ohms.

the two peaks of V_4). (7) For saturated solutions, the peak capacities of V_2 and V_3 for both the charging and discharging processes are about equal in magnitude.

On the basis of the data and facts outlined, the following conclusions can be drawn: (1) There can exist on the surface of mercury a double film layer of adsorbed alcohol molecules as indicated by four rather than two capacity peaks in both charging and discharging curves. The tendency to form double layers increases with the molecular weight of the alcohol and is probably associated with the solubility and dielectric properties of the alcohol in the aqueous phase. (2) The adsorption–desorption processes corresponding to the potential of V_4 take place over a smaller potential range than those of V_3 as evidenced by the sharper peaks of V_4. (3) For cases where four capacity peaks occur on each branch simultaneously, the formation of the layer which gives rise to the peak of V_4 is dependent on the formation of the layer which gives rise to the peak of V_3. The reverse situation does not hold. For this reason, the film layer closest to the mercury surface is associated with the capacity peaks of V_3 while the layer furthest from the electrode surface is identified with the capacity peaks of V_4. (4) The variation in potential difference between V_2 and V_3 (Table II) for the various halide solutions of *n*-hexyl and *n*-octyl alcohol indicates that the adsorption–desorption process depends not so much on potential but rather on some intrinsic property of the electrode surface. It will be shown subsequently that this property is the surface charge density of the mercury electrode. (5) Desorption processes take place either at the same rate or more rapidly than adsorption processes as evidenced by the fact that in several cases studied, sharp capacity peaks occurred for the desorption process while only rounded peaks were observed for the adsorption of the alcohol films.

This is the antithesis of Heyrovsky's[19] results with the potential–time derivative oscillograms in pyridine film formations at the mercury electrode. His findings indicated that the pyridine film builds up instantaneously, while its removal goes on slowly.

One Millimolar Solutions.—Capacity oscillograms of the 1 millimolar *n*-octyl alcohol–potassium halide solutions were made. For the potassium chloride solution, peaks were observed in the cathodic branch at all four potentials and in the anodic branch at the potentials of V_1 and V_2. There was no peak for the anodic process at V_4 and only a rounded peak at V_3. The potassium bromide solution capacity oscillogram was identical to that of the potassium chloride with the exception that no sharp peak was observed in the cathodic branch at the potential of V_4. The 1 millimolar solution in potassium iodide gave rise to rounded peaks in both the charging and the discharging curves at the potentials of V_2 and V_3, and no peaks at V_1 and V_4.

When 1 millimolar *n*-hexyl alcohol solutions were investigated for capacity peaks in all three potassium halide solutions, only the chloride solution showed any signs of electrocapillary-active phenomena. This was evidenced by the fact that the capacity maximum, occurring near the potential of the electrocapillary maximum, was increased in value by about 10% above that for a pure 1 *N* solution. There was no distortion of the differential capacity patterns for any of the halide solutions when these solutions were 1 millimolar with respect to *n*-amyl alcohol.

Surface Charge Density Relationships

Oscillograms of the S.C.D. for the pure halide solutions were obtained; a typical S.C.D. pattern is shown in Fig. 6. The S.C.D. corresponding to the potential difference between V_2 and V_3 for saturated *n*-hexyl and *n*-octyl alcohol solutions was calculated from the S.C.D. patterns of the pure solution. The results of these calculations are given in microcoulombs per square centimeter in Table IV. All values are averages of calculations from five separate S.C.D. oscillograms for each halide solution.

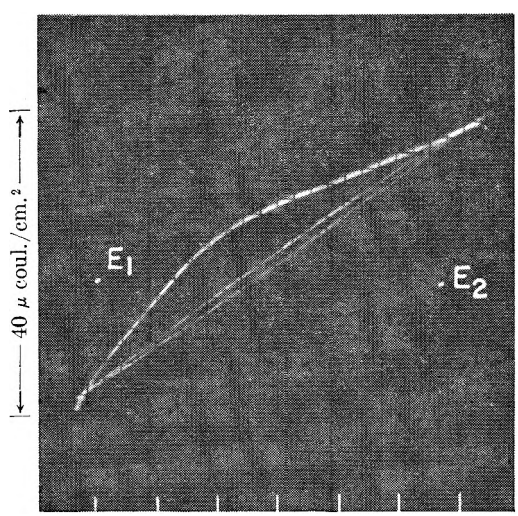

Fig. 6.—Surface charge density relation for 1 *N* KBr solution; E_1 = −0.195 v., E_2 = −1.363 v.; exposure time, 13.8 seconds; mass per second, 0.291 mg.; sensitivity resistance for curve, 70 ohms; for calibration, 170 ohms.

(19) J. Heyrovsky, F. Sorm and J. Forejt, *Collection Czechoslov. Chem. Comms.*, **12**, 1[illegible] (1947).

TABLE IV[a]

SURFACE CHARGE DENSITY DIFFERENCE OF SATURATED SOLUTIONS (DEGASSED) OVER THE POTENTIAL RANGE OF $V_3 - V_2$, μcoul./cm.²

Alcohol	1 *N* KCl	1 *N* KBr	1 *N* KI
n-Hexyl	32.1 ± 0.6	32.5 ± 0.6	32.3 ± 0.8
n-Octyl	29.2 ± 0.6	29.6 ± 0.4	29.1 ± 0.6

[a] S.C.D.D. values were obtained from oscillograms of the pure halide solutions using the potential data of Tables II and III.

The consistency of the S.C.D.D. values for both *n*-hexyl and *n*-octyl alcohol in the three different halide solutions shows that the adsorption and desorption of alcohol films, corresponding to the potentials of V_2 and V_3 for saturated solutions, are intimately connected with the surface charge property of the mercury electrode and, in fact, the potentials of adsorption and desorption are directly dependent on the surface charge density existing at the mercury surface.

The S.C.D.D. values for the saturated solutions of the two alcohols differ by about 3 microcoulombs over the potential range of $V_2 - V_3$. The S.C.D.D. for the two alcohols under supersaturated solution conditions covering the potential range of V_1 to V_4 would show little or no difference in values, since the potentials of V_1 and V_4 are almost identical for the two alcohols for each of the corresponding halide solutions. One might expect this if a double layer film exists, for the layer closest to the electrode surface corresponding to the potentials, V_3 and V_2, will be influenced directly by the S.C.D. of the electrode while the second layer corresponding to the potentials V_1 and V_4, somewhat screened from the influence of the S.C.D. of the electrode by the first layer, is less dependent on the surface property of the electrode.

At concentrations less than that of saturation, the S.C.D.D. values covering the potential range ($V_3 - V_2$) for 20 millimolar *n*-hexyl alcohol solutions (Table V) show a decided decrease in magnitude in going from the chloride to the bromide to the iodide solutions. On the other hand, the S.C.D.D. values for 1.25 millimolar *n*-octyl alcohol solutions (Table V) indicated no such decrease in values for the three halide solutions studied, but,

TABLE V[a]

SURFACE CHARGE DENSITY DIFFERENCES OF DILUTE *n*-HEXYL AND *n*-OCTYL SOLUTIONS (UNDEGASSED) OVER THE POTENTIAL RANGE OF $V_3 - V_2$, μcoul./cm.²

Alcohol	1 *N* KCl	1 *N* KBr	1 *N* KI
20 m*M* *n*-hexyl	29.7 ± 0.7	28.4 ± 0.6	26.1 ± 0.7
1.25 m*M* *n*-octyl	29.6 ± 0.6	29.9 ± 0.5	29.6 ± 0.6

[a] S.C.D.D. values were obtained from oscillograms of the pure halide solutions using the potential data of Tables II and III.

rather, these values remained constant within the experimental error of measurement.

The constancy of the S.C.D.D. values for the 1.25 millimolar *n*-octyl alcohol solutions is undoubtedly associated with the double film formation property exhibited by this alcohol. At this concentration, 2 to 4 peaks were observed in each branch for the three halide solutions. As long as the concentration of the alcohol is sufficient to produce double layers, the layer closest to the surface of the mercury will be adsorbed over the same S.C.D. range of values. At concentrations less than that required for double film formation, the S.C.D.D. values needed for adsorption will decrease as the concentration of the alcohol decreases. This, in fact, was observed to be the case for *n*-hexyl alcohol where the concentration of the alcohol is sufficiently low so that there is no indication of double film formation. When the S.C.D.D. values are considered with respect to the relative solubilities of the *n*-hexyl alcohol in the three potassium halide solutions, there is a definite relationship between the decrease in S.C.D.D. values and the decrease of concentration of the alcohols with respect to the saturation concentrations of the alcohols in going from the chloride to the bromide to the iodide. In a subsequent paper it will be shown that the S.C.D.D. value is a function of the log of the concentration.

The S.C.D. should be normal in the regions outside the adsorption region, *i.e.*, the S.C.D.D. from one end of the sweep to the other should be independent of the presence or kind of adsorbable species. Calculations were made, based on potential spans sufficient to encompass all adsorption–desorption processes, for the S.C.D.D. of the three pure electrolyte solutions and for the S.C.D.D. of various saturated and 1 m*M* *n*-heptyl and *n*-octyl alcohol solutions. The average deviation between values of corresponding solutions was 4% compared to 2% deviation in the S.C.D.D. calculations themselves; values for 1 m*M* *n*-heptyl and *n*-octyl alcohol solutions were practically identical with those for the electrolyte solution itself.

The authors wish to thank the Office of Naval Research for their support of the research project upon which the work described was done.

APPLICATION OF THE CATHODE-RAY OSCILLOSCOPE TO POLAROGRAPHIC PHENOMENA. IV. PEAK AND MINIMUM CAPACITIES OF ADSORPTION–DESORPTION PROCESSES EXHIBITED BY ALCOHOLS AT AQUEOUS SALINE SOLUTION–MERCURY INTERFACES

BY J. WEST LOVELAND[1a] AND PHILIP J. ELVING[1b]

The Pennsylvania State College, State College, Pennsylvania

Received August 22, 1951

The capacities of the adsorption and desorption peaks associated with film formation for saturated and supersaturated solutions of *n*-amyl, *n*-hexyl, *n*-heptyl and *n*-octyl alcohols were measured from differential capacity oscillograms. The values of the peak capacities are greater for supersaturated, *i.e.*, colloidal, solutions than for saturated solutions. The adsorption–desorption processes taking place at low applied negative potentials give rise to capacities about twice as great as those at more negative potentials. Desorption processes were found generally to give higher capacities than adsorption processes, especially with the higher molecular weight alcohols. This is interpreted as indicating that the rate of the desorption process proceeds as fast or faster than that of the adsorption process. The minimum capacities due to film formation for the four normal alcohols decreased as the molecular weight of the alcohol increased. This was ascribed to differences in the dielectric properties of the alcohols in aqueous solution and to the size of the alcohol molecule. Capacity peaks exhibiting an Ohm's law maximum relationship were found.

Methods have been outlined[2] whereby differential capacity and surface charge density patterns could be obtained on a cathode-ray oscilloscope. These methods were applied to the study of adsorption–desorption phenomena of various alcohols at mercury–saline solution interfaces with special emphasis on the potentials of the adsorption–desorption capacity peaks and on the surface charge density relationships involved.[3] The present study is concerned with the magnitude of the peak and minimum capacities encountered during film formation by alcohols at mercury–saline solution interfaces as observed from oscillographic capacity patterns.

(1) (a) Sun Oil Co., Norwood, Pennsylvania. (b) University of Michigan, Ann Arbor, Michigan.

(2) (a) J. W. Loveland and P. J. Elving, THIS JOURNAL, **56**, 250 (1952); (b) J. W. Loveland and P. J. Elving, *ibid.*, **56**, 255 (1952).

(3) J. W. Loveland and P. J. Elving, *ibid.*, **56**, 935 (1952).

Method of Measurement

Capacity values were calculated in the same manner as in the determination of differential capacities of pure electrolyte solutions.[1] In essence, this involves the ratio of the distances between the charging and discharging traces for the differential capacity pattern and for the calibration pattern, together with the ratio of the current sensitivity settings, the area of the mercury drop and the value of the calibrating capacitor. The latter was 0.261 ± 0.001 microfarad.

An alternate method for the determination of capacity utilizes a standard height method. The current-measuring resistance is adjusted so that the anodic and cathodic capacity peaks reach a given distance on the grid of the oscilloscope just prior to the falling of the mercury drop. The drop-time is measured for determining the area of the mercury drop. The standard capacity is then inserted in place of the dropping mercury electrode (D.M.E.) cell and the charging–discharging traces adjusted to the selected height by the current-measuring resistance. The differential capacity is calculated from the ratio of the two resistance settings, the value of the calibrating capacitor and the area of

the mercury drop. Because transient phenomena are involved, this method is not as accurate as the photographic procedure.

The sweep frequency used was 7.5 c.p.s. The cell and D.M.E. arrangement have been described.[1]

Peak Capacities

Saturated solutions of *n*-heptyl and *n*-octyl alcohols in 1 *N* potassium halide gave rise to four capacity peaks on both the charging and discharging branches of the differential capacity current oscillograms.[3] The potentials at which these peaks appeared were designated as V_1, V_2, V_3 and V_4, where V_1 was the most positive and V_4 the most negative of the four capacity peaks. The saturated solutions of *n*-hexyl alcohol were characterized by either two or three capacity peaks (V_2, V_3 and V_4) while the saturated solutions of *n*-amyl alcohol showed exclusively two peaks (V_2 and V_3) on both the charging and discharging traces.

The supersaturated undegassed solutions of these four alcohols gave one adsorption and one desorption capacity peak per branch. The potentials at which these peaks occurred were the same as those of V_1 and V_4 for the saturated solutions. The authors use the term "supersaturated" in the sense that the concentration of the alcohol in colloidal form in the aqueous phase is above that required for saturation.

The values of peak capacities in microfarads per square centimeter of mercury surface in Table I are given for the 5-minute degassed saturated solutions of the alcohols. Only the peaks corresponding to the potentials V_2 and V_3 are considered. For the C_5- and C_6-alcohols, the peak capacities of the desorption and adsorption processes at the corresponding potentials, V_2 and V_3, were, within experimental error, identical. The heptyl and octyl alcohol saturated solutions, on the other hand, usually gave different anodic and cathodic peak capacity values at the same potential. Two generalizations can be made regarding the peak capacities: (1) The peak capacities occurring at the potential of V_2, regardless of whether the adsorption or desorption process is considered, are always greater than those which appear at the potential of V_3. (2) For the C_7- and C_8-alcohols where double film formation is prevalent, the desorption processes produce higher capacity values than do the adsorption processes.

TABLE I

PEAK CAPACITIES OF SATURATED ALCOHOL SOLUTIONS IN MICROFARADS PER SQUARE CENTIMETER

		At V_2		At V_3	
Alcohol	Solution	Adsorption	Desorption	Adsorption	Desorption
n-C_5	1 *N* KCl	305	305	105	105
n-C_6	1 *N* KCl	460	460	130	130
	1 *N* KBr	410	410	127	127
	1 *N* KI	290	290	125	125
n-C_7	1 *N* KCl	250	380	72	102
n-C_8	1 *N* KCl	270	400	90	160
	1 *N* KBr	370	410	220	170
	1 *N* KI	220	380	210	115

TABLE II

PEAK CAPACITIES OF SUPERSATURATED ALCOHOL SOLUTIONS IN MICROFARADS PER SQUARE CENTIMETER

		At V_2		At V_3	
Alcohol	Solution	Adsorption	Desorption	Adsorption	Desorption
n-C_5	1 *N* KCl	370	370	110	110
n-C_6	1 *N* KCl	290	540	320	320
	1 *N* KBr	520	520	310	310
	1 *N* KI	370	370	350	350
n-C_7	1 *N* KCl	500	500	260	590
n-C_8	1 *N* KCl	600	600	190	500
	1 *N* KBr	880	880	200	580
	1 *N* KI	640	730	200	500

Very large values were found for the peak capacities (Table II) of the undegassed supersaturated solutions. The values for a given solution vary as much as 20%. The capacities measured at the potential of V_1 were usually of greater magnitude than those at V_4.

Where there are differences between the adsorption and desorption peak capacities, at the potential of either V_1 or V_4, the capacity for the adsorption process is small than that for the desorption process. This difference in peak heights is interpreted as meaning that the two processes are not completely reversible and that desorption takes place more rapidly than adsorption.

Upon degassing of the supersaturated solutions for 5 minutes for cases where three or four peaks are observed in the charging or discharging curves, the peak capacities corresponding to V_2 and V_3 were either the same or slightly greater than those given in Table I for saturated solutions. The values of peak capacity at the potentials of V_1 and V_4 could be increased or decreased by applying various voltage sweep spans or by varying the starting and ending potentials of the voltage sweep[3]; hence, any calculations on these capacity peaks are of little consequence, until a fuller understanding of the phenomenon is realized. The values given in Tables I and II have been obtained with voltage sweeps having a potential span sufficient to include all of the peaks upon which the measurements were made for each alcohol solution.

In order to determine if the presence of oxygen in the undegassed supersaturated alcohol solutions was responsible to any degree for the very high capacity values involved, oxygen was passed through the solutions for a length of time corresponding to that used in the degassing procedures. In the several cases investigated, the effect of passing oxygen through the supersaturated solutions was the same as that attained under degassed conditions, *i.e.*, the patterns observed resembled those of the supersaturated alcohol solutions which had been degassed with nitrogen.

Discussion

The magnitude of the differential capacity is directly related to the change of the surface charge density which in turn is directly related to the change of the surface tension existing at the mercury–solution interface as a function of potential. When capacity peaks occur, the surface tension of the mercury–saline solution interface is abruptly changed by the adsorption or desorption of the non-electrolyte at fairly definite potentials.

It may be concluded that the very high capacity peak values incurred with undegassed supersaturated solutions are due to the breaking of two or possibly even three layers of alcohol at the mercury surface, simultaneously and almost instantaneously. Apparently, the concentration of alcohol molecules in the vicinity of the mercury electrode under supersaturated conditions (colloidal form) is so great that the alcohol molecules are associated with each other to such a large extent that, as soon as one layer is adsorbed or desorbed, another layer is pulled along with it. Under saturated conditions where lower capacity peak values are obtained, the alcohol molecules in solution are not associated as greatly, but are dispersed in the aqueous medium. After one layer has been adsorbed, the charge on that layer is sufficient to attract a second layer of alcohol molecules. The ability to attract a second layer increases with the molecular weight of the alcohol. Such a behavior can be correlated with the dielectric characteristics of the alcohols in aqueous solution. In this connection, Frumkin[4] has stated that a definite polarity for the combination C–O must exist as (C^+, O^-) to explain the production of a potential difference associated with the adsorption of capillary-active substances at an air–water boundary. In general, the higher the dielectric constant of an alcohol, the greater the association will be between the water

(4) A. Frumkin, *Z. Physik. Chem.*, **111**, 190 (1924).

molecules and the alcohol molecules as well as between the alcohol molecules themselves, although this latter occurrence is probably negligible in aqueous solutions at the concentrations used. Infrared measurements show that the amyl alcohols in the liquid state exist in the monomer as well as the polymer form.[5] The association effect is strong enough with *n*-amyl alcohol that once the alcohol is adsorbed on the surface of the mercury, the influence of the water molecules, through hydrogen bonding, sufficiently neutralizes the charge of the OH group of the surrounding alcohol molecules that they are prevented from being adsorbed as a second layer. As the molecular weight of the alcohol increases, the neutralization of charge distribution[6] on the alcohols by the water molecules decreases, which is manifested by the increased tendency for the higher alcohols to be attracted by the small charge of the adsorbed alcohol film and to form a second layer. From another point of view, the longer the carbon chain of the alcohol, the greater the tendency will be for the alcohol to be "squeezed" out of solution with its polar end directed toward the polarized electrode surface.

Other observations are concurrent with these views. As stated, the starting potential greatly influences the height of the capacity peak at potentials corresponding to V_4. If the sweep is started at a potential between that of V_3 and V_4, the peak of V_4 completely disappeared. This indicates that there is no formation of a second layer without the first layer being present. Also as the starting potential is increased toward more negative potentials, the capacity peaks of V_4 decrease in height. As the potential span becomes more negative, a greater number of cations are drawn toward the surface of the mercury. These cations are surrounded by their solvent sheaths but the latter are presumably pushed aside[7] before the metal ions come in contact with the mercury. Regardless of whether the water molecules are shed or not by the cations at the electrode, the situation is that the concentration of the solvent molecules in the vicinity of the electrode has been substantially increased over that which would be present at more positive potentials. This has the effect of decreasing the polar attraction of the alcohol molecules to any film layer already present and may account for the decreasing peak capacity at V_4 as more negative voltage spans are applied to the D.M.E.

Minimum Capacities

Experimental.—The determinations made of minimum capacities occurring between the capacity peaks were reproducible to within 2% for saturated solutions of the alcohols. Figure 1 illustrates the type of oscillogram obtained in the determination of minimum capacities. The procedure followed for the estimation of the minimum capacity is exactly the same as that used previously for the determination of the peak capacity values.

The minimum capacities occur at or near the potentials of the electrocapillary maximum for each of the halide solutions used. Inspection of the values of Table III show a regular increase in minimum capacities for both the *n*-hexyl and *n*-octyl alcohol solutions, going from the chloride to the bromide to the iodide. From *n*-amyl to *n*-octyl in potassium chloride solutions, there is a general decrease in the minimum capacity values, with the exception of that for the *n*-heptyl solution, which is out of place in the sequence because of its lower value than the others. This abnormality cannot be explained. However, the trend of minimum capacities toward lower values with increasing molecular weight can be explained by considering the influence of the solvent molecules on the dielectric properties of the alcohols and the size of the alcohol molecules, as is done subsequently.

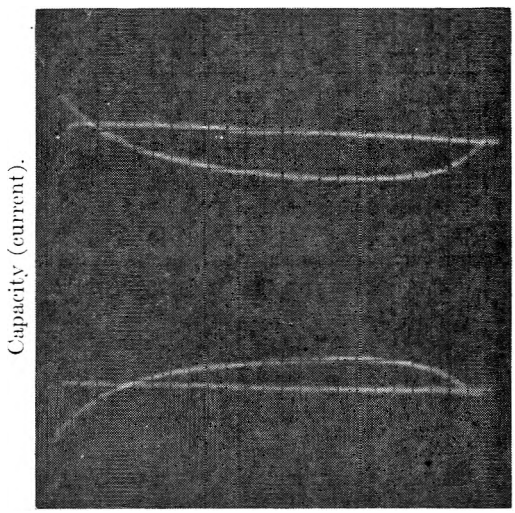

Fig. 1.—Minimum capacity for 1 *N* KBr solution saturated with *n*-$C_6H_{13}OH$. Exposure time, 12.0 seconds; mass per second, 0.291 mg.; sensitivity resistance for curve, 400 ohms; for calibration, 200 ohms.

Nature of the Capacity.—It will be beneficial for the following discussion to describe briefly and simply the nature of the total capacity. The equivalent circuit which best represents the electrical double layer in the presence of a film layer is depicted in Fig. 2[8] where C_1 is the capacity of the inner layer between the electrode surface and the Helmholtz plane (the plane which is the center of the ions nearest to the mercury surface); C_2 is the capacity of the film layer bounded on the one side by the inner layer and on the other side by the diffuse layer; C_3 is the capacity of a condenser (for clean surfaces it is formed by the diffuse layer and the Helmholtz plane) formed by the diffuse layer and the film layer; R_1 is the solution resistance and R_2 is the resistance of the film layer.

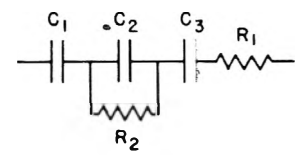

Fig. 2.—Equivalent capacity circuit for the electrical double layer in the presence of an adsorbed film layer.

As was stated in the discussion on peak capacities, the water molecules surrounding an alcohol molecule partially neutralize the polar characteristics associated with the alcohol. This partial neutralization of charges on the alcohol molecule, particularly the slight negative charge residing on the oxygen of the alcohol, is more fully realized in the case of *n*-amyl alcohol than with the higher molecular weight alcohols. This reduction in

(5) L. Pauling, "Nature of the Chemical Bond," Cornell University Press, Ithaca, N. Y., 1945, p. 327.

(6) By distributed charges is meant the fact that the alkyl portion acquires a slight positive charge which is balanced by the slight negative charge usually associated with the OH part of the alcohol.

(7) D. C. Grahame, Office of Naval Research, Technical Report No. 1 (1950).

(8) D. C. Grahame, *J. Am. Chem. Soc.*, 68, 301 (1946).

polarizability of the *n*-amyl alcohol is reflected in weaker adsorption forces than would otherwise exist. This would lead one to expect that the effective distance of the film layer between the inner and the diffuse layer for *n*-amyl alcohol to be greater than that in the case of *n*-octyl alcohol where the association effect with the solvent molecules is less. It is assumed that the capacities of C_1 and C_2 of Fig. 2 remain constant for all of the alcohol solutions of 1 *N* potassium chloride. If this is the case, then according to the equation for the capacity consisting of two plates, the capacity of the film layer C_2 may be given as

$$C_2 = DA/4\pi d \qquad (1)$$

where *A* is the area of the mercury surface, *D* is the dielectric constant of the medium, and *d* is the effective distance between the inner and outer layers.

If the coulombic forces of the *n*-amyl alcohol layer have been neutralized to a greater extent than those for a *n*-octyl layer, then the inner and the diffuse layers are to be less closely attracted by the amyl layer than by the octyl layer. Calculations of the relative capacities on this basis for the two cases indicate that a smaller capacity is expected for the amyl alcohol layer than for the octyl layer. Actually, this was not observed (Table III). There are several possible reasons why the capacity of the amyl alcohol layer is of greater magnitude than that of the octyl alcohol layer: (1) The octyl alcohol molecule is more bulky than that of the amyl alcohol which means that there is an increased distance between the inner and outer layers for the *n*-octyl alcohol over that for the *n*-amyl alcohol. This would correspond to a smaller capacity for the octyl alcohol solution. (2) More water molecules are associated with the amyl alcohol than with the octyl alcohol which would increase the capacity of the amyl alcohol layer with respect to that of the octyl alcohol layer because of an over-all increased dielectric strength for the amyl alcohol over that for the octyl alcohol. (3) The formation of double film layers is more prevalent with *n*-octyl alcohol solutions than with *n*-amyl alcohol solutions. Whenever capacities are added in series, the effective capacity decreases.

In Table III, the values of minima capacities increase going from the chloride to the bromide to the iodide solutions. This effect is explained by the increase in the capacity value of C_1 due to the presence of different halides in solution.

TABLE III

MINIMUM CAPACITIES OF SATURATED SOLUTIONS IN MICROFARADS PER SQUARE CENTIMETER

Alcohol	1 *N* KCl	1 *N* KBr	1 *N* KI
n-C_5	5.08		
n-C_6	4.72	4.78	6.17
n-C_7	3.90		
n-C_8	4.09	4.26	5.83

Supersaturated Solutions.—When any supersaturated halide solution of *n*-octyl alcohol is analyzed for minimum capacities, the patterns obtained show both a maximum and a minimum (Fig. 3). For a 1 *N* potassium chloride solution of this alcohol the minimum has a capacity value of 2.7 μf./cm.^{2} while the maximum is 7.4 μf./cm.^{2} The same general types of maximum and minimum were observed for supersaturated *n*-heptyl alcohol solutions but not for those of *n*-amyl and *n*-hexyl. These phenomena of minimum and maximum capacities can be associated with the formation of double film layers, although no exact reason can be found to explain the peculiarities.

Polarographic Maxima Relationship

The occurrence of maxima in polarographic studies is frequent. In case of oxygen maxima, an Ohm's law relationship is found for the rising portion of the peak, while the descending part is abrupt. Such a phenomenon has been observed oscillographically (Fig. 4) with *t*-amyl alcohol as well as with other alcohols in both undegassed and degassed solutions. In Fig. 4, the Ohm's law rela-

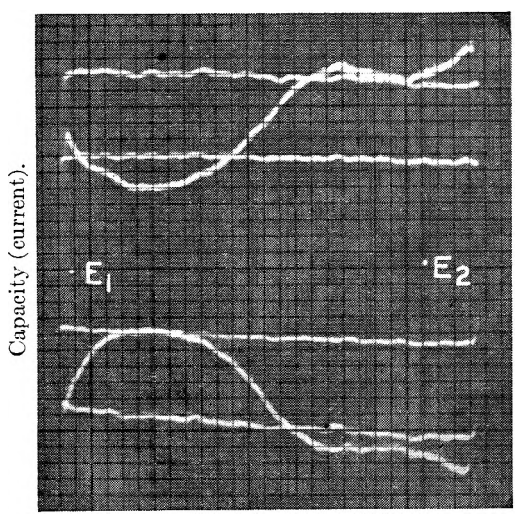

Fig. 3.—Minimum and maximum capacities for 1 *N* KCl solution supersaturated with *n*-$C_8H_{17}OH$: $E_1 = -0.284$ v., $E_2 = -0.847$ v.; exposure time, 14.3 seconds; mass per second, 0.284 mg.; sensitivity resistance for curve, 700 ohms; for calibration, 200, 400 ohms.

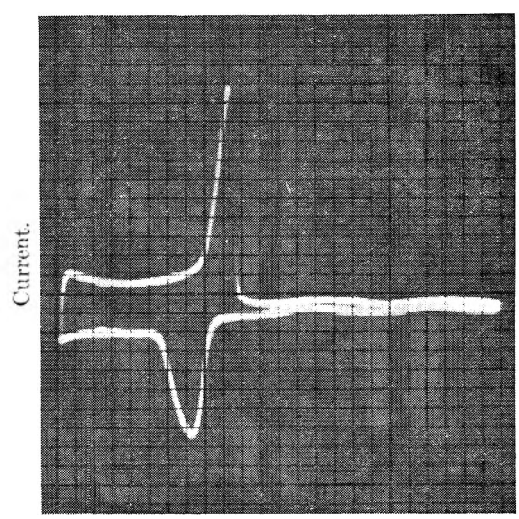

Fig. 4.—Ohm's law relationship observed with 0.05 *M* *t*-amyl alcohol in 1 *N* KCl solution.

tionship is realized only in the cathodic branch. This is also generally true of the observations made with the other alcohols, although there were instances when the anodic portion showed a reversible phenomenon.

In view of the very high capacities encountered with adsorption and desorption processes (Table II), it would be theoretically possible to observe in ordinary polarographic procedures capacity currents of several microamperes. It is the interpretation of the authors that maxima obtained in polarographic studies are due to the abnormally high capacity currents associated with adsorption or desorption processes and not to a Faradaic current.

The authors wish to thank the Office of Naval Research for their support of the research project upon which the work described was done.

APPLICATION OF THE CATHODE-RAY OSCILLOSCOPE TO POLAROGRAPHIC PHENOMENA. V. INFLUENCE OF FREQUENCY, CONCENTRATION AND STRUCTURE OF ALCOHOLS ON FILM FORMATION AT AQUEOUS SALINE SOLUTION–MERCURY INTERFACES

BY J. WEST LOVELAND[1a] AND PHILIP J. ELVING[1b]

The Pennsylvania State College, State College, Pennsylvania

Received August 22, 1952

The resistance of an alcohol film layer at the potential of the most negative capacity peak was found to vary inversely with the square of the voltage sweep frequency. The variation of peak capacities with voltage sweep rates provides a procedure for determining relative rates of adsorption and desorption of film layers at a mercury–aqueous solution interface. The potential differences between the capacity peaks for the eight isomeric amyl alcohols have been correlated with the structures of the alcohols. The surface charge density difference corresponding to the potential separation of the capacity peaks with a change in concentration for the alcohols studied was found to have the simple relationship of the surface charge density difference as a function of the log of the concentration over a tenfold range of concentration. The analytical implications are indicated.

The application of the cathode-ray oscilloscope to the determination of differential capacity and surface charge density (S.C.D.) *vs.* voltage relationships has been reported.[2] These oscilloscopic techniques have been applied to the study of film formation by alcohols from the viewpoints of the potentials at which absorption and desorption occur, of the S.C.D. values involved,[3] and of the magnitudes of the capacities observed.[4] The present study deals with the determination of the influence of such factors as voltage sweep frequency, and concentration and structure of alcohols on the capacities, potentials and S.C.D. relationships involved in film formation.

Measurement Technique

The calculation of potentials, capacities and S.C.D. from photographs of the oscillographic traces has been outlined.[1,2] Alternative procedures for the direct determination of potentials[3] and capacities[4] have been described. The results here discussed have been obtained by both photographic and direct methods.

The cell and dropping mercury electrode, D.M.E., used have also been described.[2a] The sweep frequency used was 7.5 c.p.s. unless otherwise specified.

Influence of Frequency

To determine the influence of rate of potential sweep on the peak capacities and potentials, the most negative peaks of the saturated hexyl alcohol in 1 *N* potassium chloride solution[3] were analyzed for frequency effects. As frequency increases, the potential difference between anodic and cathodic peaks increases while the peak capacity decreases; the cathodic peak is shifted to more negative potentials and the anodic peak to more positive potentials. The resistance of the film layer was calculated by dividing the potential separation of the anodic and cathodic peaks by the peak current after correcting for the *iR* drop of the solution. It was assumed that time-lag was negligible and did not account for any portion of the potential separation. These calculations are given in Table I. The drop area was 0.0173 cm.^{2}; the solution resistance 40 ohms.

TABLE I

SATURATED SOLUTION OF HEXYL ALCOHOL IN 1 *N* POTASSIUM CHLORIDE

dE/dt, volts/sec.	$V_{cathode} - V_{anode}$, millivolts	Current, peak to peak, μa.	$V_{cathode} - V_{anode}$, corrected	Resistance, film layer, ohms-cm.^{2}	Peak capacity, μf./cm.^{2}
8.93	26	46.3	22	8.3	147
17.7	35	83.5	28	5.9	134
36.0	45	148	32	3.8	119

The resistance of the film layer varies as the inverse ratio of the square root of the sweep frequency. A similar relationship was observed by Jones and Christian[5] for non-polarizable or partially polarizable electrodes and by Rozental and Ershler[6] for mercury electrodes in solutions containing mercurous ions.

(1) (a) Sun Oil Co., Norwood, Pennsylvania. (b) University of Michigan, Ann Arbor, Michigan.

(2) (a) J. W. Loveland and P. J. Elving, THIS JOURNAL, **56**, 250 (1952); (b) J. W. Loveland and P. J. Elving, *ibid.*, **56**, 255 (1952).

(3) J. W. Loveland and P. J. Elving, *ibid.*, **56**, 935 (1952).

(4) J. W. Loveland and P. J. Elving, *ibid.*, **56**, 941 (1952).

(5) G. Jones and S. M. Christian, *J. Am. Chem. Soc.*, **57**, 272 (1935).

(6) K. Rozental and B. V. Ershler, *Zhur. Fiz. Khim.*, **22**, 1344 (1948); *C. A.*, **43**, 253 (1949).

Grahame[7] found that for a potassium nitrate solution saturated with *s*-octyl alcohol, the resistance of the alcohol film at the potential of the peaks varied approximately inversely as the first power of frequency, but in the neighborhood of the electrocapillary maximum, the resistance varied almost inversely as the square of the frequency. The resistance of the *n*-hexyl alcohol film layer near the peak potential, as calculated by the present authors, is of the same order of magnitude as that found by Grahame for the *s*-octyl alcohol film layer at a frequency of 240 c.p.s. It is possible that the D.M.E., in the presence of surface-active contaminants, reacts as a partially polarized electrode, in which case the resistance of the electrode system is expected to be inversely proportional to the square root of the frequency.

The capacity values (Table I) decrease as the rate of voltage variation is increased. This same general behavior was observed by Grahame[7] for saturated *s*-octyl alcohol solutions at potentials in the vicinity of the capacity peaks. Such a variation in capacity may be used as an indication of the rate of formation or disruption of the film layer. The differential capacity being measured is a function of the S.C.D. with potential. The S.C.D. in turn is directly related to the differential of surface tension at the mercury surface with potential. Under the experimental conditions used, potential and time are interchangeable, since the applied voltage is a linear function of time, *i.e.*, dE/dt is a constant. Thus the capacity is a property of the rate of change of surface tension which is dependent to a large degree on the rate of formation of the adsorbing layer. The oscillographic technique of measuring peak capacities as a function of sweep frequency offers a rapid and convenient method for comparing the relative rates of adsorption and desorption of film layers at a mercury–aqueous solution interface.

Influence of Structure: The Amyl Alcohols

The eight isomeric amyl alcohols have been investigated at a concentration of 0.1 *M* in 1 *N* potassium chloride for peak and minimum capacities, and for peak potentials by the direct methods of measurement. Values were obtained for solutions with no degassing and with 5 minutes of degassing. The relative values of the capacities and potentials obtained for undegassed solutions were not in any way affected by degassing. Peak potentials (Table II) and capacity values (Table III) are given for the degassed solutions. The same convention of labelling the relative positions of the potentials of the capacity peaks used previously,[3,4] *i.e.*, V_2 and V_3, is used. The corresponding peak capacities are designated as C_2 and C_3, and the minimum capacities as C_m.

To explain the variation of the potential differences, $(V_3 - V_2)$, of Table II in the order given on the basis of solubility leads to confusion. But, if one considers the structural aspect and its influence on the potentials of adsorption and desorption, there is a reasonable correlation. Neopentyl alcohol shows the least potential difference, *t*-amyl the next least, etc., with *n*-amyl having the greatest potential difference between the capacity peaks. This sequence is consistent with the hindrance effects associated with methyl groups alpha and beta to the carbon attached to the hydroxyl group. The alcohols also fit nicely into the pattern according to whether they are primary, secondary or tertiary, with the notable exception of neopentyl alcohol.

TABLE II

PEAK POTENTIALS FOR 0.1 *M* AMYL ALCOHOL SOLUTIONS IN 1 *N* POTASSIUM CHLORIDE *vs.* MERCURY POOL

Alcohol	V_2, v.	V_3, v.	$V_3 - V_2$, v.
Neopentyl	0.220	1.054	0.834
t-Amyl	.237	1.099	.862
s-Isoamyl	.209	1.112	.903
s-act-Amyl	.194	1.146	.952
Diethylmethyl	.184	1.150	.966
Isoamyl	.182	1.150	.968
p-act-Amyl	.169	1.156	.987
n-Amyl	.141	1.192	1.051

TABLE III

PEAK (C_2, C_3) AND MINIMUM (C_m) CAPACITIES OF 0.1 *M* AMYL ALCOHOL SOLUTIONS IN 1 *N* POTASSIUM CHLORIDE IN MICROFARADS PER SQUARE CENTIMETER

Alcohol	C_2	C_3	C_m
Neopentyl	430	87	4.56
t-Amyl	375	79	5.35
s-Isoamyl	315	70	5.34
s-act-Amyl	325	77	5.00
Diethylmethyl	340	85	5.18
Isoamyl	310	72	5.01
p-act-Amyl	310	75	4.93
n-Amyl	270	83	5.07

When the capacities of Table III are considered, the values of C_2 and C_3 for neopentyl are greater than those for any of the others; that of C_m is the lowest for any of the alcohols. At the other extreme, the low value of C_2 for *n*-amyl seems to fit the general relationship found for potential differences. The *t*-amyl alcohol gives the second highest of the C_2 values but the fourth highest of the C_3 values, while the C_m value is the highest of all. Thus, the same relationship of the structure of the alcohols with the potential values does not hold for all the capacity values. In general, there seems to be no direct connection of capacity values with structure, except possibly when the values of C_2 are considered. In this case, if neopentyl alcohol is excluded from consideration, there is a general decrease of the C_2 values going from the tertiary to the secondary to the primary alcohols.

Concentration Effects

The effect of varying the alcohol concentration on the potentials of the adsorption and desorption processes was investigated for *n*-amyl, *t*-amyl, diethylmethyl, *n*-hexyl, *n*-heptyl and *n*-octyl alcohols in 1 *N* potassium chloride without degassing. The concentrations, the potentials (V_2 and V_3) of the two adsorption–desorption capacity peaks and their differences, and the surface charge density difference (S.C.D.D., q) values corresponding to the potential differences are given in Table IV.

(7) D. C. Grahame, *J. Am. Chem. Soc.*, **68**, 301 (1946).

Table IV

Effect of Concentration on Peak Potentials and Surface Charge Density Difference Values

Alcohol	Concn., M	V_2, v.	V_3, v.	$V_3 - V_2$, v.	q, μcoulombs/cm.^{2}
n-Amyl	0.100	0.134	1.206	1.072	31.5
	.050	.213	1.118	0.905	26.7
	.040	.243	1.097	.854	25.0
	.025	.280	1.014	.734	22.0
	.020	.312	0.994	.682	20.5
	.010	.382	.885	.503	15.8
Diethylmethyl	0.250	0.121	1.282	1.161	33.8
	.100	.203	1.182	0.979	28.0
	.050	.262	1.094	.832	24.1
	.025	.332	0.998	.656	19.3
	.0125	.413	.865	.425	13.8
t-Amyl	0.250	0.192	1.232	1.040	30.0
	.100	.252	1.113	0.861	25.0
	.050	.305	1.042	.737	21.1
	.025	.383	0.915	.532	16.0
	.020	.414	.870	.456	14.1
n-Hexyl	0.0200	0.162	1.180	1.018	29.7
	.0150	.177	1.130	0.953	27.8
	.0100	.230	1.088	.858	25.2
	.0075	.242	1.039	.797	23.8
	.0050	.292	0.997	.705	21.1
	.00375	.307	.948	.641	19.7
n-Heptyl	0.0500	0.110	1.152	1.042	31.6
	.00250	.133	1.060	0.927	28.9
	.00125	.207	1.021	.814	24.9
	.00100	.223	0.998	.775	24.2
	.000625	.235	.942	.708	22.6
n-Octyl	0.00125	0.153	1.147	0.994	29.4
	.00100	.146	1.150	1.004	29.8
	.00050	.160	1.115	0.955	28.5
	.00025	.208	1.055	.847	25.6

Application of Langmuir's Isotherm.—In a similar experiment, Heyrovsky, *et al.*,[8] determined polarographically the potentials at which pyridine over a twofold concentration range was desorbed from the D.M.E. in sodium hydroxide solutions. He assumed that the potential, v, at which desorption takes place, indicates the maximum number of pyridine molecules adsorbed at the mercury surface. The concentration at the mercury–solution interface, n_c, depends on the concentration in the solution c, according to Langmuir's isotherm

$$n_c = \frac{nwc}{1 + wc} \qquad (1)$$

where n is a proportionality constant and w is the adsorption coefficient. Moreover, Heyrovsky states that n_c is proportional to the density of charge, and therefore to the desorption potential, v, so that

$$v = \frac{kwc}{1 + wc} \qquad (2)$$

where k is another constant. Values were referred to the potential of the electrocapillary zero; k and w were evaluated from the values of v at two different pyridine concentrations. With these two values, the potentials to be expected at the other concentrations were calculated. The potentials calculated agreed with observed potentials to 0.1%.

The present authors have applied the modified Langmuir equation to the data obtained for the several alcohol solutions studied. Values of k and w were calculated for the five or six concentrations used for each alcohol, using potentials V_2 and V_3 separately as well as their difference. In no case were the values of k and w constant; the deviations of k were of the order of 8% and those of w were in some cases as great as 100%. The use of the q values in place of v did not decrease the amount of deviation of k and w to any great extent. However, at the higher concentrations, for small changes in concentration, roughly twofold in magnitude, the values of k and w agreed reasonably well for either the potential or the surface charge calculations. This is the same concentration range over which Heyrovsky, *et al.*,[8] obtained good results.

Since neither q values nor the potential values, V_2, V_3 and $(V_3 - V_2)$, over the tenfold concentration ranges involved, seem to fit the modified Langmuir equation, it was felt that possibly the Freundlich isotherm equation, if it were adapted in a fashion similar to that of the Langmuir, would provide a reasonable fit of the data. However, the results were just as incongruous as those obtained with equation 2.

Surface Charge Density Relationship.—By plotting the values of $(V_3 - V_2)$ *vs.* the logarithm of the concentration, straight line relations were obtained for most of the alcohols investigated; similarly, plots of q *vs.* log c (Fig. 1) gave straight lines in most cases.

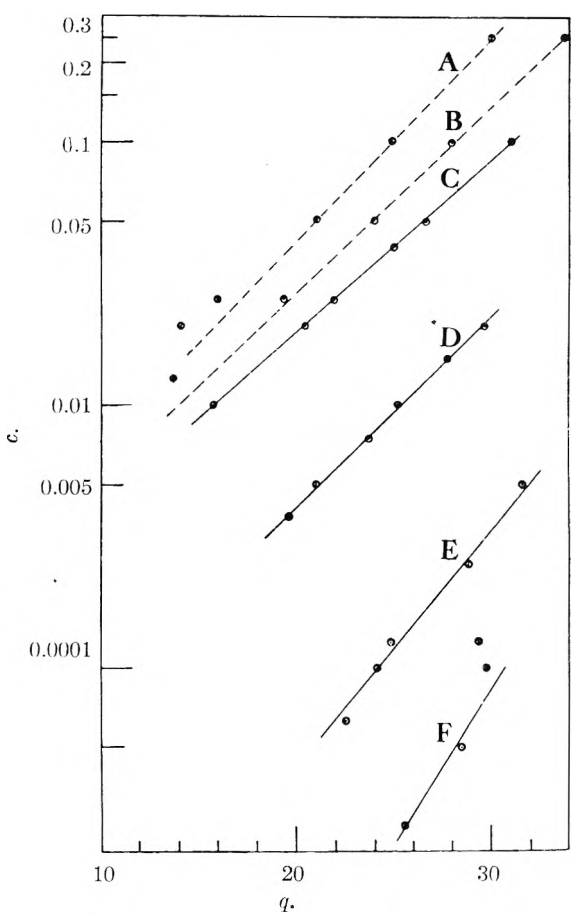

Fig. 1.—Curves of surface charge density difference (q) *vs.* concentration (c) for: A, *t*-amyl; B, diethylmethyl; C, *n*-amyl; D, *n*-heptyl; E, *n*-octyl alcohols.

(8) J. Heyrovsky, F. Sorm and J. Forejt, *Collection Czechoslov. Chem. Comms.*, 12, 11 (1947).

The authors would like to indicate the reasons why the plots of $(V_3 - V_2)$ *vs.* log c and of q *vs.* log c give straight lines. Inspection of the S.C.D. oscillogram of 1 N potassium chloride (similar to that for potassium bromide in Fig. 6, reference 3) shows a fairly linear relationship at potentials both more positive and more negative than that of the electrocapillary maximum (0.56 volt *vs.* N.C.E. for 1 N KCl) which comes at the bend of the curve. Since the variation of the values of V_3 and V_2 takes place over the linear portions of the curve, the values of $(V_3 - V_2)$ will vary in the same manner as those of q. However, if the values of V_3 and V_2 were such that one of them varied over the potential range of from 0.4 to 0.8 volt *vs.* N.C.E., then the value of q would not linearly follow those of $(V_3 - V_2)$. Accordingly, the use of potential values in equation 2 is misleading and should be replaced by the corresponding surface charge density values. The excellent agreement which Heyrovsky obtained with potential measurements is due to the fact that the S.C.D. values over the potential range used vary with potential in a fairly linear fashion. In fact, when Heyrovsky's values of v and c are plotted in the form of v *vs.* log c, excellent straight line relationships are found over the twofold concentration range involved.

n-Amyl, *n*-hexyl and *n*-heptyl alcohols give straight line relationships within experimental error (Fig. 1). For *n*-octyl alcohol the concentration range used was limited by the disappearance of the peaks being measured so that only a few points are available. The increase of the one value of $(V_3 - V_2)$ with a decrease in concentration is inexplicable except on the basis of the peculiarities of double film layers. For the diethylmethyl and *t*-amyl alcohol curves, straight line relationships are realized over the first three or four points corresponding to the higher concentrations while, at the lower concentrations, the points diverge from a straight line. This divergence is unexpected in view of the results obtained for the normal alcohols. The only explanation which can be offered for the non-linearity of these curves is that at high concentrations the molecules of diethyl carbinol and the *t*-amyl alcohol are close enough together so that structural hindrance to the alignment of the alcohol molecules at the mercury surface takes place. At lower concentrations, the molecules are further apart and the influence of structure on the lining up of molecules is less prevalent. The result of this is to require a greater S.C.D. than expected at high concentrations and a normal S.C.D. at low concentrations for adsorption to take place.

The equation which best fits the data of concentration, c, as a function of the surface charge density difference, q, is

$$q = m \log c + b \qquad (3)$$

where m and b are constants for a particular adsorbable species. Equation 3 is that for a straight line so that the value of m may be calculated from the slope of the line and the value of b from the intercept of the q axis when $c = 1$ (in terms of molarity). Using the curves of *n*-amyl, *n*-hexyl and *n*-heptyl alcohols, the values of m are calculated to be 15.3, 13.6 and 11.1, and those of b to be 46.3, 52.4 and 57.5, respectively. The significance of the b term may be associated with the solubility of the various alcohols; *i.e.*, the less the solubility the greater the value of b becomes. The slope, m, may be roughly compared to the dielectric properties and size of the alcohol molecules. Possibly, a better understanding of the true meaning of m would be forthcoming by investigating other homologous series of compounds, such as ketones and aldehydes, in the same manner as that used on the alcohols.

Analytical and Other Applications

The application of oscillographic techniques to the quantitative determination of alcohols or almost any slightly soluble organic compound in aqueous solution which give rise to adsorption–desorption capacity peaks, is in theory feasible. The procedure would be to make a calibration plot of peak potential separation *vs.* concentration for a given base solution for each organic compound used. To analyze for the concentration of the organic compound in water, the solution must be made up to correspond to the base solution used in calibration, and the potentials of the capacity peaks measured. The potential difference gives the concentration directly from the calibration curve.

The distinct advantage of this method is that the potential separation of the capacity peaks changes most rapidly at the lower concentrations, where other techniques become less accurate; thus, for *n*-amyl alcohol solutions, assuming an accuracy in potential measurements of ± 4 millivolts, the error in estimating concentrations at about 0.1 M would be about 6%, while at 0.01 M, the error would be about 2%.

A particularly appropriate application would be in measuring the change of concentration with time as in monitoring a flowing stream or in determining reaction rates.

The authors have presented this and previous papers on the application of the oscilloscope to the study of adsorption phenomena with the intent of indicating the type of information which may be obtained from the technique. It is hoped that other investigators will be encouraged to apply this method to problems involving surface tension, surface charge and capacity.

The authors wish to thank the Office of Naval Research for their support of the research project upon which the work described was done.

A THEORY OF PERCOLATION FOR THE CASE OF TWO SOLUTES

By Hiroshi Fujita

Department of Fisheries, Faculty of Agriculture, Kyoto University, Maizuru, Japan

Received August 28, 1951

The general case of the percolation problem has already been discussed in detail by many investigators for the case of a single solute, but for the case of more than one solute it has not yet been solved, though some progress has been made in the case in which the equilibrium between fluid and solid can be assumed. In this paper the writer has undertaken to solve rigorously a general case of two solutes, assuming irreversible adsorption. The results obtained show clearly the chromatographic separation of two adsorbates, as should be expected. In order to handle this problem more precisely the process of desorption should also be taken into consideration, as in the writer's previous paper[1] for the case of a single solute. However, the discussion of such a problem will be considered in a forthcoming paper.

Introduction

The theory of percolation phenomena is of much practical importance in connection with various problems in chemical engineering and chemical analysis as well. Chromatography, which has recently been widely used for chemical analysis of various kinds of organic or inorganic substances, is a direct application of these phenomena, though the exact theory of chromatography as yet has not been completed and a conventional formula is commonly used.[2] The present status of the theory of percolation was carefully summarized by Thiele[3] and Klotz[4] and lately the theory has further been developed by Amundson,[5] Brinkley,[6] Fukuda and Kawazoe,[7] Thomas,[8] Hiester and Vermeulen,[9] the present writer,[1] and others. Through the numerous investigations hitherto made almost all have mainly referred to the case in which the solution flowing through the adsorption bed contains only a single solute, while in the case of many solutes little progress has been made. In the latter case the only mathematical analysis that has been undertaken is for the rates of adsorption of all solutes on the bed assumed to be infinite. This assumption was considered to be applicable to the case of chromatography and many important contributions were made by Wilson,[10] Devault,[11] Walter,[12] Glueckauf,[13] and others.

The general case for more than one solute has not yet been solved. This is probably due not only to the mathematical complications which would appear, but also to physical obscurities regarding the behaviors of each solute in a system which is composed of the solvent, the solutes and the bed. Accordingly, any mathematical consideration of this case may not be undertaken without making assumptions as to the physical behaviors of the solutes.

In this paper, the case of two solutes which have no mutual interaction is taken and solved exactly assuming irreversible adsorption for both the solutes.

(1) H. Fujita, *Kagaki-Kikai* (*Chemical Engineering, Tokyo*), in press.
(2) K. Satake, *Kagaku no Ryoiki*, (*J. Japan Chem.*), [7] **3**, 2 (1949).
(3) E. W. Thiele, *Ind. Eng. Chem.*, **38**, 646 (1946).
(4) I. M. Klotz, *Chem. Revs.*, **39**, 241 (1946).
(5) N. R. Amundson, This Journal, **52**, 1153 (1948).
(6) S. R. Brinkley, *J. Appl. Phys.* **18**, 582 (1948).
(7) Y. Fukuda and K. Kawazoe, *Kagakukogaku to Kagakukikai* (*Chemical Engineering and Chemical Machinery, Tokyo*), **7**, 114 (1949).
(8) H. C. Thomas, *Ann. N. Y. Acad. Sci.*, **49**, 161 (1948).
(9) N. K. Hiester and T. Vermeulen, "Performance of Ion Exchange and Adsorption Columns, Part I. Saturation Theory" (manuscript submitted to *Chemical Engineering Progress*).
(10) J. N. Wilson, *J. Am. Chem. Soc.*, **62**, 1583 (1940).
(11) D. Devault, *ibid.*, **65**, 532 (1943).
(12) J. E. Walter, *J. Chem. Phys.*, **13**, 229 (1945).
(13) E. Glueckauf, *Nature*, **156**, 205 (1945).

Fundamental Equations

Consider an adsorption bed of unit cross section, through which a solute containing two different solutes flows one-dimensionally with a constant speed, with the coördinate axis, z, downstream, the entrance of the bed being $z = 0$.

Assuming irreversible adsorption for each solute, as mentioned above, and denoting by A the mean surface area per unit volume of the adsorbent: γ_i, the mean area of the adsorbent covered with the unit mass of the i-th solute, S_i, where $i = 1,2$; η_i, the amount of S_i on the bed per unit volume of the bed; C_i, the concentration of S_i in the fluid stream; then the local rate of adsorption of S_i, namely, $\partial n_i/\partial t$, will be

$$\partial n_i/\alpha\,\partial t = k_i C_i(A - \gamma_1 n_1 - \gamma_2 n_2)\ (i = 1, 2) \qquad (1)$$

where t denotes time and k_i a rate constant ($i = 1,2$).

Next, making a material balance over an elemental thickness of the bed, the following equation is obtained

$$\frac{\partial C_i}{\partial t} + V\frac{\partial C_i}{\partial z} = -\frac{1}{\alpha}\frac{\partial n_i}{\partial t}\ (i = 1, 2) \qquad (2)$$

where V is the speed of the fluid stream and α the fractional void volume of the bed.

In order to determine uniquely the solution of the above simultaneous equations (1) and (2), appropriate auxiliary conditions must be appended. In what follows the rather particular conditions which have usually been adopted by most of the authors in their studies on the percolation problem of a single solute are taken. They are stated as

$$\left.\begin{aligned} &C_i = 0;\ n_i = 0\ (t = 0, z > 0),\\ &C_i = C_i^0\ \ (t > 0, z = 0)\end{aligned}\right\}\quad (i = 1, 2) \qquad (3)$$

To facilitate the analysis it is convenient to introduce the following dimensionless variables

$$\left.\begin{aligned} &\frac{C_i}{C_i^0} = \varphi_i,\ \frac{n_i\gamma_i}{A} = \psi_i;\ \frac{z}{Vt_0} = x,\ \frac{t}{t_0} = \tau;\\ &\beta_i = \frac{A}{\alpha C_i^0\gamma_i},\ \lambda_i = k_i t_0 A\ (i = 1, 2)\end{aligned}\right. \qquad (4)$$

t_0 being an appropriate unit of time. In terms of these quantities Eq. (1) and (2) are written in the dimensionless forms

$$\frac{\partial\varphi_1}{\partial\tau} + \frac{\partial\varphi_1}{\partial x} = -\beta_1\frac{\partial\psi_1}{\partial\tau} \qquad (5)$$

$$\beta_1\frac{\partial\psi_1}{\partial\tau} = \lambda_1(1 - \psi_1 - \psi_2)\varphi_1 \qquad (6)$$

$$\frac{\partial \varphi_2}{\partial \tau} + \frac{\partial \varphi_2}{\partial x} = -\beta_2 \frac{\partial \psi_2}{\partial \tau} \tag{7}$$

$$\beta_2 \frac{\partial \psi_2}{\partial \tau} = \lambda_2(1 - \psi_1 - \psi_2)\varphi_2 \tag{8}$$

Also, the conditions (3) are expressed as

$$\begin{aligned} &\varphi_1 = \varphi_2 = 0; \quad \psi_1 = \psi_2 = 0 \ (\tau = 0, x > 0) \\ &\varphi_1 = \varphi_2 = 1 \ (\tau > 0, x = 0) \end{aligned} \tag{9}$$

After Amundson, the change of variables from (x, τ) to (ξ, η) is made according to the relations

$$\xi = \lambda x, \quad \eta = (\lambda_1/\beta_1)(x - \tau) \tag{10}$$

with ξ evidently being not negative.

Equations (5) $\sim$ (8) are then put in the forms

$$\partial \varphi_1/\partial \xi = \partial \psi_1/\partial \eta \tag{11}$$

$$\partial \Psi_1/\partial \eta = -\varphi_1(1 - \psi_1 - \psi_2) \tag{12}$$

$$\partial \varphi_2/\partial \xi = \theta(\partial \psi_2/\partial \eta) \tag{13}$$

$$\theta(\partial \psi_2/\partial \eta) = -\sigma \varphi_2(1 - \psi_1 - \psi_2) \tag{14}$$

where

$$\theta \equiv \beta_2/\beta_1 \qquad \sigma \equiv \lambda_2/\lambda_1 \tag{15}$$

These two quantities are essential parameters in this problem.

From Eq. (11) and (13) it can be seen that there exist such functions, Φ and Ψ, that

$$\begin{aligned} &\varphi_1 = \partial \Phi/\partial \eta, \ \Psi_1 = \partial \Phi/\partial \xi \\ &\varphi_2 = \theta(\partial \Psi/\partial \eta), \ \Psi_2 = \partial \Psi/\partial \xi \end{aligned} \tag{16}$$

Using these functions Eq. (12) $\sim$ (14) are reduced to the two equations

$$\frac{\partial^2 \Phi}{\partial \xi \partial \eta} = -\frac{\partial \Phi}{\partial \eta}\left(1 - \frac{\partial \Phi}{\partial \xi} - \frac{\partial \Psi}{\partial \xi}\right) \tag{17}$$

$$\frac{\partial^2 \Psi}{\partial \xi \partial \eta} = -\sigma \frac{\partial \Psi}{\partial \xi}\left(1 - \frac{\partial \Phi}{\partial \xi} - \frac{\partial \Psi}{\partial \xi}\right) \tag{18}$$

Further, putting

$$\Phi^* = \Phi - \xi, \ \Psi^* = \Psi \tag{19}$$

these are put in the forms

$$\frac{\partial^2 \Phi^*}{\partial \xi \partial \eta} = \frac{\partial \Phi^*}{\partial \eta}\left(\frac{\partial \Phi^*}{\partial \xi} + \frac{\partial \Psi^*}{\partial \xi}\right) \tag{20}$$

$$\frac{\partial^2 \Psi^*}{\partial \xi \partial \eta} = \sigma \frac{\partial \Psi^*}{\partial \eta}\left(\frac{\partial \Phi^*}{\partial \xi} + \frac{\partial \Psi^*}{\partial \xi}\right) \tag{21}$$

The object of the present paper is to solve rigorously this set of equations, both of which are nonlinear and hyperbolic.

Method of Solution

To begin with, both of the above equations are integrated once with respect to ξ, leading to

$$\partial \Phi^*/\partial \eta = f(\eta) \exp(\Phi^* + \Psi^*) \tag{22}$$

$$\partial \Psi^*/\partial \eta = g(\eta) \exp\{\sigma(\Phi^* + \Psi^*)\} \tag{23}$$

where $f(\eta)$ and $g(\eta)$ represent arbitrary functions of η. Combining Eq. (22) with Eq. (23), and putting

$$\Phi^* + \Psi^* \equiv Z \tag{24}$$

there results

$$\partial Z/\partial \eta = f(\eta)e^Z + g(\eta)e^{\sigma Z} \tag{25}$$

which can also be put in the form

$$\partial W/\partial \eta = -f(\eta) - g(\eta)W^{1-\sigma} \tag{26}$$

by putting

$$Z = -\ln W \tag{27}$$

Now, expressing the conditions (9) in terms of ξ, η and Φ^*, Ψ^*, the first equation of (9) becomes

$$\left.\begin{aligned} &\frac{\partial \Phi^*}{\partial \eta} = 0, \quad \frac{\partial \Phi^*}{\partial \xi} = -1; \\ &\frac{\partial \Psi^*}{\partial \eta} = 0, \quad \frac{\partial \Psi^*}{\partial \xi} = 0, \end{aligned}\right\} \quad (\xi > 0, \eta > 0) \tag{28}$$

and, the second

$$\partial \Phi^*/\partial \eta = 1, \ \partial \Psi^*/\partial \eta = 1/\theta \ (\xi = 0, \eta < 0) \tag{29}$$

Equations (28) give immediately

$$\Phi^*(\xi, \eta) = -\xi, \ \Psi(\xi, \eta) = 0 \ (\xi > 0, \eta > 0) \tag{30}$$

which complete the required solution in the domain: $\xi > 0, \eta > 0$. Consequently, the following considerations may be confined to the domain: $\xi > 0, \eta < 0$.

Equations (22), (23) and (29) lead to

$$\begin{aligned} &f(\eta) \exp\{\Phi^*(0, \eta) + \Psi^*(0, \eta)\} = 1 \\ &g(\eta) \exp\{\sigma[\Phi^*(0, \eta) + \Psi^*(0, \eta)]\} = \frac{1}{\theta} \end{aligned} \tag{31}$$

which yield at once a relation between $f(\eta)$ and $g(\eta)$ as

$$[f(\eta)]^\sigma = \theta g(\eta) \tag{32}$$

Thus, Eq. (26) can be written as

$$\partial W/\partial \eta = -f(\eta) - (1/\theta)[f(\eta)]^\sigma W^{1-\sigma} \tag{33}$$

On the other hand, combination of Eq. (27) with Eq. (31) gives

$$W(0, \eta) = f(\eta) \tag{34}$$

Then, putting $\xi = 0$ in Eq. (33) and inserting Eq. (34) into the equation thus obtained, provides

$$df(\eta)/d\eta = -[(1 + \theta)/\theta] f(\eta) \tag{35}$$

whence

$$f(\eta) = f(0)e^{-\frac{1+\theta}{\theta}\eta} \tag{36}$$

The integration constant $f(0)$ is easily determined by considering various relations given above, resulting

$$f(0) = 1$$

Thus

$$f(\eta) = e^{-\frac{1+\theta}{\theta}\eta} \tag{37}$$

Substituting this into Eq. (33) gives for W a partial differential equation of the first order

$$\frac{\partial W}{\partial \eta} = -e^{-\frac{1+\theta}{\theta}\eta} - \frac{1}{\theta}e^{-\frac{\sigma(1+\theta)}{\theta}\eta} W^{1-\sigma} \tag{38}$$

The general solution of this equation is easily obtained as

$$\eta = \int^{W(\xi,\eta)e^{\frac{1+\theta}{\theta}\eta}} \frac{d\zeta}{\left(\frac{1+\theta}{\theta}\right)\zeta - 1 - \frac{1}{\theta}\zeta^{1-\sigma}} + \Xi(\xi) \tag{39}$$

where $\Xi(\xi)$ is an arbitrary function of ξ. To determine the form of $\Xi(\xi)$, $\eta = 0$ is put in the above equation, and there results

$$\Xi(\xi) = -\int^{W(\xi,0)} \frac{d\zeta}{\left(\frac{1+\theta}{\theta}\right)\zeta - 1 - \frac{1}{\theta}\zeta^{1-\sigma}} \tag{40}$$

Now, since

$$W(\xi, 0) = \exp[-Z(\xi, 0)] = \exp\{-[\Phi^*(\xi, 0) + \Psi^*(\xi, 0)]\} \tag{41}$$

and $\Phi^*(\xi, 0)$ and $\Psi^*(\xi, 0)$ are determined, respectively, from the expressions for $\Phi^*(\xi, \eta)$ and $\Psi^*(\xi, \eta)$ as given by Eq. (30), causing $\eta \to 0$, we obtain

$$W(\xi, 0) = e^{\xi} \tag{42}$$

Then, the expresison for $\Xi(\xi)$ becomes

$$\Xi(\xi) = -\int_{e^{\xi}}^{} \frac{d\zeta}{\left(\frac{1+\theta}{\theta}\right)\zeta - 1 - \frac{1}{\theta}\zeta^{1-\sigma}} \tag{43}$$

In this way the result is finally obtained

$$\eta = \int_{e^{\xi}}^{We^{\frac{1+\theta}{\theta}\eta}} \frac{d\zeta}{\left(\frac{1+\theta}{\theta}\right)\zeta - 1 - \frac{1}{\theta}\zeta^{1-\sigma}}$$

which may also be written as

$$U(We^{\frac{1+\theta}{\theta}\eta}\xi;\ \sigma, \theta) = \eta \tag{44}$$

with

$$U(\zeta, \xi;\ \sigma, \theta) = \int_{e^{\xi}}^{\xi} \frac{d\zeta}{\left(\frac{\theta+1}{\theta}\right)\zeta - 1 - \frac{1}{\theta}\zeta^{1-\sigma}} \tag{45}$$

Except for some special cases of the values of σ and θ, no closed expression for U in terms of ξ and ζ may probably be obtained.

Expressions of the Solutions

Next, final expression must be found for the required solutions, namely, for φ_1, φ_2; ψ_1 and ψ_2. These quantities have already been written in terms of Φ^* and Ψ^* as

$$\begin{aligned} &\varphi_1 = \partial\Phi^*/\partial\eta,\ \psi_1 = 1 + (\partial\Phi^*/\partial\xi); \\ &\varphi_2 = \theta(\partial\Psi^*/\partial\eta),\ \psi_2 = \partial\Psi^*/\partial\xi \end{aligned} \tag{46}$$

Also, by Eq. (22), (24), (27) and (37), φ_1 is expressed as

$$\varphi_1 = 1/(We^{\frac{\theta+1}{\theta}\eta}) \tag{47}$$

First, inserting this into Eq. (44), gives

$$U(1/\varphi_1, \xi;\ \sigma\ \theta) = \eta \tag{48}$$

the equation which determines φ_1 as a function of ξ and η when the values of σ and θ are given.

Next, integrating the first relation in Eq. (46) with η, provides

$$\Phi^* = \int^{\eta} \varphi_1\, d\eta + G(\xi) \tag{49}$$

with $G(\xi)$ denoting an arbitrary function of ξ. The form of $G(\xi)$ is immediately determined by remembering that $\Phi^*(\xi, 0) = -\xi$, and thus

$$\Phi^* = -\xi + \int_0^{\eta} \varphi_1 d\eta \tag{50}$$

On putting this into the second relation in Eq. (46), namely, $\psi_1 = 1 + \frac{\partial\Phi^*}{\partial\xi}$, gives

$$\Psi_1 = \int_0^{\eta} \frac{\partial\varphi_1}{\partial\xi}\, d\eta \tag{51}$$

On the other hand, by partial differentiation of Eq. (48) with respect to ξ, there results

$$\frac{\partial\varphi_1}{\partial\xi} = -\frac{\left(\frac{\theta+1}{\theta}\right)\varphi_1 - \varphi_1^2 - \frac{1}{\theta}\varphi_1^{1+\sigma}}{\left(\frac{\theta+1}{\theta}\right) - e^{-\xi} - \frac{1}{\theta}e^{-\sigma\xi}} \tag{52}$$

and again, from Eq. (48), the relation

$$d\eta = -\frac{d\varphi_1}{\left(\frac{\theta+1}{\theta}\right)\varphi_1 - \varphi_1^2 - \frac{1}{\theta}\varphi_1^{1+\sigma}} \tag{53}$$

is also deduced. Substituting both the relations thus obtained into the integrand of Eq. (51) and integrating, the final expression for ψ_1 is arrived at

$$\psi_1 = \frac{\varphi_1(\xi, \eta) - \varphi_1(\xi, 0)}{\left(\frac{\theta+1}{\theta}\right) - e^{-\xi} - \frac{1}{\theta}e^{-\sigma\xi}} \tag{54}$$

In the same way the corresponding expressions for φ_2 and ψ_2 are readily found, giving

$$\varphi_2 = (\varphi_1)^{\sigma} \tag{55}$$

$$\psi_2 = \frac{[\varphi_1(\xi, \eta)]^{\sigma} - [\varphi_1(\xi, 0)]^{\sigma}}{\theta\left\{\left(\frac{\theta+1}{\theta}\right) - e^{-\xi} - \frac{1}{\theta}e^{-\sigma\xi}\right\}} \tag{56}$$

It will be seen here that if only the value of φ_1 is obtained, the values of ψ_1, φ_2 and ψ_2 are immediately determined by some simple computations.

Case of a Single Solute

The analysis developed on the foregoing lines has referred to the case of two solutes. However, it will be seen without difficulty that the case of a single solute, as treated by Amundson,[5] is a limiting case of the general problem when $\sigma \to 0$. Thus, to investigate whether the general formulas obtained above yield, as their limiting forms, the results of Amundson is of theoretical interest.

First, by making $\sigma \to 0$ in Eq. (45)

$$U(\zeta, \xi;\ 0, \theta) = \ln(\zeta - 1)/(e^{\xi} - 1)$$

and, therefore, Eq. (48) can be written as

$$\ln\left(\frac{1}{\varphi_1} - 1\right)\Big/\left(e^{\xi} - 1\right) = \eta$$

whence

$$\varphi_1 = \frac{1}{1 + (e^{\xi} - 1)e^{\eta}} \tag{57}$$

Then, from Eq. (54) comes

$$\psi_1 = 1 - \frac{e^{\xi+\eta}}{1 + (e^{\xi} - 1)e^{\eta}} \tag{58}$$

Also, it can be seen at once that $\varphi_2 = 1$ and $\psi_2 = 0$, as would be expected.

The results thus obtained, Eq. (57) and (58), coincide with those which are derived from Amundson's general formulas for φ_1 and ψ_1 in the case of a single solute, except for the differences in notations.

Steady State

The steady state value for various quantities are obtained from the general results given previously by proceeding to the limit $\eta \to -\infty$ which is equivalent to making τ infinitely large.

From Eq. (45) it can be seen that when $\zeta \to 1$, U becomes infinitely large in negative sign for all positive values of ξ, and, therefore, from Eq. (48), it is found that

$$\lim_{\eta \to -\infty} \varphi_1(\xi, \eta) = 1 \tag{59}$$

Again, from Eq. (45) and (48)

$$\varphi_1(\xi, 0) = e^{-\xi} \tag{60}$$

Consequently, Eq. (55) leads to

$$\lim_{\eta \to -\infty} \varphi_2(\xi, \eta) = 1 \tag{61}$$

and, further, from Eq. (54) and (56)

$$\lim_{\eta \to -\infty} \psi_1(\xi, \eta) = \frac{1 - e^{-\xi}}{\left(\frac{\theta + 1}{\theta}\right) - e^{-\xi} - \frac{1}{\theta} e^{-\sigma\xi}}$$
$$\lim_{\eta \to -\infty} \psi_2(\xi, \eta) = \frac{1 - e^{-\sigma\xi}}{\theta \left\{\left(\frac{\theta + 1}{\theta}\right) - e^{-\xi} - \frac{1}{\theta} e^{-\sigma\xi}\right\}} \tag{62}$$

Making $\xi \to 0$ in these equations the steady values of ψ_1 and ψ_2 at the entrance of the bed are found, namely

$$\lim_{\eta \to -\infty} \psi_1(0, \eta) = [\theta/(\sigma + \theta)]$$
$$\lim_{\eta \to -\infty} \psi_2(0, \eta) = [\sigma/(\sigma + \theta)] \tag{63}$$

Also, making $\xi \to \infty$ in Eq. (62) it can be seen that if $\sigma \neq 0$

$$\lim_{\eta \to -\infty} \psi_1(\infty, \eta) = [\theta/(\theta + 1)]$$
$$\lim_{\eta \to -\infty} \psi_2(\infty, \eta) = [1/(\theta + 1)] \tag{64}$$

A Numerical Example

The various analytical results obtained in the previous section are considerably complicated in form and, therefore, the concrete results of the problem may not be found directly from them alone. Thus, some numerical calculations will be carried out for attaining this purpose. Performing the extensive computations is not easy because of the analytical restrictions of solving the transcendental equation for φ_1, (48), with which the numerical computation begins.

As was mentioned previously, the evaluation of the integral in Eq. (45) cannot be made except for some special values of σ and θ. This fact makes cumbersome the numerical discussions. However, an aspect of the general character of the solution might perhaps be obtained by numerically discussing a special case.

Consider then the case in which $\sigma = 1/2$ and $\theta = 1$. Here the integration for $U(\zeta, \xi; \sigma, \theta)$ can be made analytically, so that the amount of numerical calculations is much reduced.

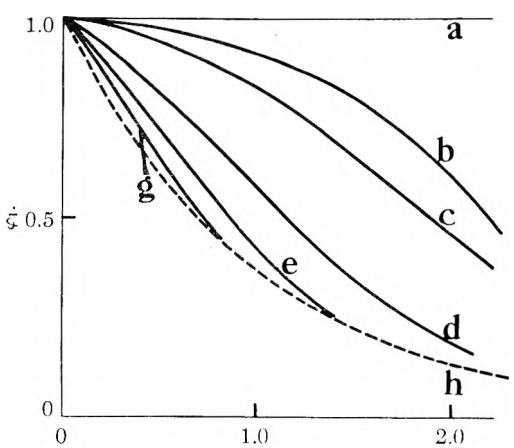

Fig. 1.—The fluid concentration history for solute 1 as a function of bed position and elapsed time: a, $\tau = \infty$; b, $\tau = 8$; c, $\tau = 5$; d, $\tau = 2.6$; e, $\tau = 1.4$; g, $\tau = 0.8$; h, $e^{-\chi}$.

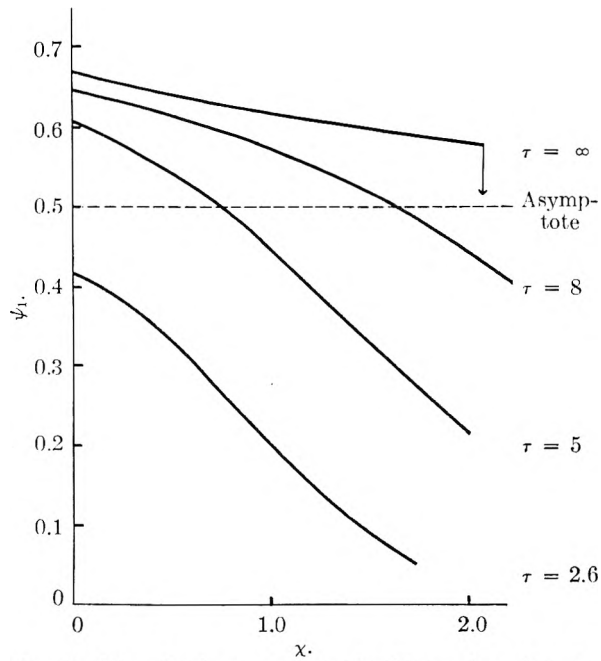

Fig. 2.—The adsorbent concentration history for solute 1.

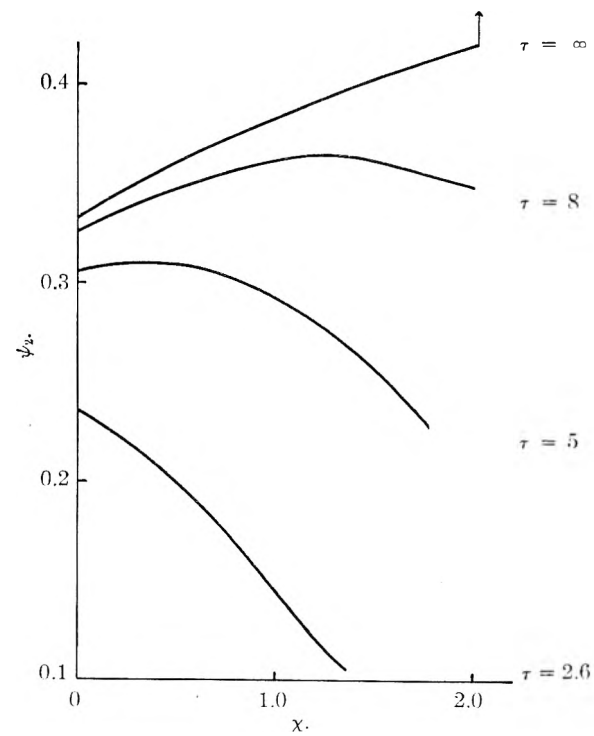

Fig. 3.—The adsorbent concentration history for solute 2.

Now, when $\sigma = 1/2$ and $\theta = 1$, Eq. (48) becomes

$$\left(\frac{1}{\sqrt{\varphi_1}} - 1\right)^2 \left(\frac{2}{\sqrt{\varphi_2}} + 1\right) = e^{3\eta} \left(e^{\xi} - 1\right)^2 \left(2e^{\xi} + 1\right) \tag{65}$$

Putting $\varphi_1 = 1/\omega^2$ and changing back the variables from (ξ, η) to (x, τ), the above equation is written as

$$(\omega - 1)^2(2\omega + 1) = e^{3\lambda_1(x - \tau)} e^{\beta_1 x} (e^{\lambda_1 x} - 1)^2 (2e^{\lambda_1 x} + 1) \tag{66}$$

To solve this numerically in terms of ω the values of λ_1 and β_1 must be assigned. In this place, they are taken as

$$\lambda_1 = 1, \beta_1 = 3 \quad (67)$$

Then, Eq. (66) is

$$(\omega - 1)^2(2\omega + 1) = e^{(x-\tau)} \times (e^{2x} - 1)^2(2e^{2x} + 1) \quad (68)$$

Since this is cubic with ω, this could be solved with the aid of the so-called Cardan's formula, or Newton's method for finding an approximate solution of any given equation. In the course of this computation we have frequently encountered the case

$$(\omega - 1)^2(2\omega + 1) = \epsilon^2 \ll 1 \quad (69)$$

In such a case, instead of the methods just cited the following expansion in ϵ has been used for the calculation of ω

$$\omega = 1 + \frac{1}{\sqrt{3}}\epsilon + \frac{1}{9}\epsilon^2 + 0(\epsilon^3) \quad (70)$$

Thus, the curves for φ_1 plotted against x for several values of τ are shown in Fig. 1.

The corresponding curves for φ_2, ψ_1 and ψ_2 can then be immediately plotted, and as an example, those for ψ_1 and ψ_2 are shown in Figs. 2 and 3, respectively.

These figures indicate that ψ_1 always has its maximum point at the entrance of the bed and decreases monotonously with increasing distance χ, while for ψ_2, though its maximum point also appears at the entrance of the bed in the early stage of the process, the maximum moves gradually downstream with time. In this way, after some time has elapsed, these two maximum points are clearly separated. This is not unlike the so-called chromatographic separation.

Acknowledgment.—The author wishes to express his appreciation to Dr. Nevin K. Hiester of Stanford Research Institute for his encouragement and assistance in preparing this work for publication in the United States.

CRITICAL CONCENTRATIONS OF POTASSIUM *n*-ALKANECARBOXYLATES AS DETERMINED BY THE CHANGE IN COLOR AND SPECTRUM OF PINACYANOLE[1]

BY SIMON H. HERZFELD

Department of Chemistry, University of Chicago, Chicago 37, Illinois

Received September 25, 1951

The critical concentrations, C_μ, of the potassium *n*-alkanecarboxylates from the hexanoate to the tetradecanoate, as determined by a titrimetric method employing pinacyanole chloride for indicator, fit closely equation (3) in which N is the number of carbon atoms in the alkyl radical. From the variation with soap concentration of the optical densities at the average wave lengths of three absorption bands in the presence of pinacyanole, the same values for C_μ are obtained for the soaps of from nine to fourteen carbon atoms as by the visual method. For the soaps of shorter chain length, the spectrophotometrically determined critical concentrations are considerably lower than those obtained by the visual means. Attention is directed to the significance given the coefficient of N in the above equation by Debye and by Corrin. According to Debye's analysis, the coefficient is the energy change during micellization per CH_2 group divided by $2.303(3kT)$, in which k is the Boltzmann constant and T the absolute temperature. Corrin evaluates both constants in terms of the standard free energy changes that accompany micellization. The light absorption characteristics of freshly prepared soap-pinacyanole solutions change with time in a manner that suggests micelle formation is not an instantaneous process. The time required for maximum formation of micelles appears to be a decreasing function of chain length.

Introduction

The occurrence of some organic electrolytes in a colloidal state was envisioned first in 1913 by McBain[2] and by Reychler.[3] The first valid demonstration of a critical passage by a solute from an ionic to a micellar distribution was made by Bury and his collaborators.[4-6] The methods that have been employed most for the determination of the critical concentration for micelle formation have been based on measurements of electrical conductivity, freezing point lowering, dew point lowering, surface and interfacial tension, density, electromotive force, solubility, solubilization and viscosity. More recently, methods based on light scattering[7-10] and absorpton spectra[11] have been introduced. In all these, the rate of change of the measured property with increase in concentration shows a more or less sharp change as micelle formation sets in.

The values obtained for the critical concentration of a long-chain electrolyte by different investigators, frequently employing the same method, have shown wide divergencies. Thus the following values have been reported or inferred for the critical concentration of potassium or sodium dodecanoate: 0.07 to 0.10 molar from freezing point data,[12] 0.025 molar by solubilization at 40°,[13]

(1) This investigation was carried out under the sponsorship of the Reconstruction Finance Corporation, Office of Rubber Reserve, in connection with the Government's synthetic rubber program. S. H. Herzfeld, Chemistry Division, Office of Scientific Research, Air Research and Development Command, Baltimore 3, Md.

(2) J. W. McBain, *Trans. Faraday Soc.*, **9**, 99 (1913).

(3) A. Reychler, *Kolloid Z.*, **12**, 277 (1913).

(4) E. R. Jones and C. R. Bury, *Phil. Mag.*, **4**, 841 (1927).

(5) D. G. Davies and C. R. Bury, *J. Chem. Soc.*, 2263 (1930).

(6) J. Grindley and C. R. Bury, *ibid.*, 679 (1929).

(7) R. F. Stamm, T. Mariner and J. K. Dixon, *J. Chem. Phys.*, **16**, 423 (1948).

(8) P. Debye, THIS JOURNAL, **53**, 1 (1949).

(9) P. Debye, *Ann. N. Y. Acad. Sci.*, **51**, 575 (1949).

(10) P. Debye and E. W. Anacker, THIS JOURNAL, **55**, 644 (1951).

(11) W. D. Harkins, H. Krizek and M. L. Corrin, *J. Colloid Sci.*, **6**, 576 (1951).

(12) M. Randall, J. W. McBain and A. McL. White, *J. Am. Chem. Soc.*, **48**, 2517 (1926).

(13) I. M. Kolthoff and W. F. Johnson, THIS JOURNAL, **50**, 440 (1946).

0.20 molar ("complete micellization") by solubilization at 25°,[14] 0.15 molar by equivalent conductivity at 18°,[15] 0.038 molar[16] and 0.034 molar[17] by density at 25°, and 0.028 molar by equivalent conductivity at 17 to 80° (average value).[18] Of the six values, three are in fair agreement and indicate a critical concentration of about 0.03 molar. On the other hand, Tartar and co-workers have obtained good agreement among four methods for the critical concentration of sodium dodecanesulfonate: 0.0097 molar by density and 0.010 molar by viscosity at 40°,[17] 0.0098 molal by solubility at 31.5°,[19] and 0.0110 molar from specific conductance data at 40°.[20]

The critical concentration for the formation of micelles, at best, is not a definite concentration but rather a concentration range throughout which the concentration of micelles increases faster than the total (stoichiometric) concentration. This has been demonstrated by the definite curvature between the two linear portions of property–composition plots,[21,21] and also by the character of the spectral changes exhibited by dyes.[22,23] From very slight to moderate variations of critical concentration with temperature have been reported. In some cases, measurements by different methods over the same temperature range have shown opposite trends. Scott and Tartar,[24] working with decyltrimethylammonium and dodecyltrimethylammonium bromides, found that the critical concentrations between 25 and 60° as indicated by conductivity increased slightly and as shown by density decreased moderately. From such findings it may be inferred that the temperature coefficient of a given property in solution may differ above and below the critical level, and no parallelism should be expected for different properties either in the concentration range of micelles or of discrete ions. Thus it is a coincidence if two methods give exactly the same value for any critical concentration at a specified temperature.

The method for the determination of critical concentration of long-chain electrolytes by the change in color or spectrum of dyes is of wide and ready applicability. The dye employed undergoes no change in spectrum in the presence of moderate concentrations of simple salts, and it need not be used in neutral solution provided the dye ion retains a charge opposite in sign to that of the long-chain ion. The dye method thus is applicable to slightly hydrolyzed long-chain ions. It measures a change in behavior involving only long-chain ions and their micelles, and to a considerable degree this procedure is independent of changes in the properties of the solvent that may be induced either by the long-chain electrolyte or by an added substance. Although the spectrogram of pinacyanole in the presence of long-chain electrolytes varies considerably with change in the nature of either the polar or non-polar group,[23] it remains essentially constant within a homologous series.

Very little work had been done on the critical concentrations of the straight chain soaps containing an odd or small number of carbon atoms. In the presently described study, the dye method was applied to the measurement of the critical molarities of all straight chain saturated soaps sufficiently soluble in water at room temperature (25°) to enable the preparation of micellar solutions.

Marked changes in the absorption spectra of cyanine dyes with environment were observed by Sheppard,[25] who found that the spectral behavior of pinacyanole chloride in water differs conspicuously from that in organic solvents of low polarity. Sheppard and Geddes[26] further showed that the spectrum in solutions of gelatin and of hexadecylpyridinium chloride approaches that in organic liquids. Sheppard ascribed this phenomenon to a reversible transition of the dye between the aggregated state found in water and a monomeric form adsorbed on the colloid. Corrin, Klevens and Harkins[22] found that a much more pronounced change in the spectrum of pinacyanole is brought about in the presence of anionic long-chain electrolytes. These investigators made a detailed study of the spectral changes exhibited in solutions of potassium dodecanoate and tetradecanoate. They discovered rapid changes in the intensities of three absorption bands in the region of the critical concentrations of these two soaps; a band shifting between 480 and 490 mμ disappeared, and two bands at about 570 mμ and 615 mμ appeared simultaneously as the concentration was increased. With alkanecarboxylates of shorter chain length, beginning with the octanoate, the maximum at 490 mμ disappears, with increase in molarity of soap, well below the value of the critical concentration established by the visual procedure developed by Corrin, Klevens and Harkins[23] and described in this report. However, even in the absence of maxima, the optical density at 490 mμ falls rapidly in the same concentration range at which the values of log I_0/I for the band maxima at the two longer wave lengths show their rapid rise (Figs. 1–5). This molarity range is interpreted as representing the critical micelle concentration. Visually, pinacyanole has a blue color in a soap solution above the critical concentration and a red color below.

Experimental Details

I. **Preparation of Soaps.**—The soaps were prepared in boiling 95% ethanol from commercially available "pure" fatty acids or from refractionated esters, by the action of reagent grade potassium hydroxide in 10% excess. The

(14) J. W. McBain and Sister A. A. Green, *J. Am. Chem. Soc.*, **68**, 1731 (1946).

(15) J. W. McBain, M. E. Laing and A. F. Titley, *J. Chem. Soc.*, **115**, 1279 (1919).

(16) C. R. Bury and G. A. Parry, *ibid.*, 626 (1935).

(17) K. A. Wright and H. V. Tartar, *J. Am. Chem. Soc.*, **61**, 544 (1939).

(18) P. Ekwall, *Kolloid Z.*, **101**, 135 (1942).

(19) H. V. Tartar and K. A. Wright, *J. Am. Chem. Soc.*, **61**, 539 (1939).

(20) K. A. Wright, A. D. Abbott, V. Sivertz and H. V. Tartar, *ibid.*, **61**, 549 (1939).

(21) K. Hess, W. Philippoff and H. Kiessig, *Kolloid Z.*, **88**, 40 (1939).

(22) M. L. Corrin, H. B. Klevens and W. D. Harkins, *J. Chem. Phys.*, **14**, 216 (1946).

(23) M. L. Corrin, H. B. Klevens and W. D. Harkins, *ibid.*, **14**, 480 (1946).

(24) A. B. Scott and H. V. Tartar, *J. Am. Chem. Soc.*, **65**, 692 (1943).

(25) S. E. Sheppard, *Rev. Modern Phys.*, **14**, 303 (1942).

(26) S. E. Sheppard and A. L. Geddes, *J. Chem. Phys.*, **13**, 63 (1945).

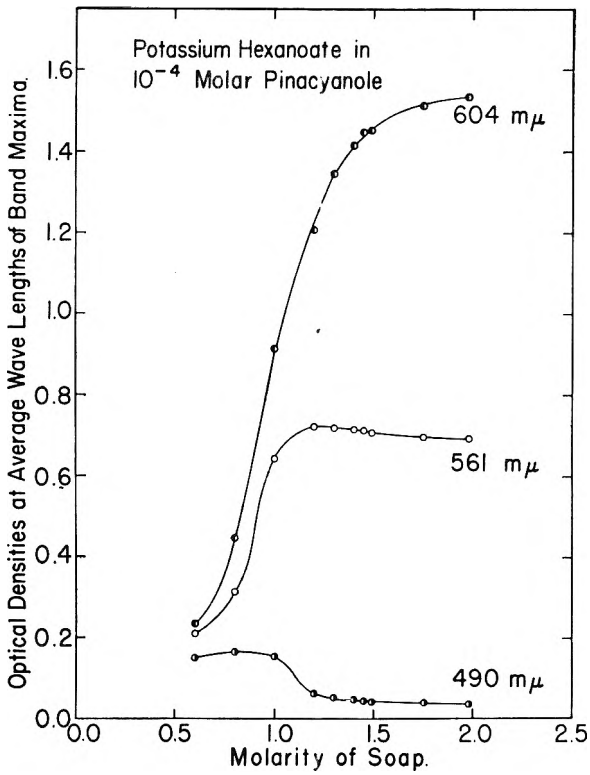

Fig. 1.—Intensities of absorption by 10^{-4} molar pinacyanole at average positions of band maxima as functions of concentration of potassium hexanoate.

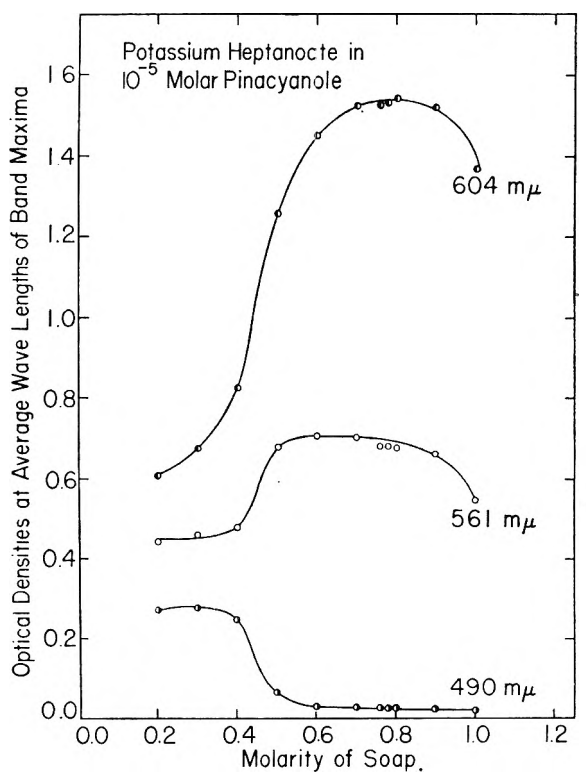

Fig. 2.—Intensities of absorption by 10^{-5} molar pinacyanole at average positions of band maxima as functions of concentration of potassium heptanoate.

filtered reaction solution was concentrated and cooled. The precipitated soap was collected and recrystallized from three to five times in absolute ethanol, until the critical concentration reached a constant value. Drying was effected by continuous evacuation at room temperature.

II. Preparation of Solutions.—All solutions were prepared by weighing the solute in a volumetric flask and bringing the solution to volume at 25°. A stock solution of pinacyanole chloride of ten times the molarity used in the subsequent measurements was made. It was found convenient to stir the dye briefly in water at 40 to 45° to effect rapid and complete solution. Before the soap solutions were brought to volume, one-tenth volume of stock

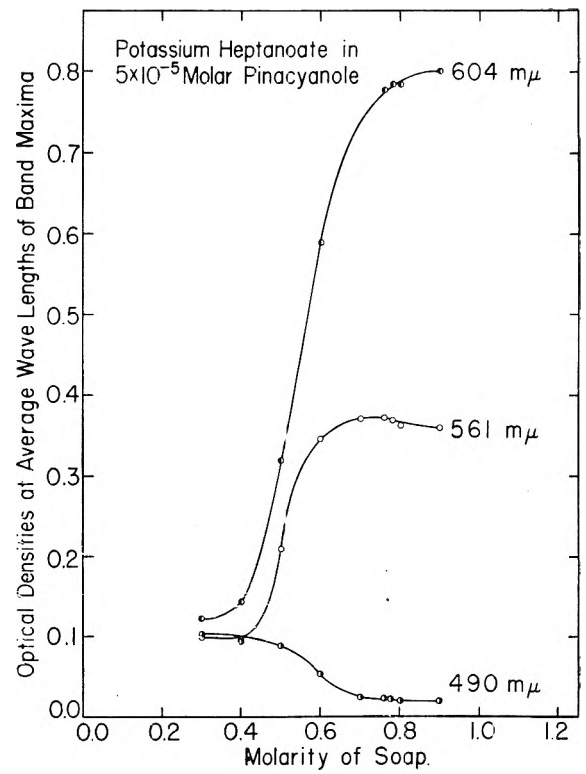

Fig. 3.—Intensities of absorption by 5×10^{-5} molar pinacyanole at average positions of band maxima as functions of concentration of potassium heptanoate.

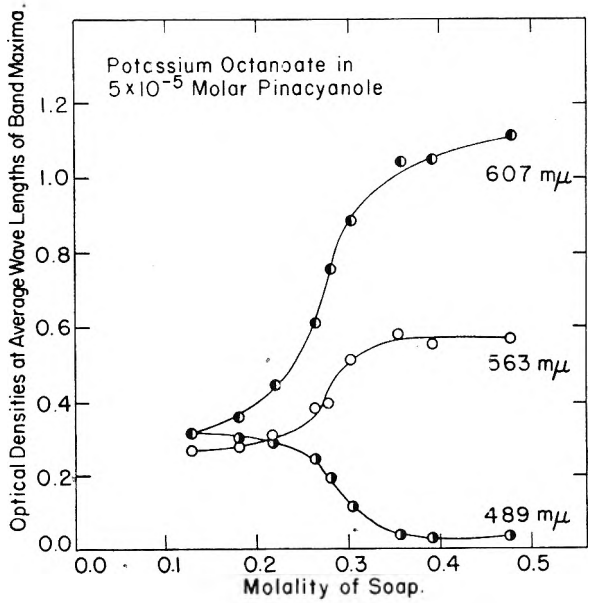

Fig. 4.—Intensities of absorption by 5×10^{-5} molar pinacyanole at average positions of band maxima as functions of concentration of potassium octanoate (by permission of M. L. Corrin, Univ. of Chicago).

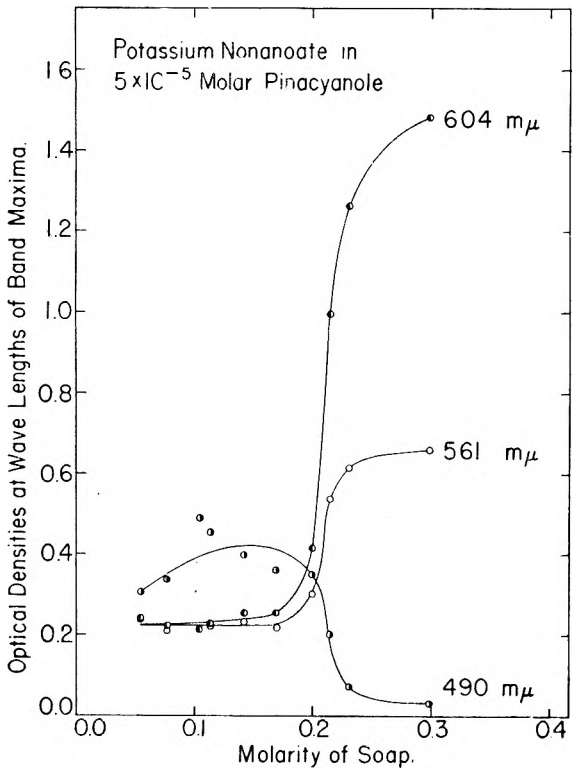

Fig. 5.—Intensities of absorption by 5×10^{-5} molar pinacyanole at average positions of band maxima as functions of concentration of potassium nonanoate.

pinacyanole was added. In the visual method with the short-chain soaps, the solutions were allowed to age briefly in order to let the color attain its maximum blue value. The initial molarity of soap in the visual studies was made about 1.5 times the anticipated critical value.

III. Analytical Procedures. (A) Visual Method.—A measured volume of soap–dye solution, usually 5.00 ml., was introduced into a 50-ml. volumetric flask. To this the dye solution in 1:10 dilution was added from a buret until the initial blue color had changed to the first definite blue-purple. This color was chosen so as to give the same critical concentration for potassium dodecanoate as that which had been obtained spectrophotometrically by Corrin, Klevens and Harkins.[22] The same end-point was used in all subsequent titrations. It was observed with light from a white fluorescent lamp through the neck of the stoppered, inverted flask held perpendicular to the line of vision. The temperature of the room was maintained at 25 ± 1°. Determinations were made at least in triplicate.

(B) Spectrophotometric Method.—From the absorption spectrograms of potassium nonanoate at ten different molarities (from 0.0539 to 0.2982) as determined with a Beckman spectrophotometer, the average positions of the band maxima were established at 490 ± 2 mμ, 561 ± 1 mμ, and 604 ± 2 mμ. The deviations from these positions for the heptanoate and hexanoate usually were less than 5 mμ. From the spectrograms for potassium octanoate as determined by Corrin,[27] the average positions appear at 489, 563 and 607 mμ. Because of the rapidity with which the transmission characteristics of pinacyanole in a freshly prepared soap solution change, it was considered desirable to measure the optical densities quickly at the average positions of the three bands. All measurements thus were made at 490, 561 and 604 mμ and were completed except in one series (Fig. 5, 490 mμ) within three minutes after the soap, pinacyanole and water were brought together. The value of $\log I_0/I$ as a function of soap concentration was then plotted for each band. No temperature control was made in these spectrophotometric studies.

IV. Choice of Pinacyanole Concentration.—In the visual method, it was found with all soaps that a minimum concentration of dye occurred above which values for the critical concentration remained constant. The concentration of 5×10^{-5} molar was above this minimum for all soaps studied except the hexanoate, and the pinacyanole was used at this molarity in all determinations from the heptanoate to the tetradecanoate. The critical concentration of the hexanoate was measured in 10^{-4} molar pinacyanole. Spectrophotometric measurements were made at the same concentrations of dye, and additional studies were conducted at lower molarities to reveal the effect of dye concentration also in this procedure.

(27) M. L. Corrin, unpublished data, Department of Chemistry, University of Chicago (1947).

Results

The values for the critical concentrations of the nine potassium *n*-alkanecarboxylates from the hexanoate to the tetradecanoate as determined by visual means with pinacyanole are shown in column 3 of Table I. They were computed by means of the equation

$$C_\mu = V_A M_A / V_T$$

where C_μ is the critical concentration in moles per liter, V_A and M_A are the initial volume and molarity of the soap solution, respectively, and V_T is the sum of the volumes of all solutions present at the end-point. The last significant digits in column 3 are somewhat uncertain.

TABLE I

CRITICAL CONCENTRATIONS OF POTASSIUM *n*-ALKANECARBOXYLATES AS DETERMINED BY MEANS OF PINACYANOLE

Soap	Molarity of pinacyanole	Critical molarity: Visual method	Critical molarity: Spectrophotometric method
Hexanoate	1×10^{-4}	1.49	1.0
Heptanoate	5×10^{-5}	0.780	0.55
Octanoate	5×10^{-5}	.401	.27[a]
Nonanoate	5×10^{-5}	.201	.21
Decanoate	5×10^{-5}	.0998	..
Undecanoate	5×10^{-5}	.0492	..
Dodecanoate	5×10^{-5}	.0234	..
Tridecanoate	5×10^{-5}	.0126	..
Tetradecanoate	5×10^{-5}	.0059	..

[a] From unpublished data by M. L. Corrin, University of Chicago, 1947.

The influence of charge in pinacyanole molarity on the indicated critical concentration is illustrated in Table II. In the visual procedure, determinations of the critical concentrations of soaps of longer chain length than the octanoate were found to be independent of pinacyanole concentration within

TABLE II

EFFECT OF PINACYANOLE CONCENTRATION ON THE INDICATED CRITICAL CONCENTRATION

Soap	Molarity of pinacyanole	Critical molarity: Visual method	Critical molarity: Spectrophotometric method
Potassium hexanoate	5×10^{-5}	1.22	..
Potassium hexanoate	1×10^{-4}	1.49	..
Potassium hexanoate	2×10^{-4}	1.48	..
Potassium heptanoate	1×10^{-5}	...	0.45
Potassium heptanoate	2.5×10^{-5}	0.670	..
Potassium heptanoate	5×10^{-5}	.780	0.55
Potassium heptanoate	1×10^{-4}	.780	..
Potassium octanoate	1×10^{-5}	.340	..
Potassium octanoate	2.5×10^{-5}	.388	..
Potassium octanoate	5×10^{-5}	.401	..
Potassium octanoate	1×10^{-4}	.402	..

the range employed. Corrin, Klevens and Harkins[23] report a slight influence of pinacyanole concentration in their spectrophotometric determinations of the critical concentrations of potassium dodecanoate and sodium hexadecyl sulfate.

The optical densities for pinacyanole chloride in the presence of potassium hexanoate, heptanoate and nonanoate at varying concentrations of soap, both above and below the critical levels as determined visually, are given in Tables III, IV, V and VI. The underlined molarity in each table is the maximum concentration at which a red component in the color of the solution was observed visually in white fluorescent light. The data are shown graphically in Figs. 1, 2, 3 and 5. Figure 4 is taken from unpublished work of M. L. Corrin.[27] These curves for the shorter-chain soaps fail to exhibit the rapid change in slope at the critical concentration that has been observed by Corrin, Klevens and Harkins[23] for the dodecanoate and tetradecanoate. Furthermore, the mid-point of the rapid drop or rise (Figs. 1–5) does not occur at the same concentration as the critical value established by visual means. This discrepancy has not been encountered with soaps of longer chain length.

TABLE III

ABSORPTION BY POTASSIUM HEXANOATE IN 1×10^{-4} *M* PINACYANOLE CHLORIDE AT AVERAGE WAVE LENGTHS OF BAND MAXIMA

Molarity	og I_0/I at 490 mμ	log I_0/I at 561 mμ	log I_0/I at 604 mμ
0.600	0.153 (M)[a]	0.212 (M)	0.285 (M)
0.800	.167 (M)	.315 (M)	.448 (M)
1.000	.155	.643 (M)	.913 (M)
1.200	.062	.721 (M)	1.252 (M)
1.300	.051	.717 (M)	1.347 (M)
1.400	.047	.715 (M)	1.415 (M)
1.450	.044	.713 (M)	1.448 (M)
1.490	.042	.706 (M)	1.451 (M)
1.751	.040	.698 (M)	1.512 (M)
1.979	.037	.692 (M)	1.535 (M)

[a] (M) signifies occurrence of a maximum at or near the indicated wave length.

TABLE IV

ABSORPTION BY POTASSIUM HEPTANOATE IN 1×10^{-5} *M* PINACYANOLE CHLORIDE AT AVERAGE WAVE LENGTHS OF BAND MAXIMA

Molarity	log I_0/I at 490 mμ	log I_0/I at 561 mμ	log I_0/I at 604 mμ
0.200	0.273 (M)[a]	0.420 (M)	0.608 (M)
.300	.278	.460 (M)	.675 (M)
.400	.250	.478 (M)	.825 (M)
.501	.068	.678 (M)	1.258 (M)
.601	.057	.706 (M)	1.452 (M)
.700	.055	.703 (M)	1.525 (M)
.760	.054	.683 (M)	1.527 (M)
.780	.053	.682 (M)	1.532 (M)
.801	.052	.678 (M)	1.541 (M)
.899	.051	.663 (M)	1.520 (M)
1.001	.048	.598 (M)	1.368 (M)

[a] (M) denotes existence of a maximum at or near the indicated wave length.

The interpretation of these graphs becomes increasingly more difficult with decrease in the chain length of the soap. If the molarity of soap at which the most rapid change in light absorption occurs is taken as the critical concentration, the values recorded in Tables I and II may be selected.

TABLE V

ABSORPTION BY POTASSIUM HEPTANOATE IN 5×10^{-5} *M* PINACYANOLE CHLORIDE AT AVERAGE WAVE LENGTHS OF BAND MAXIMA

Molarity	log I_0/I at 490 mμ	log I_0/I at 561 mμ	log I_0/I at 604 mμ
0.300	0.104	0.100 (M)[a]	0.123 (M)
.401	.096	.098 (M)	.145 (M)
.500	.090	.210 (M)	.320 (M)
.601	.055	.347 (M)	.590 (M)
.701	.026	.372 (M)	.738 (M)
.760	.025	.373 (M)	.779 (M)
.781	.024	.370 (M)	.786 (M)
.801	.021	.364 (M)	.786 (M)
.899	.021	.361 (M)	.802 (M)

[a] (M) denotes occurrence of a maximum at or near the indicated wave length.

TABLE VI

ABSORPTION BY POTASSIUM NONANOATE IN 5×10^{-5} *M* PINACYANOLE CHLORIDE AT AVERAGE WAVE LENGTHS OF BAND MAXIMA

Molarity	log I_0/I at 490 mμ	log I_0/I at 561 mμ	log I_0/I at 604 mμ
0.0539	0.309 (M)[a]	0.238	0.240 (M)
.0764	.338 (M)	.210	.220 (M)
.104	.490 (M)	.215	.215 (M)
.113	.430 (M)	.220	.227 (M)
.142	.398 (M)	.234	.255 (M)
.169	.361 (M)	.219 (M)	.256 (M)
.200	.351 (M)	.303 (M)	.417 (M)
.215	.204	.537 (M)	.995 (M)
.230	.072	.615 (M)	1.264 (M)
.298	.031	.658 (M)	1.482 (M)

[a] (M) denotes occurrence of a maximum at or near the indicated wave length.

Soaps of shorter chain length than the hexanoate were not included in this study. Micellization of sodium pentanoate has been reported by Hess, Philippoff and Kiessig,[21] on the basis of X-ray evidence, to occur at 2.24 to 2.35 molar. Bunbury and Martin,[28] from observation of washing power, density, and conductivity, concluded that micellization was not exhibited by the alkanecarboxylates below the hexanoate. Davies and Bury[5] came to the same conclusion from density measurements. The visual method with pinacyanole ceases to be applicable with the pentanoate.

Discussion

From Figs. 1–5 it is seen that the intensity of absorption at or near 604 mμ continues to increase with increasing molarity of soap after the optical densities at the shorter wave lengths have come to essentially constant values. It may be inferred from this that the human eye is sufficiently sensitive to light in the region of 604 mμ to see a red component in the dye–soap solution until the absorption of this wave length has reached nearly its maximum intensity. Until such time as the theory of micellization has been more completely and unequivocally

(28) H. M. Bunbury and H. E. Martin, *J. Chem. Soc.*, **105**, 417 (1914).

worked out, it will be difficult to reconcile the spectrophotometric and visual findings for the shorter-chain soaps.

It has been found that the critical concentrations of the homologous alkanecarboxylates, as obtained by the visual method with pinacyanole (Table I), fit the empirical equation

$$\log C_\mu = a + bN \qquad (2)$$

in which N is the number of carbon atoms in the alkyl. This relationship is shown in Fig. 6. The

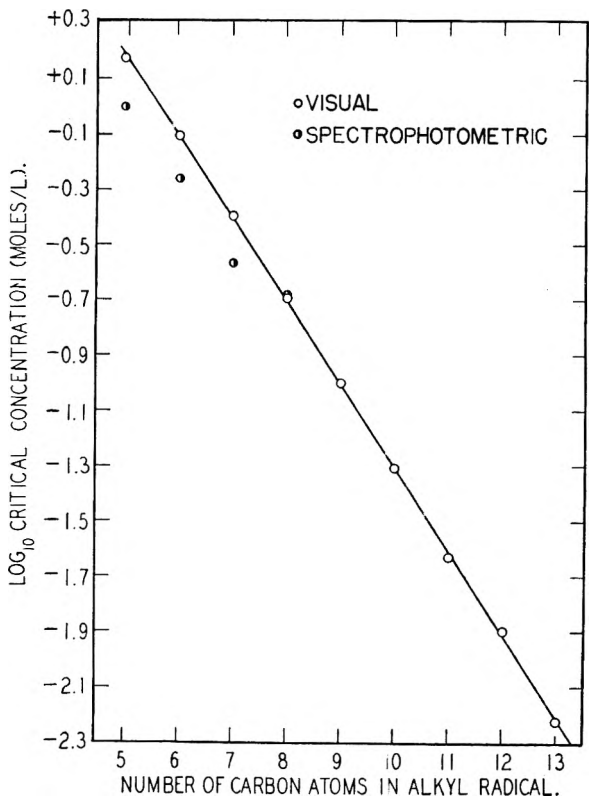

Fig. 6.—Variation of the critical concentration of the *n*-alkane-carboxylates with chain length.

linearity of log C_μ with N had been noted previously for several homologous series of electrolytes by Stauff,[29] by Hartley,[30] by Hess, Philippoff and Kiessig,[21] and by Scott and Tartar.[24] Computation by the method of least squares of the parameters in equation (2) from the visually determined critical molarities gives the following specific equation for the potassium *n*-alkanecarboxylates

$$\log C_\mu = 1.70 - 0.301\ N \qquad (3)$$

In a homologous group of long-chain electrolytes, provided the chain lengths are sufficiently great, the work done against the coulomb forces can be taken as independent of chain length. The work performed by a number of chains in the transition from a free to an associated state, however, clearly increases linearly with the number of methylene groups in each chain. Debye[8] has shown that this work is a logarithmic function of C_μ, and it follows that N should be a logarithmic function of C_μ. The coefficient of N in equation (2) has been shown by Debye to be the energy change per CH_2 group divided by $2.303(3kT)$, k being the Boltzmann constant and T the absolute temperature. Combination of this relationship with equation (3) gives the energy equivalent of a single methylene group as equal to $(2.303 \times 0.301 \times 3kT)$, or $2.08\ kT$. On a gram mole basis at 25°, this becomes 1230 cal./mole. This value is 4.2% higher than the increase of 1180 cal./mole for each additional CH_2 group in the experimental heats of vaporization of normal alkanes.[31] The difference may be laid to the decrease in the quasi-interfacial energy that accompanies micellization, provided that vaporization and the separation of long chains in solutions are associated with identical energy changes. Corrin[32] arrives at equation (2) from concepts based entirely on the law of mass action and attempts to evaluate the constants from considerations of the free energy changes that accompany micellization.

In Fig. 6, all critical molarities by the visual method fall closely on the straight line defined by equation (3). Corresponding values by the spectrophotometric procedure for the six, seven and eight carbon homologs clearly fall below this straight line. Deviations from the linear relationship between log C_μ and the number of carbon atoms have been found for the short-chain members of homologous groups by several earlier investigators. Scott and Tartar,[24] for example, by means of measurements of equivalent conductivity and density, found the linear relationship to hold from decyl- to hexadecyltrimethylammonium bromide. The value of log C_μ for the octyl homolog, however, was observed to fall below the extrapolated line. For the alkanesulfonic acids, the same authors report a linear relationship from eleven to fourteen carbon atoms but find that the value for the nine carbon homolog falls below the extrapolated line.

A partial explanation of the adherence of the soaps of shorter chain length to the linear relationship between log C_μ and N found in the presently described visual investigation may be drawn from the spectrophotometric findings as represented in Figs. 1 to 5. The curves show that for alkanecarboxylates of fewer than nine carbon atoms, not only do the changes in the optical densities in the regions of the three band maxima occur over wide ranges of concentration, but the intensity of absorption at 604 mμ continues to rise with increase in molarity of soap even beyond the critical concentration as established by visual means. In the light of these observations, the critical concentrations for the six, seven and eight carbon soaps obtained by the visual method and shown in Table I appear to represent upper limits.

Changes with time were noted in the color of freshly prepared solutions of the short-chain soaps and pinacyanole, both visually and spectrophotometrically. The rate of change decreased with shortening of the carbon chain. When a 2.25 molar solution of potassium hexanoate with pina-

(29) J. Stauff, *Z. physik. Chem.*, **A183**, 55 (1938).
(30) G. S. Hartley, *Kolloid Z.*, **88**, 22 (1939).
(31) U. S. Bureau of Standards, American Petroleum Institute Research Project No. 44.
(32) M. L. Corrin, *J. Colloid Sci.*, **3**, 333 (1948).

cyanole was first prepared, it was distinctly reddish-violet. On standing, the color became blue, and the change appeared complete in about 20 minutes. With a solution of the heptanoate of above the critical concentration, the change to blue seemed complete in about 10 minutes. Spectrophotometrically, it is found that at 490 mμ the intensity of absorption decreases with time, whereas at 561 and 604 mμ the optical densities increase with time. This time effect is very pronounced with the six and seven carbon soaps. The wide scattering of points at 490 mμ in Fig. 5 below the indicated C_μ which were determined at from three to 15 minutes after the solutions were made, illustrates the importance of the time effect. The rate of change in optical density with time varies with soap concentration but in general is significant only for $^1/_2$ hour. The readings at 490 mμ may decrease by nearly 50% during that period, and at 561 and 604 mμ they may increase by as much as 10%. Ultimately, due to the instability of the dye, all three bands will fade. These observations are not in disagreement with the view that micelles continue to form for a considerable time after the long-chain electrolyte has been dissolved. The discrepancies between the visual and spectrophotometric results reported herein may in part be explained by this phenomenon.

EFFECT OF SALT ON THE CRITICAL CONCENTRATIONS OF POTASSIUM *n*-ALKANECARBOXYLATES AS DETERMINED BY THE CHANGE IN COLOR OF PINACYANOLE[1]

By Simon H. Herzfeld

Department of Chemistry, University of Chicago, Chicago 37, Illinois

Received September 25, 1951

It has been shown that for the potassium *n*-alkanecarboxylates, the critical concentration and also the rate of change of the critical concentration with increase in the concentration of added potassium chloride, are decreasing functions of the concentration of the salt. The data are found to fit equation (1) in which C_μ is the critical molarity and C_i the total volume normality of counterion. The slope of this line is found to be essentially independent of chain length. Hobbs[2] interprets a as a function of the thermal energy and the work of micelle formation. Corrin[3] reasons that b is the ratio of the number of counterions to that of long-chain ions in the micelle at the critical concentration, and argues that the ratio is independent of the concentration of added salt. Both Hobbs and Corrin arrive at equations of the same form as the empirical equation shown above.

Introduction

Numerous workers[4-14] have reported that the presence of salt increases the tendency of long-chain electrolytes to micellize. The first systematic investigation of salt effect was carried out by Corrin and Harkins,[15] who studied the effects of various inorganic salts over wide ranges of concentration on both anionic and cationic long-chain electrolytes. Corrin and Harkins, within the limits of their experiments, found that these effects were independent of the valence and composition of the ion possessing a charge of the same sign as that of the aggregating ion. Ions of opposite sign were restricted to sodium, potassium, chloride and bromide. The rate of decrease of the critical molarity, C_μ, with increasing normality of added salt was found to diminish rapidly with rise in salt concentration. In the cases studied, the data fitted the equation

$$\log C_\mu = a + b \log C_i \qquad (1)$$

in which C_i is the total concentration in gram equivalents per liter of ions opposite in sign to the long-chain ion. The slope of this line was observed to vary moderately with the constitution of the micellizing ion and to remain less than one in all cases. Merrill and Getty[16] confirmed the findings of Corrin and Harkins for the case of sodium dodecanoate.

The present investigation was undertaken to study the salt effect in a homologous series of long-chain electrolytes. The findings at lower concentrations of salt have been demonstrated to fit equation (1), and the slope has been shown to remain constant within the limits of accuracy of the method.

Experimental Methods

The soap and pinacyanole were of the same lots used in the work described in the preceding report. The salt, potassium chloride of reagent grade, was dried at 110°. Measured volumes of soap and salt solutions of known normalities, prepared at 25°, were mixed in varying ratios. Each mixture was brought by dilution at constant concentration of dye to the critical molarity in the manner employed in the earlier work. The end-points usually became

(1) This investigation was carried out under the sponsorship of the Reconstruction Finance Corporation, Office of Rubber Reserve, in connection with the Government's synthetic rubber program. S. H. Herzfeld, Chemistry Division, Office of Scientific Research, Air Research and Development Command, Baltimore 3, Md.

(2) M. E. Hobbs, This Journal, **55**, 675 (1951).

(3) M. L. Corrin, *J. Colloid Sci.*, **3**, 333 (1948).

(4) G. S. Hartley, *Trans. Faraday Soc.*, **30**, 444 (1934).

(5) R. C. Murray, *ibid.*, **31**, 199 (1935).

(6) G. S. Hartley and D. F. Runnicles, *Proc. Roy. Soc. (London)* **A168**, 420 (1938).

(7) G. S. Hartley, *J. Chem. Soc.*, 1968 (1938).

(8) K. A. Wright, A. D. Abbott, V. Sivertz and H. V. Tartar, *J. Am. Chem. Soc.*, **61**, 544 (1939).

(9) H. V. Tartar and R. D. Cadle, This Journal, **43**, 1173 (1939)

(10) H. F. Walton, *J. Am. Chem. Soc.*, **68**, 1180 (1946).

(11) R. S. Stearns, H. Oppenheimer, E. Simon and W. D. Harkins, *J. Chem. Phys.*, **15**, 496 (1947).

(12) P. Debye, *Ann. N. Y. Acad. Sci.*, **51**, 575 (1949).

(13) P. Debye and E. W. Anacker, This Journal, **55**, 644 (1951).

(14) H. A. Scheraga and J. K. Backus, *J. Am. Chem. Soc.*, **73**, 5193 (1951).

(15) M. L. Corrin and W. D. Harkins, *ibid.*, **69**, 683 (1947).

(16) R. C. Merrill and R. Getty, This Journal, **52**, 774 (1948).

TABLE I

VARIATION OF THE CRITICAL CONCENTRATIONS OF POTASSIUM *n*-ALKANECARBOXYLATES WITH ADDED POTASSIUM CHLORIDE AT 25° AS DETERMINED BY THE CHANGE IN COLOR OF PINACYANOLE CHLORIDE

Salt Concn., *M*	Critical Concn., *M*
Heptanoate in 5×10^{-5} *M* dye	
0	0.780
0.146	.728
.346	.691
.633	.633
1.08	.542
1.72	.430
2.38	.340
2.80	.280
Heptanoate in 2.5×10^{-5} *M* dye	
0	0.670
0.066	.662
.154	.617
.289	.577
.407	.543
.522	.522
.728	.485
1.08	.430
1.50	.374
1.79	.335
2.00	.307
2.28	.285
2.45	.263
2.64	.247
2.76	.230
2.91	.218
Octanoate in 5×10^{-5} *M* dye	
0	0.400
0.075	.376
.309	.309
.530	.265
.865	.216
1.22	.175
1.52	.152
2.22	.111
2.73	.091
2.97	.085
3.20	.080
Nonanoate in 5×10^{-5} *M* dye	
0	0.200
0.037	.187
.087	.175
.159	.159
.278	.139
.461	.115
.677	.097
.855	.086
1.29	.064
1.63	.054
1.92	.948
2.11	.042
2.39	.040
2.64	.038
2.88	.036
3.27	.033
Decanoate in 5×10^{-5} *M* dye	
0	0.0998
0.0105	.0949
.0229	.0917
.0379	.0885
.0559	.0838
.0787	.0787
.110	.0731
.151	.0645
.227	.0568
.344	.0469
.386	.0429
Undecanoate in 5×10^{-5} *M* dye	
0	0.0492
0.0048	.0478
.0144	.0456
.0187	.0437
.0273	.0409
.0386	.0386
.0534	.0356
.0764	.0327
.103	.0294
.133	.0266
.169	.0242
.216	.0216
.287	.0191
.403	.0161
.506	.0145
.642	.0128
.830	.0111
1.01	.0101
1.18	.0094
1.35	.0090
1.52	.0087
1.70	.0085
2.01	.0081
2.22	.0074
Tridecanoate in 5×10^{-5} *M* dye	
0	0.0126
0.00134	.0121
.00291	.0116
.00478	.0112
.00706	.0106
.00929	.00929
.0134	.00892
.0156	.00842
.0187	.00800
.0251	.00717
.0276	.00690
.0327	.00654
.0411	.00587
.0529	.00529
.0616	.00492
.0913	.00406
.116	.00357
.144	.00319
.169	.00294
.194	.00277
.216	.00262
.241	.00253
.268	.00238
.312	.00227

sharper with increasing concentration of salt. Computation of C_μ again was made by means of

$$C_\mu = V_A M_A / V_T \qquad (2)$$

in which V_A and M_A are the initial volume and molarity of the soap solution, and V_T the sum of the volumes of all solutions added up to the end point. Calculation of the concentration of salt, C_S, at the end-point was made in a like manner.

Results

The variation of critical concentration with added potassium chloride has been determined for six potassium soaps: heptanoate, octanoate, nonanoate, decanoate, undecanoate and tridecanoate. The measurements for the dodecanoate made by Corrin and Harkins[15] were not repeated. The new data are recorded in Table I. The values for the first four soaps are plotted in Fig. 1, which shows that the initial effect of added salt increases with lengthening of the carbon chain. Figures 2 and 3 illustrate in greater detail the very rapid initial drop of C_μ as a function of C_S that is exhibited by the eleven and thirteen carbon soaps. In all cases studied, the absolute value of dC_μ/dC_S was found to be a decreasing function of C_S. Most of the decrease in C_μ occurs before C_S reaches 25 C_μ. It is significant[17] that with added alcohol, either in the absence of salt or in the presence of a constant concentration of salt, the value of dC_μ/dC_a, where C_a is the molarity of added alcohol, is a linear function of C_a and is independent of C_S.

Plots of log C_μ as a function of log C_i are shown in Figs. 4 to 10. It is seen that the relationship is linear for all soaps at relatively low normalities of counterion. Departure from linearity was demonstrated for five of the systems, which were studied to relatively high concentrations of added salt. The parameters of equation (1) were computed for the linear portions of the plots from the data in Table I by the method of least squares. The results are collected in Table II, together with values for the dodecanoate obtained by Corrin and Harkins.[15] The maximum ratio of equivalents of

TABLE II

VALUES OF PARAMETERS IN LOG $C_\mu = a + b$ LOG C_i FOR POTASSIUM *n*-ALKANECARBOXYLATES

Number of carbon atoms	Molarity of pinacyanole $\times 10^5$	*a*	*b*
7	5	−0.160	−0.565
7	2.5	− .270	− .568
8	5	− .641	− .621
9	5	−1.068	− .532
10	5	−1.561	− 562
11	5	−1.990	− .521
12	5	−2.617	− .570[a]
13	5	−2.937	− .538

[a] From data of Corrin and Harkins.[15]

(17) S. H. Herzfeld, M. L. Corrin and W. D. Harkins, THIS JOURNAL **54**, 271 (1950).

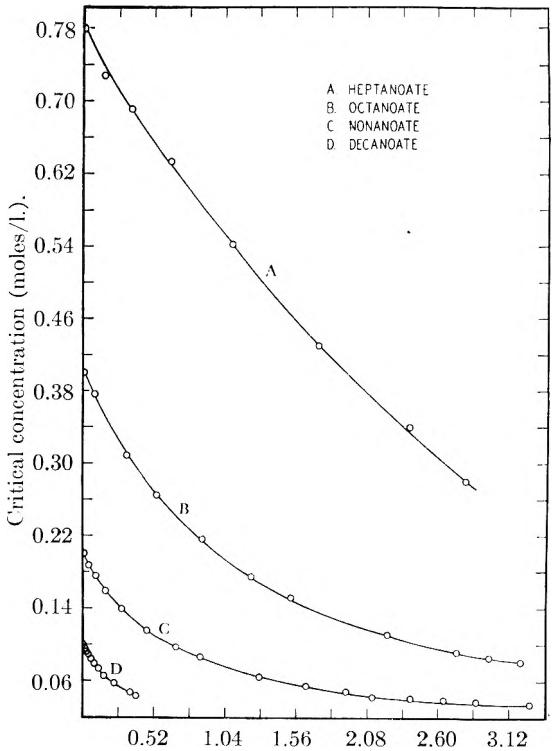

Fig. 1.—Plots of the critical concentrations of four potassium *n*-alkanecarboxylates showing the relative effect of added salt at 25° in 5×10^{-5} molar pinacyanole.

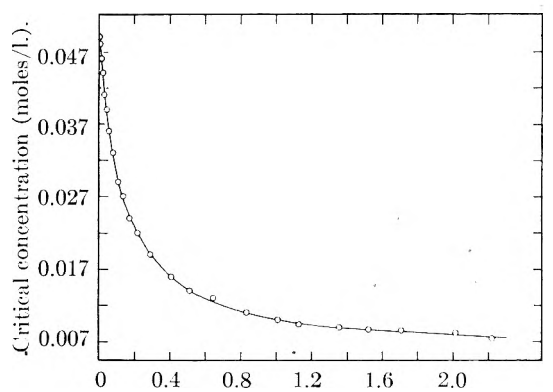

Fig. 2.—Variation of the critical concentration of potassium undecanoate with added salt at 25° in 5×10^{-5} molar pinacyanole.

salt to equivalent weights of soap that falls on a straight line rises from about 4 for the heptanoate to more than 140 for the tridecanoate. The actual maximum salt concentration, however, drops from 1.7 to 0.3 normal. The cause for the departure from linearity is not known to the writer. It is possible that linearity ceases when coalescence of micelles into microcrystals begins.

It is significant that the values of a show a definite trend with increase in chain length, whereas b appears to be essentially independent of the carbon content in the homologous series investigated. The arithmetic mean of b for the seven soaps is -0.560 ± 0.022. The variations in the slope of the straight line from the mean value show no trend and are compatible with the limits of accuracy

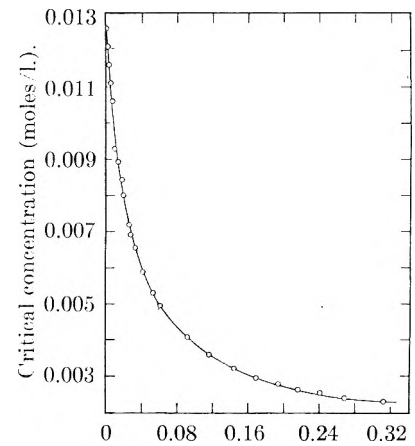

Fig. 3.—Variation of the critical concentration of potassium tridecanoate with added salt at 25° in 5×10^{-5} molar pinacyanole.

of the titrimetric method applied to different members of a homologous series. The determinations with a single soap exhibit much smaller deviations from the best straight line.

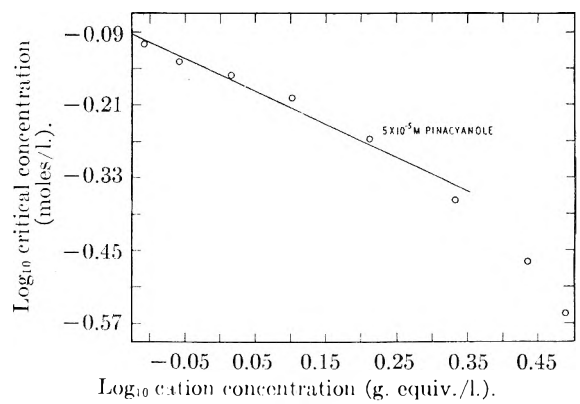

Fig. 4.—Linear logarithmic relation between critical concentration of potassium heptanoate and total counterion concentration at 25° in 5×10^{-5} molar pinacyanole.

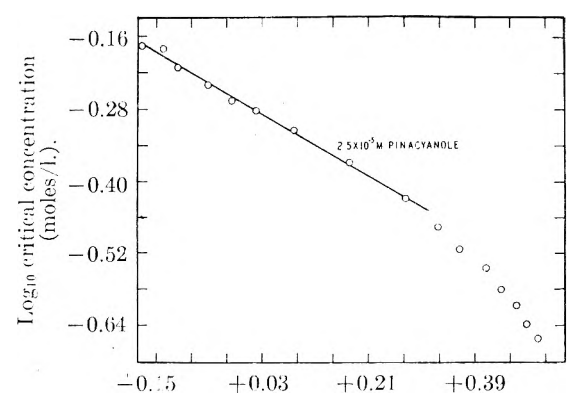

Fig. 5.—Linear logarithmic relation between critical concentration of potassium heptanoate and total counterion concentration at 25° in 2.5×10^{-5} molar pinacyanole.

Discussion

All measurements of equivalent conductivity have shown that ionic compounds containing large water-insoluble organic groups behave as typical

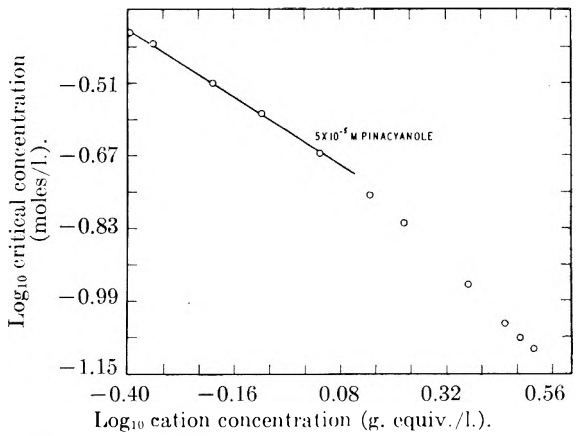

Fig. 6.—Linear logarithmic relation between critical concentration of potassium octanoate and total counterion concentration at 25° in 5 × 10^{-5} molar pinacyanole.

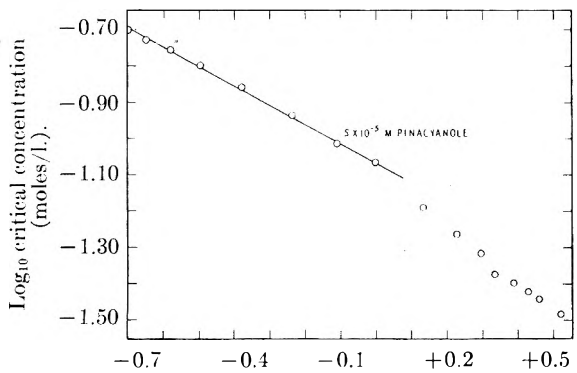

Fig. 7.—Linear logarithmic relation between critical concentration of potassium nonanoate and total counterion concentration at 25° in 5 × 10^{-5} molar pinacyanole.

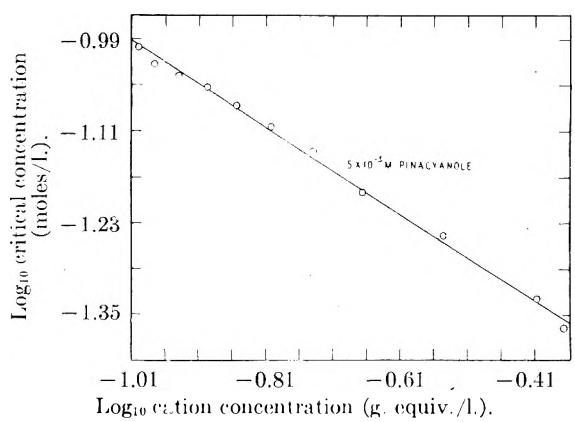

Fig. 8.—Linear logarithmic relation between critical concentration of potassium decanoate and total counterion concentration at 25° in 5 × 10^{-5} molar pinacyanole.

strong electrolytes at concentrations below their respective critical values. In dilute solutions of strong electrolytes, when the interionic potential energy is small in comparison to the average thermal energy, the repulsion between ions of like sign rises with increase in the magnitude of the charge in the manner prescribed by the principle of ionic strength and the more inclusive Debye–Hückel theory. With the onset of aggregation in solutions of long-chain electrolytes, the charge on one ion undergoes a manifold increase; and the interionic potential

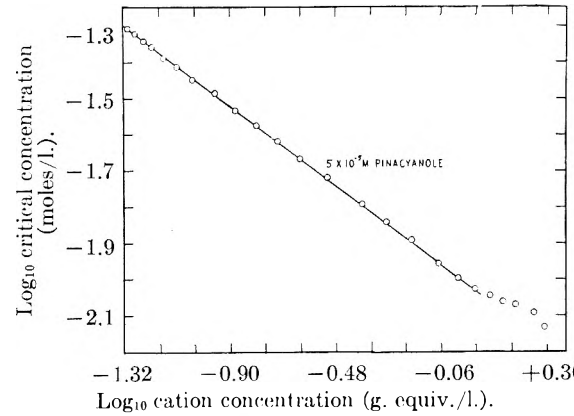

Fig. 9.—Linear logarithmic relation between critical concentration of potassium undecanoate and total counterion concentration at 25° in 5 × 10^{-5} molar pinacyanole.

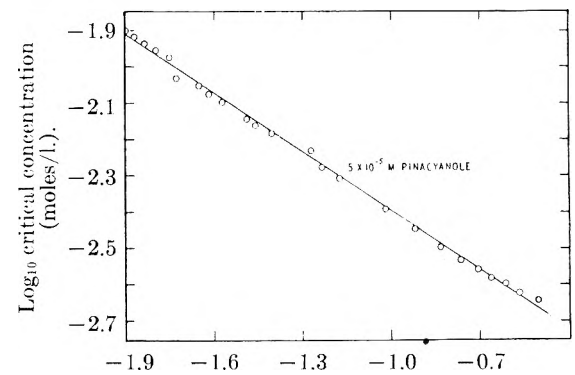

Fig. 10.—Linear logarithmic relation between critical concentration of potassium tridecanoate and total counterion concentration at 25° in 5 × 10^{-5} molar pinacyanole.

energy is no longer much less than the average thermal energy. Furthermore, the large potential thus established on the surface of a micelle repulses added salt ions of like sign so strongly that the concentration of the latter on the surface of the micelle becomes insignificant. Debye[18] has computed that this concentration is no more than 3 × 10^{-4} of that in the bulk of the solution. The magnitude of the charge on unaggregated ions of the same sign as the micelles acquires much less significance than before aggregation, therefore; and the influence of added salt is governed by the sum total of ionic charges rather than by the quantity of charge on individual ions bearing the same sign as the micelles.

The composition or valence of salt ions of unlike sign of charge to that of the long-chain ion, however, may have a profound effect on the stability of the micelle. It has been demonstrated by Lottermoser and Püschel[19] and by Samis and Hartley[20] that the tendency of negative long-chain ions to micellize rises markedly with increase in the valence of the counterion. With positive long-chain ions, Samis and Hartley were able to find only insignificant variations in the critical concentration with change in the valence and composition of the coun-

(18) P. Debye, THIS JOURNAL, **53**, 1 (1949).

(19) A. Lottermoser and F. Püschel, *Kolloid Z.*, **63**, 175 (1933).

(20) C. S. Samis and G. S. Hartley, *Trans. Faraday Soc.*, **34**, 1305 (1938).

terion. Recent work by Kraus and co-workers,[21,22] however, has demonstrated for several quaternary ammonium and pyridinium salts a very marked effect of the constitution of the counterion upon the critical concentration. In a group of five *n*-octadecyltrimethylammonium salts, four of which were of the uni-univalent type, the critical concentration varied more than fourfold, with the lowest value being exhibited by the oxalate. On the basis of available data, therefore, no correlation can be drawn between the critical concentration of a cationic long-chain electrolyte and the valence of the anion associated with it. Possibly the influence of valence exists but is masked by a stronger force.

The parameter a in equation (1) has been given a meaning recently by Hobbs,[2] who adopts the view that the micelle is a double layer of long-chain molecules of approximately cylindrical symmetry, with the polar groups oriented in the flat surfaces of the disk-shaped structure. Hobbs deduces that a is a function of both the energy of micelle formation and the thermal energy of the solute. He supports the view of Debye[18] that the effect of salt on the critical concentration is associated with an increase in the number of molecules per micelle.

The slope of the line given by equation (1) has been interpreted by Corrin[3] to represent the ratio of the number of attached counterions to the number of long-chain ions in the micelle at the critical concentration. Corrin makes no assumption regarding the shape of the micelle, and treats the effect of added salt on C_μ by a direct application of the mass law to the equilibrium between the unassociated long-chain ions and counterions, and the aggregates. Corrin argues that the micelle content is unchanged by the addition of salt and shows that the value of b should be independent of the concentration of counterion, of the valences of the two kinds of ions composing the micelle, and, in the case of a homologous series of long-chain electrolytes, of the chain-length. The first and third of these statements are not in disagreement with the findings of the present report. The other remains to be tested.

Acknowledgment.—The kindly guidance and inspiration given the author during this and the previous investigation by the late Professor William Draper Harkins are recognized gratefully. The pursuance of the work was facilitated greatly also by the constructive criticisms freely offered by Dr. M. L. Corrin.

(21) E. C. Evers and C. A. Kraus, *J. Am. Chem. Soc.*, **70**, 3049 (1948).

(22) P. F. Grieger and C. A. Kraus, *ibid.*, **70**, 3803 (1948).

FOAMING OF NON-IONIC SURFACE ACTIVE AGENTS

By Manuel N. Fineman, George L. Brown and Robert J. Myers

Research Laboratories, Rohm and Haas Co., Philadelphia, Pa.

Received September 27, 1951

The foaming properties of non-ionic surface active agents vary markedly with the temperature of the test and with the solubility of the surfactants as characterized by their cloud points. The principal effect of temperature is that of altering the solubilities. An attempt has been made to deduce information concerning the shapes of their ethylene oxide distribution curves from analysis of their foaming behavior.

Non-ionic surface active agents have become widely available only within the past decade. Because of their comparatively recent origin, the literature contains relatively few accounts of their properties, in contrast to the voluminous investigations reported for soap and synthetic ionic surface active compounds.

The reaction of ethylene oxide with an alcohol or phenol is capable of producing a spectrum of non-ionic surface active materials. For a given alcohol or phenol, the hydrophilic nature is increased as the polyoxyethylene chain is lengthened; and for a specific polyoxyethylene chain the hydrophobic nature increases with the length of the hydrocarbon base.

In view of a lack of published reports on the subject, the foaming of aqueous solutions of several materials of this type has been examined. The compounds studied in greatest detail were those obtained from reaction of *p-t*-octylphenol with ethylene oxide. The prototype molecule may be represented by the symbol OPE_x, where x represents the average number of moles of ethylene oxide. The foam of homologous compounds containing longer aliphatic chain substituents on the aromatic nucleus was also examined briefly.

In view of the nature of the reaction of ethylene oxide with the various organic groups, the molecular weight must be regarded only as a number average. Presumably the molecular weight distribution could be calculated by the method of Flory.[1]

As opposed to colloidal electrolytes, for which the solubility in water increases with increasing temperature, these ethylene oxide polymers are insolubilized as the temperature is raised, presumably as the result of loss of water associated with the hydrophilic ether linkages in the chain. Upon heating, a dilute aqueous solution becomes turbid at a definite temperature known as the cloud point. The cloud point is substantially constant for solutions of 0.5 to 10% concentration,[2] and measurements are customarily conducted on 1% solutions. Compounds of the OPE_x series in which x is 6 or less are very hydrophobic, and since they are in-

(1) P. J. Flory, *J. Am. Chem. Soc.*, **62**, 1561 (1940).

(2) J. M. Cross, Official Proceedings, 36th Mid-Year Meeting, Chemical Specialties Manufacturing Association.

soluble in water at all temperatures, they do not have a measurable cloud point. As x is varied between 7 and 15 the cloud point ranges from room temperature to 100°, and where x is greater than 15 the compounds are so hydrophilic that their aqueous solutions remain clear even at the boiling temperature. Where it can be measured, the cloud point may be used as an index of the balance of the hydrophilic and hydrophobic properties in these non-ionics.

The importance of the concept of the cloud point in connection with selection of materials with optimum wetting and detergency has been discussed by Cross.[2]

Cohen[3] has studied the effect of the hydrocarbon chain length on solubility for a series of ethylene oxide adducts of aliphatic alcohols. He has shown that butanol requires addition of 0.8 mole of ethylene oxide to form a water soluble product, and for each succeedingly higher alcohol, an additional mole of ethylene oxide is needed to maintain water solubility. Apparently the hydrophilic character of an ethylene oxide group is just enough to balance the hydrophobic character of an additional $-CH_2-$ group in the hydrocarbon chain.

A number of studies have indicated that non-ionic surface active agents are effective solubilizers.[4,5] These materials are of limited efficiency in dispersing and suspending solid particles.[6-9]

Apparatus.—The foaming properties of the non-ionics were examined in the Ross and Miles Pour Apparatus.[10] The procedure involves release of a fixed volume of detergent solution from a pipet set at a given height above a lesser amount of the solution contained in a thermostatic graduated cylinder and measurement of the volume of the foam thus produced. Results are expressed as foam heights in a cylinder of uniform diameter. Since this test is simple and rapid, and the results are very reproducible, it is currently under consideration as an A.S.T.M. standard. It permits examination of foam and foam stability at any desired temperature and is limited only by the temperature range of the circulating medium.

Foam of OPE$_x$ Series.—Figure 1 shows the foam heights obtained with 1% solutions of members of the OPE$_x$ series when examined at 120°F., (49°) the standard temperature of the Ross and Miles test.

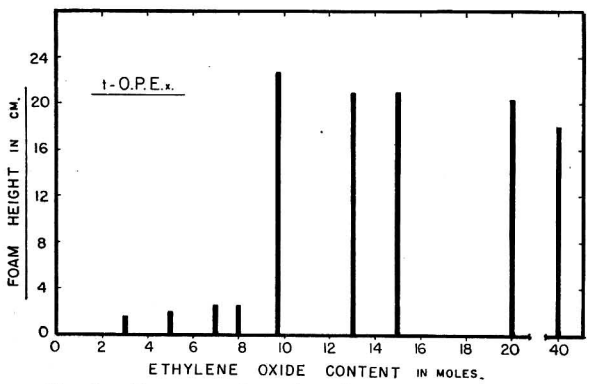

Fig. 1.—Foam as a function of composition at 49°.

(3) M. Cohen, *Compt. rend.*, **226**, 1366 (1948).
(4) A. A. Green and J. W. McBain, THIS JOURNAL, **51**, 286 (1947).
(5) R. C. Merrill, *ibid.*, **54**, 482 (1950).
(6) R. C. Merrill and R. Getty, *ibid.*, **54**, 489 (1950).
(7) L. Greiner and R. D. Vold, *ibid.*, **53**, 67 (1949).
(8) T. M. Doscher, *ibid.*, **53**, 1362 (1949).
(9) R. D. Vold and C. C. Konecny, *ibid.*, **53**, 1262 (1949).
(10) J. Ross and G. D. Miles, *Oil & Soap*, **18**, 99 (1941).

The lower analogs produced very little foam at this temperature; whereas the higher analogs, containing more than 8 moles of ethylene oxide, produced appreciable foam. Moreover, among the latter, foam did not seem to vary much with ethylene oxide content.

This abrupt transition in foam height was also noted at lower concentrations although the foam produced by the higher analogs was slightly less.

Correlation of Foam with Cloud Point.—Figure 2 shows that the unusually abrupt transition in foam properties observed for members of the OPE$_x$ series was also noted when the foam of similar non-ionics was examined. Analogs of the OPE$_x$ series containing 9 and 12 branched chain carbon atoms (*i.e.*, *t*-C_9PE_x and *t*-$C_{12}PE_x$) showed a similar behavior as did also the series of non-ionics based upon lauryl alcohol (*n*-$C_{12}E_x$).

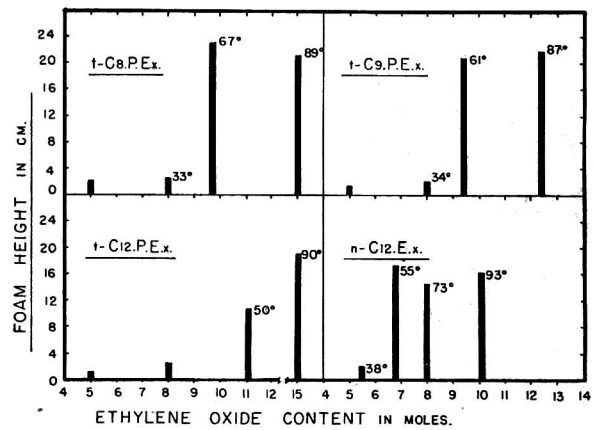

Fig. 2.—Foam as a function of composition at 49°.

The cloud point of each compound is noted adjacent to the bar representing its foam height. Examination of these temperatures, and comparison with the temperature of the test, reveals that compounds with cloud points below the temperature of the test produced little or no foam; compounds with cloud points above it produced appreciable foam. Moreover in the case of one compound, *t*-$C_{12}PE_{11}$, whose cloud point almost coincided with the temperature of the test, an intermediate amount of foam was produced.

Foam as a Function of Temperature.—Since the temperature of the test appeared to be an important

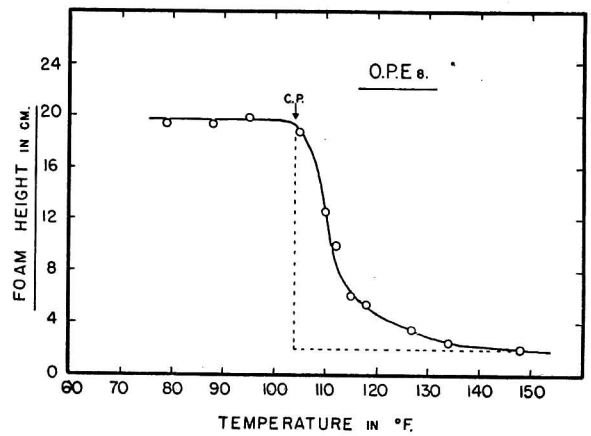

Fig. 3.—Foam as a function of temperature.

criterion which determined the amount of foam produced, the foaming properties of several members of a series were examined as a function of temperature.

As shown in Fig. 3, at temperatures below its cloud point, the foam height produced by OPE_8 was fairly constant and fairly high. However, at the cloud point (indicated by the arrow) the non-ionic started to precipitate out of solution and, as its solubility decreased with increasing temperature, the foam height decreased to less than one-tenth of the original value.

Since the Ross and Miles is essentially a "static" foam test, the above observations were checked by a "dynamic" method in which the solutions were stirred vigorously in a high speed mixer. This behavior was also obtained with other types of non-ionics. In general, at temperatures *below* the cloud point, foam of non-ionics may be appreciable; however, at temperatures *above* the cloud point, it is reduced markedly, often by a factor of 10.

Of theoretical interest is the fact that foam volume seems to be more dependent on the actual amount of surface active agent in solution rather than on its surface activity. Other work in this Laboratory has shown that the surface activity of aqueous solutions decreases with increased ethylene oxide content. For example, at 25° surface tension values rise from 29 dynes/cm. for a 1% dispersion of OPE_5 to 42 for a 1% solution of OPE_{40}. These values change little with temperature in the range 25 to 75°.

Thus the materials which are least soluble have the greatest surface activity and are poorest in foam. However, it may be that a high concentration in solution is required in order to have an adequate amount of surfactant available for adsorption over the tremendous surface produced by the foam bubbles.

The data in Table I show that surface and interfacial activities do not change appreciably with temperature and show no abrupt transition even above the cloud point. Presumably, above the cloud point, molecules of the non-ionic are still present in an amount sufficient to adsorb at the surface of limited area used with the duNouy Tensiometer and depress the surface tension. This amount is quite inadequate over the much larger surface of a foam.

TABLE I

SURFACE AND INTERFACIAL ACTIVITIES AS A FUNCTION OF TEMPERATURE $OPE_{9.7}$ (CLOUD PT. 67°)

Concn., %	Surface tension 25°	50°	75°	Interfacial tension[a] 25°	50°	75°
1.0	30.4	29.3	28.1	1.2	1.3	5.2
0.3	30.2	29.0	28.1	2.0	..	..
.1	30.0	28.7	27.9	2.5	..	..
.03	29.7	28.7	27.8	4.2	..	..
.01	31.1	29.5	29.8	9.9	9.7	11.5
.003	39.4	35.7	35.2	17.2	..	..
.001	46.2	44.6	42.9	21.5	..	..

[a] Against mineral oil.

If OPE_8 were monodisperse, we anticipate that all of the sample would precipitate out of solution at the cloud point and foam would drop sharply to a low value. However, as has already been pointed out, these ethylene oxide adducts are polydisperse and contain many molecules which have less than, or more than, 8 ethylene oxide units per octylphenol group. If these concepts are correct, a measure of the ethylene oxide distribution for a given non-ionic can be deduced from the shape of its foam curve in the region of the cloud point.

If a rectangle is drawn with sides formed by the ordinate through the cloud point, and the abscissa through the point of minimum foam, the percentage area of this rectangle below the foam curve is a measure of the degree of molecular weight dispersion of the non-ionic. Compounds which tend to be monodisperse should have foam curves of steep slope with minimum area below the curve; compounds which tend to be polydisperse will have less steep curves and appreciable area below them.

For OPE_8, the percentage area below the curve was 22.4%. For another member of the series, $OPE_{9.7}$, the area was 26.7% (Fig. 4).

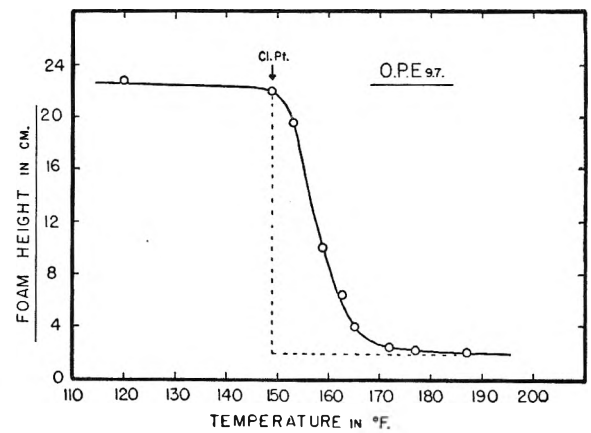

Fig. 4.—Foam as a function of temperature.

Where the polydisperse character of $OPE_{9.7}$ was artificially extended by addition of 10% of the lowest analog, OPE_1, the area below the foam curve increased to 29.0% of the reference rectangle (Fig. 5).

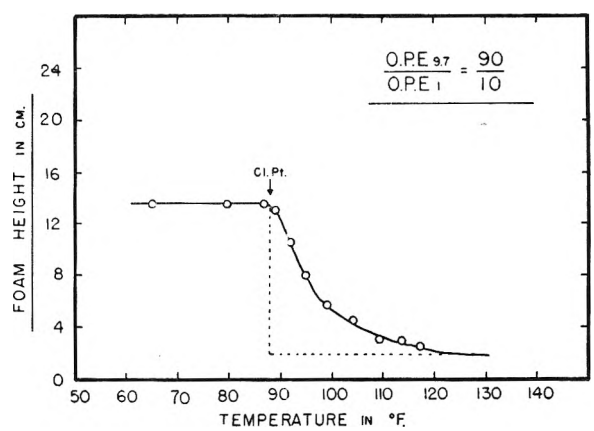

Fig. 5.—Foam as a function of temperature.

$OPE_{9.7}$ must contain a fairly large proportion of the lower analogs since, as shown by Fig. 6, addition of as much as 35% of OPE_5 did not alter the foam-temperature behavior of $OPE_{9.7}$ as much as might have been expected. However, it must be noted

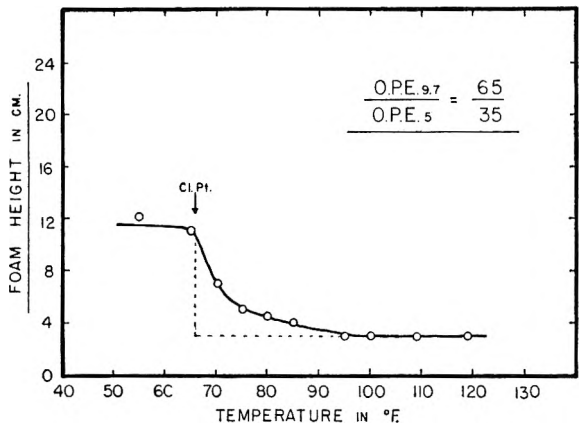

Fig. 6.—Foam as a function of temperature.

in this as well as in the preceding graph, that the addition of lower analogs caused an appreciable reduction in the amount of foam obtainable even at temperatures below the cloud point. Mutual solubilization of the various species doubtless complicates any interpretation.

These curves represent the shapes of the ethylene oxide distribution curves if the following assumptions hold true: (1) The cloud point depends linearly upon the ethylene oxide content. (2) The foam of each monodisperse species drops sharply to the minimum value with an infinitesimal temperature increase above its cloud point.

Since these curves are derived from analysis of foaming properties which in turn are a function of solubility, and the latter, in turn, is a function of ethylene oxide distribution, it is apparent that the curves have been obtained by a very devious procedure and are, therefore, subject to error. Consequently they should be interpreted with reservation. It may be possible to obtain much more accurate ethylene oxide distribution curves by fractionation of these compounds, or by examination of changes in turbidity as a function of temperature. Thus far, efforts at resolving these mixtures have proved unsuccessful. Mutual solubilization effects make solvent fractionations unattractive, and the low volatility makes fractional distillation difficult.

Acknowledgment.—The assistance of Mr. J. P. Scullin, who made the surface and interfacial tension measurements reported here, is gratefully acknowledged.

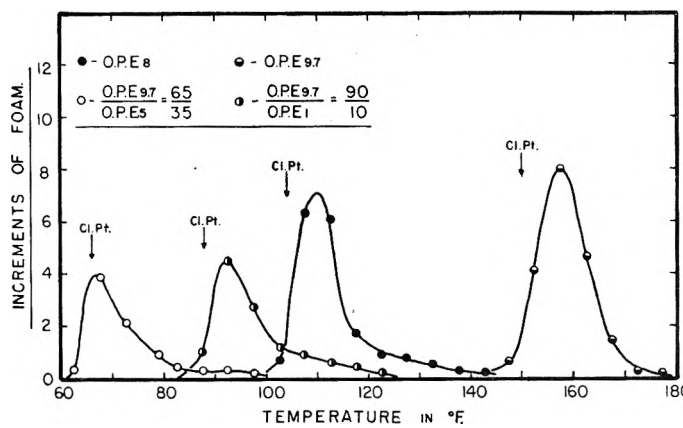

Fig. 7.—Ethylene oxide distribution curves.

Plotting increments of foam for a fixed increment of temperature, against temperature, the four preceding graphs may be redrawn as shown in Fig. 7.

REACTIONS OF ETHYL RADICALS

By K. J. Ivin,[1] M. H. J. Wijnen[2] and E. W. R. Steacie

Division of Chemistry, National Research Council, Ottawa, Canada

Received October 23, 1951

The reactions of ethyl radicals are reviewed with special emphasis on combination and disproportionation. It is concluded that existing data are compatible with activation energies of about zero for both reactions. Hydrogen abstraction by ethyl radicals is also reviewed, with the conclusion that the frequency factors of these reactions are similar to those for methyl radicals. The decomposition of the ethyl radical is also discussed.

Introduction

Recently quantitative data have been forthcoming on the reactions of methyl radicals, especially on the combination of methyls[3,4] and on hydrogen-abstraction reactions of the type[5-12]

$$CH_3 + RH = CH_4 + R$$

The reactions of ethyl radicals are in a much more uncertain state. This is due to two causes, the difficulty of finding a satisfactory source of ethyl radicals, and the greater complexity of their reactions even at low temperatures. With methyl radicals the only important types of reaction are hydrogen-abstraction and combination. With ethyl radicals decomposition and disproportionation occur as well. In the present paper it is proposed to review the information in the literature on these reactions, as well as certain new work which seems to lead to a more quantitative picture of the elementary reactions of ethyl radicals.

I. Disproportionation and Combination

Introduction.—When two identical radicals interact and disappear from a system with the formation of stable products two main types of reaction are possible, which for the ethyl radical may be represented by the equations

$$2C_2H_5 = C_2H_4 + C_2H_6 \quad \textit{disproportionation} \quad (1)$$

$$2C_2H_5 = C_4H_{10} \quad \textit{combination} \quad (2)$$

The relative ease of occurrence of the two processes seems to vary from radical to radical, and the evidence on the behavior of some of the more complex radicals has recently been collected by Melville and Valentine.[13] Reaction (1) is of the general hydrogen-abstraction type, and might therefore by analogy be expected to have an activation energy of 5–8 kcal. However, because of the formation of the double bond in C_2H_4 in the process it is far more exothermic than the usual reaction of the type

$$C_2H_5 + RH = C_2H_6 + R$$

where R is an alkyl radical. It is, therefore, quite possible that reaction (1) may have a very low activation energy.

Review of Earlier Work.—There has been a considerable divergence of opinion in the past over the prevalence of disproportionation. Original estimates of the relative importance of reactions (1) and (2) were made merely by the examination of the products of reactions in which ethyl radicals were supposed to participate, and the assumption that

$$\frac{\text{Rate of formation of } C_4H_{10}}{\frac{1}{2}\text{ rate of formation of } (C_2H_4 + C_2H_6)} = \frac{k_{\text{combination}}}{k_{\text{disproportionation}}}$$

Summaries of experiments which have been interpreted on this basis have been made by Moore and Taylor[14] and by Semerano, Riccoboni and Callegari.[15]

It is apparent from these reviews that there are large discrepancies in the relative amounts of C_4 and C_2 hydrocarbon produced in the reactions. It is, however, obvious and has been emphasized by Moore and Taylor, that a mere analysis of the products does not give a reliable estimate of the relative rates of the combination and disproportionation reactions. Especially in cases where the ethane produced is not equal to the ethylene it is evident that complicating processes are occurring. In particular account must be taken of processes of the type of reaction (3)

$$C_2H_5 + (C_2H_5)_2X = C_2H_6 + C_2H_5{\cdot}X{\cdot}C_2H_4 \quad (3)$$

The fact that ethane and ethylene are not always formed in equal amounts may be due to various complications, including: (i) Reaction (3) followed by a process in which the radical $C_2H_4{\cdot}X{\cdot}C_2H_5$ disappears without forming ethylene; (ii) $C_2H_5 + C_2H_4 = C_4H_9$, etc.

It is evident that no real information about the ratio k_1/k_2 can be obtained without a thorough investigation which establishes the mechanism of the particular reaction with reasonable certainty.

We will, therefore, confine our discussion to reactions in the gas phase, which in all probability involve ethyl radicals, and in which a reasonable correction may be made for the reactions of ethyl radicals with molecules other than themselves, or for subsequent reactions of the products of the disproportionation and combination reactions. These provisos immediately eliminate from further con-

(1) National Research Council of Canada Postdoctorate Fellow, 1948–1950.

(2) National Research Council of Canada Postdoctorate Fellow, 1949–1951.

(3) R. Gomer, *J. Chem. Phys.*, **18**, 998 (1950).

(4) D. M. Miller and E. W. R. Steacie, *ibid.*, **19**, 73 (1951).

(5) A. F. Trotman-Dickenson and E. W. R. Steacie, This Journal, **55**, 908 (1951).

(6) A. F. Trotman-Dickenson and E. W. R. Steacie, *J. Chem. Phys.*, **18**, 1097 (1950).

(7) A. F. Trotman-Dickenson and E. W. R. Steacie, *ibid.*, **19**, 163 (1951).

(8) A. F. Trotman-Dickenson and E. W. R. Steacie, *ibid.*, **19**, 169 (1951).

(9) A. F. Trotman-Dickenson and E. W. R. Steacie, *ibid.*, **19**, 329 (1951).

(10) L. M. Dorfman and W. A. Noyes, Jr., *ibid.*, **16**, 557 (1948).

(11) R. Gomer and W. A. Noyes, Jr., *J. Am. Chem. Soc.*, **71**, 3390 (1949).

(12) R. Gomer and W. A. Noyes, Jr., *ibid.*, **72**, 101 (1950).

(13) H. W. Melville and L. Valentine, *Trans. Faraday Soc.*, **46**, 210 (1950).

(14) W. J. Moore and H. S. Taylor, *J. Chem. Phys.*, **8**, 396 (1940).

(15) G. Semerano, L. Riccoboni and F. Callegari, *Ber.*, **74B**, 1297 (1941).

sideration a number of the reactions listed by Semerano, Riccoboni and Callegari[15] and by Moore and Taylor.[14] Thus the decomposition of sodium ethyl in ether was shown by Schorigin[16] to involve the solvent; and it is very doubtful whether the decomposition of certain ethyl cyanogold compounds to give butane involves ethyl radicals.[17] The decomposition of silver ethyl has only been studied in solution and has been stated by Bawn and Whitby[18] not to initiate the polymerization of styrene or methyl methacrylate, a fact which weighs against, though does not necessarily exclude, a radical mechanism. The thermal decompositions of the vapors of lead tetraethyl,[19] silicon tetraethyl[20] and germanium tetraethyl[21] have only been studied at high temperatures with a resulting diversity of products and intractability of data. In the photolysis of ethyl iodide[22] it appears that the disproportionation and combination reactions are negligible compared with other reactions of ethyl radicals so that it is not possible to make a reasonable correction for the latter.

The following gas phase reactions, however, almost certainly involve ethyl radicals to some degree, and reliable data exist, which, when combined with reasonable assumptions, enable one to estimate the relative rates of the disproportionation and combination reactions.

The Photolysis of Mercury Diethyl.—The photolysis of mercury diethyl has recently been investigated by Ivin and Steacie.[23] The products of the reaction were almost entirely ethylene and ethane in equal amounts, and butane. Figure 1 gives a plot of the $^1/_2C_2/C_4$ ratio against pressure at various temperatures. The fact that the ratio is pressure dependent means that in addition to combination and disproportionation of ethyl radicals, there must occur reactions involving the attack of an ethyl radical on a molecule of mercury diethyl.

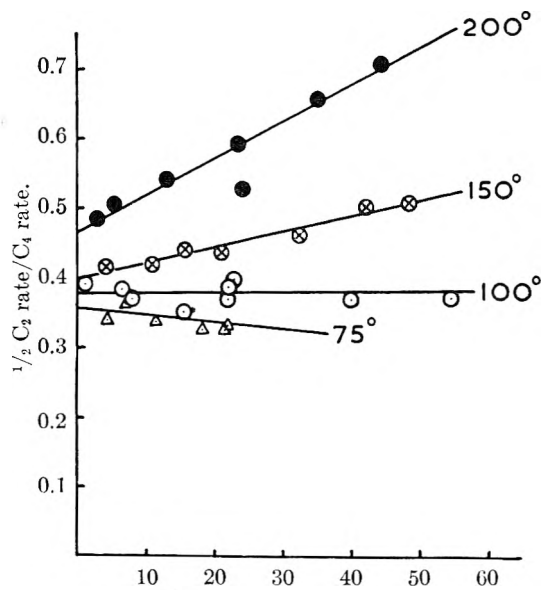

Fig. 1.—Photolysis of mercury diethyl at various temperatures and pressures.

The results are well fitted by the mechanism

$$Hg(C_2H_5)_2 + h\nu = Hg + 2C_2H_5 \qquad \phi_a I_a$$
$$2C_2H_5 = C_2H_6 + C_2H_4 \qquad (1)$$
$$2C_2H_5 = C_4H_{10} \qquad (2)$$
$$C_2H_5 + Hg(C_2H_5)_2 = C_2H_4 + C_2H_6 + Hg + C_2H_5 \qquad (3)$$

A further unidentified reaction producing butane at a rate proportional to the pressure and incident intensity also occurs to a slight extent. The assumption is made that the entire reaction proceeds *via* the formation of radicals. This is justified by the fact that the energy of light absorbed is not less than 95 kcal. per mole while the sum of the two Hg–C bonds is only about 40 kcal. per mole.

The usual steady-state treatment of the above mechanism gives

$$\frac{d([C_2H_4] + [C_2H_6])}{dt} = \frac{2k_1\phi_a I_a}{k_1 + k_2} + \frac{2k_3[Hg(C_2H_5)_2](\phi_a I_a)^{1/2}}{(k_1 + k_2)^{1/2}}$$
$$\frac{d[C_4H_{10}]}{dt} = \frac{k_2\phi_a I_a}{k_1 + k_2}$$
$$[d(^1/_2C_2)/d(C_4)]_{p=0} = k_1/k_2$$

From the temperature coefficient of the intercepts in Fig. 1 at zero pressure $E_1 - E_2$ can be obtained, and from the slope of the line when the C_2 rate is plotted against pressure E_3 can be obtained. In this way, it is found that

$$E_1 - E_2 = 0.8 \pm 0.2 \text{ kcal.}$$
$$A_1 \approx A_2$$
$$P_3 \approx 1.3 \times 10^{-4}$$

Rotating sector experiments (see later) at 150° show that E_2, the energy of activation of the combination reaction, cannot be greater than 0.65 kcal. per mole, while the steric factors P_1 and P_2 are not smaller than 0.1.

Only slight effects could be detected on varying the frequency of absorbed light, the proximity of surface and the amount of excess inert gas. It may be safely said that the combination reaction does not normally require the presence of a third body.

It should be noted from Fig. 1 that the ratio k_1/k_2 can only be obtained from the intercepts, and a mere determination of the products at some arbitrarily chosen pressure can give quite false results.

The results of Moore and Taylor[14] on the photolysis of mercury diethyl and zinc diethyl are not sufficiently detailed to permit correction for side reactions.

The Photolysis of Diethyl Ketone.—This reaction was studied by Dorfman and Sheldon[24] using 3130 Å. at low intensity. The kinetics conform to the mechanism

$$(C_2H_5)_2CO + h\nu = 2C_2H_5 + CO \qquad (0)$$
$$2C_2H_5 = C_2H_4 + C_2H_6 \qquad (1)$$
$$2C_2H_5 = C_4H_{10} \qquad (2)$$
$$C_2H_5 + (C_2H_5)_2CO = C_2H_6 + C_2H_5COC_2H_4 \qquad (3)$$
$$C_2H_5 + C_2H_5COC_2H_4 = C_2H_5COC_4H_9 \qquad (4)$$
$$2C_2H_5COC_2H_4 = (C_2H_5COC_2H_4)_2 \qquad (5)$$

(16) P. Schorigin, *Ber.*, **53**, 1931 (1910).
(17) A. Burawoy, C. S. Gibson and S. Holt, *J. Chem. Soc.*, 1024 (1935).
(18) C. E. H. Bawn and F. J. Whitby, *Faraday Soc. Discussion*, **2**, 228 (1947).
(19) R. N. Meinert, *J. Am. Chem. Soc.*, **55**, 979 (1933).
(20) C. E. Waring, *Trans. Faraday Soc.*, **36**, 1142 (1940).
(21) R. L. Geddes and E. Mack, *J. Am. Chem. Soc.*, **52**, 4372 (1930).
(22) W. West and L. Schlessinger, *ibid.*, **60**, 961 (1938).
(23) K. J. Ivin and E. W. R. Steacie, *Proc. Roy. Soc. (London)*, **A208** 25 (1951).
(24) L. M. Dorfman and Z. D. Sheldon, *J. Chem. Phys.*, **17**, 511 (1949).

The assumption is made that the entire photolysis proceeds *via* the formation of radicals. This assumption is less easy to justify than in the case of the mercury diethyl photolysis since the energy of the radiation is rather less than the sum of the two C_2H_5–CO bond energies. It has been shown by Blacet and his co-workers[25] that in analogous photolyses of aldehydes an appreciable amount of reaction occurs by intramolecular processes. Assuming that such processes may be neglected, Dorfman and Sheldon derive by an extrapolation to infinite intensity the following values of k_1/k_2

T, °C.	56.6	120.3
k_1/k_2	0.25	0.82

However, these values are subject to considerable error, particularly at the upper temperature, owing to the uncertainties in the extrapolation. The value of $E_1 - E_2 = 4.8$ kcal. per mole derived from these two values is probably in error by rather more than the 1.5 kcal. per mole suggested by Dorfman and Sheldon.

Ells and Noyes give[26] details of four experiments at room temperature, two using a full aluminum spark and two using 1850–2000 Å., in which butane and equal amounts of ethylene and ethane are formed. The intensity appears to be sufficiently high that reactions (3), (4) and (5) can be neglected. The values of k_1/k_2 obtained from the $^1/_2C_2/C_4$ rate ratio are 0.23 and 0.25 for the first two experiments and 0.13 and 0.30 for the latter two.

Much more detailed investigations of the photolysis of diethyl ketone over the temperature range 25 to 300° have recently been made at Ottawa and at Rochester, and the results have been published in a joint paper by Kutschke, Wijnen and Steacie.[27] The results are in general agreement with the mechanism of Dorfman and Sheldon, but deviations at high temperatures necessitate the inclusion also of the reaction

$$C_2H_5COC_2H_4 = C_2H_4 + CO + C_2H_5 \qquad (6)$$

The mechanism is thus essentially similar to that for mercury diethyl except that the pentanonyl radical has some considerable stability. From the above mechanism the following relationships can be derived, if reactions (4), (5) and (6) are neglected

$$\frac{R_{C_2H_6} - R_{C_2H_4}}{R_{C_4H_{10}}} = \frac{k_2[C_2H_5COC_2H_5]}{k_2^{1/2}R_{C_2H_{10}}^{1/2}}$$

$$\frac{R_{C_2H_6} + R_{C_2H_4}}{R_{C_4H_{10}}} = \frac{2k_1}{k_2} + \frac{k_3[C_2H_5COC_2H_5]}{k_2^{1/2}R_{C_4H_{10}}^{1/2}}$$

$$\frac{R_{C_2H_4}}{R_{C_4H_{10}}} = k_1/k_2$$

Variations of concentration and of intensity show the validity of these relationships at low temperatures. At higher temperatures deviations occur because of (6), but to a good approximation these can be neglected. From the results at various temperatures the following values are obtained

$$E_1 = E_2 = 0$$
$$E_3 = 7.4 \text{ kcal.}$$
$$P_3 \approx 2.5 \times 10^{-4}$$

There thus seems to be good agreement between the results for diethyl ketone and for mercury diethyl. There is, however, one pronounced discrepancy. From the results with mercury diethyl, the values of the k_1/k_2 ratios are

T, °C.	75	100	150	200
k_1/k_2	0.36	0.38	0.40	0.46

The values for the corresponding ratios from diethyl ketone are approximately 0.10 ± 0.02 independent of temperature. It is possible that energy carry-over from the primary step in the case of mercury diethyl might be the cause of the discrepancy.

The Mercury Photosensitized Hydrogenation of Ethylene.—This reaction was studied by LeRoy and Kahn,[28] who suggested the mechanism

$$C_2H_4 + H = C_2H_5 \qquad (0)$$
$$2C_2H_5 = C_2H_4 + C_2H_6 \qquad (1)$$
$$2C_2H_5 = C_4H_{10} \qquad (2)$$
$$C_2H_5 + H_2 = C_2H_6 + H \qquad (3)$$

Reaction (3) only becomes important above 200°. While it is possible in principle to allow for reaction (3) by extrapolation to zero hydrogen pressure, the data in this paper are not sufficient to enable this to be done with any confidence. The following values of k_1/k_2 have been obtained from the C_2H_6/C_4H_{10} ratio. The scatter is quite large. The value of 25° is taken from the data of Moore and Taylor.[14]

T°C.	k_1/k_2
42	0.44, 0.61, 0.22, 0.28
200	0.45, 0.49
25	0.17

The Mercury Photosensitized Decomposition of Ethane.—This reaction is believed to proceed by the mechanism[29]

$$Hg^* + C_2H_6 = Hg + C_2H_5 + H \qquad (0)$$
$$2C_2H_5 = C_2H_4 + C_2H_6 \qquad (1)$$
$$2C_2H_5 = C_4H_{10} \qquad (2)$$
$$H + C_2H_6 = C_2H_5 + H_2 \qquad (3)$$
$$H + C_2H_5 = C_2H_6^* \qquad (4)$$
$$C_2H_6^* = 2CH_3 \qquad (5)$$
$$C_2H_6^* + M = C_2H_6 + M \qquad (6)$$
$$CH_3 + H = CH_4 \qquad (7)$$

Darwent and Steacie were unable to detect any ethylene in the products and did not include the disproportionation reaction (1) in their scheme. However, it must undoubtedly occur under the conditions of the experiments and the absence of ethylene is to be accounted for by the occurrence of the very fast reaction

$$C_2H_4 + H = C_2H_5 \qquad (8)$$

At high pressures methane formation is negligible and on calculating the stationary concentration of ethylene from reactions 0, 1, 2, 3 and 7 we find it to be $(k_1k_3/k_2k_7)(C_2H_6)$, while the limiting quantum yield of hydrogen at high pressures is given by $1/(1 + k_1/k_2)$. At room temperature k_1/k_2 is about 0.2 while k_3k_7 is probably of the order 0.01. Hence the stationary concentration of ethylene will be only about 0.2% of that of the ethane. The cal-

(25) F. E. Blacet, THIS JOURNAL, **52**, 534 (1947).

(26) V. R. Ells and W. A. Noyes, Jr., *J. Am. Chem. Soc.*, **61**, 2492 (1939).

(27) K. O. Kutschke, M. H. J. Wijnen and E. W. R. Steacie, *ibid.*, **74**, 714 (1952).

(28) D. J. Leroy and A. Kahn, *J. Chem. Phys.*, **15**, 816 (1947).

(29) B. deB. Darwent and E. W. R. Steacie, *ibid.*, **16**, 381 (1948).

culated limiting quantum yield of hydrogen is about 0.8 which is quite compatible with the data of Darwent and Steacie. Recent experiments by Darwent[30] indicate that ethylene *is* formed in the reaction.

The Reaction of Ethyl Iodide with Sodium Vapor.—This reaction has been studied by Bawn and Tipper[31] using the Polanyi flame technique. Under the conditions of the experiments it appears that the reaction between ethyl radicals and ethyl iodide (which is very marked in the photolysis of ethyl iodide) is relatively slight. Partial polymerization of the ethylene occurs so that k_1/k_2 is best given by the ratio C_2H_6/C_4H_{10}. The values calculated from the data in which nitrogen is used as the carrier gas are scattered at random between 1.71 and 2.21 for the temperature range 300–367°. The mean of 8 values is 1.85. In the presence of hydrogen as carrier gas one would expect the reactions $C_2H_5 + H_2 = C_2H_6 + H$ and $C_2H_4 + H = C_2H_5$ to occur readily with a net increase in the C_2H_6/C_4H_{10} ratio. In actual fact little change can be detected.

Attention must be drawn to the fact that although this is a gas phase reaction, one of the products, sodium iodide, condenses in the reaction zone. Hence, the radical reactions may occur wholly or in part on the surface thus formed and we may expect deviations from the results obtained for the purely homogeneous reactions.

Propionaldehyde and Methyl Ethyl Ketone.—Recent work by Pitts and Blacet[32] on the photolysis of propionaldehyde yields a value of approximately 0.1 for the ratio k_1/k_2 at room temperature.

The ratio of $R_{C_2H_4}/R_{C_4H_{10}}$ in the photolysis of methyl ethyl ketone by the same authors gives a value slightly less than 0.2 at low temperatures and increases with temperature in a manner similar to diethyl ketone. A value of 0.1 to 0.2 and a reaction analogous to reaction (4) in the diethyl ketone photolysis gives a reasonable explanation of the results.

Discussion

If the values of log k_1/k_2 obtained from the various reactions are plotted against reciprocal temperature, it is found that while there is general agreement as to the order of magnitude of the k_1/k_2 values, detailed agreement is not good. There is, however, a general negative slope corresponding to $E_1 > E_2$ as expected. It is probable that some of the discrepancies are due to inadequate allowance for the effect of side reactions. The cases in which there is a lack of internal consistency clearly require reinvestigation. It is possible that even after full allowance for side reactions we may still be left with different k_1/k_2 values at a given temperature, for the following reason. When first formed, the ethyl radicals will possess varying amounts of energy depending on the energetics of the primary process. If any of this excess energy is retained until the collision of two ethyl radicals, we may expect an increase in k_1/k_2 for two reasons. Firstly, the effective energy of activation of disproportionation will be reduced and secondly, though probably less important, there will be an increased probability of redissociation of freshly formed butane molecules. There is some evidence of a slight "hot radical" effect in the photolysis of mercury diethyl, but the effects reported are too small to be conclusive.

Finally we may make some remarks on the mechanism of the disproportionation reaction. It seems likely that one ethyl radical removes a methyl hydrogen rather than a methylene hydrogen from a second ethyl radical; that is, combination is favored by a head-to-head collision of radicals while disproportionation is favored by head-to-tail collisions. Recent experiments on the photolysis of partially deuterized diethyl ketone bear this out.[33] Diethyl ketone was used, in which the secondary hydrogens were replaced by deuterium, *viz.*

$$CH_3CD_2COCD_2CH_3 + h\nu = 2CH_3CD_2 + CO$$

While there were certain complications in the reaction, the results showed unequivocally that disproportionation occurred by a head-to-tail mechanism

$$CH_3CD_2 + CH_3CD_2 = C_2H_4D_2 + C_2H_2D_2$$

II. The Absolute Rate of the Disproportionation and Combination of Ethyl Radicals

Since in the photolysis of mercury diethyl the rate of production of C_2-hydrocarbons is given by an expression of the form

$$d(C_2)/dt = aI_a + bI_a^{1/2}$$

the rate is not directly proportional to the light intensity. Hence, in a certain range of values, with a rotating sector, the rate with intermittent light will be a function of the sector speed. It is thus possible to determine the average lifetime of ethyl radicals under given experimental conditions. From this the concentration of ethyl radicals may be calculated, and hence the absolute values of k_1 and k_2 the velocity constants for disproportionation and combination.

VALUES GIVEN BY IVIN AND STEACIE[28]

E, kcal. per mole; A, cc. mole^{-1} sec.$^{-1}$; Z_2 (assuming normal kinetic theory cross-sections, for an average temperature over the range investigated) = 1.2×10^{14}

E_2 assumed	0	0.65
E_1	0.8	1.45
$A_1 \times 10^{-13}$	1.65	5.5
$A_2 \times 10^{-13}$	1.57	1.2

It thus appears that, as with methyl radicals, the frequency factor for combination is quite high. It is of interest that the frequency factor for disproportionation is of the same magnitude.

III. Hydrogen Abstraction Reactions

A variety of methyl reactions of the type

$$CH_3 + RH = CH_4 + R$$

have been investigated.[5–12] It is of great interest to compare these with the corresponding ethyl radical reactions

$$C_2H_5 + RH = C_2H_6 + R$$

Unfortunately, the data on such reactions are very scanty. Until recently virtually no quantitative information existed, with the exception of the reaction

$$C_2H_5 + H_2 = C_2H_6 + H \qquad (5)$$

For this reaction rough estimates had been made by a number of workers. Thus, Leermakers[34] estimated the activation energy to be 15 kcal., Moore and Taylor[14] about 9 kcal., and Jungers and

(30) B. deB. Darwent, private communication.

(31) C. E. H. Bawn and C. F. H. Tipper, *Faraday Soc. Discussion*, **2**, 104 (1947).

(32) F. E. Blacet and J. N. Pitts, private communication.

(33) M. H. J. Wijnen and E. W. R. Steacie, *Can. J. Chem.*, **29**, 1092 (1951).

(34) J. A. Leermakers, *J. Am. Chem. Soc.*, **55**, 4508 (1933)

Taylor[35] about 11 kcal. If the value of the activation energy of the reverse reaction is taken as 9 kcal., then E_5 would be about 14 kcal. However, this is quite uncertain.

Quantitative data for a few reactions have been obtained recently. Dorfman and Sheldon[24] have estimated the activation energy

$$C_2H_5 + C_2H_5COC_2H_5 = C_2H_6 + \text{etc.}$$

to be 4.1 kcal., while Kutschke, Wijnen and Steacie[27] obtain 7.4 kcal., with a steric factor of about 3×10^{-4}.

For the reaction with diethyl mercury

$$C_2H_5 + C_2H_5HgC_2H_5 = C_2H_6 + C_2H_4HgC_2H_5$$

Ivin and Steacie[23] obtained 6.2 kcal., with a steric factor of the order of 10^{-4}. It is interesting to note that this is of the same order of magnitude as the steric factor of typical methyl radical reactions. The activation energies also are relatively low, and suggest that the difference between reactions of methyl and of ethyl radicals is not great.

Wijnen and Steacie[36] have recently investigated the reaction of ethyl radicals with deuterium. Diethyl ketone was photolyzed in the presence of deuterium over a range of temperature from 54 to 257°. On the basis of the previous discussion of the diethyl ketone photolysis, the mechanism of the reaction in the presence of deuterium may be assumed to be

$$C_2H_5COC_2H_5 + h\nu = 2C_2H_5 + CO$$
$$C_2H_5 + C_2H_5 = C_2H_6 + C_2H_4 \quad (1)$$
$$C_2H_5 + C_2H_5 = C_4H_{10} \quad (2)$$
$$C_2H_5 + C_2H_5COC_2H_5 = C_2H_6 + C_2H_5COC_2H_4 \quad (3)$$
$$C_2H_5 + D_2 = C_2H_4D + D \quad (5)$$
$$D + C_2H_5COC_2H_5 = HD + C_2H_5COC_2H_4 \quad (6)$$
$$C_2H_5COC_2H_5 = C_2H_4 + CO + C_2H_5 \quad (4)$$

Reaction (4) is only of importance at high temperatures. If this is excluded, we have

$$k_5/k_3 = \frac{R_{C_2H_5D}[C_2H_5COC_2H_5]}{R_{C_2H_6-C_2H_4}[D_2]}$$

Actually, it may be shown that the occurrence of (4) at high temperatures will make no significant difference as is the case in the photolysis of diethyl ketone above.

By a plot of log k_5/k_3 against $1/T$ it is, therefore, possible to obtain $E_5 - E_3$. In this way it is found that

$$E_5 - E_3 = 5.9 \text{ kcal.}$$

Hence

$$E_5 = 7.5 + 5.9 = 13.4 \pm 0.5 \text{ kcal.}$$

If a value of 3×10^{-4} is accepted for the steric factor of reaction (3), then the steric factor of reaction (5) is about 10^{-3}.

With the above value of E_5 it is possible to correlate satisfactorily the activation energy of the reverse reaction with the bond dissociation energy of ethane D (C_2H_5–H).

IV. The Decomposition of Ethyl Radicals

At high temperatures the ethyl radical can decompose

$$C_2H_5 = C_2H_4 + H$$

This reaction was postulated by Rice and Herzfeld[37] as an essential step in the thermal decomposition of ethane.

Rice[38] assigned a value of 49 kcal. to the activation energy of the reaction in order to explain the over-all activation energy for the thermal decomposition of ethane. Most of the activation energies for the elementary steps, however, were assigned on a speculative basis to fit observed activation energies and some have been shown later to be very inaccurate. The bond strength values used are no longer those generally accepted and the mechanism postulated itself is in places doubtful. Thus the activation energy values are open to very large errors.

Bawn[39] has estimated the activation energy for the decomposition of the ethyl radical by a transition state calculation and has obtained a value of 48–50 kcal. This estimate appears to be somewhat more reliable than the values deduced for various other radicals since it is largely independent of the bond strength chosen for the removal of the first hydrogen atom in ethane. However, all transition state calculations of this kind have only qualitative significance.

A minimum value for the activation energy of the decomposition can be arrived at on thermochemical grounds since the reaction is endothermic. All the necessary thermochemical values have been established with reasonable certainty giving a heat of reaction of 37.5 kcal. Thus the activation energy of the reaction will be 37.5 kcal. plus the activation energy of the reverse reaction. This would suggest an activation energy of 38–43 kcal.[40]

A more direct estimate has recently been made by Bywater and Steacie,[41] who investigated the mercury photosensitized decomposition of ethane at high temperatures. There seems to be little doubt that the mechanism of the reaction at low temperatures is[29]

$$Hg(^3P_1) + C_2H_6 = Hg(^1S_0) + C_2H_5 + H \quad (1)$$
$$H + C_2H_6 = C_2H_5 + H_2 \quad (2)$$
$$2C_2H_5 = C_4H_{10} \quad (3)$$
$$2C_2H_5 = C_2H_6 + C_2H_4 \quad (4)$$

In agreement with this, hydrogen production is only very slightly temperature dependent. At high temperatures, however, there is a sudden very abrupt increase in the rate of hydrogen production which is undoubtedly due to the onset of (5)

$$C_2H_5 = C_2H_4 + H \quad (5)$$

which together with (2) constitutes a reaction chain. If the low-temperature "non-chain" hydrogen is allowed for, the remaining high temperature production of hydrogen gives a very good Arrhenius plot corresponding to $E_5 = 39.5$ kcal. This is in excellent agreement with the thermochemical value for the heat of reaction, and the assumption

(35) J. C. Jungers and H. S. Taylor, *J. Chem. Phys.*, **6**, 325 (1938).
(36) M. H. J. Wijnen and E. W. R. Steacie, *ibid.*, in press.
(37) F. O. Rice and K. F. Herzfeld, *J. Am. Chem. Soc.*, **56**, 284 (1934).
(38) F. O. Rice *ibid.*, **56**, 488 (1934).
(39) C. E. H. Bawn, *Trans. Faraday Soc.*, **31**, 1536 (1935).
(40) E. W. R. Steacie, "Atomic and Free Radical Reactions," Reinhold Publ. Corp., New York, N. Y., 1946.
(41) S. Bywater and E. W. R. Steacie, *J. Chem. Phys.*, **19**, 326 (1951).

that the activation energy of the reverse of (5) will be very small.

Conclusion

Much less information exists on the reactions of ethyl radicals than for methyl radicals, and until recently there has been little quantitative information. Recent work is of a more quantitative nature, and the following conclusions may be drawn: (a) The activation energy of the decomposition of ethyl radicals is about 39.5 kcal. (b) Both disproportionation and combination of ethyl radicals have very low activation energies. The frequency factors are similar. Hence both reactions may be expected to occur simultaneously in the normal temperature range in which photochemical measurements are carried out. (c) The collision efficiency of the combination process $2C_2H_5 = C_4H_{10}$ is high, and is of the order of magnitude of 0.1 to 1. (d) Hydrogen abstraction reactions are responsible for most of the apparent discrepancies in earlier work. Such reactions appear to have steric factors of the order of 10^{-3} to 10^{-4} as with methyl radical reactions. The activation energies of such reactions indicate that ethyl radicals are not much less reactive than methyls.

SOME RECENT DEVELOPMENTS IN REACTION RATE THEORY

BY HENRY EYRING AND RICHARD P. SMITH

Department of Chemistry, University of Utah, Salt Lake City, Utah

Received October 23, 1941

A brief review of the status of theoretical calculations of reaction rates is given. New developments in organic reaction rate theory are discussed; particular attention is given the development of a theory for charge distributions in aliphatic molecules and the correlation of the calculated charge distributions with organic reaction rates. The reaction of sodium atoms with organic halides and the chlorination of aliphatic molecules are discussed in some detail. The parallelism between changes in electrical resistance and hardness of alloys is discussed in terms of electronic availability.

Modern reaction rate theory reduces most ordinary problems in reaction rates to problems in molecular structure and the potential of interaction between molecules. Specifically, the theory of absolute reaction rates, as formulated by Eyring[1] in 1935 for the general case where one or more molecules combine to form the activated complex has for the specific rate constant

$$k' = \kappa \frac{kT}{h} \frac{F^{\ddagger}}{F_A F_B \cdots} e^{-E_0/RT} = \kappa \frac{kT}{h} K^{\ddagger} \qquad (1)$$

Here k' is the specific rate constant, R is the gas constant, h is Planck's constant, T is the absolute temperature, E_0 is the activation energy per mole of the reaction at absolute zero, κ is the "transmission coefficient" and $F^{\ddagger}$, F_A, F_B, etc., are the partition functions of the "activated complex" and of the reactants A, B, etc., respectively, per unit volume and $K^{\ddagger}$ is the equilibrium constant between reactants and activated complex. The "activated complex" is defined to be the configuration of the reactant atoms and/or molecules corresponding to maximum energy along the most favorable reaction path. The transmission coefficient allows for the possibility that not every system of reactant molecules reaching the top of the barrier (*i.e.*, the activated complex configuration) and moving along the coördinate of decomposition leads to reaction. For normal adiabatic reactions, such as those usually encountered by the organic chemist, this factor may satisfactorily be taken to be unity.

The theory of absolute reaction rates is, then, a statistical theory relating the very important quantity k', the specific rate constant, to (a) statistical quantities, such as the average translational energy of a molecule ($(3/2)kT$) and partition functions $F^{\ddagger}$, F_A, F_B, etc.; (b) the transmission coefficient, which is primarily related to the shape of the "barrier," *i.e.*, "hump" in the potential energy plotted as a function of the reaction coördinate, and which will not concern us here, the deviations of this factor from unity being negligible for the reactions of particular interest to us; and (c) the activation energy, which must be calculated quantum mechanically, estimated semi-empirically or empirically, or determined experimentally.

Equation (1) is often written in the quasi-thermodynamic forms

$$k' = \kappa \frac{kT}{h} e^{-\Delta F^{\ddagger}/RT} \qquad (2)$$

$$k' = \kappa \frac{kT}{h} e^{\Delta S^{\ddagger}/R} e^{-\Delta H^{\ddagger}/RT} \qquad (3)$$

where $\Delta F^{\ddagger}$ is the "free energy of activation," $\Delta S^{\ddagger}$ is the "entropy of activation," $\Delta H^{\ddagger}$ is the "heat of activation," (all per mole, referred to standard states which must be designated), and R is the gas constant. The heat of activation, $\Delta H^{\ddagger}$, is practically the same as the previously introduced activation energy, E_0, the two differing essentially by RT for unimolecular gas reactions and for reactions in solution where the standard states are unit concentrations; for other types of reactions, the relationships are readily derived.[2]

Equation (1) is derived for the rate process

$$A + B + \cdots \longrightarrow C^{\ddagger} \longrightarrow D + E + \cdots \qquad (4)$$

Here species A and B, etc., unite to form the activated complex $C^{\ddagger}$ which breaks up to form D and E, etc. Thus the velocity of reaction is

$$v = k'(A)(B)\cdots = C^{\ddagger}\kappa(kT/h) \qquad (5)$$

The relation $v = C^{\ddagger}\kappa(kT/h)$ holds equally well for a reaction of the type

$$A + B + \cdots \longrightarrow C^{+} + M^{+} \cdots \longrightarrow D + E \cdots \qquad (6)$$

(1) H. Eyring, *J. Chem. Phys.*, **3**, 107 (1935).

(2) S. Glasstone, K. J. Laidler and H. Eyring, "The Theory of Rate Processes," McGraw-Hill Book Co., Inc., New York, N. Y., 1941.

In this case

$$v = \kappa \frac{kTe}{h} - E_0/RT \frac{F^{\ddagger} F_m \cdots}{F_A F_B} \frac{(A)(B)\cdots}{(M)\cdots} =$$

$$\kappa \frac{kT}{h} K^{\ddagger} \frac{(A)(B)\cdots}{(M)\cdots} = k' \frac{(A)(B)\cdots}{(M)\cdots} = C^{\ddagger} \kappa \frac{KT}{h} \quad (7)$$

Ordinarily the Arrhenius plot of the specific rate constant against $1/T$ yields a negative slope in the accustomed manner. This is, however, not necessary since $K^{\ddagger}$ like any equilibrium constant may possess a temperature maximum. Thus many biological reactions show a maximum with temperature ordinarily interpreted as the superposition on the customary Arrhenius speed-up with temperature rise of an accompanying enzyme inactivation. Alternatively one may simply say that $K^{\ddagger}$ shows a temperature maximum and that above this temperature maximum the activated complex is less energy rich than the constituents from which it is assembled. One cannot emphasize too much that $K^{\ddagger}$ must be expected to show just the complexities of any other equilibrium constant.

The main problems to be dealt with in calculating reaction rates then, are (a) calculation of the entropy of activation, and (b) calculation of the heat of activation (or energy of activation).

It is not difficult to estimate the entropy of activation with fair accuracy once the approximate configuration of the activated complex is known. This is fortunate not only for the sake of calculating the "frequency factor" (*i.e.*, the coefficient of $e^{-\Delta H^{\ddagger}/RT}$) for a reaction, but this also provides us with a powerful tool for the elucidation of reaction mechanisms. Various forms for the activated complex of a reaction may be postulated, and the entropy of activation estimated for each. This is possible because masses and moments of inertia are the most important factors entering these calculations, other than universal constants. By comparing the various calculated entropies of activation with that which is observed, the mechanism of the reaction may be decided upon in many cases.[2] A particularly striking example is a reaction which we shall discuss more fully later in this paper: the reaction of sodium atoms with halides. When a sodium approaches a halide molecule, the valence electron of the sodium transfers to the halide, which promptly dissociates, the result being the formation of a sodium halide and a free atom or radical. Magee[3] has shown that the very high frequency factors observed can be accounted for only by assuming a separation of five to seven ångström units between the halide center of gravity and the sodium atom nucleus, so that the electron must prefer to jump from the sodium to the halogen even when quite a large separation exists.

Large, important areas in the field of reaction rate theory apparently would be in good condition, then, if means were available for calculating (or successfully estimating from empirical considerations) activation energies. This is the part of reaction rate theory which has caused the most trouble.

It is quite evident that entirely new methods must be found for determining activation energies theoretically. In principle, straightforward quantum mechanical calculations should be used. However, by using this approach, it has so far been possible only to show that, for the simplest reaction, $H + H_2$ para $= H_2$ ortho $+ H$, the activation energy is less than 19 kcal., while the experimental value is about 7 kcal. Thus it appears that this can only be a successful approach, as new approximations are found which will both simplify and improve the calculations.

An alternative approach was devised by Polanyi and Eyring[4] which is usually known as the "semi-empirical" method for calculating activation energies. They used London's approximate formula for the energy E for four monovalent atoms, which is

$$E = Q - \{1/2((\alpha - \beta)^2 + (\beta - \gamma)^2 + (\gamma - \alpha)^2)\}^{1/2} \quad (4)$$

Here Q represents the total "coulombic" binding, and α, β and γ are exchange interactions between various atoms. Following Sugiura's calculations[2] on the hydrogen molecule, the "coulombic" terms were assumed to be about 14% of the total binding, and the total binding energies between pairs of atoms were assumed to be satisfactorily approximated by means of Morse curves between the atoms. These approximations made possible the construction of potential surfaces, and these were sufficiently accurate for at least qualitative discussion of the nature of a chemical reaction; and, in many cases, the calculated activation energies were in good agreement with experiment.

The method described above for the calculation of activation energies is now seldom used, and the *a priori* calculation of activation energies is a task that few have ventured to try during the last decade. The reasons for this shyness on the part of chemists appear to be, first, that the "semi-empirical" method has been applied to most of the simple gas reactions with results ranging from poor to excellent, and no one is sure of how to consistently improve the calculations; and, second, the reactions which are at once most interesting and most numerous, namely, the reactions of organic chemistry, are not suited to treatment by the "semi-empirical" method. This latter fact is well illustrated by the poorness of the results which have been obtained with what has been called the simplest of organic reactions, namely, the reaction of sodium atoms with organic halides. Here the agreement with experiment is very rough indeed. Furthermore, in this particular case, one is not at all sure of how to take account of the changing properties of, for example, the C–Cl bonds when calculating the energies of activation for a series of chlorides, such as CH_3Cl, CH_2Cl_2, $CHCl_3$ and CCl_4, where the activation energy differential is about 10 kcal.

It therefore seems evident that neither the Eyring–Polanyi method nor strict quantum mechanical methods can at present be very fruitful for solving the activation energy problem, in view of the difficulties involved and the large number of reactions the chemist is interested in. Hence a high degree of successful empiricism seems to be demanded.

An empirical but very successful method for qualitatively considering relative organic reaction rates

(3) J. L. Magee, *J. Chem. Phys.*, **8**, 687 (1940).

(4) H. Eyring and M. Polanyi, *Z. physik. Chem.*, **B12**, 279 (1931).

has been built up by the "electronic interpretations" school, led particularly by such English workers as Ingold, Robinson, Lowry and Lapworth. Simple concepts for discussing changes in electronic densities on various atoms in molecules due to substituent charges are used, and these charges are in turn qualitatively correlated with reaction rates and equilibria. In 1940 Ree and Eyring[5] decided that here was a good place to start in attempting to attain a more quantitative treatment of organic reactions, and the result was the demonstration that the simple rules of the electronic school could equally simply be mathematically formulated and applied to the consideration of relative amounts of ortho, meta and para nitration of substituted benzenes.

The success of these calculations clearly demanded further explorations in this field. Efforts were begun in 1940 toward the development of a simple theory for estimating charge distributions in simple aliphatic molecules, such as methylene chloride. The war interrupted this work, but it has finally been continued in the recent paper by Smith, Ree, Magee and Eyring,[6] wherein a simple, semi-empirical scheme is detailed for the calculation of charge distributions in aliphatic molecules. The validity of the method was demonstrated by the calculation of dipole moments of polysubstituted methanes and ethyl halides, using the moments of the methyl halides as the bases. A following paper by Smith and Eyring[7] shows that the net charges thus calculated may be simply correlated with the activation energies for reactions of halides with sodium atoms, thereby lending support to the charge distribution theory and at the same time showing how charge distributions are easily correlated with reaction rates, at least for certain types of reactions.

For details of the charge distribution theory the reader is referred to the appropriate paper.[6] There it was shown how, to the approximations used, atoms in molecules may be considered to have "net charges" associated with them, and these may be calculated by a simple scheme. It was found that certain moments were needed as bases, among them being the C–H bond moment in methane. This is certainly small, and the calculations based on the assumption that it is zero were satisfactory. All calculations presented in this paper are based upon this assumption.

The net charges for CH_3Cl, CH_2Cl_2, $CHCl_3$ and CCl_4 were calculated to be as follows.

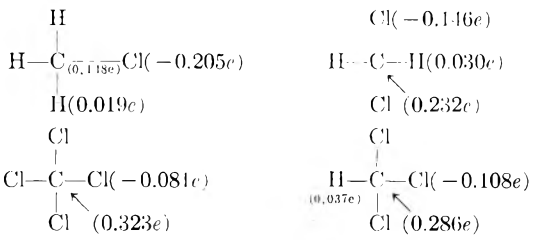

Here e is the negative charge of an electron. This series clearly portrays the main features of the "inductive effect," *i.e.*, the change in the moment of a bond with the bond environment. As the carbon becomes more heavily substituted with chlorines, the latter take more electronic charge from the carbon, thereby increasing its effective nuclear charge, making further removal of charge more difficult. Hence two chlorines cannot remove twice as much charge as one, *i.e.*, the chlorines in CH_2Cl_2 have smaller net negative charges than has the chlorine in CH_3Cl, and so on.

In the reactions of the above molecules with sodium atoms, it is found that the activation energies decrease as we go through the series, the total change being about 9.5 kcal./mole. This seems qualitatively understandable when the net charges shown above are considered. As the chlorine atom becomes more negatively charged, its electron affinity decreases, and the electron from the sodium atom therefore is not transferred to the chlorine so easily. Remarkably enough, the plot of the net charges against the activation energies yields a straight line.[7] Still more remarkable is the fact that if net halogen charges are divided by the polarizabilities of the carbon–halogen bonds, not only do the chlorides fall on a straight line (the polarizabilities of all C–Cl bonds are taken to be the same), but bromides and iodides are brought onto the *same* straight line. This relationship is so accurate that one wonders about the possibility of showing how it may be made to follow from theoretical considerations. So far, not much progress has been made in this direction, so that this remains as a challenge. A very rough argument that indicates how such a relationship might arise is as follows. Let us treat the "extra" charge on the halogen, *i.e.*, the halogen net negative charge, by the "particle in a box" model, using a one dimensional model for simplicity. If L is the length in which the particle may move, the ground-state energy of such a system is

$$E = h^2/8mL^2 \qquad (5)$$

Suppose the available space is shortened an amount dL. The corresponding energy change is then

$$dE = -(h^2/4mL^3)dL \qquad (6)$$

Suppose that, before the "loose" electron of the sodium atom can be transferred to the halogen atom, the "extra charge" of the halogen atom must be pushed over onto the carbon atom. This is equivalent to a reduction in L. If this reduction is constant, then eq. (6) shows the energy differential to be inversely proportional to L^3 for a unit of charge. Multiplying this by the fraction of a charge to be transferred, we arrive at a proportionality of energy differential to net charge divided by L^3. Now L^3 has the same dimensions as polarizability, and might be expected to be proportional to the polarizability; hence a rough justification of our empirical relation. Similar arguments, made more precise, might lead to the desired relationship.

Two very different types of reactions, then, have so far yielded to treatment by the new methods, where other methods have failed. They are, (a) an electrophilic attack on a carbon atom by an ion (the nitration of substituted benzenes); (b), an electron-transfer reaction (reaction of sodium atoms with halides). Many important organic reactions are essentially of these types, and may be expected

(5) T. Ri (Ree) and H. Eyring, *J. Chem. Phys.*, **8**, 433 (1940).

(6) R. P. Smith, T. Ree, J. L. Magee and H. Eyring, *J. Am. Chem. Soc.*, **73**, 2263 (1951).

(7) R. P. Smith and H. Eyring, *ibid.*, **74**, 229 (1952).

to yield to similar treatment. Other types, such as a dissociation reaction (acidic ionization) will be shown to be amenable to such treatment in a future paper.

In all the reactions discussed above, net charges residing on atoms are the fundamentally important factors. In another class of reactions, namely, free radical reactions, it is well known that not net charges, but rather charge availabilities, are the important factors. Our inductive effect theory is, as we shall now demonstrate, capable of providing indices of electron availability for various positions in molecules, and these can be correlated with rates of free-radical attack on various positions.

The reaction we shall consider is one for which many data have been assembled, namely, the free radical chlorination of aliphatic hydrocarbons and aliphatic chlorides. Ash and Brown[8] have recently reviewed the data on this reaction. Here a chlorine atom comes up to a hydrogen atom in the chlorinated (or unsubstituted) alkane; an electron is pulled out of the C–H bond, so that an H–Cl bond may be formed, leaving a free radical.

In order to understand how the experimental results for this reaction may be explained, let us first consider *n*-butane. Here the secondary carbons are favored toward chlorination. In $(CH_3)_2CHCH_2$-CH_3, the tertiary carbon is highly favored. These facts have previously been explained only by the suggestion that a methyl group may be considered to activate the adjoining carbon, though the nature of this activating influence is not elucidated. Our explanation is simply this: The more easily an electron can be pulled out of a given C–H bond to form the H–Cl bond, the lower the activation energy should be. The more easily a carbon atom can regain electronic charge from other bonds, the more willing it will be to give up a C–H bond electron. Carbon–carbon bonds will be much better suppliers of charge than carbon–hydrogen bonds, because of the greater longitudinal polarizability of the former. A primary carbon has only one C–C bond through which to partially make up charge deficit; a secondary carbon has the benefit of two C–C bonds; and a tertiary carbon has three. Hence the results mentioned above are readily explained.

We turn now to the chlorination of *n*-butyl chloride, which is a bit more complicated. Here we have not only the "reservoir" effect just considered, but superimposed on this is the inductive effect. The relative amounts of attack at the various carbons are as follows.[1]

$$\underset{24}{C}—\underset{47}{C}—\underset{22}{C}—\underset{7}{C}—Cl$$

Numbering the positions 1, 2, 3, 4 from the left, we see that the "reservoir" effect will explain the greater amount of attack at position 2 over position 1. Carbons 3 and 4 have equally good "reservoirs," but they are already electron deficient because of the influence of the chlorine already present in the molecule.

To show that the above explanation will actually account for the trend shown, we have assumed that, in the activated state, the incomplete H–Cl bond has removed about as much charge from the carbon concerned as a chlorine would remove if attached directly to the carbon. Then we may use the charge actually removed by a chlorine substituted in a position as a measure of the "electron availability" at that position. That is, we simply calculate charge distributions for the four compounds Cl-$(CH_2)_4Cl$, $CH_3CHCl(CH_2)_2Cl$, $CH_3CH_2CHClCH_2Cl$ and $CH_3(CH_2)_2CHCl_2$. The charges we calculate to reside on the second chlorine then are, respectively, in units of 10^{-10} e.s.u., -1.056, -1.129, -1.024, -0.799. These figures parallel the amounts of substitution previously given very well. Similar calculations have been made for the chlorination of $CH_3(CH_2)_2CHCl_2$ and $CH_3(CH_2)_2CCl_3$. The results are tabulated below. For each molecule, the experimental amounts of substitution are given on the first line, and the charges a chlorine will remove are given on the second line (units of 10^{-10} e.s.u.).

C	C	C	C	X
24	47	22	7	Cl
−1.056	−1.129	−1.024	−0.799	
37	49	12	2	Cl_2
−1.051	−1.071	−0.966	−0.618	
51	49	0	...	Cl_3
−1.043	−1.058	−0.925	...	

Experiment shows carbons 1 and 2 in the last molecule to be about equally attacked, while our "electron availability indices" also become almost equal for these positions, as contrasted with the two other molecules. In other words, the strong inductive effect of the three chlorines seems to just counterbalance the different "reservoir" effects here.

It is intended to discuss this reaction in more detail elsewhere. Meanwhile, it is hoped that we have indicated how useful the simple concepts of our inductive effect theory can be for semi-quantitative understanding of diverse types of organic reactions.

One other concept which involves electronic availability serves to explain the parallelism between changes in the electrical resistance and in the hardness of alloys.[9] One should think of conductance electrons as a solvent surrounding the positive atomic kernels holding them together and permitting them to slip past each other readily, providing there is sufficient electron solvent. A useful and close analogy is clay held together and made plastic by added moisture which surrounds the clay particles. Now if one does anything to tie up the electrons, say, by causing them to be adsorbed on individual atoms as occurs whenever atoms of different electronegativity are added to the alloy, the solvent electrons tend to disappear and the alloy hardens becoming more brittle and at the same time increases in its electrical resistance as it tends toward the semi-conducting state. If additions reach the point where compounds start precipitating out of the alloy, the situation becomes complex and the simple parallelism between hardness and resistance requires closer analysis. We will pursue this matter no further here.

(8) A. B. Ash and H. C. Brown, *Record Chem. Progress*, **9**, 81 (1948).

(9) R. F. Vines, "The Platinum Metals and Their Alloys," The International Nickel Co., 1941.

In reactions involving the fusion of more than one saturated molecule into an activated complex, electronic promotion is involved. This activation energy of promotion is lessened by coördination of the activated complex with a suitable electron acceptor. Metals as shown by their work functions have long been recognized to have this catalytic virtue of temporarily accepting unwanted electrons. We have been able to mention only a few of the cases where electron displacement lowers activation energy. In most cases suitable quantitative theories are still much needed.

FREQUENCY FACTORS OF SOME BIMOLECULAR REACTIONS

BY G. K. ROLLEFSON

University of California, Berkeley, California

Received October 23, 1951

The facts discussed in this paper show that there are two values for the frequency factor for bimolecular reactions between neutral molecules which may be considered normal. These values are 10^{11} and 10^{7}. The first corresponds to reaction every time the molecules come within a distance of the order of a molecular diameter of each other, whereas the second requires that in the activated complex the two molecules are essentially bonded to each other. These values are equally valid in the gas phase and in solution which leads to the conclusion that the caging action of the solvent postulated by Franck and Rabinowitch is usually small or negligible. For reactions between ions in solution the same factors hold but must be modified by a factor which takes into account the difference in entropy of solvation of the activated complex and the reactant ions.

The factor A in the Arrhenius expression for the rate constant for a bimolecular reaction $k = Ae^{-E/RT}$ may be called a frequency factor, although it does not have the dimensions of frequency, since it determines the frequency with which the molecules react when the system possesses the necessary activation energy. In this paper the magnitude of this factor for a number of systems is to be discussed in terms of the "collision theory" and of the "absolute reaction rate theory."

There are many reactions in the gaseous state for which, if the concentrations are expressed in moles per liter and the time in minutes, the frequency factor has been found to be about 10^{11}. This is true for example in the formation or decomposition of hydrogen iodide, the conversion of para- to ortho-hydrogen by oxygen, the reaction of bromine atoms with hydrogen, etc. In fact, this value has been found so frequently that it is usually referred to as the normal value, and explanations are sought for deviations from it. In terms of the collision theory this characteristic value is explained as reaction occurring at every collision when the system possesses the requisite activation energy. Lower values are accounted for by assuming that in order for the molecules to react they must be oriented in some special way with respect to each other and, in addition, there is the possibility that the necessary changing of bonds will not occur so that the molecules will separate without reacting although the necessary activation energy was available. The weakness of this theory is that it offers no quantitative means for the evaluation of these specific orientations or probabilities.

The absolute reaction rate theory expresses the frequency factor as $\kappa(k_b T/h)e^{\Delta S^*/R}$ in which κ is the transmission coefficient and is usually assumed to be unity, ΔS^* is the entropy change associated with the formation of the activated complex from the two reactant molecules. The remainder of the expression is a constant believed to be characteristic of all reactions. In principle this factor can be calculated if we know the energy states of the reactant molecules and of the activated complex. In practice the energy states of the activated complex are not known from experiment and, therefore, assumptions must be made concerning them. The number of adjustable parameters available is usually so great that it is always possible to show that any experimental result is understandable, although it might not have been predicted. However, at least for bimolecular reactions, there are some generalizations based on the known entropy changes for complete reactions which we wish to point out.

A survey of the entropy changes which are associated with the addition of two atoms or molecules to form a new molecule reveals that such a process is usually accompanied by an entropy decrease of about thirty. Such a value can be attributed to the loss of translational entropy of one molecule. If the formation of the activated complex is analogous to such an addition reaction, the entropy of activation should be about -30 and, correspondingly, the frequency factor should be about 10^{7} or only one ten-thousandth of the so-called normal value. On the other hand, if the only condition which must be fulfilled in forming the activated complex is that the two molecules must approach within some specified distance of each other, then we could expect that the entropy change would correspond to the loss of translational entropy with respect to only one degree of freedom and, hence, it should be about -10. Such a value leads to a frequency factor of 10^{11}. Thus, according to this theory, the "normal" value should be found for reactions for which the formation of the activated complex requires only the condition stated above.

There is another group of reactions for which the observed frequency factors are about 10^{7}. As examples we may cite the dimerization of cyclopentadiene,[1] and the reactions of methyl radicals with several organic molecules.[2] In the latter cases 10^{7} is said to be the upper limit, but it is probably close to the actual value. Such a value is readily under-

(1) A. Wasserman, *J. Chem. Soc.*, 1028 (1936).

(2) L. M. Dorfman and R. Gomer, *Chem. Rev.*, **46**, 499 (1950).

stood in terms of the absolute rate theory if we assume that the formation of the activated complex is essentially the same as an addition reaction and, therefore, has an entropy change of -30 as has been mentioned above. For this condition to be fulfilled it is not necessary that any long-lived intermediate be formed; it may well be sufficient that the attachment of the molecules last only for a period comparable with the time of a vibration. The collision theory has, as yet, not provided a means for the quantitative calculation of such a frequency factor. In general, it may be said that the ideas presented here require that both 10^{11} and 10^{7} be considered "normal" values for the frequency factor. The first value can be expected to apply to reactions of atoms, quenching of fluorescence, or any reaction which requires nothing more specific than that the reactant molecules come within a distance of the order of a molecular diameter of each other. The second value should be found whenever there is need for any highly specific orientation of the reacting molecules. For example, in the series of reactions discussed by Dorfman and Gomer, the methyl radical and the organic molecule may be thought of as being temporarily bonded in the activated complex by the hydrogen atom which is to go with the methyl radical to form methane.

It has been found that bimolecular reactions in solution have frequency factors similar to those found in the gas phase. This fact has been discussed extensively by Moelwyn-Hughes[3] in connection with the collision theory of reactions in solution. Few data are available for reactions which follow simple bimolecular rate laws, both in the gas phase and in solution. A search of the literature reveals three examples: (1) the dimerization of cyclopentadiene[4]; (2) the conversion of para- to ortho-hydrogen by oxygen[5]; (3) the reaction of iodine atoms with ethylene iodide.[6] The values obtained for the constants of the Arrhenius equation for the first of these reactions are listed in Table I.

TABLE I

CONSTANTS FOR THE REACTION

Medium	Dimerization log A	Dimerization E, kcal.	Dissociation log A	Dissociation E, kcal.
Gas	6.1	16.7	13.1	35.0
Pure liquid	5.7	16.0	13.0	34.5
CCl_4	5.9	16.2		
CS_2	5.7	17.7		
Benzene	7.1	16.4		
Parffian	8.1	17.4	13.0	34.2

The second reaction has been studied at only one temperature in solution and found to have the same value for the rate constant as in the gas phase. The third reaction is one of the steps in the decomposition of ethylene iodide, which is found to follow the same mechanism in solution and in the gas phase, and the constants are found to be the same in both phases within the limits of experimental error.

Recently some experiments have been carried out at the University of California in which the rate of a bimolecular reaction was studied in the gas phase and in solution in overlapping temperature ranges.[7] The reaction studied was that between carbon tetrachloride and photoactivated β-naphthylamine. Since the reaction was followed by the decrease in fluorescence of the β-naphthylamine, it will be referred to as the quenching of the fluorescence, although there are grounds for believing that the actual reaction involves more change than such a statement implies.[8]

Both the fluorescence and its quenching depend to some extent on the frequency of the exciting light in the gas phase but are independent of it in the liquid phase. This fact can be explained by saying that in the liquid phase the excited molecules are brought to the lowest vibrational level of the upper electronic state before they can react with another molecule or fluoresce; in the gas phase several vibrational levels are involved. In order to compare the rates of the same process in the two states it is necessary to study the rate of quenching in the gaseous state for molecules in the lowest vibrational level of the upper electronic state. This was accomplished by introducing ethane or cyclohexane vapor, substances which can remove vibrational energy but do not return the photoexcited molecule to its lowest electronic state. The results for the gas phase given in Table II are the limiting values reached with high pressures of the inert gas. The

TABLE II

CONSTANTS FOR NAPHTHYLAMINE CCl_4

Medium	Rate constant	ΔS^*
Gas	5.9×10^{10}	-9.7
Cyclohexane	$4.5 \times 10^{11}\, e^{-2470/RT}$	-7.2
Isooctane	$2.0 \times 10^{11}\, e^{-1600/RT}$	-8.8

entropies of activation listed in the last column have been calculated assuming that the transmission coefficients are unity. It is apparent that there is no significant difference between the values listed. In each case the observed entropy change is reasonably consistent with the assumption that the only condition imposed in forming the activated complex is that the two molecules must be at some definite distance from each other. The activation energies are not under discussion in this paper, but it might be mentioned that they are somewhat smaller than the values found for viscosity in these solvents.

The results which have been cited show that in an inert solvent the frequency factor for a bimolecular reaction is not significantly different from what it is in the gas phase. The slight variations which exist might well be due to the solvent not being completely inert. The slightly higher values found for solutions in the quenching of the fluorescence of β-naphthylamine may also be explained from the point of view of the collision theory as being caused by a limitation of the space available for the solute molecules, thus, giving rise to an effect much like that which is provided for in the van der Waals

(3) E. A. Moelwyn-Hughes, "Kinetics of Reactions in Solution," Oxford University Press, 1947.

(4) A. Wasserman, *et al.*, *Nature*, **137**, 196 (1936); *J. Chem. Soc.*, 1028 (1936); *Nature*, **139**, 669 (1937); *Trans. Faraday Soc.*, **34**, 128 (1938).

(5) L. Farkas and H. Sachsse, *Z. physik. Chem.*, **B23**, 119 (1933)

(6) M. J. Polissar, *J. Am. Chem. Soc.*, **52**, 956 (1930).

(7) H. G. Curme, Ph.D. Thesis, University of California, 1950.

(8) The experimental details are to be published elsewhere.

equation by the introduction of the correction term b to the volume.

The data which have been cited offer a possibility for estimating the magnitude of the caging effect on the decomposition of a molecule which was discussed by Franck and Rabinowitch.[9] According to their hypothesis the rate of decomposition of a molecule into two parts should be decreased by a solvent, since the solvent molecules would tend to hold the parts together and thus favor recombination rather than separation. We have seen that the solvent has relatively little effect on the rate with which the molecules come together. Therefore, if the solvent does not form a solvate with the addition product and thus alter the equilibrium, the principle of microscopic reversibility requires that the rate of decomposition cannot be affected appreciably. In the case of the decomposition of the dimer of cyclopentadiene the rate has been measured in two condensed systems, and it is apparent from an inspection of Table I that the solvent does not retard the decomposition significantly. Since this system involves a rather large molecule, it is not likely that this caging effect is ever of great importance. It is more reasonable to attribute any significant alteration of the rate (or efficiency) of dissociation in passing from the gas phase to solution to the formation of a solvate which essentially changes the reaction.

Reactions involving ions cannot be studied both in the gas phase and in solution, but they can be used to study a number of other factors which influence the frequency factors in solvents. One of these is the effect of the change in solvation which occurs when two ions react. According to theoretical treatments which have been published the frequency factor should change by a factor of 100 for each unit change in the value of the product of the charges of the reacting ions. The data shown in Table III are usually cited[10] in support of this rule. The agreement between the calculated and observed values is reasonably good for the first four examples, but the others deviate too much. The magnitude of the disagreement between theory and experiment is particularly noticeable if one considers that the experimental values for the last five examples vary over a range covered by a factor of four hundred, whereas the theory calls for a variation of a factor of one hundred million. There is probably no simple explanation for these deviations since the observed effects are both higher and lower than the theoretical. It is possible that the original investigators of these reactions have presented over-simplified interpretations of their data, but similar deviations show up in such simple systems as are found in the study of the quenching of fluorescence. A comparison of the quenching of quinine in acid solution by chloride ion, of acridone by iodide, and of uranin in alkaline solution by iodide shows that, according to the theory, the relative entropy factors should be 10^4, 1 and 10^{-4}. Experimentally, they are all approximately the same. The entropy decrease associated with the formation of the activated complex is about 2 or 3 in each of these reactions. This small value might be taken as evidence that in these cases the measured entropy change is the one associated with a diffusion process. However, it was shown by Rollefson,[11] by a study of the temperature coefficients of the constants in the equation for the deviations from the Stern–Volmer quenching law derived by Boaz and Rollefson, that for the reaction of acridone with iodide[12] the entropy change for the bimolecular quenching process was the same as that involved in getting the two molecules into the same solvent cage. It seems, therefore, that it may be possible for the activated complex to be formed in some systems without any great changes in the restraints imposed on the solvent by the charges.

The discussion up to this point has assumed that the transmission coefficient which appears in the absolute rate theory equation for the rate constant is unity. Although this condition is probably fulfilled in many cases, it is not necessarily true and some of the discrepancies between theory and experiment shown in Table III may be due to a deviation of this factor from unity. One condition which might lead to a small transmission coefficient is the restriction on transitions from a singlet to a triplet state or *vice versa*. However, in general, this selection rule is inclined to break down in a collision process. In the reaction between β-naphthylamine and carbon tetrachloride, which has been mentioned previously, there is a possibility that the quenching action involves a transfer of the naphthylamine molecule from an excited singlet state to a triplet state. In order to test this idea some experiments were carried out in a rigid solvent in which the triplet state could be detected by its phosphorescence. It was found that when the fluorescence intensity was reduced to about half its initial value the phosphorescence intensity was increased noticeably. No tests were made to determine whether or not the triplet state was also deactivated by the carbon tetrachloride, but the experiment as it stands is sufficient to show that the singlet-triplet transfers occur with a frequency which is at least comparable with any other changes which may occur. It is, of course, possible that there are other quantum restrictions which play a

TABLE III

ENTROPY FACTORS FOR IONIC REACTIONS

Reaction	Calcd.	Obsd.	Calcd./obsd.
$Cr(H_2O)_6^{+++} + CNS^-$	10^6	10^6	1
$Co(NH_3)_5Br^{++} + OH^-$	10^4	2×10^4	$1/2$
$NH_4^+ + CNO^-$	10^2	0.6	16
$C_6H_5NClCOCH_3^+ + Cl^-$	10^2	0.8	12
$ClO^- + ClO_2^-$	10^{-2}	4×10^{-5}	250
$C_6H_5C(CCOO^-) + I_3^-$	10^{-2}	7×10^{-6}	1400
$CH_2ClCOO^- + S_2O_3^{--}$	10^{-4}	6×10^{-7}	160
$Co(NH_3)_5Br^{++} + Hg^{++}$	10^{-8}	6×10^{-6}	1.6×10^{-3}
$AsO_3^{---} + TeO_4^{--}$	10^{-12}	10^{-7}	10^{-5}

(9) J. Franck and E. Rabinowitch, *Trans. Faraday Soc.*, **30**, 120 (1934).

(10) Moelwyn-Hughes derived an equation which leads to such a value (*Proc. Roy. Soc.* (*London*), **155A**, 308 (1936)) from the collision theory point of view; the absolute reaction rate point of view has been presented in books such as Laidler's "Chemical Kinetics," McGraw-Hill Book Co., Inc., New York, N. Y., 1950, p. 133.

(11) Unpublished results presented at the meeting of the American Chemical Society held in Detroit, April, 1950.

(12) H. Boaz and G. K. Rollefson, *J. Am. Chem. Soc.*, **72**, 3435 (1950).

part in some of these reactions, but at present there is no experimental evidence concerning them.

The considerations which have been presented in this paper offer a possibility of extending the remarks of Rollefson and Boaz[13] to account for the extreme specificity so often found in the study of the quenching of fluorescence. In their discussion it was pointed out that a high degree of specificity could be accounted for if the quenching consisted of a transfer of energy between the reacting molecules only when the quencher molecule has an energy state separated from the lowest state by approximately the same amount as the excited state of the fluorescer differs from a lower state of the molecule. Under such conditions the transfer can occur if the molecules merely come close to each other; *i.e.*, the entropy of activation would be about −10. If this condition is not fulfilled, the quencher can still remove energy from the fluorescer, but in order to do so they will have to essentially form an addition compound and thus fulfill the condition for which the entropy change is −30. Such a change will reduce the quenching constant by a factor of 10^4 and thus put it below the range which can be studied by the usual type of experiment.

(13) G. K. Rollefson and H. Boaz, THIS JOURNAL, **52**, 518 (1948).

ADSORPTION OF CARBON DIOXIDE BY GLASS

BY JOHN B. THOMPSON,[1] E. ROGER WASHBURN AND L. A. GUILDNER[2]

Avery Laboratory, University of Nebraska, Lincoln, Nebraska

Received November 15, 1951

The continued interest in the adsorptive properties of glass has given rise to the present study of low temperature CO_2 adsorption on some commercially available kinds of glass. The present report includes Pyrex wool and two kinds of "Scotchlite" brand glass beads. In the course of this study, an extreme case of capillary condensation was encountered, the effect of etching the glass was studied, and some data on the effect of water on CO_2 adsorption was obtained.

Experimental

The small surface areas of the adsorbents required an apparatus with which accurate measurements of small adsorptions could be obtained at pressures up to atmospheric. The apparatus, which is shown in Fig. 1, is essentially a U tube, one arm of which is one meter long and the other arm about 40 cm. The two arms form an absolute pressure manometer, a vacuum being maintained in the long arm by Germann's method.[3] The short arm, in a water jacket, is a gas buret of variable volume. The advantage of using a uniform tube instead of the conventional series of bulbs is that the pressure in the tube is continuously variable. The mercury levels were read to the nearest 0.05 mm. with a 1-meter cathetometer. The short tube was volumetrically calibrated in terms of cathetometer readings from the weights of discharged mercury.

The apparatus is operated in the conventional way: after the adsorbent is degassed, stopcock A is closed, gas is admitted to the gas buret, and stopcock B is closed. Three or four readings of the mercury levels are then made with the gas in the short tube at various pressures. Stopcock A is then opened and the adsorption measurements are made in the usual way. Dead space values were determined with helium.

With the present apparatus, good accuracy may be obtained even when the ratio of gas adsorbed to gas in the dead space is as low as 0.1, as was the case with the unetched type 520 glass beads. Relative adsorption may be measured when the ratio is as low as 0.005, the absolute accuracy in this case being limited by the experimental error in dead space determination.

The results of the adsorption measurements were calculated using the equation of state

$$PV(1 + ZP) = nRT$$

where P, V, n, R and T have their usual meanings and Z is a function of temperature. For CO_2 at 25°, $Z = 0.00000774$ when P is expressed in mm. of mercury, and at −78°, $Z = 0.0000329$. These values of Z were calculated from density data of CO_2. For helium, Z was assigned the value zero.

The CO_2 was generated from Dry Ice and dried with Anhydrone or Drierite, from which other gases had been removed by repeated evacuation and flushing with CO_2.

Adsorbents. 1.—"Scotchlite" brand glass beads type 520: This material is a high density glass supplied in the form of microspheres by the Minnesota Mining and Manufacturing Company. According to the manufacturer, these spheres have fire polished surfaces and have not been subjected to the etching action of water. It may therefore be expected that the surface of the material is smooth enough that the geometric area would be in good agreement with the area determined by gas adsorption. This expectation was fulfilled as discussed below.

2.—"Scotchlite" brand glass beads type 120: This material is a lime-soda glass in the form of fire polished microspheres.

3.—Pyrex wool: Pyrex brand glass wool (Owens-Corning Fiberglass Corp.) Catalog Number 800 was used.

Results

1. Unetched Adsorbents. Type 520 Beads.—These beads gave S-shaped CO_2 adsorption isotherms at temperatures from − 77.0 to − 77.6°. Experimental error obscures the temperature dependence of the isotherms in this range. The results of five isotherm determinations are shown in Fig. 2. The simple (two constant) Brunauer, Emmett and Teller equation[4] applied to this adsorbent gives a linear plot for relative pressures less than about 0.2. The specific surface area calculated by the BET method is 0.158 square meter per gram using the value 17.0 Å.^{2} per molecule for CO_2.[5] It is interesting to note that the surface area calculated from Emmett and Brunauer's point B[5] is 0.16 square meter per gram, a value which is in reasonable agreement with the BET value.

The specific surface area calculated from the size distribution of the beads and their density is 0.151 square meter per gram. The size distribution was determined from samples totaling 392 beads with the results shown in Fig. 2. While this small a

(1) E. I. du Pont de Nemours and Company, Research Fellow, 1950–1951. Present address: E. I. du Pont de Nemours and Company, Wilmington, Delaware.

(2) Franklin E. and Orinda M. Johnson Fellow, 1948–1949. Present address: Massachusetts Institute of Technology, Cambridge, Mass.

(3) A. F. O. Germann, *J. Am. Chem. Soc.*, **36**, 2456 (1914).

(4) S. Brunauer, P. H. Emmett and E. Teller, *ibid.*, **60**, 309 (1938).

(5) P. H. Emmett and S. Brunauer, *ibid.*, **59**, 1559 (1937).

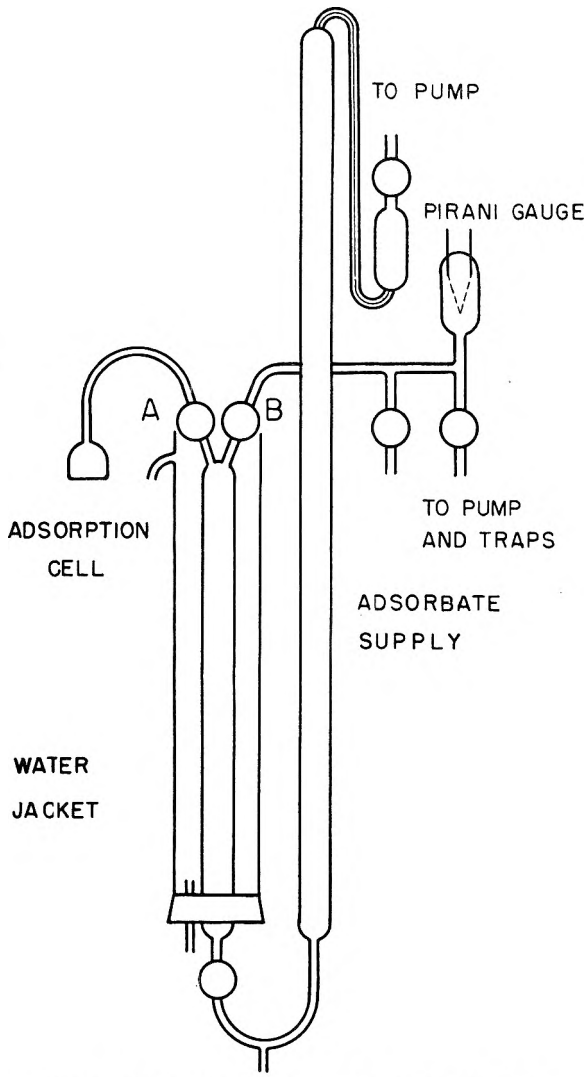

Fig. 1.—Adsorption apparatus (schematic diagram).

count of the beads cannot give a highly accurate value for the geometric surface, we feel that it is nevertheless sufficient to establish the fact that the geometric surface and the surface determined from adsorption data are equal within the limitations of the BET method. In other words, the adsorbent is approximately smooth on the molecular scale, at least with respect to CO_2 molecules. The geometric surface was calculated by the equation

$$S = \frac{6\Sigma nd^2}{\Sigma nd^3} \times \frac{1}{\text{density}}$$

where S is the specific surface area and n is the number of beads having a mean diameter d.

The adsorbent was degassed at 150 to 180° for 18 hours initially and between determinations. Some gas was still being evolved at the end of these degassing periods while the adsorbent was hot, but the evolution ceased when the adsorbent was cooled below about 60°.

Type 120 Beads.—A further study of degassing conditions was made on the Type 120 glass beads. This adsorbent contains considerable water, which was observed to condense in the gas buret when the

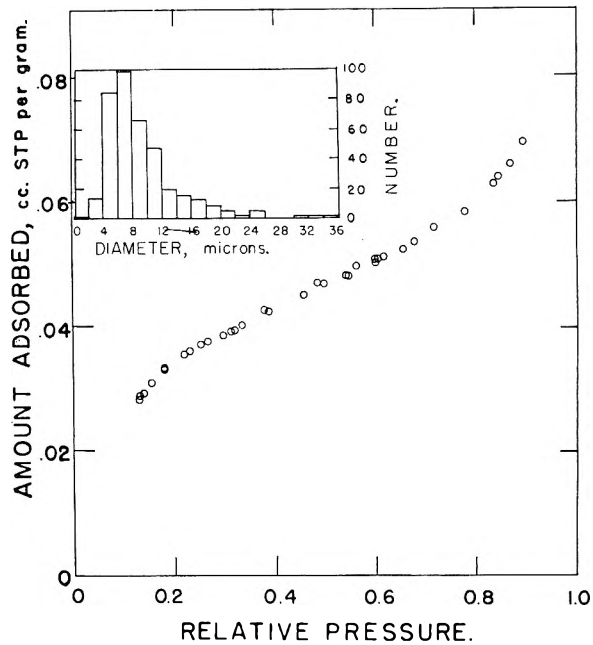

Fig. 2.—Type 520 glass beads; size distribution and CO_2 adsorption isotherm.

glass was heated in the adsorption cell with the vacuum pump shut off.

Curve A is the CO_2 isotherm at −78° obtained after degassing the adsorbent 1 hour at 70° and 17 hours at 25° at 10^{-4} mm. pressure. The surface water remaining after this treatment results in a relatively large CO_2 adsorption. Curve B is the

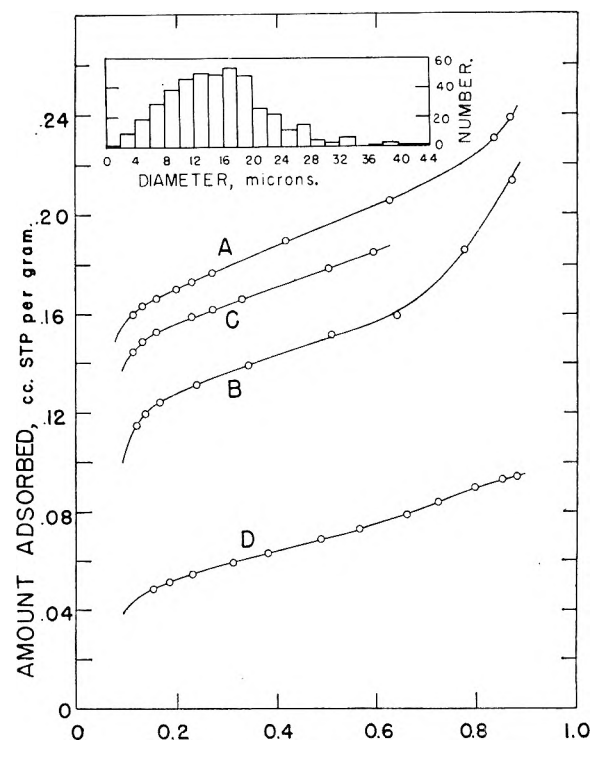

Fig. 3.—Type 120 glass beads: size distribution and CO_2 isotherms showing the effect of water on CO_2 adsorption and the effect of water diffusing to the surface of superficially dried glass.

CO_2 isotherm obtained after further degassing at 40 to 50° for 18 hours. The smaller adsorption after this treatment we ascribe to the partial depletion of the surface water under these degassing conditions. Curve C is the CO_2 isotherm obtained after evacuating the sample to 10^{-4} mm. at 25° and allowing it to stand without further pumping overnight. The increase in adsorption over the previous amount is due to an increase in the amount of surface water as a result of outward diffusion of water dissolved in the glass. Curve D is the CO_2 isotherm obtained after degassing 18 hours at 170–180°. This treatment removes nearly all the surface water and the CO_2 adsorption is only 1.7 times that calculated for the geometric surface of the sample. This factor of 1.7 may be due either to roughness of the surface or to water not removed by the 180° degassing. The loss in weight due to the degassing amounted to about 0.22 wt. %.

The fact that the middle portions of the isotherms are of the same shape, differing only in vertical displacement, indicates that a given amount of surface water takes up a constant amount of CO_2 above relative pressures of about 0.2 or less. The process by which this CO_2 is taken up may be regarded as a chemical combination of CO_2 and the surface water phase or as a case of chemisorption of CO_2 by water. The remainder of the CO_2 is held by physical adsorption which is approximately equal for dry glass and for the water–CO_2 surface presented by wet glass. It is more than possible that the rate of diffusion of water through a glass membrane may be measured by the influence of water on the adsorption of CO_2.

Pyrex Wool.—This adsorbent gives a CO_2 isotherm at −78° which is everywhere convex to the pressure axis, the familiar Type III isotherm. However, during determinations of the isotherm, it was frequently observed that extremely large amounts of CO_2 disappeared from the gas phase, only to reappear after a short time. The small adsorption, referred to hereafter as normal adsorption, was always less than about $1/3$ of a molecular layer (based on geometric surface) up to relative pressures of 0.82, while the large adsorption, hereafter called abnormal adsorption, occasionally was equivalent to 30 molecular layers at relative pressures as low as 0.62. The abnormal adsorption could not be made to take place in a reproducible manner, but started to occur as the relative pressure was increased to values, different for each determination, greater than 0.6. Normal adsorption could often be obtained at relative pressures less than 0.8, but attempts to further increase the pressure while normal adsorption was being observed always resulted in abnormal adsorption.

The abnormal adsorption is thought to be not true adsorption but rather capillary condensation of CO_2 in the interfibrillar spaces of the Pyrex wool. The Kelvin equation for capillary condensation does not, however, account for the amount of CO_2 condensed, giving values of only about $1/100$ of that observed even assuming the fibers were hexagonally close packed so as to give the maximum capillary space, which they were not.

Etched Adsorbents.—Samples of both types of glass beads were allowed to stand with occasional stirring in carefully purified water at room temperature for 33 days. The samples were then filtered, washed and air dried at room temperature for 8 days. CO_2 isotherms at −78° were then determined for the samples, which were degassed 18 hours at 150–170° initially and between determinations. The initially determined (Type II) isotherms agreed with those made after further degassing, indicating that the increased adsorption observed was not due to incomplete removal of water. The adsorption by etched Type 520 beads was 21 times that of an equal weight of untreated beads. The adsorption by etched Type 120 beads was 12 times that of the untreated beads. The increased adsorption by the etched beads was taken to indicate an increase in surface area as the result of etching by water. Analysis of the filtrates from the etched samples and microscopic examination of the samples indicated that no important increase in specific surface resulted from a decrease in size of the spheres by the solvent action of water.

THE ADSORPTION OF COBALT AND BARIUM IONS BY HYDROUS FERRIC OXIDE AT EQUILIBRIUM

By J. E. Duval and M. H. Kurbatov

Department of Chemistry, The Ohio State University, Columbus 10, Ohio

Received November 30, 1951

A study of the adsorption of barium and cobalt ions in quantities less than 10^{-8} gram atom per 30 ml. of solution was pursued with the purpose of effecting the separation of these elements as they appear in radioactive forms after activation of stable isotopes or in fission and spallation nuclear reactions. The behavior of these divalent ions in such extreme dilution, with respect to adsorption phenomena at equilibrium, was investigated in order to verify the previously derived adsorption equation. It was found that under comparable conditions cobalt is adsorbed to a greater extent than barium, the ratio of the two being as high as four in some cases shown. The amount of cobalt or barium adsorbed at equilibrium increases with *p*H and quantity of adsorbent in a manner consistent with the law of mass action, when the *p*H of the solution is above 6.5 to 7.0. At *p*H less than 6.5 to 7.0 the adsorption of cobalt is greater than expected from the simplified mass law equation, in which the effect of anions, such as chloride, is considered constant. Barium and cobalt ions which occur together in low concentration in fission products can be separated from one another only partially by adsorption on hydrous ferric oxide.

Introduction

The adsorption of ions by hydrous ferric oxide has been used as a means of preparing carrier free samples of radioactive species of high specific activity. Samples in which there is a high ratio of the number of radioactive atoms to the total number of isotopic atoms are important for: (1) studies of the radiations from the species themselves, (2) tracer experiments in chemistry, medicine, biology, etc., (3) determining the behavior of ions at such low concentrations that the interactions between these ions themselves are negligible.

In this paper is presented a study of the adsorption of cobalt and barium ions by hydrous ferric oxide at equilibrium. These experiments were performed to determine the relative extent of adsorption of cobalt and barium ions and to show that their adsorption follows the law of mass action. The amount of material adsorbed was determined by radioactive tracer methods, utilizing cobalt-60 and barium-133.

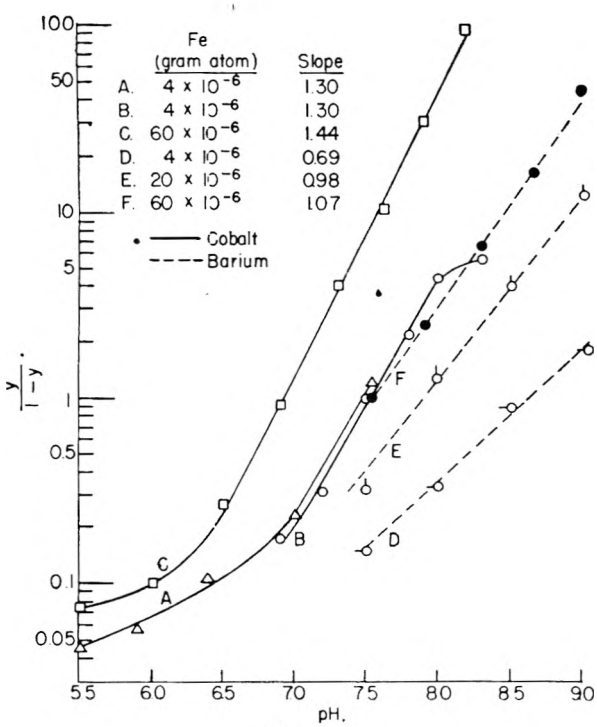

Fig. 1.

Tracer Preparation.—The cobalt used in these experiments was a mixture of cobalt-60 and cobalt-59, obtained from the Isotopes Division of the Oak Ridge National Laboratory. It was prepared by neutron pile activation of spectroscopically pure cobalt-59.

The barium used was barium-133, $T_{1/2}$ = 38.8 hours, which was obtained by deuteron bombardment of spectroscopically pure cesium chloride in The Ohio State University cyclotron. The barium produced was separated by adsorption on hydrous ferric oxide.

The target was allowed to stand for three hours, after activation, to permit the decay of 38-minute chlorine-38. The target material was then dissolved in about 25 ml. of dilute hydrochloric acid, and this solution was concentrated by evaporation to about 5 ml. Five milliliters of 0.01 *M* ferric chloride was added, and the solution was made strongly basic with ammonia. Adsorption of barium by the precipitated hydrous ferric oxide was allowed to proceed for one hour, after which the solution was filtered. The precipitate was washed with ammonium chloride–ammonia solution to remove monovalent ions. After the precipitate had been washed, it was dissolved in concentrated hydrochloric acid.

The ferric chloride solution containing barium was evaporated to dryness, and the residue was dissolved in hydrochloric acid. The solution was then titrated to *p*H 5.5 with 0.1 *N* ammonium hydroxide. Hydrous ferric oxide was precipitated at this *p*H, but it adsorbed only a small fraction of the barium (less than 1%). The solution was filtered, and the precipitate was washed with a dilute ammonium chloride solution the *p*H of which was 5.3.

The filtrate was evaporated to dryness, and the ammonium chloride in the residue was sublimed. Traces of cesium were removed by a repetition of the adsorption procedure.

The barium was finally obtained as a solution of barium chloride in 0.01 *N* hydrochloric acid. The concentration of barium ions was estimated to be less than 1×10^{-9} gram atom per 2 ml.

Adsorption Procedure.—All adsorption experiments were conducted with a constant chloride ion concentration in solution of 2.79×10^{-1} gram atom, a final volume of solution after titration of 32 ± 0.3 ml., and at room temperature, about 27°.

Samples were prepared which contained 2 ml. of ferric chloride solution of desired strength and 2 ml. of tracer. Varying amounts of triply distilled water and 0.01 *N* hydrochloric acid were added to the samples in order to keep the final volume and the chloride ion content constant. The samples were prepared in outside ground weighing bottles. Immediately after the samples had been titrated to various *p*H values, they were stoppered, and the adsorption of barium or cobalt ions by the coagulated hydrous ferric oxide was allowed to reach equilibrium. The adsorption time was about 50 hours.

After the adsorption had reached equilibrium, the bottles were opened, and 5-ml. portions were pipetted from the supernatant liquid. These were evaporated to dryness in small dishes, and the activities were measured by means of a mica end-window Geiger–Müller tube. Since the amount of activity used per sample and the total volume were known, the amount of tracer adsorbed (y), and the amount

TABLE I

*p*H EFFECT: COBALT

Constant factors: cobalt, 2.8×10^{-9} gram atom; chloride, 2.79×10^{-4} gram atom; volume, 32.1 ± 0.2 ml.

Experiment A, Fe, 4×10^{-6} gram atom			Experiment B, Fe, 4×10^{-6} gram atom			Experiment C, Fe, 60×10^{-6} gram atom		
*p*H	$y/1-y$	Adsorbed, %	*p*H	$y/1-y$	Adsorbed, %	*p*H	$y/1-y$	Adsorbed, %
5.50	0.45	4.3	6.90	0.18	15.0	5.50	0.07	6.8
5.90	.56	5.4	7.20	.31	22.9	6.02	.10	8.9
6.40	.11	10.0	7.50	.99	49.7	6.50	.26	20.7
7.00	.23	18.9	7.80	2.18	68.6	6.90	.91	47.5
7.54	1.20	54.6	8.00	4.38	81.4	7.30	4.00	80.0
			8.30	5.52	84.7	7.62	10.20	91.1
						7.91	30.20	96.8
						8.20	92.20	98.9

BARIUM

Constant factors: barium, 1×10^{-9} gram atom or less; chloride, 2.79×10^{-4} gram atom; volume, 32.1 ± 0.2 ml.

Experiment D, Fe, 4×10^{-6} gram atom			Experiment E, Fe, 20×10^{-6} gram atom			Experiment F, Fe, 60×10^{-6} gram atom		
*p*H	$y/1-y$	Adsorbed, %	*p*H	$y/1-y$	Adsorbed, %	*p*H	$y/1-y$	Adsorbed, %
7.51	0.15	13.2	7.51	0.32	24.0	7.53	1.01	50.1
8.01	.34	24.8	7.99	1.28	56.1	7.90	2.47	71.1
8.51	.88	46.8	8.51	3.98	79.9	8.31	6.49	86.7
9.03	1.78	64.0	9.02	12.22	92.5	8.67	16.50	94.3
						9.00	45.56	97.9

TABLE II

EFFECT OF ADSORBENT QUANTITY

Cobalt

Constant factors: cobalt, 2.8×10^{-9} gram atom; chloride, 2.79×10^{-4} gram atom; volume, 32.0 ± 0.2 ml.

Experiment G, *p*H 6.8			Experiment H, *p*H 7.5		
Fe (g. atoms $\times 10^6$)	$y/1-y$	Adsorbed, %	Fe (g. atoms $\times 10^6$)	$y/1-y$	Adsorbed, %
4	0.12	10.4	4	0.81	44.7
6	.17	14.3	6	1.20	54.7
10	.23	18.9	8	1.48	59.8
20	.41	27.2	10	1.67	62.6
60	.91	47.5	20	3.44	77.5
			60	10.24	91.1

Barium

Constant factors: barium, 1×10^{-9} gram atom or less; chloride, 2.79×10^{-4} gram atom; volume, 32.0 ± 0.1 ml.

Experiment J, *p*H 7.5		
Fe (g. atoms $\times 10^6$)	$y/1-y$	Adsorbed, %
4	0.12	10.9
6	.15	12.7
10	.21	17.2
20	.39	27.8
60	.72	41.8

not adsorbed ($1-y$), were calculated from the activity of the 5 ml. of solution.

The procedure used to study the effect of varying quantities of adsorbent was the same as for the *p*H effect shown above, except that the quantities of adsorbent were varied, while the *p*H of the samples were constant.

Adsorption Results

Results of the adsorption experiments are given in Tables I and II. In addition the data of Table I have been plotted in order to show the nature of the curves. The fraction $y/(1-y)$ is the ratio of the quantity of tracer adsorbed to the quantity unadsorbed at constant volume. It is related to the *p*H and quantity of adsorbent by the previously derived[1,2] equation

$$K = \frac{y}{1-y} \times \frac{(H_3O^+)^z}{(\text{adsorbent})^z}$$

This equation results from the treatment of the adsorption system as a cation exchange system in equilibrium which follows the law of mass action when the activities of the ions in solution are their molar concentrations and when other ion concentrations, such as chloride, are effectively constant. It can be seen from the equation that if the quantity of adsorbent is maintained constant, a plot of log $y/(1-y)$ *vs.* *p*H should give a straight line provided the volume and chloride ion concentrations are constant. Likewise, if the *p*H is maintained constant, a plot of log $y/(1-y)$ *vs.* log (gram atoms of iron) should also produce a straight line.

These experiments indicate that, (1) the adsorption of barium and cobalt follows the law of mass action. The curves obtained by plotting $y/(1-y)$ *vs.* *p*H or quantity of adsorbent are straight lines over most of the region studied. The fact that the straight line portions of the curves for either cobalt or barium are not of the same slope but that the slopes are increased when the quantity of hydrous oxide is greater, is taken to indicate that the actual quantity of adsorbent depends not only on the quantity of hydrous oxide precipitated but upon the *p*H as well. This is consistent with the view that the adsorbent is both an anion and a cation exchanger, and that the nature and quantity of anion affects the quantity of cation adsorbed.[1]

(2) For cobalt below *p*H 7 and 6.5, experiments A and C, respectively, the adsorption does not follow the equation. Possibly, under these conditions the adsorption becomes more strongly dependent on

(1) M. H. Kurbatov, Gwendolyn B. Wood and J. D. Kurbatov, THIS JOURNAL, **55**, 1170 (1951).

(2) M. H. Kurbatov, G. B. Wood and J. D. Kurbatov, *J. Chem. Phys.*, **19**, 258 (1951).

other factors such as chloride ion concentration than it is at higher *p*H.

(3) Cobalt is adsorbed to a greater extent than barium under comparable conditions, the ratio between the two being as high as four in some cases. In experiment B at *p*H 7.50, 49.7% of the cobalt was adsorbed, while in experiment D at *p*H 7.51, 13.2% of the barium was adsorbed. In experiment H with the quantity of adsorbent 4×10^{-6} gram atom, the adsorption of cobalt was 44.7%, while in experiment J with this same quantity of adsorbent the adsorption of barium was 10.9%. Despite this difference in per cent. adsorbed, barium and cobalt which occur together in low concentrations in fission products cannot be separated from one another to give samples of high radioactive purity, since the amount of barium adsorbed, while considerably less than the amount of cobalt adsorbed, is still quite large.

(4) The relative extent of adsorption of cobalt and barium is the reverse of that reported by Kressman and Kitchener for the adsorption of these ions on a phenol sulfonic acid resin.[3] They indicate that the extent of adsorption of cobalt is determined by the ion association of cobalt ions and a "primary determining factor, which may or may not be ionic size." In the case of adsorption on hydrous ferric oxide, it is believed that a more significant factor is the weakly basic character of cobalt, that is, the hydrolysis of cobalt ion is a controlling factor in its adsorption by the very weakly acidic adsorbent, hydrous ferric oxide. Cobalt and barium ions are adsorbed on hydrous ferric oxide in the reverse order of the basicities of their hydroxides.

The support of this research by the Development Fund of The Ohio State University and grants received through the Graduate School from the Research Foundation are gratefully acknowledged by the authors.

(3) T. R. E. Kressman and J. A. Kitchener, *J. Chem. Soc.*, 1201 (1949).

MATHEMATICS OF ADSORPTION IN BEDS. VI. THE EFFECT OF LONGITUDINAL DIFFUSION IN ION EXCHANGE AND CHROMATOGRAPHIC COLUMNS[1]

BY LEON LAPIDUS[2] AND NEAL R. AMUNDSON

University of Minnesota, Minneapolis 14, Minnesota

Received January 2, 1952

The effect of longitudinal diffusion in chromatographic and ion exchange columns is considered. Calculations made under the assumption of pointwise local equilibrium show that sharp boundaries are smoothed out, thus casting some doubt on the column method for determining isotherms. The problem in which the local rate of removal follows a first order kinetic law is also solved and this solution is a new one.

Of the many factors which may determine the dynamic behavior of an adsorption column, the effect of diffusion has received the least attention. The diffusional effects may manifest themselves, in general, in three ways under the most simple assumptions. If there is a resistance to mass transfer between the fluid and solid, it is usually assumed that this is a diffusional phenomenon. If the particles used as adsorbent are of some size and if the whole particle is to be used effectively, it is necessary that the adsorbate diffuse through the fluid in the intraparticle volume before adsorption can take place inside the particle. These two effects have already been considered by the writers.[3] The third effect, that of longitudinal diffusion in the interparticle fluid, was considered partially by Glueckauf, Barker and Kitt,[4] and it is the purpose of this paper to generalize and extend this work. Longitudinal diffusion causes a flow of adsorbate which is superimposed upon the convective flow of fluid through the column. Physically, it is clear that diffusion will tend to smear out sharp adsorption bands formed in the column and this is substantiated by the calculations.

Certainly longitudinal diffusion will be a small effect on the total flow of adsorbate through the column. This brings up, however, a rather interesting conflict on the basic character of chromatographic analysis. The early theory of chromatography assumed that equilibrium between adsorbent and adsorbate solution was immediately established. Later work showed that this required an extremely small rate of flow through the column, in which case the effect of diffusion becomes more pronounced. On the other hand, if flow rates are high the equilibrium theory becomes questionable and some rate process must be used for the local adsorption mechanism.

It is assumed here that a column of unit cross sectional area is packed with a finely divided adsorbent such that the interparticle volume is filled with solvent or solution. The column may have an initial adsorbate content on the adsorbent as well as in the interparticle volume. At time zero a solution, whose concentration may vary with the time, is admitted to the column. It is desired to know the concentration of the interparticle solution and the adsorbate content of the adsorbent at any time and at any position in the bed. Let

c = concentration of adsorbate in the fluid stream, moles per unit volume of solution

(1) Presented at the XIIth International Congress of Pure and Applied Chemistry, New York, N. Y., Sept. 13, 1951.

(2) Forrestal Research Center, Chemical Kinetics Division, Princeton University, Princeton, New Jersey

(3) P. R. Kasten, L. Lapidus and N. R. Amundson, THIS JOURNAL, 56, 683 (1952).

(4) E. Glueckauf, K. H. Barker and G. P. Kitt, *Discussions of the Faraday Soc.*, No. 7, 199 (1949).

n = amount of adsorbate on the adsorbent, moles per unit volume of bed as packed
V = velocity of fluid through interstices of the bed
z = distance variable along the bed
D = diffusion coefficient of the adsorbate in solution in the bed
$c_0(t)$ = concentration of solution admitted to the bed.
$c_i(z)$ = initial concentration of solution in the interparticle volume in the bed
$n_i(z)$ = initial adsorbate concentration on the adsorbent
α = fractional void volume in the bed

Then on analyzing an elemental length of bed Δz, the equation

$$D\frac{\partial^2 c}{\partial z^2} = V\frac{\partial c}{\partial z} + \frac{\partial c}{\partial t} + \frac{1}{\alpha}\frac{\partial n}{\partial t} \qquad (1)$$

results.

It is necessary to make some assumption concerning the mechanism of adsorption, that is, the local relation between c and n. Although it would be desirable to use a general relation of the form

$$\frac{\partial n}{\partial t} = f(n,c)$$

two special cases will be treated here

$$n = k_1 c + k_2 \qquad (2)$$
$$\partial n/\partial t = k_1 c - k_2 n \qquad (2')$$

The first implies that equilibrium is established at each point in the bed while the second assumes the rate of adsorption is finite. The second also contains in it the special case of mass transfer at the particle surface in which the equilibrium is linear as assumed by Hougen and Marshall,[5] *i.e.*

$$\partial n/\partial t = k_f(c - c^*)$$

where k_f is a mass transfer coefficient and $n = k_1 c^*$. The additional relations

$$c = c_0(t) \quad \text{when } z = 0,\ t > 0 \qquad (3)$$
$$\left.\begin{aligned} c &= c_i(z) \\ n &= n_i(z) \end{aligned}\right\} \quad \text{when } t = 0,\ z > 0 \qquad (4)$$

describe, respectively, the inlet fluid and the initial condition of the bed.

The problem as stated above is the most general one with the assumptions used here. One assumption which is generally not valid but which has been tacit in practically all previous work concerns the character of the hydrodynamic velocity profile. If the velocity profile is not uniform one would not expect the concentration profile to be uniform. Hence equation 1 is in error in not only neglecting the hydrodynamic variations but also the consequent concentration effects.

Equilibrium Case.—If pointwise equilibrium is established in the column at each point, it is necessary to solve equations 1, 2, 3 and 4. This is possible since the problem may be easily reduced to problems which have already been solved. Details of the solution are given in the appendix. The solution is

$$c(z,t) = [f_1(z,t) + f_2(z,t)]\exp\left(\frac{Vz}{2D} - \frac{V^2 t}{4D\gamma}\right) \qquad (5)$$

(5) O. Hougen and W. R. Marshall, *Chem. Eng. Prog.*, 43, 197 (1947).

where

$$f_1(z,t) = \frac{1}{2}\sqrt{\frac{\gamma}{\pi D t}}\int_0^\infty c_i(s)\exp\left(\frac{-Vs}{2D}\right)\left[\exp\left(\frac{-\gamma(s-z)^2}{4Dt}\right) - \exp\left(\frac{-\gamma(s+z)^2}{4Dt}\right)\right]ds \qquad (6)$$

and

$$f_2(z,t) = \frac{z}{2}\sqrt{\frac{\gamma}{\pi D}}\int_0^t c_0(s)\exp\left[\frac{V^2 s}{4D\gamma} - \frac{\gamma z^2}{4D(t-s)}\right]\frac{ds}{(t-s)^{3/2}} \qquad (7)$$

Special cases of equation 5 may be obtained with ease. Suppose, for example, that $c_0(t)$ and $c_i(z)$ are constants, c_0 and c_i, respectively, then straightforward manipulation of the integrals produces

$$\frac{c - c_i}{c_0 - c_i} = H(v) \qquad (8)$$

where $Vt\alpha = v$ and

$$H(v) = \frac{1}{2}\left[1 + \operatorname{erf}\left(\sqrt{\frac{vV}{4\gamma\alpha D}} - z\sqrt{\frac{\gamma\alpha V}{4vD}}\right) + e^{\frac{Vz}{D}}\operatorname{erfc}\left(\sqrt{\frac{vV}{4\gamma\alpha D}} + z\sqrt{\frac{\gamma\alpha V}{4vD}}\right)\right] \qquad (9)$$

where erf and erfc are the error and complementary error functions, respectively.

From equations 8 and 9 it is seen that the concentration ratio is dependent upon two variables, V/D and $v/\gamma\alpha$. In Fig. 1 equation 8 is plotted as concentration ratio c/c_0 *versus* v for $z = 50$ and with values of $V/D = 1, 2, 10$ and 100 for $\gamma\alpha = 5$ and $\gamma\alpha = 25$. Curves A, B, C and D are for decreasing diffusivity with fixed velocity or for increasing velocity and fixed diffusivity. Hence as the velocity decreases through the bed the sharp breakthrough point which would normally be expected tends to be smeared out. Curves E, F, G are for a smaller value of $\gamma\alpha$ and illustrate the effect of a lower capacity adsorbent. In this case the effect of diffusion is not as pronounced.

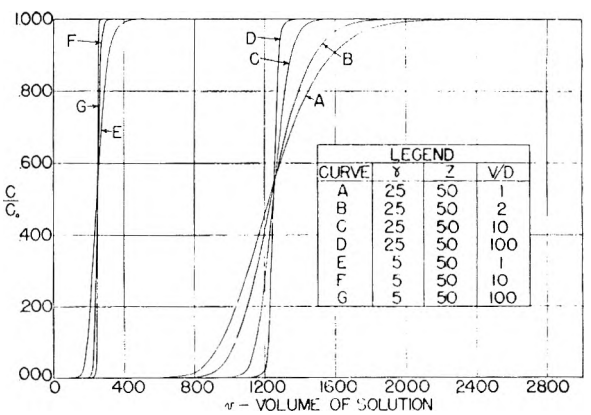

Fig. 1.—Plot showing the effect of longitudinal diffusion for an infinite column in which equilibrium is established locally. Initial adsorbate concentration is zero. Influent concentration is c_0.

It is well known that the solution for no diffusion, $D = 0$, is

$$c = \begin{cases} c_i\left(z - \dfrac{v}{\gamma\alpha}\right), & z > v/\gamma\alpha \\ c_0\left(\dfrac{v}{V\alpha} - \dfrac{\gamma z}{V}\right), & v > z\gamma\alpha \end{cases}$$

and hence the graph corresponding to Fig. 1 is a step function, the steps occurring at $v = 250$ and 1250. The graphs in Fig. 1 are seen to converge to these step functions.

A second special case of some interest is that one in which the feed solution contains a pulse in composition. It is supposed the concentration is c_0 from zero time to time $\bar{t}$, after which it jumps to c_{00} and remains so after $\bar{t}$. Let c_i be zero for convenience only. Equation 5 reduces to

$$\begin{aligned} c(z,t) &= c_0 H(v) + (c_{00} - c_0)\, H(v - \bar{v}), && \bar{v} < v < \infty \\ &= c_0\, H(v) && v < \bar{v} \end{aligned} \qquad (10)$$

where $V\bar{t}/\alpha = \bar{v}$ with $H(v)$ defined in Equation 9.

Figure 2 contains plots of Equation 10 with the same parameter values used in Fig. 1 and with $\bar{v} = 300$ and $c_{00} = 0$. One can see here how the unit pulse, expected for $D = 0$, is smoothed out by diffusion and reduced to less than half its expected value. In Fig. 3 the same equation is plotted with $c_{00} = c_0/2$.

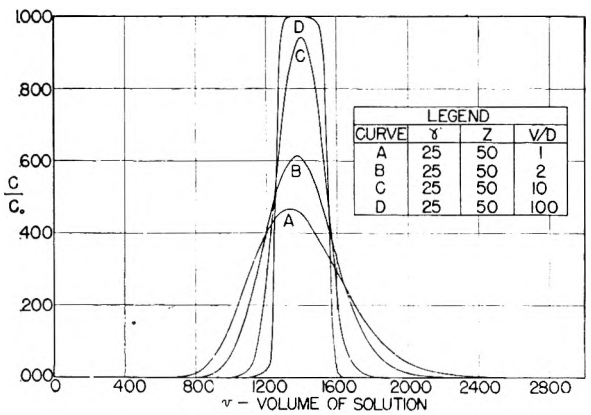

Fig. 2.—Plot showing the effect of longitudinal diffusion for an infinite column in which equilibrium is established locally. Initial adsorbate concentration is zero and the influent solution has a pulse in concentration of c_0 of duration equivalent to 300 cc. of feed.

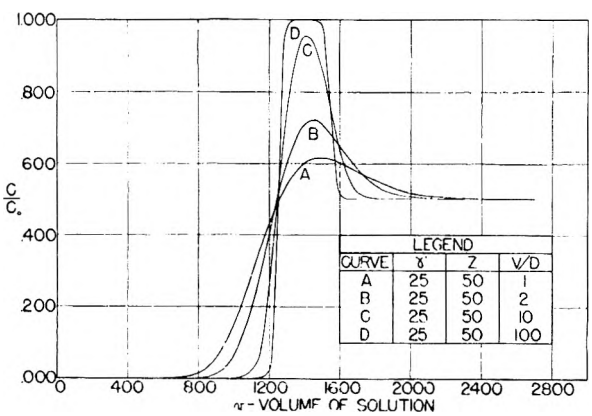

Fig. 3.—Plot showing the effect of longitudinal diffusion for an infinite column in which equilibrium is established locally. Initial adsorbate concentration is zero and the influent solution has a pulse in concentration of c_0 of duration equivalent to 300 cc. of feed followed by a solution whose concentration is $c_0/2$.

Non-equilibrium Case.—The equilibrium assumption is probably not realistic at flow rates commonly encountered. As a first approach the solution will be obtained for the system consisting of Equations 1, 2′, 3 and 4. The details will be presented in the appendix. The solution is

$$c(z,t) = e^{\frac{Vz}{2D}}(Y_1 + Y_2) \qquad (11)$$

where

$$Y_2 = \int_0^t [F'(\tau) + kF(\tau)]c_0(t - \tau)\mathrm{d}\tau \qquad (12)$$

$$F(t) = e^{-kt}\int_0^t I_0\left[2\sqrt{\frac{k_1k_2x}{\alpha}(t - x)}\right]\frac{z}{2\sqrt{\pi D x^3}}\, e^{-\frac{z^2}{4Dx} - xd}\, \mathrm{d}x \qquad (13)$$

and

$$Y_1 = \int_0^\infty \{[H'(t,z - s) - H'(t,z + s)]X + [H(t,z - s) - H(t,z + s)]Y\}\, \mathrm{d}s \qquad (14)$$

$$H(t,q) = \sqrt{\frac{D}{\pi}}\, e^{-k_2t}\int_0^t I_0\left[2\sqrt{\frac{k_1k_2x}{\alpha}(t - x)}\right] e^{-\frac{q^2}{4x} - xd}\, \frac{\mathrm{d}x}{\sqrt{x}} \qquad (15)$$

$$X = \frac{1}{D}\, c_i(s)\, e^{\frac{Vs}{2D}} \qquad (16)$$

$$Y = \frac{k_2}{2D}\,[n_i(s) + \alpha c_i(s)]e^{\frac{Vs}{2D}} \qquad (17)$$

where I_0 is the modified Bessel function of zero order.

Equation 11 is rather complicated to use, although it contains only well tabulated functions. The complexity of this solution is characteristic of those problems involving fixed bed operation when any but the most trivial assumptions are made concerning the local mechanism. For the special case $c_i = n_i = 0$ and $c_0(t) = c_0$, a constant, equation 11 reduces to

$$\frac{c}{c_0} = e^{\frac{Vz}{2D}}\left[F(t) + k_2\int_0^t F(t)\,\mathrm{d}t\right]$$

If diffusion is neglected, this solution reduces to

$$\begin{aligned} \frac{c}{c_0} &= e^{-\frac{kz}{V\alpha}}\left[e^{-k_2\left(t - \frac{z}{V}\right)} I_0\left(2\sqrt{\frac{k_1k_2z}{\alpha V}\left(t - \frac{z}{V}\right)}\right) + k_2\int_0^{t - \frac{z}{V}} e^{-k_2s} I_0\left(2\sqrt{\frac{k_1k_2zs}{\alpha V}}\right)\mathrm{d}s\right], && t > z/V \\ &= 0 && t < z/V \end{aligned}$$

The above solution has been obtained by many writers.

It is thus possible to obtain analytical solutions to problems with linear isotherms or linear kinetics; almost all effects may be taken into consideration. It is of the utmost importance to obtain experimental data to determine the pertinence of these effects. It is essential also to obtain experimental data on the hydrodynamical characteristics of flow through packed beds of solids. Data for large particles are available, but data for small particles are almost non-existent.

Note that these calculations assume a column of infinite extent. The values shown in Figs. 1, 2 and 3 for c/c_0 are not those of an effluent from a column 50 cm. in length, but are the concentration ratios 50 cm. from the inlet of an infinite column. The corresponding problems for a finite column have as yet been unsolved.

Appendix

Equilibrium Case.—From Equation 2 and with the substitution

$$c = g \exp\left(\frac{Vz}{2D} - \frac{V^2t}{4D\gamma}\right)$$

Equations 1, 3 and 4 may be written

$$\frac{D}{\gamma}\frac{\partial^2 g}{\partial z^2} = \frac{\partial g}{\partial t}$$

$$g = c_i(z) \exp\left(-\frac{Vz}{2D}\right), \text{ when } t = 0,\ z > 0$$

$$g = c_0(t) \exp\left(\frac{Vt^2}{4D\gamma}\right), \text{ when } z = 0,\ t > 0$$

where it has been assumed that $c_i(z)$ and $n_i(z)$ are equilibrium values. The system of equations may be split into two problems

$$\frac{D}{\gamma}\frac{\partial^2 f_1}{\partial z^2} = \frac{\partial f_1}{\partial t} \qquad \frac{D}{\gamma}\frac{\partial^2 f_2}{\partial z^2} = \frac{\partial f_2}{\partial t}$$

$$f_1 = c_i(z) \exp\left(-\frac{Vz}{2D}\right),\ t = 0 \qquad f_2 = 0 \quad ,\ t = 0$$

$$f_1 = 0 \quad ,\ z = 0 \qquad f_2 = c_0(t) \exp\left(\frac{V^2t}{4D\gamma}\right),\ z = 0$$

where it can easily be seen that $g = f_1 + f_2$.

From Churchill[6] the solution f_1 is given by equation 6 and from the same source[7] the solution f_2 may be derived to give equation 7.

Mention should be made here concerning the calculations. In equation 9 the product of an exponential and the erfc must be taken. The erfc is always small while the exponential is large since the exponent may be as high as 5000. This difficulty may be circumvented by using the assymptotic expansion for erfc(x).

$$\text{erfc}(x) = \pi^{-\frac{1}{2}} e^{-x^2}\left(\frac{1}{x} - \frac{1}{2x^3} + \frac{1\cdot3}{2^2x^5} - \frac{1\cdot3\cdot5}{2^3x^7} + \cdots\right)$$

Non-equilibrium Case.—The equilibrium assumption is probably not realistic at flow rates commonly encountered. As a first approach the solution will be obtained for the system consisting of equations 1, 2′, 3 and 4

$$D\frac{\partial^2 c}{\partial z^2} = V\frac{\partial c}{\partial z} + \frac{\partial c}{\partial t} + \frac{1}{\alpha}\frac{\partial n}{\partial t} \qquad (1)$$

$$\frac{\partial n}{\partial t} = k_1 c - k_2 n \qquad (2')$$

$$= c_0(t) \quad ,\ \text{when } z = 0,\ t > 0 \qquad (3)$$

$$\left.\begin{matrix} c = c_i(z) \\ n = n_i(z) \end{matrix}\right\} \ ,\ \text{when } t = 0,\ z > 0 \qquad (4)$$

This system seems to be a new one so that its solution will be discussed in some detail. The solution will be obtained by the method of the Laplace transformation. The definition of the transforms will be taken as

$$L[c(z,t)] = \int_0^\infty e^{-pt} c(z,t)\, dt = h(z,p) = h$$

$$L[n(z,t)] = N(z,p) = N$$

The transforms of equations 1 and 2 are

$$D\frac{d^2h}{dz^2} = V\frac{dh}{dz} + ph - c_i(z) + \frac{1}{\alpha}[pN - n_i(z)]$$

$$pN - n_i(z) = k_1 h - k_2 N$$

Elimination of N between these two equations gives

$$\frac{d^2h}{dz^2} - \frac{V}{D}\frac{dh}{dz} - \frac{h}{D}\left[\frac{\alpha p(p + k_2) + pk_1}{\alpha(p + k_2)}\right] = -\frac{1}{D}\left[c_i(z) + \frac{k_2 n_i(z)}{\alpha(p + k_2)}\right]$$

This must be solved subject to the conditions

$$h = L[c_0(t)] = h_0(p)$$

h finite as $z \longrightarrow \infty$

The latter condition ensures that the concentrations remain finite for large z.

It is convenient to make the change of variable

$$y = he^{-\frac{Vz}{2D}}$$

which reduces the above system to

$$\frac{d^2y}{dz^2} - gy = \frac{\alpha p c_i(z) + k_2[n_i(z) + \alpha c_i(z)]}{\alpha D(p + k_2)} e^{\frac{Vz}{2D}} = P(z)$$

$$y = h_0(p), \text{ when } z = 0$$

$$y = 0 \quad , \text{when } z \longrightarrow \infty$$

where

$$g = \frac{1}{D}\frac{p^2 + Ap + B}{p + k_2}$$

$$A = \frac{V^2\alpha + 4D(k_1 + \alpha k_2)}{4D\alpha}$$

$$B = \frac{V^2 k_2}{4D}$$

This problem may be split into two others

$$\frac{d^2y_1}{dz^2} - gy_1 = P(z) \qquad \frac{d^2y_2}{dz^2} - gy_2 = 0$$

$$y_1 = 0, \text{ when } z = 0 \qquad y_2 = h_0(p), \text{ when } z = 0$$

$$y_1 = 0, \text{ when } z \longrightarrow \infty \qquad y_2 = 0 \quad , \text{when } z \longrightarrow \infty$$

where $y = y_1 + y_2$

Consider y_1 first. The general solution may be written[8]

$$y_1 = C_1 e^{z\sqrt{g}} + C_2 e^{-z\sqrt{g}} + \frac{2}{\sqrt{g}}\int_0^z P(s) \sinh \sqrt{g}\,(z - s)\, ds$$

When $z = 0$, $C_1 = -C_2$ and when $z \to \infty$

$$C_1 = -\frac{1}{\sqrt{g}}\int_0^\infty P(s) e^{-s\sqrt{g}}\, ds$$

Therefore with a little manipulation

$$y_1 = -\frac{2}{\sqrt{g}}\int_0^z P(s) e^{-z\sqrt{g}} \sinh \sqrt{g} s\, ds - \frac{2}{\sqrt{g}}\int_z^\infty P(s) e^{-s\sqrt{g}} \sinh \sqrt{g} z\, ds$$

$$= \int_0^\infty P(s) G(z,s)\, ds$$

where the Green's function $G(z,s)$ is defined by

$$G(z,s) = \begin{cases} -\frac{2}{\sqrt{g}} e^{-z\sqrt{g}} \sinh \sqrt{g} s, & s < z \\ -\frac{2}{\sqrt{g}} e^{-s\sqrt{g}} \sinh \sqrt{g} z, & s > z \end{cases}$$

It is obvious that the solution for y_2 is

$$y_2 = h_0(p) e^{-z\sqrt{g}}$$

Since $h = y e^{\frac{Vz}{2D}}$, it is clear that the inverse transforms of y_1 and y_2 may be taken directly. Now y_2 may be written in the form

$$y_2 = k_2 h_0(p)\frac{e^{-z\sqrt{g}}}{p + k_2} + h_0(p) p \frac{e^{-z\sqrt{g}}}{p + k_2}$$

Consider the quantity

$$\frac{e^{-z\sqrt{g}}}{p + k_2}$$

The inverse of this function is not available directly from tables and its inversion by means of the inversion integral

(6) R. V. Churchill, "Modern Operational Mathematics in Engineering," McGraw-Hill Book Co., Inc., New York, N. Y., 1944, p. 117.

(7) Reference 6, p. 109.

(8) Kamke, "Differentialgleichungen," Chelsea Publishing Co., New York, N. Y., 1948, p. 607.

is beset with difficulties. However, by using a seldom used operational form the answer may be obtained.

The Laplace transform of the function

$$\int_0^t J_0\left[2\sqrt{x(t-x)}\right] f(x)\,dx$$

where J_0 is the zero-order Bessel function, is

$$\frac{1}{p}\phi\left(p+\frac{1}{p}\right)$$

where $\phi(p)$ is the transform of $f(t)$. (See reference 9, the eighth formula on the page and note also the difference in notation.) From this it is a simple matter to show that the transform of

$$e^{-k_2 t}\int_0^t J_0\left[2\sqrt{ax(t-x)}\right] f(x)dx$$

is

$$Q = \frac{1}{p+k_2}\,\phi\left(p+k_2+\frac{a}{p+k_2}\right)$$

If one chooses for $\phi(p)$

$$\phi(p) = e^{-k\sqrt{p+d}}$$

then

$$Q = \frac{1}{p+k_2}\exp\left[-k\sqrt{\frac{p^2+(2k_2+d)p+k_2^2+k_2 d+a}{p+k_2}}\right]$$

Therefore if one chooses

$$d = A - 2k_2 = \frac{V^2}{4D} + \frac{k_1}{\alpha} - k_2$$

$$-a = -B + k_2 A + k_2^2 = +\frac{k_1 k_2}{\alpha}$$

$$k = z/\sqrt{D}$$

then the inverse of Q is $L^{-1}(Q) = F(t)$, defined in Equation 13.

The inverse of $\phi(p)$ is

$$\frac{k}{2\sqrt{\pi t^3}}\,e^{-\frac{k^2}{4t}-td}$$

It is somewhat natural to expect this latter function to appear here since it occurred in the equilibrium case. Note that $F(o) = 0$ so that the inverse of y_2 may be written as a convolution, as in equation 12.

(9) N. W. McLachlan and Pierre Humbert, *Mem. des Science Math.*, **100**, 12 (1941).

In order to find the inverse transform of y_1 it is necessary to consider the inverse $P(s)G(z,s)$. $P(s)$ may be written

$$\frac{-pX-Y}{p+k_2} = P(s)$$

with X and Y defined in Equations 16 and 17.

Consider the function

$$R = (pX+Y)\,\frac{1}{\sqrt{g}}\,\frac{e^{-q\sqrt{g}}}{p+k_2} \qquad (18)$$

with q independent of p. The inverse of this function may be found by the method used on y_2 by taking $\phi(p)$ to be

$$\frac{e^{-q\sqrt{p+d}}}{\sqrt{p+d}}$$

whose inverse is

$$\frac{e^{-\frac{q^2}{4t}-td}}{\sqrt{\pi t}}$$

Hence the inverse of equation 18, omitting for the moment the factor $pX + Y$, is given by equation 15.

Now $H(o,q) = 0$ so that the inverse of R is

$$L^{-1}(R) = XH'(t,q) + YH(t,q)$$

with the prime denoting differentiation with respect to t.

The quantity q used here needs some elucidation. From the definition of the Green's function $G(z,s)$ the following may be written

$$e^{-z\sqrt{g}}\sinh\sqrt{g}s = \frac{1}{2}\left(e^{-\sqrt{g}(z-s)} - e^{-\sqrt{g}(z+s)}\right)$$

$$e^{-s\sqrt{g}}\sinh\sqrt{g}z = \frac{1}{2}\left(e^{-\sqrt{g}(s-z)} - e^{-\sqrt{g}(s+z)}\right)$$

Therefore in taking the inverse transform above, q must be chosen successively as

$$\frac{1}{\sqrt{D}}(z-s),\ \frac{1}{\sqrt{D}}(z+s),\ \frac{1}{\sqrt{D}}(s-z),\ \frac{1}{\sqrt{D}}(s+z)$$

but since q appears only as q^2 in Equation 13 only two values of q need be used

$$q^2 = (z-s)^2/D \quad , \quad (z+s)^2/D$$

Because of this fortuitous incident the Green's function has an inverse which may be represented by a single expression for all z and is given in equation 14. It can be shown that this solution satisfies all the conditions originally set down but these details will be omitted.

It may be rigorously shown that the solutions obtained in this paper converge to the solutions obtained from the equations when the diffusion is neglected, as $D \to 0$. This has some mathematical interest.

AN IMPROVED APPARATUS FOR THE STUDY OF FOAMS[1]

CHEVES WALLING, EDGAR E. RUFF AND JAMES L. THORNTON, JR.

Research and Development Division, Lever Brothers Company, Cambridge, Mass.

Received January 10, 1952

Foam drainage measurements on the five systems discussed here indicate that our apparatus gives useful results primarily with rapidly draining films (*e.g.*, sodium Oronite), in which, under the conditions studied, loss of liquid from the foam occurs entirely by loss of water from the films of the intact foam. With slow-draining foams (*e.g.*, soaps), initial foam densities are more erratic and foams collapse rather than drain, so that the present method of study is inapplicable. A more general (and probably intrinsically more interesting) application of the apparatus is to foam composition studies, and results obtained indicate that it can be used to determine surface concentrations on any system producing a stable enough foam with sufficiently uniform bubble size. The results with sodium myristate and dodecylamine hydrochloride show that it is particularly useful in determining surface concentrations of each component in polycomponent systems, and that, while absolute concentrations are subject to uncertainties in determining total film areas, relative surface concentrations may be determined with precision depending only on the analytical techniques employed. Further studies are in progress on both single- and polycomponent systems. The latter show particularly complicated and interesting behavior, which we hope to describe at a later date.

Introduction

Important physical properties of bulk foams such as drainage of liquid from the foam, viscosity and rate of bubble collapse appear to be determined primarily by the nature and amount of surfactant material concentrated in the surfaces of the bubble films. Although calculation of this surface concentration is theoretically possible for systems containing a single surfactant species from surface tension measurements *via* the Gibbs equation, experimental verification has proved difficult.[2] For multicomponent systems, no adequate theory exists, and direct measurements appear to offer the only feasible approach. A number of pieces of equipment have been devised for the determination of foam compositions and results have been summarized by Abribat,[3] and more recently by Bikerman[4] and by Shedlovsky,[5] while a simple device for the study of the drainage properties of single films has been described by Miles and co-workers.[6]

This paper describes a modified apparatus for the study of both foam drainage and foam composition which appears to offer several advantages over most previous devices. First, it distinguishes between drainage of liquid from the interstices of intact foams and drainage due to bubble collapse. Second, it permits the collection over a range of drainage times of large enough samples of foams for analysis. Finally, since the surface area of the foam being collected can be measured with reasonable accuracy, actual surface concentrations of surfactant materials in the foam can be calculated on the basis of a simple model.

Apparatus and Method

The apparatus employed is illustrated in Fig. 1. The foaming solution is contained in a 5-liter spherical vessel A with a 94 mm. i.d. (100 mm. o.d.) flat-ground neck C. Foam is produced by bubbling nitrogen through the inlet G, consisting of a 0.9 mm. glass nozzle. The foam produced rises through the column D, which consists of interchangeable units 30.5, 61.0 and 122 cm. in length, flat ground on the ends and joined to the foaming vessel with an adhesive tape. On reaching the top of the column D, the foam passes into the collector head E, 15.24 cm. in height, and is destroyed and thrown to the outer walls of the annular receiver by the whirling paddle F. In order to minimize evaporation from the foam, the collector head E is surmounted by a plastic cover with only a small hole for the shaft of the paddle F.

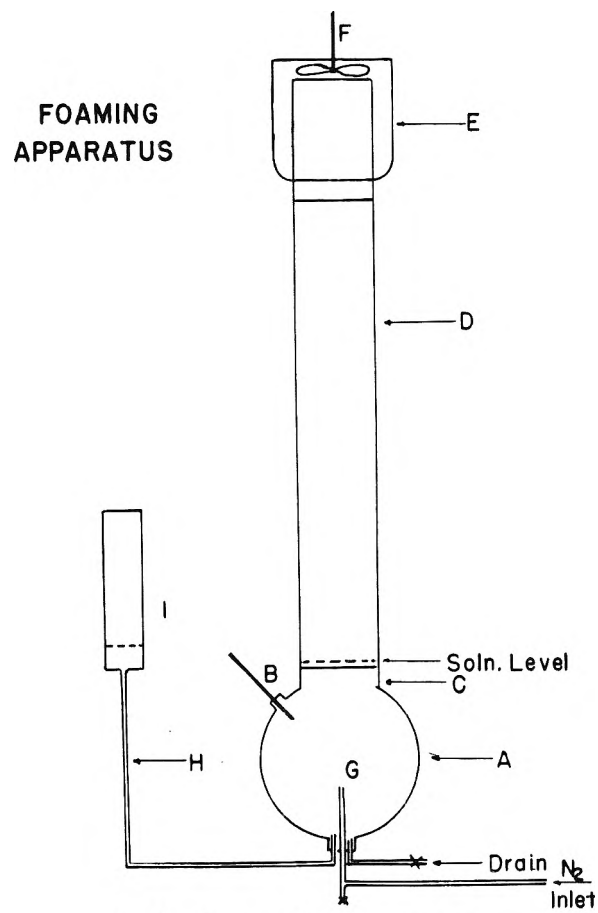

Fig. 1.—Diagram of foaming apparatus.

Rates of foam drainage are measured by determining the weight of foam collected in E for different heights of the column D at a constant rate of bubbling, either by periodically removing and weighing the collector head, or by observing the change in position of a toluene–water interface in the differential manometer H. The manometer consists simply of a vertical tube surmounted by a cylindrical reservoir containing toluene to which a small amount of oil-soluble dye has been added. The elevation of the manom-

(1) Presented in part at the XII International Congress of Pure and Applied Chemistry, New York, September 10, 1951.

(2) J. W. McBain and L. A. Wood, *Proc. Roy. Soc. (London)*, **A145**, 286 (1940).

(3) M. Abribat, *Actualites Scientifiques et Industrielles*, 123 (1942).

(4) J. J. Bikerman, "Surface Chemistry for Industrial Research," Academic Press Inc., New York, N. Y., 1947.

(5) L. Shedlovsky, *Ann. N. Y. Acad. Sci.*, **49**, 279 (1948).

(6) G. D. Miles, J. Ross and L. Shedlovsky, *J. Am. Oil Chemists Soc.*, **27**, 268 (1950).

eter is adjusted so that the toluene–water interface lies in the tube, and its sensitivity depends primarily upon the ratio of cross-sectional areas of the reservoir and the vertical tube. For convenience in changing surfactant solutions, the manometer is connected to the system through a stopcock, and all observations of interface level are made with foam rising in the column as the viscous drag of the rising foam displaces the interface level slightly. The manometer method provides a more continuous record, and the multiplication factor of the manometer is such that a 1-mm. movement of the interface corresponds to only 0.16 mm. change in the level of the foaming solution, or the production of 1.1 g. of foam. The temperature of the foaming solution is determined by a thermometer at B and, although the experiments reported here have all been made at approximately room temperature (28°), the apparatus has subsequently been thermostated to higher temperatures by warming the solution vessel with a Glascol heater and surrounding the column with a pasteboard tube containing an electric heating element.

Good foams are produced from many synthetic detergents and soaps at bubbling rates of 18.8 to 45.1 cc./sec., giving rates of foam rise of 2.7 to 6.5 mm./sec. By varying column heights, and placing the collector head directly on the flask, drainage times can thus be varied from 25 to 500 seconds. In this range, a number of surfactant materials give stable foams in which there is negligible breakage of bubbles as they rise through the column. Further, for many materials these bubbles prove to be surprisingly uniform in size throughout the volume of the column, except for a few very small bubbles trapped where the film between larger bubbles touches the column walls, and consist of polyhedra averaging 3 to 5 mm. in diameter. By stopping the flow of nitrogen, measuring and averaging the diameters of a number of bubbles, and calculating the total surface area as though the bubbles were spheres, a reasonably accurate value for the rate of surface production can be calculated by the relation $S = 3V/r$ where V is the total volume of foam and r the (average) bubble radius. This rate proves to be in the range of 100–300 sq. m./hr.

Since each bubble film has a surface on either side, the average film thickness may also be computed from the surface area and (collapsed) volume of foam produced per unit time by the relation film thickness = 2 × foam volume/foam area. Results at our bubbling rates vary from 0.5 to 10 × 10^{-4} cm.

By analysis of collapsed foam gathered in the collector head, any difference between its composition and that of the original solution may be determined. If the foam structure can be considered essentially as surface in which such concentration of surfactant material must have occurred, and liquid trapped between the surfaces with the same composition as the original foaming solution,[7] the actual concentration of material in the surface may be calculated by considering this analytically determined excess as spread over the measured surface area. The significance of such a calculation, of course, depends upon the validity of this assumption; but, as shown below, actual results are reasonable, indicating each molecule of adsorbed surfactant material occupies 24 to 90 Å.^{2} of surface.

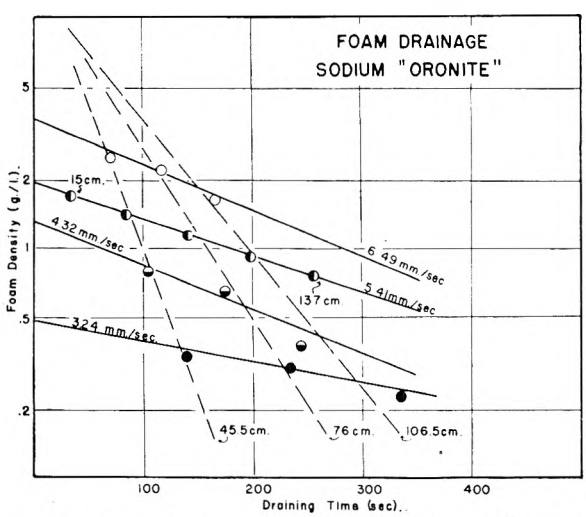

Fig. 2.—Foam drainage properties of sodium "Oronite," 0.05% solution at 28°.

(7) Note that this assumption is only valid in a system such as this in which there is negligible bubble collapse which would feed extra surfactant material back into the liquid filling between bubble surfaces.

A final quantity which may be determined with the apparatus is the minimum rate of foam rise which will just permit the foam from a given solution to reach the top of a column of particular height. This rate gives a measure of ultimate foam stability, a matter of some practical importance in many fields.

Foam Measurements

The application of this apparatus, as well as some of its limitations, may best be shown by reporting measurements on some actual surfactant systems. For this purpose, five have been chosen: a technical sodium dodecylbenzene sulfonate, sodium myristate, sodium lauryl sulfate, dodecylamine hydrochloride and an octylphenol–ethylene oxide condensation product.

Sodium Dodecylbenzene Sulfonate.—The material employed was a technical material supplied by the Oronite Chemical Company and marketed under the name of "Sodium Oronite." It consists of the sodium salt of a mixture of sulfonated alkyl benzenes with branched side chains averaging twelve carbons in length and derived from polymerized propylene.[8] Since it gives particularly satisfactory and reproducible foams in the apparatus, it was used in much of the preliminary investigation. The material used had been almost completely separated from inorganic salts, and contained 95.67% alcohol soluble solids considered to be active material.

Foam drainage measurements, determined on 0.05% solutions in distilled water, are plotted in Fig. 2. Foam weights/hour are, in general, the average of several measurements, the median deviation of duplicate determinations from the average being of the order of 4%. In Fig. 2, the data are plotted as foam density *vs.* draining time on a semilogarithmic plot. The solid lines pass through series of points obtained at different column heights at constant rates of foam rise. Since the lines are straight and roughly parallel, they indicate that, in this range, the rate of drainage is proportional to foam density over a tenfold range with a value of 0.45%/sec. Extrapolation of the solid lines back to zero draining time gives foam densities at the instant of foam formation, and show this to increase with bubbling rate, a reasonable enough result, as increased agitation would be expected to entrap more liquid in the foam. The relation between experiments carried out at different bubbling rates but a single column height is indicated by the dashed lines in the figure. Interestingly, extrapolations of these (dashed) lines all lead to intersection with the zero draining time axis at a foam density of about 20 g./liter, representing a sort of (hypothetical) maximum wetness for foam produced at a very high rate.

The bubbles which make up the foam have approximately the same size at all bubbling rates, ranging in diameter from 3.0 to 4.0 mm. with an average diameter of 3.5 mm., corresponding to a

(8) A. H. Lewis, U. S. Patents 2,477,382, 2,477,383 (July 26, 1949).

surface area of 17.1 cm.^{2}/cm.^{3} of foam. Analysis of the collected foam was accomplished by diluting to a sodium Oronite concentration of approximately 0.01%, and determining the optical density of the solution at 261 mμ with a Beckman spectrophotometer. At this wave length, a 0.01% solution of sodium Oronite in a 1-cm. cell has an absorbency of 1.505. Foam analysis results are summarized in Table I, and show that the concentration of sodium Oronite is 2–4 times that of the bulk solution.

TABLE I

SOME FOAM CHARACTERISTICS OF SODIUM ORONITE. 0.054% ACTIVE IN DISTILLED WATER, TEMP. 28°; FOAM RISE 5.41 MM. PER SEC.

Column height, cm.	15	45.5	76	106.5	137
Foam weight, g./hr.	220	174	152	125	104
Na Oronite in foam, %	0.120	0.148	0.173	0.178	0.213
Surface excess, mg./g.	0.66	0.94	1.19	1.24	1.59
Foam volume, cm.^{3}/hr. × 10^{-5}	1.35	1.35	1.35	1.35	1.35
Foam surface, cm.^{2}/hr. × 10^{-6}	2.31	2.31	2.31	2.03	2.31
Av. bubble diam., cm.	0.35	0.35	0.35	0.40	0.35
Film area per molecule, sq. Å.[a]	93	83	75	77	82
Av. film thickness, cm. × 10^4	1.90	1.51	1.32	1.23	0.90

[a] Assuming an average molecular weight of 352.

From these data, the surface area occupied by each molecule (assuming adsorption as a unimolecular layer) has been calculated. Results at different column heights (*i.e.*, different draining times) are in good agreement indicating that, for this system at least, equilibrium between surface and solution is rapidly attained, and that our basic assumption that liquid draining from the foam has the same composition as bulk solution is essentially correct. A further check of the method may be obtained by comparing the average area/molecule (82 Å.^{2}) by that predicted from surface tension measurements *via* the Gibbs equation. This value has been determined by Dr. C. R. Sporck of this Laboratory as 65 Å.^{2}, a reasonable agreement in view of the uncertainties of the two methods.

Inspection of Fisher–Hirschfelder models show that close-packed extended sodium Oronite molecules should occupy only 35–50 Å.^{2} apiece. A value of 82 Å.^{2} about corresponds to the packing of molecules in which the benzene rings and sulfonate groups are both lying on the surface with the hydrocarbon "tails" erect.

By progressively decreasing bubbling rates, it was found that the lowest rate of foam rise which would just bring foam to the top of a 2-ft. column was 0.89 mm./sec.

Sodium Myristate.—The foaming properties of sodium myristate were studied, both to compare the behavior of a typical soap with a synthetic detergent, and to see whether, in our apparatus, it showed the preferential adsorption of free fatty acid in the foam surface first reported by Perrin[9] and Laing[10] for oleate foams.

Drainage properties of sodium myristate solutions prove to be quite different from those of sodium Oronite, and it was found necessary to use 0.10% solutions to obtain satisfactory results. Foams were much wetter (about 4.5 g./liter at a rate of foam rise of 5.4 mm./sec.) and showed little decrease in density with column height, although densities decreased markedly with lowered bubbling rate. Further, there appeared to be considerable bubble collapse, particularly at lower foaming rates, and some variation in rate of bubble rise at different points in the column. Apparently, with such soap foams, in our apparatus drainage from intact foam bubbles is very slow, and foam density is determined almost entirely by the initial conditions of foam formation, and the collapse of bubbles within the foam. Typical results are listed in Table II but should be regarded as of only qualitative significance.

TABLE II

SODIUM MYRISTATE

Density Measurements of Foam from 0.10% Solution in Distilled Water

Height of column, cm.	Rate of bubble rise in mm. per second 6.49	5.41	2.16
	Weight of foam produced per hour, grams		
45.5		570	
76		608	
106.5		567	
137	860	634	146
	Density of foam, mg. per liter		
45.5		4222	
76		4504	
106.5		4200	
137	5309	4696	2703

Analyses were carried out on foams collected from 0.10% sodium myristate solutions which had risen through 137-cm. columns at 2.16 and 6.49 mm./sec. Total fatty acid was determined by acidifying 200-ml. portions of condensed foam and extracting with ether, and sodium by ashing with sulfuric acid. Blanks by these techniques on the original solution gave molar concentrations of fatty acid and sodium of 3.99 × 10^{-3} and 4.00 × 10^{-3} (calcd. 3.95 × 10^{-3}). Results, together with calculation of surface concentrations as previously outlined, are given in Table III, and indicate that the surfactant adsorbed at the bubble surfaces occupies an area of 24–30° Å.^{2}/molecule and consists of approximately 1 molecule of myristic acid to 2 of sodium myristate. This value corresponds to rather close packing of a unimolecular layer of paraffin chains.

Sodium Lauryl Sulfate.—Foam drainage and composition studies were carried out on a sample of sodium lauryl sulfate prepared from commercial lauryl alcohol (du Pont Lorol No. 5) and purified by recrystallization from alcohol followed by washing with acetone to remove the last traces of unsulfated lauryl alcohol.

Results of foam drainage experiments carried out on a 0.05% solution in distilled water are plotted in Fig. 3. They show that, while rather wet foams have first order drainage rates only slightly lower than those obtained from sodium Oronite (about 0.3%/sec. compared with 0.45), as films become thinner, the drainage rate drops off, becoming negligible at a rate of foam rise of 3.24 mm./sec. at which point the average film thickness is about 3000 Å. The foam drainage properties of sodium

(9) J. Perrin, *Ann. Phys.*, [9] **10**, 160 (1918).

(10) M. E. Laing, *Proc. Roy. Soc. (London)*, **109A**, 28 (1925).

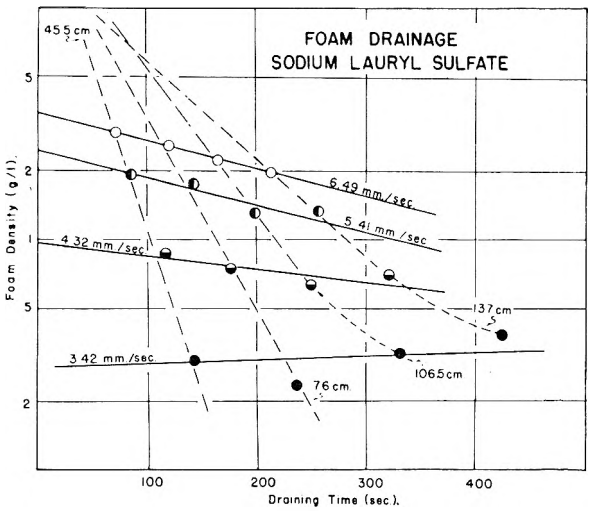

Fig. 3.—Foam drainage properties of sodium lauryl sulfate, 0.05% solution at 28°.

lauryl sulfate, in our apparatus, thus appear to be intermediate between sodium Oronite and sodium myristate.

TABLE III

PROPERTIES OF FOAM COLLECTED AT TOP OF 137-CM. COLUMN FROM 0.1012% Na MYRISTATE

Rate of foam rise, mm./sec.	6.49	2.16
G./hr. collected	860	146
Na myristate in foam, %	0.1265	0.1738
Surface excess, mg./g. foam	0.253	0.726
Free myristic acid in foam, %	0.0143	0.0319
Surface excess, mg./g.	0.143	0.319
Molar ratio soap:acid in surface	1:0.62	1:0.48
Foam surface, cm.²/hr. × 10^{-6}	2.56	0.90
Area/molecule, soap + acid (Å.²)[a]	30	24
Av. film thickness (cm. × 10^{4})	6.72	3.24

[a] Molecular weight of myristic acid determined as 231.

Foam compositions were determined by analysis of initial collected foam by methylene blue titration as described by Jones[11] and show a 4–8 fold enrichment over the initial solution. Results of six experiments at one rate of foam rise and four column heights are given in Table IV. The average value for the surface area per molecule of adsorbed lauryl sulfate is 34 Å.², with the individual values all within 10% of this value except for the two measurements in the 137-cm. column. Sodium lauryl sulfate thus appears to form rather a close-packed film only slightly less dense than that formed by sodium myristate.

TABLE IV

FOAM PROPERTIES OF 0.05% Na LAURYL SULFATE SOLUTION FOAM RISE 5.41 MM./SEC.

Column height, cm.	45.5	45.5	76	106.5	137	137
Foam weight, g./hr.	155	160	122	102	99	94
Na lauryl sulfate in foam, %	0.20	0.21	0.22	0.29	0.22	0.40
Surface excess, mg./g.	1.5	1.6	1.7	2.4	1.7	3.5
Foam volume, cm.³/hr. × 10^{-5}	1.35	1.35	1.35	1.35	1.35	1.35
Av. bubble diam., cm.	0.52	0.51	0.53	0.52	0.50	0.53
Foam surface, cm.²/hr. × 10^{-6}	1.55	1.59	1.53	1.56	1.62	1.53
Area/molecule in surface, Å.²[a]	33	31	37	32	48	23
Av. film thickness, cm. × 10^{4}	2.0	2.0	1.6	1.3	1.2	1.2

[a] Molecular weight of sodium lauryl sulfate taken as 302.

(11) J. H. Jones, *J. Assn. Off. Agricultural Chemists*, **28**, 398 (1945).

Dodecylamine Hydrochloride.—As an example of the foaming properties of a cationic surfactant, a 0.05% solution of dodecylamine hydrochloride was studied at four column heights and one rate of foam rise. The material employed was a sample of Armour and Company dodecylamine neutralized with the calculated quantity of hydrochloric acid and results are listed in Table V. This material showed rather unsatisfactory behavior in the apparatus giving erratic foam densities (although the foam appears to be of the slow-draining type), and a wide distribution of bubble sizes. Foam compositions were determined by both chloride and Kjeldahl nitrogen analyses of the collected foams and indicate an average area/molecule of 24 Å.² and negligible hydrolysis of the amine salt in the foam surface. This last conclusion, incidentally, based upon the quite good check between chloride and nitrogen analyses, is unaffected by the irreproducibility in foam density and uncertainty as to average bubble size.

TABLE V

FOAM PROPERTIES OF 0.05% DODECYLAMINE HYDROCHLORIDE SOLUTION; FOAM RISE 5.41 MM./SEC.

Column height, cm.	45.5	76	106.5	137
Foam weight, g./hr.	75	54	66	80
RNH_3Cl in foam, %				
by Cl	0.175	0.406	..	0.256
by N	0.190	0.395	..	0.285
Surface excess (Cl) mg./g.	1.25	3.56	..	2.06
(N) mg./g.	1.40	3.45	..	2.35
Foam volume, cm.³/hr. × 10^{-5}	1.35	1.35	1.35	1.35
Av. bubble diam., cm.	0.88	0.93	0.90	0.95
Foam surface, cm.²/hr. × 10^{-6}	0.92	0.87	0.90	0.95
Area/molecule Å.² (Cl)[a]	36	17	..	21
(N)	32	17	..	19
Av. film thickness, cm. × 10^{4}	1.6	1.2	1.5	1.7

[a] Molecular weight of dodecylamine taken as 185.

Triton X-100.—In addition to the ionic surface active materials investigated, a series of measurements was also made on a typical non-ionic polyethylene oxide condensation product, Triton X-100. This material, manufactured by Rohm and Haas, is stated by them to be the reaction product of octylphenol and 8–10 moles of ethylene oxide, *i.e.*

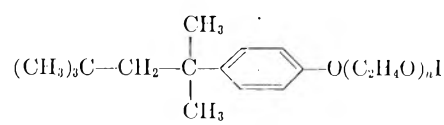

with n having a range of values averaging 8–10. Results of foam measurements on a 0.05% solution at four column heights are given in Table VI. At this rate of bubble rise, Triton X-100 produces quite a reproducible foam of even bubble size with a drainage rate of approximately 0.23%/sec., comparable to sodium lauryl sulfate.

TABLE VI

FOAM PROPERTIES OF 0.05% TRITON X-100 SOLUTION
FOAM RISE 5.41 MM./SEC.

Column height, cm.	45.5	76	106.5	137
Foam weight, g./hr.	96	85	67	65
X-100 in foam, %	0.33	0.36	0.46	0.55
Surface excess, mg./g.	2.8	3.1	4.1	5.0
Foam vol., cm.^{3}/hr. $\times 10^{-5}$	1.35	1.35	1.35	1.35
Av. bubble diam., cm.	0.46	0.42	0.40	0.41
Foam surface, cm.^{2}/hr. $\times 10^{-6}$	1.76	1.93	2.03	1.98
Area/molecule, Å.^{2}[a]	71	78	79	66
Av. film thickness, cm. $\times 10^4$	1.09	0.88	0.66	0.66

[a] Molecular weight of Triton X-100 taken as 647.

Foam compositions were determined by evaporating the collected foam to dryness, re-evaporating with a little petroleum ether, and weighing. The value of 74.5 Å.^{2}/molecule obtained for the density of adsorbed material at the film surface is in a reasonable range, and suggests that this rather long, heavy molecule (m.w. 647 for $n = 10$) is more nearly extended in a direction normal to the surface than loosely coiled at the air–water interface.

The authors wish to acknowledge the advice and helpful discussion of Dr. C. R. Sporck in connection with this work, and also the aid of the members of our Analytical Section in carrying out the foam composition analyses described.

COMPLEXES OF VARIOUS METALS WITH ETHYLENEDIAMINETETRAACETIC ACID

BY ARTHUR E. MARTELL AND ROBERT C. PLUMB[1]

Department of Chemistry, Clark University, Worcester 3, Mass.

Received January 14, 1952

In a recent article the relative tendencies of various transition metals to form complexes with ethylenediaminetetraacetic acid (EDTA) in a number of buffer solutions was reported. In the present paper the interpretation of the results is extended and new data are presented for a number of rare earth ions.

Introduction

In a previous publication,[2] a new approach to the determination of equilibria between metal ions and complexing agents was described. The experimental method consisted of treating a solution of the complexing agent simultaneously with two metal ions, the amounts of all three species employed being equal. Thus only half the quantity of reagent required to react with both metals was present, assuming the usual 1:1 complex to be formed. Depending on the various buffers employed, the "uncomplexed" form of the metal either remained in solution or precipitated as a solid phase. Thus it was possible to compare the stabilities of two metal complexes in the presence of other reagents. The purpose of the present paper is to offer a theoretical interpretation for this method for conditions involving (1) precipitation of the excess metal ion and (2) presence of a single solution phase, and to present new results involving rare earth complexes of ethylenediaminetetraacetic acid (EDTA).

Experimental

Measurements.—The method employed is the same as that described previously.[2] All comparisons of the rare earths were made to Nd at 582 mμ in 0.2 *M* carbonate buffer. After each reaction the buffer was checked and adjusted to the original *p*H when necessary. The solutions employed were 0.01 molar in metal complex. Absorption measurements were made with a Beckman quartz spectrophotometer, Model DU, operated at maximum sensitivity and with 1-cm. quartz cells. The only rare earth complex which showed strong absorption bands is that of Nd. The absorption bands observed were: strong, Nd 358 and 582 mμ; moderately strong, Pr 446 mμ and Sm 404 mμ; weak, Nd 331 and 514 mμ. The peaks of the absorption bands observed are listed in Table I. It was not necessary to consider or correct for the absorption of Nd^{+3}, since the concentration of free metal ion was negligible at equilibrium, as previously described.[2]

TABLE I

ABSORPTION BANDS OF 0.01 *M* RARE EARTH EDTA COMPLEXES
0.2 *M* carbonate buffer *p*H 8.65

Rare Earth	λ mμ	Transmission, %
Pr	446	86.3
Nd	358	94.0
	514	96.0
	582	81.9
	331	96.9
Sm	404	90.0
La	None	
Y	None	

All comparisons of stability of complexes using mixtures of metal ions as previously described were made with reference to neodymium at 582 mμ. None of the other pure metal complexes absorbed in this region. The results of the absorption measurements on the mixtures, made up 0.01 *M* with EDTA and each of two metal ions, are indicated in Table II.

TABLE II

MIXED COMPLEXES[a]

Mixture	Transmission, %	*S*[b]
Y–Nd	94.8	Y, 2.74
Pr–Nd	89.0	Pr, 0.71
Sm–Nd	92.1	Sm, 1.43
La–Nd	86.1	La, 0.33
		Nd, 1.00

[a] Concentration of each metal and of EDTA was 0.01 *M*. [b] *S* = moles of metal complexed/moles of Nd complexed.

(1) Aluminum Company of America, New Kensington, Pa.

(2) R. C. Plumb, A. E. Martell and F. C. Bersworth, THIS JOURNAL, **54**, 1208 (1950).

Calculations

For the mathematical development given below, it is assumed that metal ion and ligand form a 1:1 complex as indicated by the equation

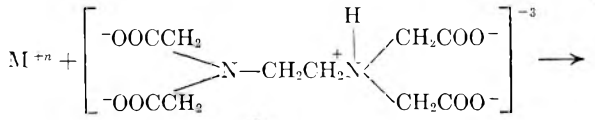

I

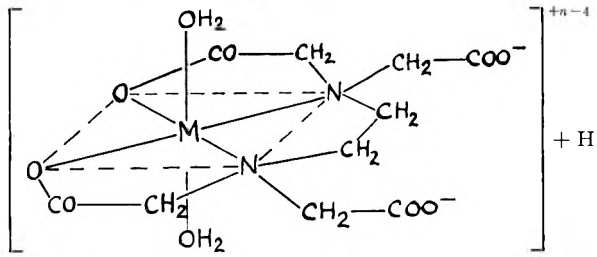

II, Tetradentate EDTA Chelate

II

The trinegatively charged anion (I) is chosen to represent the active form of the amino acid since this is the form which predominates in the buffer solution employed (carbonate buffer at *p*H 8.65). For rare earth ions the tetradentate chelate structure shown may be in equilibrium with higher chelate forms in which the donor may be pentadentate (III) or even hexadentate (IV). The assumption of a coördination number of six is not unreasonable for the rare earth metals in solution.[3] A 1:1 lanthanum–EDTA complex having the formula $NaLa(EDTA)\cdot 5H_2O$ has recently been prepared and recrystallized.[4] In this case it is not possible to state how much of the water is directly coördinated to the lanthanum ion. However, knowledge of this type is not required for the interpretation of the experimental work outlined below. In connection with the assumption of a 1:1 complex, it is significant that just such a structure was favored by Moeller and Brantley.[5] Schwarzenbach[6] showed the 2:1 complex (M_2EDTA) to be quite unstable relative to the 1:1 complex. Further, it is not likely that complexes involving more than one mole of ligand were formed in the present investigation, in view of the excess of metal ion employed.

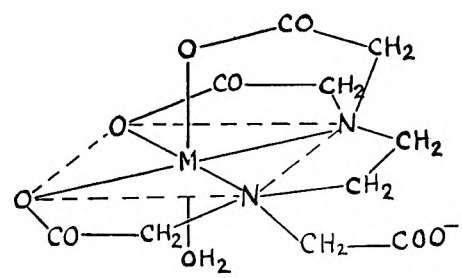

III
Pentadentate EDTA Chelate

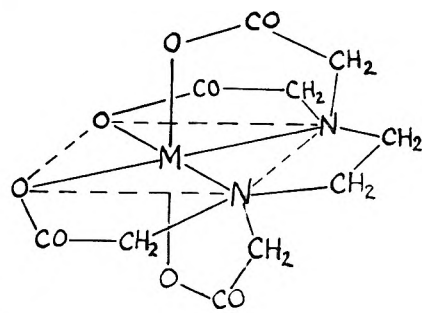

IV
Hexadentate EDTA Chelate

Consider first the case of precipitation of excess metal ion by the buffer. Since the metal complexes were determined directly (by absorption measurements), the concentration of free complexing agent has no effect on the replacement reaction, and the equilibrium may be written as

M, carbonate buffer, *p*H 8.65 + M′EDTA $\rightleftharpoons$ M′, carbonate buffer, *p*H 8.65 + M EDTA

where M and M′ represent the two metal ions in equilibrium with the precipitating agent and with the complexing agent, while M EDTA and M′ EDTA represents the metal complexes. Electrical charges of ions are omitted for clarity. The equilibrium constant for this reaction has the form

$$K_c = \frac{(\text{M}', \text{ carbonate buffer, } p\text{H } 8.65)(\text{M EDTA})}{(\text{M, carbonate buffer, } p\text{H } 8.65)(\text{M}' \text{ EDTA})} \quad (1)$$

where ( ) represents molar concentrations. Since both metals are in equilibrium with carbonate ion, the equilibrium constant may also be written in terms of the solubility products of the rare earth carbonates

$$K_c = \frac{(\text{M EDTA})}{(\text{M}' \text{ EDTA})}\left[\frac{K'_{sp}}{K_{sp}}\right]^{1/2} = S_{M/M'}\left[\frac{K'_{sp}}{K_{sp}}\right]^{1/2} \quad (2)$$

where K_{sp} and K'_{sp} are solubility products of $M_2(CO_3)_3$ and $M'_2(CO_3)_3$, respectively, and $S_{M/M'}$ is the ratio of the concentration of the complexes of M and M′ present at equilibrium.

In the special case where the uncomplexed metal does not precipitate (*i.e.*, in acetate buffer at *p*H 4) equation (1) becomes

$$K_c = (\text{M}')(\text{M EDTA})/(\text{M})(\text{M}' \text{ EDTA}) \quad (3)$$

Under the conditions employed (1) the total amounts of M, M′ and EDTA are equal. Therefore it follows that

$$(\text{M}) + (\text{M EDTA}) = (\text{M}') + (\text{M}' \text{ EDTA})$$
$$(\text{M EDTA}) + (\text{M}' \text{ EDTA}) = (\text{M}) + (\text{M}')$$

and

$$(\text{M}')/(\text{M}) = (\text{M EDTA})/(\text{M}' \text{ EDTA}) = S_{M/M'}$$

where S is the ratio of the metal complexes at equilibrium. Thus equation (3) becomes

$$K_c = S^2_{M/M'} = K/K'$$

where K and K', the formation constants of the metal complexes, are given by

$$K = (\text{M EDTA})/(\text{M})(\text{EDTA}^{-4})$$
$$K' = (\text{M}' \text{ EDTA})/(\text{M})'(\text{EDTA}^{-4})$$

Therefore when the excess metal does not precipitate, the ratio of the complex formation constants may be calculated directly from S. This method is applied below to the data of the previous paper[2] for the calculation of the stability constants of the EDTA complexes of certain transition metals.

Discussion of Results

Rare Earth Complexes (Excess Metal Precipitates).—Figure 1 shows an interesting correlation between the index S, indicating relative quantities of the complexes at equilibrium, and the atomic number, except in the case of yttrium. The correlation is extended to this metal by assuming an "effective" atomic number of 66.3, according to standard practice,[7] which places it between dysprosium and holmium. Such a correlation suggests a relationship between ionic radius and stability of the complex. Comparison of these two quantities indicates that the stability increases with decreasing ionic radius or increasing charge–radius ratio, the so-called "ionic potential" of the metal. The weakest complex is formed with lanthanum, the strongest with yttrium. It should be kept in mind that the index S is not actually the ratio of stability constants. If, however, the

(3) M. Calvin and A. E. Martell, "The Chemistry of the Metal Chelate Compounds," Prentice-Hall, Inc., New York, N. Y., in press, Chapter VII.

(4) A. E. Martell and M. Calvin, unpublished results.

(5) T. Moeller and J. C. Brantley, *J. Am. Chem. Soc.*, **72**, 5477 (1950).

(6) G. Schwarzenbach and H. Ackermann, *Helv. Chim. Acta*, **31**, 1029 (1948).

(7) B. H. Ketelle and G. E. Boyd, *J. Am. Chem. Soc.*, **69**, 2800 (1947).

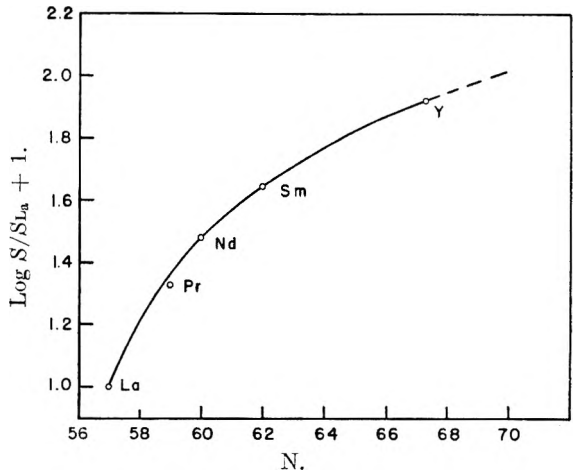

Fig. 1.—Correlation with atomic number of relative stabilities of rare earth–EDTA chelates in 0.2 *M* carbonate buffer at *p*H 8.65.

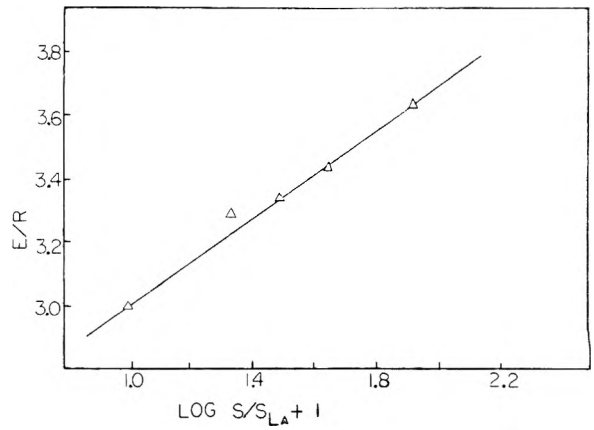

Fig. 2.—Correlation with ionic radius of relative stabilities of rare earth–EDTA chelates in 0.2 *M* carbonate buffer at *p*H 8.65. *E*/*R* represents charge–radius ratio.

relative solubilities of the carbonates are nearly the same, the precipitation of excess metal as carbonate would produce only a second-order effect on the observed values of *S*. Hence it would seem that the values of *S* may be close to the relative values of the stability constants of the complexes.

The linearity of the relationship between ionic radius and the relative values of the stability function is strikingly illustrated by Figure 2. If the relative solubilities of the rare earth carbonates have an appreciable influence on *S*, it becomes apparent that the logarithms of the solubilities must also vary in a linear manner with charge–radius ratio.

The *S* values of the rare earths listed in Table II are appreciably different. Since the values of *S* actually represent relative distribution ratios of the rare earth ions between liquid and solid phases, this difference suggests that such a distribution may offer a convenient method of separating rare earths. A search of the literature failed to reveal similar or analogous data for comparison. The only information available on the separation of the rare earths by equilibration between liquid and solid phases is the well-known work on separations by means of cation exchange resins. The equilibrium measurements of Tompkins and Mayer[8] offer a good example of the kind of data which may be compared with our *S* values as a measure of separability. Their measurements resulted in the evaluation of the distribution ratios of the rare earths between the cation exchanger and citrate solution at controlled *p*H. Their values of K_d, the distribution ratios, are listed in Table III, and compared with the value of *S* by reducing to α', the distribution ratios relative to yttrium. The reciprocal of *S* was taken to allow a direct comparison with ion exchange data.

TABLE III

At. No.	Rare earth	K_d[a]	α'[b]	S_y^{-1}
57	La	87	7.6	8.3
58	Ce	87	7.6	...
59	Pr	40	3.5	3.9
60	Nd	...	...	2.7
61	Pm	21	1.8	...
62	Sm	...	...	1.9
65	Tb	14	1.2	...
66.3	Y	11.5	1	1

[a] Tompkins and Mayer, *J. Am. Chem. Soc.*, 69, 2859 (1947). K_d for 0.23 *M* citrate, 0.5 *M* NH_4ClO_4, Dowex 50 ammonium form, tracer amts. of metal. [b] α = K_d(metal)/K_d(yttrium). [c] S_y^{-1} = moles of metal precipitated/moles of yttrium precipitated.

It is apparent that the separabilities of the rare earths of Table III by these two methods (*i.e.*, EDTA complexing in carbonate buffer and citrate complexing in the presence of a cation exchange resin) are of the same order of magnitude. The use of water-soluble complexing agents similar to EDTA may be of value in certain cases for the separation of rare earth ions. Although it is difficult to see how the EDTA–carbonate buffer reaction may be applied to a column method of separation, it seems that the use of EDTA for elution of cation exchange columns at relatively high *p*H certainly should be investigated.

Transition Metals (Uncomplexed Metal Remains in Solution).—The method outlined in the introduction was applied to the determination of the ratios of the stability constants of the transition metals. The results are given in Table IV. The absolute values of the constants listed were calculated using the value of 18.4 given by Schwarzenbach[9,10] for the logarithm of the stability constant of the copper complex. Assuming that the relative values of the stability constants are not greatly affected by small changes in ionic strength, the values listed in Table IV should hold approximately for an ionic strength of 0.1.

It was pointed out by Schwarzenbach[10] that the results obtained by this method must be corrected for acetate complexing if they are to be interpreted in terms of stability constants. A search of the literature revealed that the stability data for the transition metal chelates are incomplete. However, from the results of Edmonds and Birnbaum,[11]

(8) E. R. Tompkins and S. W. Mayer, *J. Am. Chem. Soc.*, **69**, 2859 (1947).

(9) G. Schwarzenbach and H. Ackermann, *Helv. Chim. Acta*, **30**, 1798 (1947); **32**, 1543 (1949).

(10) G. Schwarzenbach and Freitag, *ibid.*, **34**, 1503 (1951).

(11) S. M. Edmonds and N. Birnbaum, *J. Am. Chem. Soc.*, **62**, 2367 (1940).

Pedersen,[12] Cannan and Kibrick,[13] Ferrell, Ridgeon and Riley,[14] the stability constants of the 1:1 acetate complexes may be assumed, to a first approximation, to be: Pb, 2.0: Cu, 1.6; and only slightly less for the other transition metals such as Ni and Co (about 1.4). Assuming these values to represent the relative effects of acetate on the observed stability constants, the "corrected" values of Table IV are obtained. It may be seen that there is considerable deviation from the carefully-measured values of Schwarzenbach,[10] also listed for comparison. The discrepancy is probably due to differences in ionic strength, temperature, approximations in the corrections for acetate complexing, and to various unknown factors such as the influence of sodium ion on the equilibria.

No attempt was made to calculate the stability constant of $Cr^{III}EDTA$, for which data were available, because of extensive hydrolysis of the chromic ion under the conditions employed.

Further work using this absorption method for the determination of relative stabilities of metal chelates in the absence of buffers and in a controlled ionic atmosphere has been initiated in these laboratories, and it is hoped that further results will be forthcoming soon.

TABLE IV

Metal ion	S_{Cu}	K/K_{Cu}	log K	log K^a	log K^b_{cor}
Cu^{+2}	100	1.0	18.4	18.4	18.4
Ni^{+2}	39.0	0.15	17.6	18.4	17.4
Pb^{+2}	27.2	.074	17.3	18.2	17.7
Co^{+2}	8.9	.0079	16.3	16.1	16.1

[a] Values given by Schwarzenbach.[10] [b] Corrected for acetate complexing.

Acknowledgment.—The authors are indebted to F. C. Bersworth of the Bersworth Chemical Company, Framingham, Massachusetts, for financial support.

(12) K. Pedersen, *Kgl. Danske Videnskab. Math.-Phys. Medd.*, **22**, No. 10 (1945).

(13) R. K. Cannan and A. Kibrick, *J. Am. Chem. Soc.*, **60**, 2314 (1938).

(14) E. Ferrell, J. M. Ridgeon and H. L. Riley, *J. Chem. Soc.*, 1440 (1934).

ADSORPTION AT WATER–HELIUM, –METHANE AND –NITROGEN INTERFACES AT PRESSURES TO 15,000 P.S.I.A.

BY E. W. HOUGH, B. B. WOOD, JR., AND M. J. RZASA

Stanolind Oil and Gas Company, Tulsa, Oklahoma

Received January 26, 1952

The adsorption of helium, methane and nitrogen at the gas–water interface is estimated from the isothermal change of interfacial tension[1] with pressure, by the application of the Gibbs adsorption isotherm. The pressure range is from 15 to 15,000 p.s.i.a., and the temperature is from 80 to 280°F. Lower limits for the excess surface concentrations of gas molecules are calculated, and estimates of the change in total volume per unit increase in surface area, due to decreased density at the surface, are made.

Introduction

Adsorption at gas–liquid interfaces can be calculated from the isothermal change of interfacial tension with pressure by a relation due to Gibbs.[2] Related methods have been described by Adam[3] and Rice.[3a] The data for the interfacial tension of simple systems, even at moderate pressures, are not very extensive. Kundt[4] has reported work at 70°F. for several organic liquids with several gases up to about 3200 p.s.i.a. Recently, interfacial tension data for the water–methane system were reported at several temperatures for pressures to 15,000 p.s.i.a.[5]

Results and Discussion

Interfacial tensions in the water–nitrogen system and in the water–helium system have been determined by the technique described for the water–methane system,[5] which employs the pendant drop. Analyses of the nitrogen and helium used are given in Table I. The water used was triple-distilled and had a specific resistance in excess of 350,000 ohm cm. Frequent checks, in the apparatus, of the interfacial tension of the water sample against air at atmospheric pressure and at 80°F. were used to test the purity of the water. Volumetric data employed were obtained from Wiebe and Gaddy[6] for nitrogen, from Wiebe, Gaddy and Heins[7] for helium, and from Dorsey[8] for water.

TABLE I

ANALYSES OF GAS SAMPLES

Gas impurity	Nitrogen[a] (Mole per cent.)	Helium[b] (Mole per cent.)	Gas impurity	Nitrogen[a] (Mole per cent.)	Helium[b] (Mole per cent.)
CO_2	0.00	0.00	C_3H_6	0.00	0.00
CO	.00	.00	C_3H_8	.00	.00
H_2	.00	.00	C_4H_8	.00	.00
N_2	..	.16	C_4H_{10}	.00	.00
CH_4	.03	.02	Total C_5	.00	.00
C_2H_4	.00	.00	Total C_6	.00	.00
C_2H_6	.00	.00	Helium	.00	..

[a] Sample of Prepurified Grade obtained from Air Reduction Co. [b] Obtained from the Bureau of Mines, Amarillo, Texas, through the National Cylinder Gas Co.

The experimental values for the interfacial tensions of the water–nitrogen system and the water–helium system are

(1) The term "interfacial tension" will be used for the specific free surface energy between two phases having different compositions, while the term "surface tension" will be used for the specific free surface energy between two phases having the same composition.

(2) J. W. Gibbs, "Collected Works," Longmans, Green, and Co., New York, N. Y., 1931.

(3) N. K. Adam, "The Physics and Chemistry of Surfaces," Third Ed., Oxford University Press, London, 1941, Chapt. 3.

(3a) O. K. Rice, *J. Chem. Phys.*, 15, 333 (1947).

(4) Kundt, *Ann. Physik*, 12, 538 (1881); "International Critical Tables," Vol. 4, McGraw-Hill Book Co., Inc., New York, N. Y., 1928, p. 475.

(5) E. W. Hough, M. J. Rzasa and B. B. Wood, Jr., *Petr. Trans. AIME*, 192, 57 (1951).

(6) R. Wiebe and V. L. Gaddy, *J. Am. Chem. Soc.*, 60, 2300 (1938).

(7) R. Wiebe, V. L. Gaddy and C. Heins, *ibid.*, 53, 1721 (1931).

(8) N. E. Dorsey, "Properties of Ordinary Water-Substance," Reinhold Publishing Corp., New York, N. Y., 1940, pp. 207–225.

shown in Figs. 1 and 2. These data were obtained by successive series of isothermal pressure changes for 15-second-old drops having a diameter of about 0.08 in., formed on a tip having an external diameter of 0.0472 in. For pressures of 5000 p.s.i.a. or below and temperatures of 160°F. or below, the precision of a given measurement was better than 1 dyne/cm. Under these conditions, the effects of pressure hysteresis, which are shown but not explained in Figs. 1 and 2, were as much as several times this value. The precision at the highest pressure (15,000 p.s.i.a.) and temperature (280°F.) is estimated to be 2 dyne/cm. and the effect of pressure hysteresis is probably several times this value. Smoothed values of interfacial tension are reported in Table II. The values in the table are given to 0.1 dyne/cm. al-

TABLE II

SMOOTHED VALUES OF INTERFACIAL TENSION

Temp., °F Press., p.s.i.a.	80	100	160	220	280
	Interfacial tension,[a] dynes/cm.				
	A. Water–nitrogen system				
15	75.0	72.4	66.6		
1,000	71.7	69.3	63.9	58.0	52.3
2,000	68.2	66.1	61.0	55.6	50.3
3,000	64.8	62.9	58.2	53.2	48.4
4,000	61.5	59.8	55.5	50.9	46.5
5,000	58.3	56.8	52.8	48.6	44.6
10,000	44.9	44.0	41.4	38.8	36.3
15,000	39.0	38.3	36.2[b]	34.1	32.2[b]
	B. Water–helium system				
15	68.5	66.4	60.7		
1,000	69.1	67.0	61.4	55.4	49.4
2,000	69.7	67.6	62.0	55.9	49.8
3,000	70.2	68.1	62.4	56.4	50.3
4,000	70.6	68.5	62.9	56.8	50.8
5,000	71.0	68.9	63.2	57.2	51.2
10,000	72.4	70.2	64.6	59.1	53.2
15,000	73.3	71.1	65.7	60.6	55.0

[a] Values obtained 15 seconds after exposure of water to nitrogen containing water vapor. See text for remarks on precision. [b] Extrapolated. [c] Values obtained 15 seconds after exposure of water to helium containing water vapor. See text for remarks on precision.

though the absolute experimental uncertainties are greater than this amount, because the slopes of the isotherms are used in the calculation of surface excesses. It is not to be inferred, however, that the experimental uncertainties at 80°F. and 15 p.s.i.a. are as great as might be at first suspected from inspection of the value of 75.0 for water and nitrogen and 68.5 for water and helium, when compared to the accepted value of 71.7[9] for water and air. Some liquids have been observed to have a percentage difference in interfacial tension of this order of magnitude for various gases. For instance, the interfacial tension of mercury and hydrogen at 25° is 462 dyne/cm. and that of mercury and water vapor is 470 dyne/cm. according to the "International Critical Tables."[10] The surface tension at 25° (*in vacuo*) is 475 dyne/cm.[10] The interfacial tension between ethanol and air at 21° and 1 atm. is reported by the "International Critical Tables"[4] as 22.2 dyne/cm. while the same reference reports the interfacial tension at 21° and 1 atm. of ethanol and hydrogen as 21.3 dyne/cm. The present work suggests the need for further experimentation in regard to this point which could be investigated with a pendant drop cell of the atmospheric pressure type. Positive slopes for the interfacial tension–pressure isotherms apparently have not been observed in the case of liquid–gas combinations before, but have been observed for water and decane by Michaels and Hauser.[11] In addition, Rice[3a] has indicated that such behavior is feasible from a thermodynamic viewpoint.

(9) A. Weissberger, "Physical Methods of Organic Chemistry," Vol. I, Interscience Publishers, Inc., New York, N. Y., 1945. See p. 163, W. D. Harkins, "Determination of Surface and Interfacial Tension."

(10) "International Critical Tables," Vol. IV, McGraw-Hill Book Co., Inc., New York, N. Y., 1928, p. 475, see Fig. 1.

(11) A. S. Michaels and E. A. Hauser, THIS JOURNAL, **55**, 408 (1951).

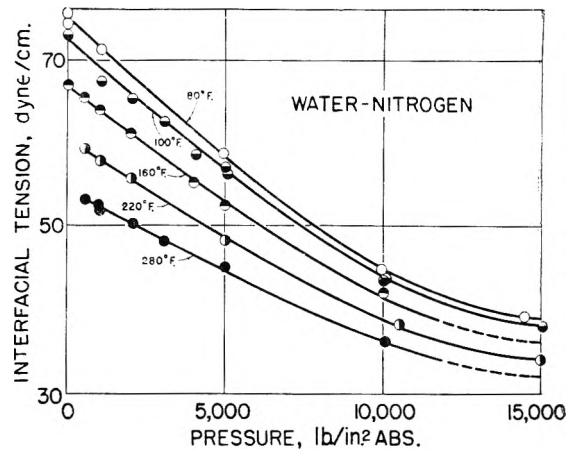

Fig. 1.—Interfacial tension in the water–nitrogen system.

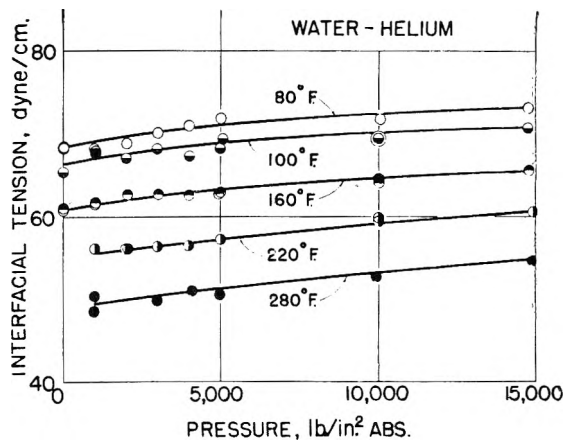

Fig. 2.—Interfacial tension in the water–helium system.

Values of a lower limit of excess surface concentration, Γ, of the gas molecules, have been calculated for nitrogen, helium and methane. The equation 3a employed in the calculations is shown in Table III. The total volume change per unit increase in surface, ΔV_σ, due to decreased density at

TABLE III

CALCULATION OF EXCESS SURFACE CONCENTRATION

A. Equation used[a]

$$(\partial\gamma/\partial p)_\sigma = \frac{-\Gamma ZkT}{p} + \Delta V_\sigma$$

B. Nomenclature

- k = gas constant per molecule (erg/molecule °K.)
- p = absolute pressure (dynes/cm.²)
- T = absolute temperature (°K.)
- Z = compressibility factor for gaseous phase
- Γ = Excess surface concentration of gas molecules (molecules/cm.²)
- γ = surface tension (dynes/cm.)
- ΔV_σ = change in total volume per unit increase in surface area due to decreased density at the surface (cm.³/cm.²)
- σ = refers to constant surface when used as subscript on partial derivative

C. Assumption

$\Delta V_\sigma = 0$ (The Γ calculated with this assumption would be less than the correct value)

[a] Taken from Rice.[3a]

the surface, is assumed zero. The values obtained are given in Figs. 3, 4 and 5. The points at which slopes were determined are indicated by circles on the curves. Uncertainty in these data is probably about 0.3×10^{14} molecules/cm.², except for the case of methane in the vicinity of 5000 p.s.i.a. where the uncertainty is several times this value.

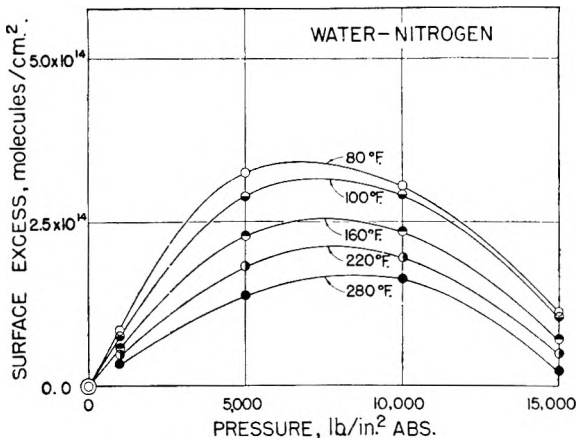

Fig. 3.—Nitrogen surface excess concentration ($\Delta V_\sigma = 0$).

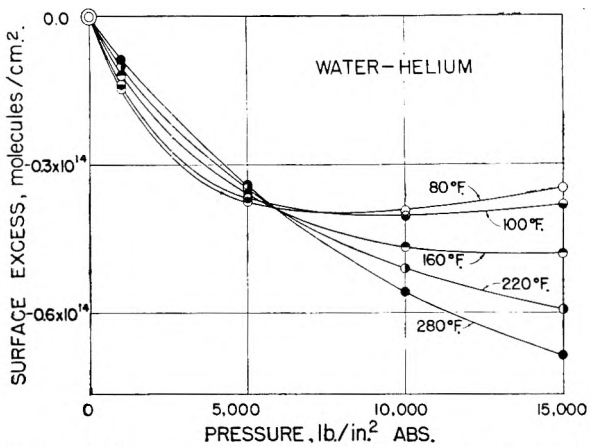

Fig. 4.—Helium surface excess concentration ($\Delta V_\sigma = 0$).

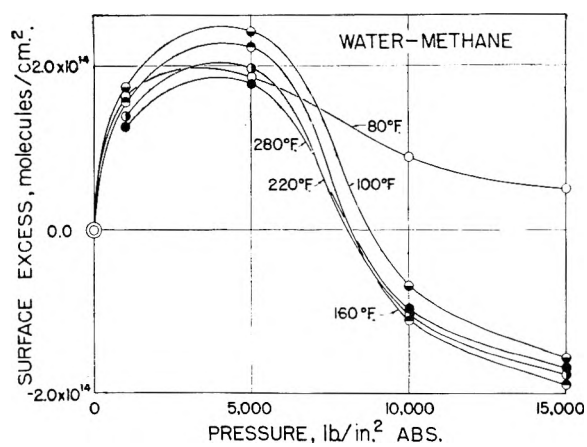

Fig. 5.—Methane surface excess concentration ($\Delta V_\sigma = 0$).

An incomplete set of observations has revealed the presence of plastic films in the water–nitrogen and water–methane systems at certain pressures and temperatures, but not in the water–helium system. The films observed are strong enough to distort drops having a diameter of about 0.05 inch and were detected by letting a drop having about twice that diameter stand for periods from 3 to 10 minutes and removing some water from the drop. The films are not detected when water is removed from 15-second-old drops. The plastic film has been observed as many as 10 times in succession, discarding each film-bearing drop from the tip when film appeared, without noticeable diminution of the effect. When a drop coated with a plastic film is allowed to stand, the angular contours disappear after a period of several minutes. In the water–nitrogen system, plastic films were observed at 160°F. at about 7500 p.s.i.a. and 10,000 p.s.i.a. when 5-minute-old drops were reduced in size. They were also observed at 220°F. at about 8,000 p.s.i.a. In the water–methane system, plastic films were observed at 280°F., for pressures of about 5,000 and 10,000 p.s.i.a. The drops which were reduced in size were from 2 minutes to 10 minutes old. At 15,000 p.s.i.a., however, no observable film was obtained when a drop 10 minutes old was reduced in size. Systematic attempts to obtain evidence of plastic film in the helium–water system for drop ages of about 5 minutes were unsuccessful. No information was obtained on the nature of the films so that very little can be said of their probable composition. A guess may be made, however, that they are hydrates, since both methane[12] and nitrogen[12] are known to form hydrates in the bulk phase, and since no film was observed at the water–helium interface.

A picture of a plastic film between water and nitrogen at about 7600 p.s.i.a. and 160°F. is shown in Fig. 6.

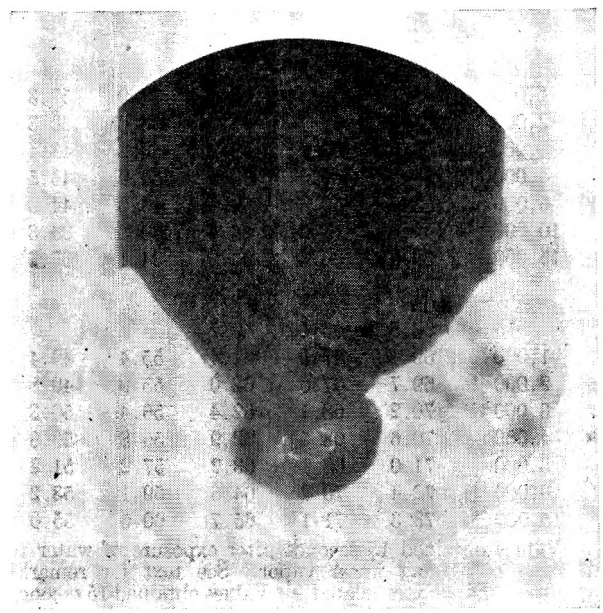

Fig. 6.—Plastic film in water–nitrogen system at about 160°F. and 7600 p.s.i.a.

The maximum values for the lower limit of excess surface concentration for nitrogen in the water–nitrogen system (shown in Fig. 3) appear to approximate the concentration for a monolayer. This idea appears reasonable because an extrapolation of isobaric values near the maximum value to a temperature of −321°F. appears to be in the vicinity of the value of surface concentration for a monolayer of nitrogen on a solid surface at that temperature given by Livingston,[13] 6.49 × 10^{14} molecules per square centimeter. A similar statement can be made for the water–methane system. It is evident, however, from the information on plastic film formation, that the actual values of surface excess concentration are considerably above these lower limit values for the pressures above 5,000 p.s.i. and the temperatures where film formation was obtained.

The lower limit values of excess surface concentrations for the helium–water system are negative, and plastic films were not observed, so that similar conclusions about the probable existence of surface excess concentrations at least as great as a monolayer cannot be drawn.

A lower limit value of the increase in the total volume change per unit increase in surface area, ΔV_σ, can be estimated for nitrogen and water by assuming that the excess surface concentration does not decrease when pressure is above the maximum concentration value indicated in Fig. 3. These values of ΔV_σ at 10,000 p.s.i. and 15,000 p.s.i. are about 0.3 × 10^{-8} cm., respectively, and are not greatly dependent on temperature. Corresponding values for methane and water are about 3 × 10^{-8} cm. at 10,000 p.s.i. and

(12) M. de Forcrand, *Compt. rend.*, **135**, 959 (1902).
(13) H. K. Livingston, *J. Colloid Sci.*, **4**, 447 (1949).

3.2×10^{-8} cm. at 15,000 p.s.i. Values of ΔV_σ, calculated for helium and water, assuming the surface excess concentration, Γ, is zero, are about 0.4×10^{-8} cm. at 10,000 p.s.i. and 0.3×10^{-8} cm. at 15,000 p.s.i.

Conclusions

Interfacial tension in the water–nitrogen system shows a decrease as pressure and as temperature are increased. The value at 15,000 p.s.i. and 280°F. is about 32 dyne/cm. Interfacial tension in the water–helium system shows an increase as pressure is increased. The value at 15,000 p.s.i. is about 5 dyne/cm. above that at 15 p.s.i. at 80°F. The interfacial tension decreases when temperature is increased isobarically. Lower limit values of surface excess concentration of the gas molecules have been calculated for these two systems and for the water–methane system. The existence of at least monolayer concentration above several thousand p.s.i. pressure is indicated for the water–nitrogen and water–methane systems. The observation of plastic film formation indicates that the actual values may be considerably larger than the lower limit values in some parts of the pressure range. Lower limit values of volume change per unit surface, due to decreased density of the surface upon adsorption of gas molecules, are estimated.

Acknowledgment.—The authors wish to thank the Stanolind Oil and Gas Company for permission to publish this material.

A NEW METHOD FOR MEASUREMENT OF THE HIGH FIELD CONDUCTANCE OF ELECTROLYTES (THE WIEN EFFECT)[1]

BY JOHN ALAN GLEDHILL[2,3] AND ANDREW PATTERSON, JR.[4]

Department of Chemistry of Yale University, New Haven, Conn.

Received February 12, 1952

A new method utilizing a differential pulse transformer bridge is described for the measurement of conductance of electrolytes under high fields. This method is useful not only for high field work but also for impedance measurement in general, and for low-field conductance work when it is desirable to avoid the platinization of electrodes required for the satisfactory operation of the usual conductance bridges. The bridge method is a general one for all impedance measurements and for use at frequencies and with pulses or wave forms limited only by the design of the transformer. Measurements of the high field conductance of magnesium and zinc sulfates and of acetic acid indicate that repeated measurements on the same solution at the same value of field give rise to differences in the per cent. fractional high field conductance quotient, $\Delta\lambda/\lambda_0$ (%), of 0.03 or less; in other words, the precision of measurement is 0.03%, *absolute*. Preliminary measurements are presented for these two salts and for the acid which indicate conformity with the results of Wien and his co-workers.

I. Introduction

In 1927 Max Wien[5] announced the significant discovery that the conductances of electrolytic solutions do not conform to Ohm's law under the influence of high potential gradients. In the years prior to 1939 Wien and his co-workers studied in great detail the behavior of electrolytes under the influence of high fields. This work has been summarized by Eckstrom and Schmelzer.[6] Onsager[7] and Onsager and Wilson[8,9] have worked out theories to account for the variation of the conductance with field strength for weak and for symmetrical valence type strong electrolytes. It is thus surprising to find that during the passage of almost a quarter century since Wien's discovery there is only one set of precise data for a strong electrolyte in aqueous solution to test the theory of Onsager and Wilson. In this case the temperature at which the measurement was made is in doubt. For weak electrolytes in aqueous solution, the situation is no better; Schiele[10] specified neither the concentrations nor the temperature for his work with acetic acid. It was with the intention of remedying this situation that the investigation reported herewith was begun.

Quite high field strengths must be applied in order to obtain appreciable conductance changes with aqueous solutions of most electrolytes. This places a number of peculiar restrictions on the measurement method which are not encountered in dealing with solutions of very low conductivity or with measurements at low fields. The practical considerations of economical power generation and of reasonable temperature rise in the conductance cells dictate that the high field may be applied only for periods in the order of 0.1 to 10 microseconds. This places the frequencies involved out of the range of audio frequency bridges, while the high voltage gradients cannot be accommodated by any conventional bridge design. Wien and Malsch[5] overcame these difficulties most ingeniously and developed their barretter bridge method into one of remarkable precision. Since 1939, however, pulsed power generation and the observation, study and measurement of pulses in the range of 0.1 to 10 microseconds have become commonplace although prior to that time such matters were quite unknown.

(1) This material is taken from a dissertation submitted by John Alan Gledhill to the Faculty of the Graduate School of Yale University in partial fulfillment of the requirements for the degree of Doctor of Philosophy, May, 1949.

(2) Department of Chemistry, Rhodes University, Grahamstown, South Africa.

(3) Queen Victoria Scholar of the University of South Africa, 1947–1949.

(4) The support of an American Chemical Society Postdoctoral Fellowship, 1946–1948, is gratefully acknowledged.

(5) M. Wien and J. Malsch, *Ann. Physik*, [4] **83**, 305 (1927).

(6) H. C. Eckstrom and C. Schmelzer, *Chem. Revs.*, **24**, 367 (1939).

(7) L. Onsager, *J. Chem. Phys.*, **2**, 599 (1934).

(8) W. S. Wilson, Dissertation, Yale University, 1936.

(9) H. S. Harned and B. B. Owen, "The Physical Chemistry of Electrolytic Solutions," 2nd ed., Reinhold Publishing Corp., New York, N. Y., 1950, pp. 95–114.

(10) J. Schiele, *Ann. Physik*, [5] **13**, 811 (1932).

Since these techniques were so obviously applicable to a study of the Wien effect and since it seemed possible that a method more convenient and consistent than that of Wien and Malsch might be devised, we set upon this latter task before attempting to develop more experimental data.

In the barretter bridge method of Malsch and Wien[5] a critically damped sine wave is applied to a double Wheatstone bridge network; temperature sensitive barretter elements in the auxiliary bridge permit one to determine if the main bridge is in balance. The principal drawbacks of the method are that it does not permit observation of pulse shape or behavior and that its operation is tedious. Later, Fucks[11] and Hüter[12] developed oscillographic methods of observation which were less time consuming, but also less precise. Adcock and Cole[13] have reported a method of measurement which employs square pulse excitation and oscillographic presentation of the bridge balance. Blüh and Terentiuk[14] have also reported a method incorporating a number of electronic advances.

In the present investigation a novel bridge circuit is employed having a number of advantages over bridges previously reported for high field conductance measurement. Conductance cell designs and methods of manipulation are reported which make it possible to perform high field conductance measurements with simplicity and speed, but with no sacrifice of precision. This is in contrast with previously reported methods, in which high precision and simplicity of manipulation have been found incompatible. Some preliminary high field conductance measurements are reported for magnesium and zinc sulfates and for acetic acid to indicate the capabilities of the method.

II. Apparatus

A block diagram of the apparatus is shown in Fig. 1.

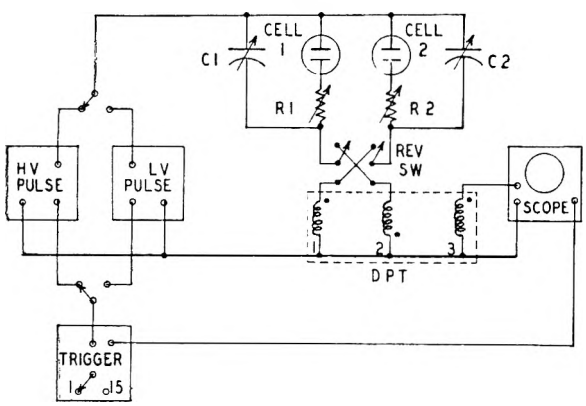

Fig. 1.—Block diagram of high field conductance measurement apparatus.

Pulse Power Supplies.—The high voltage pulse power supply consisted of a MIT Model 9 one-megawatt pulse modulator unit. This device has been adequately described by Glasoe and Lebacqz.[15] The unit is capable of developing over one megawatt of pulse power into a 500-ohm load. It was modified according to Glasoe and Lebacqz,[15] pp. 158–159, to give pulses between 0.5 and 5.0 microseconds duration. In addition, the inductive recharging path for the output storage condenser was entirely removed, so that the conductance cells constituted the recharging circuit. This caused the majority of the energy of one pulse to flow in reverse direction through the cells during a short period after a pulse and thus had the effect of converting what otherwise would have been an unidirectional flow of current into the equivalent of a single sine wave. Such an arrangement was found to contribute markedly to the stability of conductance in cells subject to pulse excitation.

Because of the convenience of the procedure, cell conductances at low fields were measured with square pulse excitation also. Low voltage square pulses were provided by a conventional arrangement of multivibrator and power amplifier capable of providing pulses in the 0.1–10 microsecond range at voltages adjustable from zero to 50 volts.

Oscilloscope.—A Tektronix Type 511A oscilloscope was used for observation of pulse wave forms. The single triggered sweep feature of this unit was essential to high field conductance measurement, where balancing was done on single pulses separated by periods of time as long as half an hour. An actinic P-11 screen was employed for photographic purposes. The second anode voltage was raised to 5000 volts for added intensity when single pulses were to be observed.

Trigger Generator.—In order to coördinate the operation of the oscilloscope and the low and high power pulse modulators, a trigger generator was constructed. With this unit it was possible to produce single pulses at will, or to produce repeated pulses at a rate of 15 per second synchronized with the line frequency. In either case, two output trigger pulses were provided: one to the oscilloscope, and at an appropriate time later a second trigger to the modulator in use. It was thus possible to start the sweep of the oscilloscope and to center any length pulse on the scope trace for convenience in observation.

Cells.—The conductance cells were used in pairs to take advantage of the cancellation of heating effects due to the passage of high field pulses. Measurements made under such circumstances were relative, not absolute. Potassium chloride or hydrochloric acid were the reference electrolytes. Both cells were made from liter Pyrex flasks with standard taper closures (see Fig. 2). The electrodes were sealed

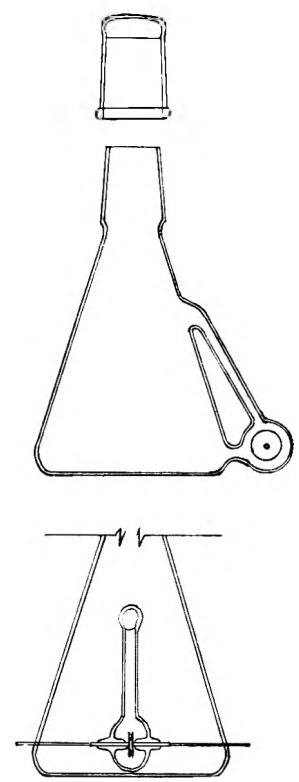

Fig. 2.—Cell for high field conductance measurement.

(11) W. Fucks, *Ann. Physik*, [5] **12**, 306 (1932).

(12) W. Hüter, *ibid.*, [5] **24**, 253 (1935).

(13) W. A. Adcock and R. H. Cole, *J. Am. Chem. Soc.*, **71**, 2835 (1949).

(14) O. Blüh and Z. Terentiuk, *J. Chem. Phys.*, **18**, 1664 (1950).

(15) G. N. Glasoe and J. V. Lebacqz, "Pulse Generators," Vol. 5, Radiation Laboratory Series, McGraw-Hill Book Co., Inc., New York, N. Y., 1948, pp. 152–160.

in a compartment on the side of the flask with one connection near the bottom and another near the top of the flask. When the solution in the flask was stirred with a magnetic stirrer, effective circulation took place through the cell compartment. The provision of a large volume of solution and the circulation of the solution through the cell compartment were found to be essential to the avoidance of conductance drifts after the passage of high field pulses. At the same time, the closed cell could be handled in accordance with the best conductance measurement practice.

The electrodes were of polished platinum discs, 16 mm. in diameter and 0.5 mm. thick. A 14-gage platinum wire was welded to the center of the disc, and a 2-mm. diameter platinum tube of 0.1-mm. wall thickness was welded to the wire near the disc. The thin walled tubing was intended for sealing to Pyrex glass, but it was found easier to work uranium glass into a tube seal. Accordingly, uranium glass was used for the entire cell compartment and was sealed directly to the Pyrex glass of the cell flask. (Corning 3321 glass would probably be suitable.) The electrodes were spaced one millimeter apart with a machined high purity Armco iron spacer, and were clamped in correct axial alignment with two Armco iron clamps. The surfaces of the spacer were carefully ground plane and parallel on a surface grinder and later micrometer calipered to within one part in 1000. See Fig. 3 for a detail of the electrodes and electrode clamp. After completion of the glass working, the spacer and clamp were dissolved in 6 M nitric acid. The electrodes were polished with fine abrasive paper before assembly in the clamps. No platinization was employed. After removal of the spacer assembly the cells were repeatedly washed with distilled water and finally steamed for one hour. The electrodes were kept wet after an initial weighing of the cells thoroughly dry to establish the weight of the cells for determination of concentration of solutions.

The cells were mounted on a Lucite insulating support in a thermostat filled with high quality transformer oil. The oil was maintained dry by a bag of silica gel immersed therein. The leads from the cells dipped into mercury cups to make contact with the bridge circuit directly above the bath. The solutions in the cells were stirred by small magnets covered with Pyrex glass, coupled to magnets under the Lucite support. These latter magnets were operated from without the bath by a flexible shaft. The thermostat was adjusted to 25.00 ± 0.01° with a recently calibrated platinum resistance thermometer.

It is to be noted that no attempt was made to avoid spreading of the field at the edges of the electrodes. With electrodes 16 mm. in diameter and a spacing of only 1 mm. the ratio of diameter to separation was considered to be large enough that fringing effects might be neglected. Plans are under way, however, to calibrate this type of cell against a cell with guard ring, in order that an estimate of fringing effects may be obtained.

Impedance Balancing.—Since two conductance cells were employed in a relative measurement of the Wien effect, it was necessary to balance only the change of conductance with increasing field and any stray capacitance differences in the cells and bridge wiring. Variable condensers C_1 and C_2 were provided to balance capacitance. These capacitors were variable high voltage insulated air dielectric units with a rating of 15–75 $\mu\mu$f. at 20 kv. maximum. The maximum field obtainable in the cells was limited by the breakdown of these condensers. Variable vacuum condensers would be preferable.

Variable resistors R_1 and R_2 in series with the cells were used to compensate for cell unbalance resulting from conductance changes with increasing field. The change in R_1 and R_2 necessary to effect balance was taken as a direct measure of the change in resistance of the cells. Three General Radio type 668 compensated decade resistance units were used in series for both R_1 and R_2 to give a resistance of 111 ohms maximum in 0.1-ohm steps.

The cell leads and all other leads in the bridge wiring were kept as short as possible. All other connections were made with properly terminated lengths of coaxial cable in order to preserve the quality of wave forms and to avoid unwanted radiation and reflections.

Differential Pulse Transformer Bridge Circuit.—The bridge circuit employed in these measurements consisted of a differential pulse transformer (DPT), shown within dotted lines in Fig. 1. Identical twin primary windings were connected in opposition in series with the impedances presented by the cells, balancing resistors and condensers. The oscilloscope was used to observe the wave form of the voltage developed across the third winding. If equal currents, both in amplitude and in phase, should flow through the two opposed primary windings, no net flux would result in the core of the transformer and no voltage would be induced in the third winding. If the impedances connected in series with the power supply and the transformer windings should be unequal, unequal currents would accordingly flow in the two windings, a net flux proportional to the degree of unbalance would result, and a signal would be observed upon the oscilloscope. Balance of the bridge circuit was thus shown by a null in voltage from winding 3. This circuit has been mentioned briefly elsewhere.[16]

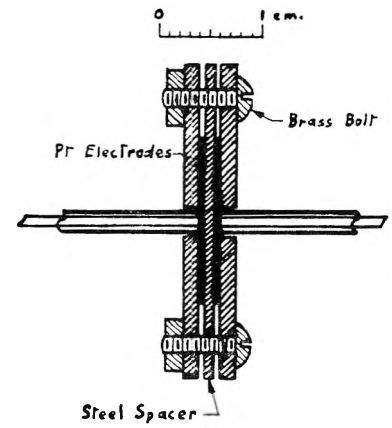

Fig. 3.—Detail of electrodes and electrode spacer assembly.

The DPT circuit has been analyzed by applying the procedures outlined by Gardner and Barnes[17] with the following results pertinent to its use as a bridge: (1) The circuit is a general impedance bridge; any impedance Z_1 in one arm of the bridge may be balanced by a like impedance Z_2 in the other arm. (2) The balance point is independent of the form of the excitation function applied to the circuit, that is, the balance is independent of frequency. The bridge may be excited by a rectangular pulse, a distorted pulse, a step function, or a sine wave so long as the transformer is capable of passing the frequencies involved in the excitation function. (3) The sensitivity of the bridge is proportional to the amplitude of the applied excitation. For maximum sensitivity, the magnetizing inductance of the transformer should be as large as possible and the coupling between the primaries and the secondary should be as close as possible. Also, the leakage inductance of the primaries should be small, which requires that the primaries be closely coupled. The unbalance voltage developed across the output winding is directly proportional to the unbalance in the conductances of the complex impedances in series with the two primaries. For small differences, the unbalance voltage is proportional to the resistive unbalance in the two impedances. One is thus justified in the use of linear interpolation on photographs of the oscilloscope patterns to find the true balance from two off-balance signals produced by a known change of resistance in one arm of the bridge. (4) To minimize the effect of residual capacitances and inductances in the transformer itself, as well as to obtain the desirable features which contribute to high sensitivity (as in 3, above), the physical dimensions of the whole transformer must be small and insulating materials with low dielectric constant are to be preferred. (5) In addition, if pulse excitation is to be employed in the 0.1 to 10 microsecond range, good frequency and pulse response will again require that most of the above criteria for good design be fulfilled. In particular, close coupling, small size, small number of turns, and small distributed capacitance are necessary.

These requirements have been successfully met in a differential pulse transformer wound on a 3-mil Hypersil core (Westinghouse No. 131 7996) with two windings each of 88 turns of #30 heavy Formvar insulated copper wire and one

(16) J. A. Gledhill and A. Patterson, Jr., *Rev. Sci. Instruments*, **20**, 960 (1949).

(17) M. F. Gardner and J. L. Barnes, "Transients in Linear Systems," John Wiley and Sons, Inc., New York, N. Y., 1942.

of 107 turns of # 32 Formvar layer wound and distributed on both legs of the core. The primaries were kept in as nearly identical geometrical relation as possible.[18] The resulting transformer was impregnated with a thermosetting varnish.

An analysis of the entire circuit including the pulse power supplies, the measured impedances, and the transformer reveals these additional features: (1) Since it will not in general be possible to wind the transformer so that the two primaries are precisely similar electrically, it will be necessary to insert a reversing switch to interchange the two windings and to determine the true balance from the mean of the two values thus obtained. As is customary, if the difference is small, the arithmetic mean may be employed. (2) If the source of power has a finite internal impedance the balance conditions are not affected. The off-balance currents are necessarily reduced somewhat by a finite source impedance so that it is advisable to keep the latter as low as possible for maximum sensitivity. (3) The resistances of the transformer windings will affect the sensitivity in much the same way, and are thus best kept small. In order that the reversing of the two windings may give a correct result for the balance, the resistances of the two primaries must be as nearly equal as possible. (4) The presence of transients in the output voltage from the transformer which coincide with discontinuities in the input pulse impose two limitations on the applicability of the circuit. The input pulse must be long enough so that there is an undisturbed portion of the output pulse long enough to permit one to judge the approach to a null, and the transients must not be of such amplitude as to saturate the transformer core or oscilloscope amplifiers or to puncture the insulation of the transformer or associated circuits. (5) The influence of differing earth admittances on this bridge circuit is greatly minimized in comparison to the usual bridge. The close coupling required between the windings causes any effect in one arm of the bridge to be reflected almost equally in the other arm. As a result, elaborate shielding of the bridge components with all its attendant difficulties is not necessary. (6) When the bridge is in balance, no flux exists in the transformer core and consequently no reverse electromotive force exists across the primary windings. In consequence, all of the input pulse power is applied across the impedances in series with the primary windings. This results in considerable economy in pulse power generation; greatly simplifies the construction of the transformer, which need not thus be insulated for high voltages; and permits one easily to compute the field strength applied to the impedances. This is in contrast with the usual Wheatstone bridge, where, for maximum sensitivity, equal bridge arms are required. In such a case only half the input voltage would be applied to the measured elements, the bridge arms would have to be constructed to withstand high voltages, and the measuring arm would be raised high above ground potential. This is of obvious importance in high field measurements, and constitutes one of the most attractive features of the DPT bridge performance.

III. Experimental Procedure

A solution, the high field conductance of which was to be measured, was placed in one cell and a solution of potassium chloride or hydrochloric acid was placed in the other. Because the high voltage pulse modulator would not operate properly into a load impedance much less than 500 ohms, each cell was required to have a resistance of 1000 ohms. The concentration of electrolytes investigated was thus limited to approximately 10^{-4} molar with the cells employed. Each cell had previously been weighed while dry. Before use each cell was steamed for one hour, cooled, and filled with approximately 1000 g. of conductivity water. The cells were closed with a standard taper cap containing a sintered glass gas bubbler tube extending nearly to the bottom of cell. Purified nitrogen was then bubbled through the water. With the cell at room temperature, 25°, the resistance was measured with the DPT bridge circuit with 10-volt 4-microsecond pulses applied. When the conductivity of the water had reached a satisfactorily low value the bubbler was removed and the cell capped with its usual closure. The joints were lightly greased near the lower perimeter with Apiezon grease. The cells and water contents were each weighed. Each cell was then placed in the thermostat on the Lucite cell holder, an operation which at the same time established the necessary connections to the bridge circuit. The cells were allowed to come to temperature equilibrium and the conductance of the water determined; this was usually lower than 0.4×10^{-6} ohm. A suitable amount of stock solution of electrolyte was placed in one cell at a time from a weight buret. The resistance of the cell was measured during this operation *versus* a decade resistance box and variable condenser in parallel in the other arm of the bridge. Addition was cautiously continued until the cell showed a resistance in the vicinity of 1000 ohms. The resistance of the cell containing the electrolyte which would show the larger change in conductance with high field excitation was made appropriately larger than that of the cell containing the reference electrolyte. Thus, at the highest fields the cells would have nearly the same resistances. In this way the values of the compensating resistors in the circuit with the high fields applied would be at a minimum, lessening the voltage gradients and possibility of dielectric breakdown in the decade resistors. The cells were allowed to come to equilibrium until the conductance was stable to within a few tenths of an ohm. All these measurements were carried out with low field pulse excitation using 15 pulses per second repetition rate.

Measurements were then made with successively increasing pulse voltage up to a maximum of 200 kv./cm. field in the conductance cells. Each high field measurement was alternated with a low field measurement to assure that the cell was at proper temperature and that no untoward or unnoticed irreversible conductance changes were taking place. High field measurements were made with single pulses to minimize heating and other conductance-disturbing effects of passing large currents (*e.g.*, 10 amperes at 20 kv.) through the cells. Because of the special properties of the DPT bridge circuit (to be discussed below with details of the bridge balancing procedure) this could be accomplished with a minimum of repetition of the high field excitation.

Pulse voltages were determined by direct measurement with a calibrated capacitative voltage divider and the oscilloscope.

C.P. potassium chloride was recrystallized twice from conductivity water, dried in an oven, and fused in a current of dry nitrogen in a weighed platinum boat. A stock solution was made up by weighing the boat and contents and dissolving the contents into a weighed quantity of conductivity water. The platinum boat was left in the solution.

C.P. magnesium sulfate was recrystallized three times from conductivity water. The resulting salt was dried at 70°, ground in an agate mortar, dried at 125°, again ground, and finally heated at 400° for two hours in a platinum dish. The salt, assumed to be anhydrous magnesium sulfate, was dissolved in the requisite amount of conductivity water to give a stock solution. This solution was analyzed by weighing a portion, evaporating the water carefully, and finally heating the platinum dish to 1000°. The residue was assumed to be magnesium oxide. Three such determinations by evaporation together with the concentration determined from the weighed quantity of anhydrous magnesium sulfate dissolved to make the solution gave the result 0.1180 ± 0.0002 molar.

A zinc sulfate stock solution was prepared and analyzed in essentially the same manner.

(18) The resistances of the windings of two transformers constructed in this manner were measured on a General Radio type 650A impedance bridge with the following results: transformer 1, winding 1 1.51 ohms, W 2 1.47 ohms, W 3 2.73 ohms; Tr 2, W 1 1.46 ohms, W 2 1.49 ohms, W 3 2.73 ohms. The inductances of the windings and the DQ dial readings measured at 1000 c.p.s. on the same bridge were: Tr 1, W 1 3.19 millihenries, DQ = 7.5, W 2 3.20 mh., DQ = 7.5, W 3 4.73 mh., DQ = 6.5; Tr 2, W 1 2.38 mh., DQ = 6.0, W 2 2.39 mh., DQ = 6.0, W 3 3.59 mh., DQ = 5.1. The inductance of winding 1 of transformer 1 was measured as a function of frequency on a Western Electric D170370 bridge; this bridge is capable of much greater precision than the GR 650A bridge, as well as being more accurate. The results were as follows: at 2 kilocycles, 2.8440 millihenries; 5 kc., 2.8044 mh.; 10 kc. 2.7389 mh.; 20 kc., 2.5961 mh.; 50 kc., 2.2278 mh.; and 100 kc., 1.7863 mh. The resistance balance was not recorded for these measurements, but was found to change appreciably as the inductance dropped. These figures all suggest that an improved core material such as the recently available ferrites would decrease the losses in the transformer and markedly improve the frequency response. Also, the different inductance and Q values for the two transformers indicate that considerable care in the assembly and core positioning and closure of the transformers will be necessary.

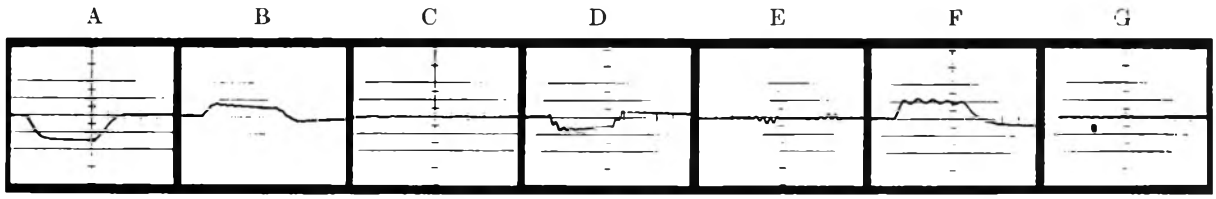

Fig. 4.—Pulse forms observed with differential pulse transformer bridge circuit: A, two microsecond input pulse; B, unbalance wave form with two carbon resistors; C, balance wave form with two carbon resistors and GR 670 F decade resistance box; D, E, same as A and B, respectively, except with ordinary uncompensated decade resistance boxes; F, unbalance wave form with capacitors; G, balance wave form with capacitors and GR 722 variable capacitor.

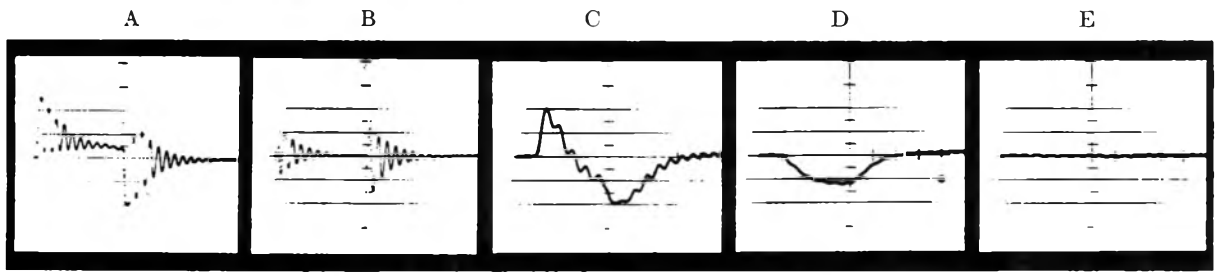

Fig. 5.—Pulse forms observed with differential pulse transformer bridge circuit: A, B, unbalance and balance wave forms with inductances and 1000 microsecond pulse; C, parallel R–C circuit, both unbalanced; D, parallel R–C circuit, capacitance approximately balanced but resistance unbalanced; E, parallel R–C circuit, both R and C in balance.

Suitably diluted solutions of reagent quality acetic and hydrochloric acids were used without purification.

IV. Results

The three components of impedance—resistance, capacitance and inductance—affect the shape of square pulses differently in the differential pulse transformer bridge circuit. In a parallel combination of R, L and C not balanced by a like combination of R, L and C in the other arm of the bridge, unbalanced R gives a voltage output proportional to the degree of unbalance, unbalanced L integrates the pulse, and unbalanced C differentiates the pulse. It is thus possible to determine from a glance at the pulse which components are out of balance and to correct for each independently by removing, for L, the slope on the center of the pulse, for C, the oppositely directed spikes at the beginning and end of the pulse, and for R, the deviation of the oscilloscope trace from the base line. Complex combinations of reactive elements are difficult to interpret on the basis of pulse shape. The photographs of Figs. 4 and 5 show some typical pulse shapes. These photographs were made with repeated exposures; single pulse photographs, while perfectly readable, are not well suited for reproduction. Accordingly no pulse signatures with conductance cells are shown. The R–C combination, Fig. 5, C, D and E, gives a good representation of conductance cell patterns at low fields.

In Fig. 4A, a 2-microsecond input pulse is shown. Figure 4B was obtained with two 1000-ohm nominal valued carbon resistors. Figure 4C shows the balance condition when the resistance unbalance was made up by the insertion of resistance from a General Radio Type 670 F compensated decade resistance box. Carbon resistors are comparatively free from reactive components at these frequencies. Ordinary decade resistance boxes have distributed inductance and capacitance, however, and give rise to less clean-looking pulse shapes such as in Figs. 4D and 4E. The residual reactive components introduce the oscillatory transients at the beginning and end of the pulse. A perfectly satisfactory balance could nevertheless be obtained on units which were never intended to operate at frequencies near 500 kc. In Figs. 4F and 4G are shown the results of balancing two 300 $\mu\mu$f. capacitors. One of the capacitors was variable and had appreciable lead inductance; this is reflected in the oscillatory transient on the pulse.

In Figs. 5A and 5B are shown pulse shapes obtained on balancing two 2.8 millihenry inductances, one of which was variable. The pulse length was 1000 microseconds. The inseparable distributed capacitance in the inductances gives rise to the violent oscillations. The DPT in this case was an ordinary audio output transformer. Figs. 5C, D and E show a common case in conductance measurement, a parallel R–C circuit. In Fig. 5C both R and C are out of balance. In Fig. 5D the capacitance has been approximately balanced, and in 5D both are in balance.

After an extensive series of measurements to study the utility of the bridge for short pulse behavior of various R–L–C combinations we have concluded that it is comparatively easy to attain precisions of measurement in the order of 0.1% while employing pulses of 1–5 microseconds duration and ordinary variable and decade impedance standards. If sufficiently simple combinations are being measured, and if it is possible under practical circumstances to balance residual inductances and capacitances, precision of measurement in the range 0.01% may be readily achieved. The accuracy attainable will be comparable if the standards are sufficiently well known. These measurements are not of particular interest here, but it is important to recognize that the conductance cell is a complex impedance which is only approximated by a parallel R–C circuit, and that the precision of measurement with conductance cells will depend markedly upon the degree to which the assumption of a parallel R–C circuit approaches

the equivalent circuit of the cell. Accordingly, precisions of measurement such as those mentioned may not necessarily be claimed when conductance cells are the unknown impedance.

In high-field conductance measurements with magnesium and zinc sulfates measured relative to potassium chloride we have found the assumption of a parallel R–C circuit to be reasonably satisfactory. It was found that the external capacitance necessary to achieve balance between the cells containing the two solutions did not change appreciably—less than 5 $\mu\mu$f.—at all field strengths thus far studied. No difficulty was noted in achieving balance with unplatinized electrodes, a fact which is to be attributed to the high frequencies employed. (It will be recalled that the Fourier analysis of a single square pulse contains all frequencies.) However, the oscilloscope wave forms obtained at high fields with conductance cells are noticeably less well defined than with R–C circuits made up of relatively pure circuit elements. This can only be interpreted as meaning that there are residual reactive components which have not been properly accounted for.

Although the principal claim for this new bridge technique is its usefulness for high field conductance measurement, it may be mentioned that low field conductance measurements may be carried out in the same manner. Since the high frequencies involved make balancing possible without resort to platnization of the electrodes or tedious multi-frequency measurements, it is then possible to work with extremely dilute solutions without difficulty due to adsorption of the electrolyte on the electrode surfaces. Further, pulsed-bridge studies of pulse-rated components, *e.g.*, radar pulse transformers, vacuum tubes, high power electroacoustic transducers, and so on, have not been previously reported, so far as is known to the authors; for high power pulse impedance measurements, this bridge network is especially well suited.

Table I lists experimental data and results for a determination of the high field conductance of magnesium sulfate relative to potassium chloride. Theoretical values computed from the equation of Onsager and Wilson[9]

$$\Lambda = \Lambda^0 - \frac{|e_j|^2\kappa\Lambda^0}{2DkT}\,g(x) - \frac{96\,500\,|\,k\,e_j\,|\,2\kappa}{6\sqrt{2}\,\pi\eta\,300}f(x) \quad (1)$$

are included for reference. The symbols are those of Harned and Owen.[9,19] The disparity between the experimental and theoretical results is of the same order as found by Wien,[20] although the data cannot be directly compared with those of Wien because of his different concentration and uncertainty as to the temperature of his measurements. The fact that the experimental results are higher than the theoretical has been attributed to the presence of ion pairs in the 2–2 electrolyte.[19]

Table II lists similar data for the high field conductances of zinc sulfate relative to potassium chloride. In both Tables I and II the Wien effect of the potassium chloride reference solution has been corrected in the theoretical results by computation, using equation (1). See also ref. 19.

TABLE I

THE HIGH FIELD CONDUCTANCE OF AN AQUEOUS SOLUTION OF MAGNESIUM SULFATE RELATIVE TO POTASSIUM CHLORIDE AT 25°

$MgSO_4$: 1.733×10^{-4} molar R_0 = 1010.75 ohms KCl: 2.942×10^{-4} molar R_0 = 985.95 ohms

Experimental results:

Field, kv./cm.	R_v ($MgSO_4$)	$\lambda_v = 1/R_v$	$\Delta\lambda$	$\frac{\Delta\lambda}{\lambda_0}$, %
0	1010.75	9893.64	0.0	0.0
10	1008.00	9920.63	26.99	.273
20	1003.10	9969.10	75.46	.763
30	998.00	10020.0	126.40	1.278
40	994.60	10054.3	160.65	1.624
50	991.35	10087.2	193.61	1.957
60	989.40	10107.1	213.50	2.158
70	986.85	10133.2	239.61	2.422
80	985.10	10151.2	257.61	2.604
90	983.50	10167.8	274.13	2.771
100	982.30	10180.2	286.55	2.896
120	980.25	10201.5	307.84	3.111
150	977.50	10230.2	336.54	3.402
180	975.35	10252.7	359.09	3.630
200	974.10	10265.9	372.25	3.763

Onsager–Wilson theory:

Field, kv./cm.	Λ^0 $MgSO_4$ = 133 Λ_x	%	Λ^0 KCl = 149.86 Λ_x	%	Relative, %
0	126.62	0.0	148.24	0.0	0.0
10	127.01	0.308	148.29	.033	0.275
30	128.21	1.249	..	..	1.10
60	129.02	1.891	..	..	1.61
100	129.51	2.281	148.78	.362	1.920
200	130.02	2.684	148.91	.454	2.230
300	130.23	2.845	148.97	.492	2.353

TABLE II

THE HIGH FIELD CONDUCTANCE OF AN AQUEOUS SOLUTION OF ZINC SULFATE RELATIVE TO POTASSIUM CHLORIDE AT 25°

$ZnSO_4$: 1.64×10^{-4} molar R_0 = 1044.90 ohms KCl: 2.88×10^{-4} molar R_0 = 998.25 ohms

Experimental results:

Field, kv./cm.	R_v ($ZnSO_4$)	$\lambda_v = \frac{1}{R_v}$	$\Delta\lambda$	$\frac{\Delta\lambda}{\lambda_0}$, %
0	1044.90	9570.3	0.0	0.0
10	1041.50	9601.5	31.25	.327
20	1035.50	9657.2	86.88	.908
50	1023.30	9772.3	202.02	2.111
80	1015.50	9841.4	277.08	2.895
100	1012.05	9880.9	310.64	3.246
150	1008.15	9919.2	348.87	3.645
180	1006.25	9937.9	367.60	3.841

Onsager–Wilson theory:

Field, kv./cm.	Λ^0 $ZnSO_4$ = 133 Λ_x	%	Λ^0 KCl = 149.86 Λ_x	%	Relative, %
0	126.79	0.0	148.24	0.0	0.0
50	128.92	1.674	148.61	.248	1.426
100	129.63	2.233	148.78	.362	1.871
200	130.12	2.619	148.91	.454	2.165
300	130.31	2.773	148.97	.492	2.281

Table III lists high field conductance data for acetic acid relative to hydrochloric acid. It was found impossible to determine the high field conductance of acetic acid relative to potassium chlo-

(19) See also, F. E. Bailey and A. Patterson, *J. Am. Chem. Soc.*, **74**, 4756 (1952).

(20) M. Wien, *Ann. Physik*, **85**, 795 (1928).

ride. Effects which appeared to result from polarization in the case of the acetic acid made it impossible to obtain a balance on the oscilloscope. These effects were not noticeable when acids were used in both cells. Since the change of resistance is in this case much larger than with the strong electrolytes above, the high fields have been corrected for the voltage drop across the compensating resistors, R_1 and R_2. The data extrapolate to a negative intercept which has been interpreted as due to the incomplete attainment of unit activity, even in the dilute solutions employed. This intercept, -1.50%, corresponds to an activity coefficient of 0.985. The theoretical computation, made with the aid of Onsager's equations[7]

$$F(b) = 1 + b + \frac{b^2}{3} + \frac{b^3}{18} + \cdots$$

where $b = 9.636\ V/DT^2$ for a 1-1 electrolyte (2)

$$K(x) = K(0)F(b) = \frac{c\alpha^2}{1 - \alpha}$$

$$\frac{\alpha}{\alpha_0} - 1 = \frac{\lambda - \lambda_0}{\lambda_0} = \frac{\Delta\lambda}{\lambda_0}$$

has been corrected for this negative intercept. The experimental data correspond closely to the theoretical, falling slightly below at high values of the field. Schiele's values[10] fall above the theoretical by a somewhat larger amount.

In these determinations the precision of measurement of the quantity $\Delta\lambda/\lambda_0$ is in the order of 0.03%, absolute. In other words, the difference between the per cent. fractional conductance change on successive measurements on the same solutions at the same value of field is no greater than 0.03. This is a factor limited principally by the uncertainty of balance due to transient oscillations on the pulses observed, rather than the precision ultimately attainable with the circuit. It is hoped that a better understanding of the equivalent circuit of the conductance cells will permit an improvement in residual impedance balancing and a reduction in the transients observed. The field strength is believed to be known to within 1%.

It should be pointed out in comparing these results with those of Wien and his co-workers that square pulse excitation eliminates any uncertainty as to the proper maximum value of field strength, and that an oscilloscopic presentation which permits balancing of the several components of an impedance will eventually permit a better understanding of conductance cell behavior under high field excitation. The DPT circuit makes this possible for the first time. The general method described makes possible a rapid measurement of high field conductance with a precision comparable to the tedious integrating method of Malsch and Wien. Since the present method is not an integrating one, but one which permits an instantaneous view of circuit behavior, it is felt that the precision claimed is truly indicative of the success with which the item actually sought, $\Delta\lambda/\lambda_0$, has been measured.

TABLE III

THE HIGH FIELD CONDUCTANCE OF AN AQUEOUS SOLUTION OF ACETIC ACID RELATIVE TO HYDROCHLORIC ACID AT 25°

HAcO: 7.7×10^{-4} molar HCl: 1.1×10^{-4} molar
R_0 = 1069.75 ohms R_0 = 1027.0 ohms

Experimental results:

Field, kv./cm.	R_v(HAcO)	$\lambda_v = \frac{1}{R_v}$	$\Delta\lambda$	$\frac{\Delta\lambda}{\lambda_0}$, %
0	1069.75	9348.0	0.0	0.0
20	1066.0	9380.9	32.88	.351
30	1061.6	9419.7	71.76	.768
50	1051.3	9512.0	164.05	1.755
60	1045.9	9561.1	213.16	2.280
90	1028.0	9727.6	379.65	4.061
100	1022.1	9783.9	435.80	4.662
136	1001.1	9989.0	641.03	6.857
145	996.1	10039.1	691.17	7.394
172	983.0	10172.9	824.95	8.825
189	975.3	10253.2	905.27	9.684

Onsager's theory: Λ^0 HCl = 426.16

Field, kv./cm.	HAcO, %	HCl, %	Relative, %
0	0.0	0.0	0.0
50	3.135	.174	2.961
100	6.419	.209	6.210
200	12.923	.236	12.687

The slope of the above curve corresponds to an intercept of -1.50%:

Field, kv./cm.	(Relative, %) − 1.5
0	− 1.50
50	1.461
100	4.710
200	11.187

Acknowledgment.—The authors are indebted to Capt. W. L. Pryor, USN, for making available certain of the equipment employed, to Mr. Frederick E. Bailey, Jr., for some of the experimental work, and to Prof. H. S. Harned for his suggestion of the problem and for continued assistance and encouragement. Part of the work reported was performed under contract with the Office of Naval Research, Contract Nonr 215 (00), the assistance of which is gratefully acknowledged.

THE ALKALINE HYDROLYSIS OF MONOETHYL MALONATE ION IN ISODIELECTRIC MEDIA

BY W. J. SVIRBELY AND BEVERLEY W. LEWIS[1]

The Department of Chemistry, University of Maryland, College Park, Maryland

Received February 18, 1952

The effects on the kinetics of the alkaline hydrolysis of monoethyl malonate ion due to changing dielectric constant and to changing solvent system were studied at 25.08°. The rate constants were determined for solvent systems having dielectric constants of 50, 60, 70 and 75. The solvent systems were dioxane–water, acetone–water, ethyl alcohol–water and isopropyl alcohol–water. Studies in methyl alcohol–water systems were unsuccessful. The data are examined in light of existing theories.

The alkaline hydrolysis of monoethyl malonate ion has been studied previously.[2-4] Recent studies by Svirbely and Mador[4] were carried out in two solvent systems, namely, dioxane–water and *t*-butyl alcohol–water in the dielectric range of 50 to 60. In this research, data were obtained at 25.08° in the dielectric constant range of 60 to 75 for the dioxane–water system and in the dielectric range of 50 to 75 for three other solvent systems, namely, acetone–water, isopropyl alcohol–water, and ethyl alcohol–water, with the purpose of testing the theory of the change in rate with changing dielectric constant of the medium for an ion–ion reaction of like charge sign.

Materials and Apparatus

Potassium Ethyl Malonate.—This salt was prepared by Mador.[4] Saponification analysis indicated a purity of 100 ± 0.1%.

Dioxane.—Commercial dioxane was purified by a standard procedure.[5] $n^{20}D$ was 1.4221.

Acetone.—Commercial acetone was purified by a standard procedure.[6] $n^{20}D$ was 1.3588.

Ethyl Alcohol.—Absolute ethyl alcohol was purified by the method of Lund and Bjerrum as described by Fieser.[7] $n^{20}D$ was 1.3613.

Isopropyl Alcohol.—Commercial isopropyl alcohol was purified by a method given by Weissberger and Proskauer.[8] $n^{20}D$ was 1.3777.

Water.—Freshly boiled, distilled water was used in preparing all solutions.

Apparatus.—All apparatus used and their calibrations have been previously described.[4]

Experimental Method

The preparation of reaction mixtures and the experimental procedure in carrying out a run were essentially the same as before.[4]

In the case of acetone–water mixtures, the color change of the mixed indicator of phenolphthalein and thymol blue was not distinct. A 0.1 molar solution of phenolphthalein in alcohol was determined by *p*H measurements to be suitable as an indicator for the titration in the acetone–water system.

The weight percentages of dioxane, acetone, ethyl alcohol and isopropyl alcohol–water mixtures corresponding to any specific dielectric constant at 25.08° were obtained by interpolation of the data of Åkerlöf.[9]

The densities of acetone, ethyl alcohol and isopropyl alcohol at 25° were taken from the literature.[10a] The density of dioxane was taken[10b] as 1.030 at 25°. These values were used in transforming weight data to volume data.

Calculations and Discussion

Evaluation of Rate Constants.—The time–concentration data at 25.08° for the reaction in the ethyl alcohol–water mixtures having a dielectric constant of 50 are given in Table I. The k's were calculated by use of the second-order equation where both reactants have initial concentrations, namely

$$k(t_2 - t_1) = \frac{1}{C_2} - \frac{1}{C_1} \qquad (1)$$

A pair of consecutive samples for a run was used in each calculation of k.

The ionic strength for this reaction can be expressed[4] by the equation

$$\mu = 2C_0 + x + S \qquad (2)$$

where C_0 is the initial normality of both reactants

TABLE I

DATA IN ETHYL ALCOHOL–WATER MIXTURES, D = 50, t = 25.08°

Time, min.	Normality	$\sqrt{\mu(\text{mean})}$	k, liter/mole-min.	k^0, liter/mole-min.
	Run 1	Initial N = 0.01393		
6.0	0.01353	...	...	...
21.5	.01276	0.1693	0.288	0.147
46.0	.01171	.1719	.287	.145
120.0	.00938	.1768	.286	.142
	Run 2	Initial N = 0.01441		
6.0	0.01371	...	...	...
21.0	.01294	0.1703	0.289	0.147
46.5	.01179	.1731	.296	.149
76.0	.01069	.1763	.296	.147
120.0	.00944	.1796	.283	.139
	Run 3	Initial N = 0.01389, NaCl = 0.1966 N		
6.0	0.01289	...	...	...
16.0	.01188	0.4753	0.660	0.145
28.5	.01082	.4763	.659	.145
43.0	.00980	.4775	.665	.146
65.0	.00857	.4787	.665	.146
	Run 4	Initial N = 0.01398, NaCl = 0.1965 N		
7.0	0.01286	...	...	...
17.0	.01186	0.4755	0.656	0.145
29.5	.01079	.4766	.669	.147
66.0	.00857	.4783	.656	.144
				k^0_{av} = 0.146

(1) Abstract from a thesis submitted by B. W. Lewis to the Graduate School of the University of Maryland in partial fulfillment of the requirements for the degree of Master of Science.

(2) M. Ritchie, *J. Chem. Soc.*, **139**, 3112 (1931).

(3) F. H. Westheimer, W. A. Jones and R. A. Lad, *J. Chem. Phys.*, **10**, 478 (1942).

(4) W. J. Svirbely and I. L. Mador, *J. Am. Chem. Soc.*, **72**, 5699 (1950).

(5) L. F. Fieser, "Experiments in Organic Chemistry," 2nd ed., D. C. Heath and Co., New York, N. Y., 1941, p. 368.

(6) Reference 5, p. 383.

(7) Reference 5, p. 359.

(8) A. Weissberger and E. Proskauer, "Organic Solvents," Clarendon Press, New York, N. Y., 1935, p. 125.

(9) G. Åkerlöf, *J. Am. Chem. Soc.*, **54**, 4125 (1932); G. Åkerlöf and O. A. Short, *ibid.*, **58**, 1241 (1936).

(10) (a) "International Critical Tables," Vol. III, p. 27–33; (b) I. L. Mador, Thesis, University of Maryland, 1950.

(equal concentrations), S is the normality of the uni-univalent electrolyte and x is the amount of material in moles per liter which has reacted. Since each value of k corresponds to an ionic strength range, the mean value of the ionic strength for two consecutive samples is given in the third column of Table I.

The values of the limiting velocity constant k^0 at $\sqrt{\mu} = 0$ were obtained by use of the equation[4]

$$\log k^0 = \log k - \frac{3.647 \times 10^6 \sqrt{\mu}}{(DT)^{3/2} + 5.028 \times 10^9 a_i DT\sqrt{\mu}} \quad (3)$$

As before,[4] a value of a_i was determined by trial and error through use of equation 3 which gave the most consistent values of k^0 over the ionic strength range. The values of a_i which were found to fulfill the above criterion in each solvent system are given in the second column of Table II. It is evident that they depend on the nature of the solvent. The last column of Table I lists the values of k^0 for the reaction in ethyl-alcohol mixtures at a dielectric constant of 50 as an illustration of the consistency of the k^0 values using a value of a_i equal to 2.3 A.

TABLE II

Solvent system	a_i (vol. concn.), Å.	r (vol. concn.), Å.	r (mole fraction), Å.
Water[a]	4.8	4.0	2.6
Dioxane–water	4.8[a]	5.7	3.9
t-Butyl alcohol–water	4.3[a]	...	...
Acetone–water	4.0	2.3	1.7
Isopropyl alcohol–water	3.5	3.7	2.4
Ethyl alcohol–water	2.3	2.1	1.6

[a] These results were obtained in the previous study, ref. 4.

The average values of the limiting velocity constants (k^0) based on volume concentrations in liters mole^{-1} min.$^{-1}$ are given in Table III. These limiting velocity constants (k^0) were corrected to mole fraction rate constants (k_N^0) by use of the equation[4]

$$k_N^0 = 1000 \frac{\Sigma n k^0}{V} \quad (4)$$

and the results are given in Table III. A comparison of the data in the *t*-butyl alcohol–water and dioxane–water media, had previously led[4] to the conclusion that mole fraction units were necessary. On the basis of the data presented here for the alkaline hydrolysis of the monoethyl malonate ion carried out in a variety of solvent systems, one must conclude that a choice between mole fraction concentration units and volume concentration units cannot be made with any certainty.

TABLE III

SUMMARY OF k^0 AND k_N^0 VALUES AT 25.08° IN THE VARIOUS SOLVENT SYSTEMS

Dielectric constant	Dioxane–water k^0	Dioxane–water k_N^0	Acetone–water k^0	Acetone–water k_N^0	Isopropyl alcohol–water k^0	Isopropyl alcohol–water k_N^0	Ethyl alcohol–water k^0	Ethyl alcohol–water k_N^0
78.47[a]	0.807[b]	44.7[b]	0.799	44.2	0.792	44.4	0.774	42.8
75	.722	38.7	.686	35.7	.724	38.8	.654	34.3
70	.653	33.5	.560	26.7	.633	31.1	.506	24.5
60	.513[b]	23.9[b]	.430	17.1	...	..	.271	11.1
50	.374[b]	15.6[b]	.356	11.8	.320	11.5	.146	5.04

[a] The values of k^0 and k_N^0 for dielectric constant 78.47, *i.e.*, pure water as the solvent, were calculated using the particular value of a_i which was determined to be best for the solvent system under consideration. [b] Data taken from ref. 4.

Salt Effects.—The data in column 4, Table I show the existence of a positive primary salt effect for the reaction in the ethyl alcohol–water mixtures, $D = 50$. Experiments carried out over an ionic strength range in acetone–water mixtures, $D = 60$, and in isopropyl alcohol–water mixtures, $D = 50$, also showed the existence of a positive primary salt effect. These results are in accord with previous work.[4]

Effect of Solvents on the Rate at Zero Ionic Strength.—Figure 1 is a plot of log k^0 *versus* $100/D$ for the solvent systems studied. Figure 2 is a similar plot of log k_N^0 *versus* $100/D$. The equation developed by Scatchard,[11] namely

$$\left(\frac{\partial \log k^0}{\partial \frac{1}{D}}\right)_T = \frac{-\epsilon^2 Z_A Z_B}{2.303 rTk} \quad (5)$$

predicts a straight line plot at a given temperature having a slope independent of the solvent except for the possibility that the radius of the activated

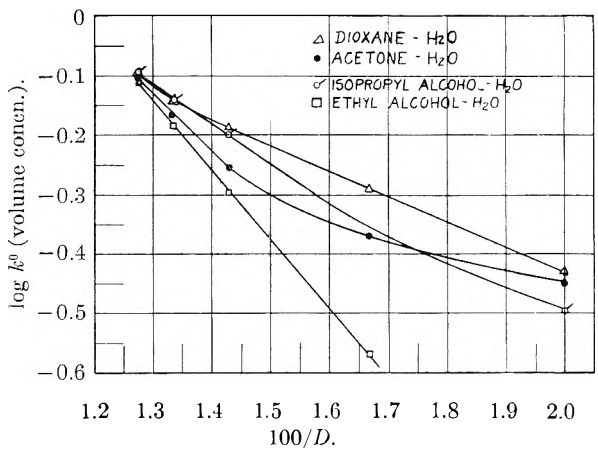

Fig. 1.—Influence of dielectric constant on the reaction rate at zero ionic strength.

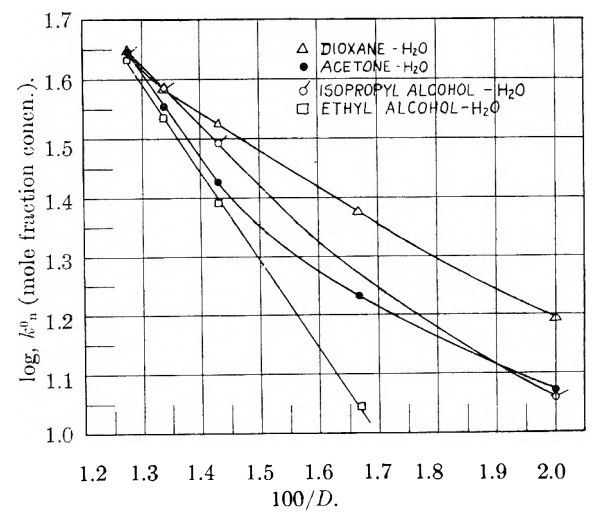

Fig. 2.—Influence of dielectric constant on the reaction rate at zero ionic strength.

(11) G. Scatchard, *Chem. Revs.*, **10**, 229 (1932).

complex differs with the solvent system. Reference to Figs. 1 and 2 shows that linearity is obtained in all cases at the higher dielectric values. With the exception of the dioxane–water system, the linearity extends to the inclusion of the k^0 data obtained in pure water as the solvent. It should be emphasized that a separate calculation of k^0 was made from the data[4] obtained in the runs with water as the solvent for each solvent system, using the particular value of a_i for that system. If the value of a_i determined for water as a solvent is used to calculate the value of k^0 in water, then one k^0 value only is obtained. The use of this single k^0 value in the plots of Figs. 1 and 2 would lead to curvature at the water end of the ethanol–water, isopropyl–water and acetone–water curves. Since this curvature is eliminated by our first method of calculation, which is essentially a method that allows for correction in water due to specific solvent influences operating in a mixed solvent pair, it appears to us in light of the linearity predicted by equation 5 that our first method of calculation is to be preferred.

By use of equation 5 and the slopes obtained from the linear portions of Figs. 1 and 2, the values of r, the radius of the complex, have been calculated and are given in Table II. The order of magnitude of the radii is not unreasonable in either concentration scale. However, it is apparent that as in the case of the a_i values, the values of r depend on that nature of the solvent.

We would also like to report that runs were made in methanol–water systems. However, values of k increased markedly as the run proceeded. Reference to the fourth column of Table I shows that in each run the values of k were essentially constant over the small ionic strength range investigated. Thus it was evident that some other reaction was occurring in the methanol–water system which was not taking place in the other systems studied. Work in the methanol–water systems was therefore abandoned.

VISCOSITIES OF SEVERAL LIQUIDS[1]

By D. M. Mason, O. W. Wilcox and B. H. Sage

Chemical Engineering Laboratory, California Institute of Technology, Pasadena, California

Received February 25, 1952

The viscosity of ethylenediamine, ethylenediamine hydrate, hydrazine and isopropylamine in the liquid phase was measured with a steel rolling ball viscometer over the temperature ranges 30 to 210°, 30 to 170°, 10 to 80° and 0 to 180°, respectively. These measurements were carried out at pressures from bubble point to 250 atm. Investigations also were made of the viscosity in the liquid phase of commercial samples of red fuming nitric acid, white fuming nitric acid and furfuryl alcohol at bubble point over the temperature ranges 10 to 120°, 10 to 120° and 30 to 130°, respectively. The latter measurements were made in a rolling ball viscometer constructed of glass since the nature of these materials at high temperature precluded the use of a steel instrument.

Experimental

In principle, the rolling ball viscometer involves an inclined tube in which a closely fitting ball is permitted to roll under the influence of gravity. The roll time may be empirically related to the viscosity of the fluid. This type of instrument was proposed by Flowers.[2] A schematic diagram and description of the steel viscometer used for the measurements at elevated pressures in the present investigation are available.[3] The sample was added to the evacuated system through a suitable inlet. The roll time of the ball was determined by the time elapsed between the signals recorded on a chronograph when the ball passed inductance coils wound on the exterior of the roll tube. These coils were spaced 19.05 cm. apart. The uncertainty in time measurements was 0.1%. Mercury was added or withdrawn from an auxiliary chamber in order to change the effective volume of the system. The pressure within the viscometer was measured by a balance.[4] The tubing from the balance was filled with oil and was connected to the viscometer through an oil–mercury interface. The probable uncertainty in the measured pressure was less than 0.1 atm. The absolute temperature was established within 0.02° by means of a platinum resistance thermometer. The temperature of the agitated oil-bath surrounding the viscometer was controlled within 0.04° of the desired temperature by means of an electrical heater used in conjunction with a modulated, droop corrected electronic circuit.

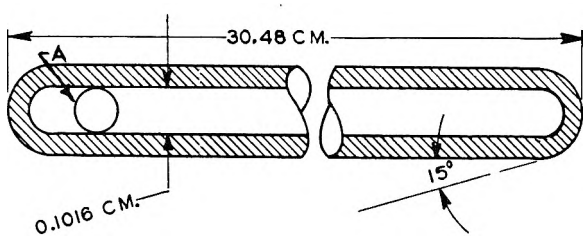

Fig. 1.—Glass rolling ball viscometer.

In Fig. 1 are presented the principal dimensions and arrangement of the glass rolling ball viscometer employed in the measurement of the viscosity of fuming nitric acid and furfuryl alcohol. The sample was introduced by high vacuum technique into the tube, which was closed at one end. The other end of the tube was sealed while the lower end was immersed in liquid air. A small glass ball shown at A cleared the interior of the tube by approximately 0.03 cm. The tube was located in an agitated air-bath and the temperature of the sample was known within 0.5°. The roll time between marks on the tube was determined visually. No difficulty was experienced in reproducing roll time within 0.5%.

Density data for the samples were obtained by measurements with a pycnometer over the range of temperatures where the vapor pressure is below that of the atmosphere. Values of density at higher pressures were determined by generalized relationships given in the literature.[5] As has been described[3] the viscometers were calibrated with fluids of known viscosity and for those cases where flow was not in the laminar region suitable corrections[2,3,6] were made for

(1) This paper presents the results of research carried out for the Jet Propulsion Laboratory, California Institute of Technology, under Contract No. W-64-200 ORD-455 sponsored by the U. S. Army Ordnance Department.

(2) A. E. Flowers, *Proc. Am. Soc. Test. Mat.*, 14, II, 565 (1914).

(3) B. H. Sage and W. N. Lacey, *Trans. Am. Inst. Mining Met. Engrs.*, 127, 118 (1938)

(4) B. H. Sage and W. N. Lacey, *ibid.*, 174, 102 (1948).

(5) K. M. Watson, *Ind. Eng. Chem.*, 35, 398 (1943).

(6) M. D. Hersey and H. Shore, *Mech. Eng.*, 50, 221 (1928).

deviation from the simple functional relationship that exists between viscosity and roll time in the laminar region. The theory of a rolling ball viscometer has been discussed in some detail elsewhere.[7,8]

TABLE I

VISCOSITY OF ETHYLENEDIAMINE

Temp., °C.	Bubble point	Pressure, atmospheres 50	100	150	200	250
30	1.586[a]	1.632	1.689	1.720	1.760	1.789
40	1.260	1.292	1.328	1.364	1.392	1.412
50	1.033	1.053	1.082	1.116	1.140	1.162
60	0.853	0.873	0.896	0.922	0.946	0.970
70	.704	.724	.742	.761	.781	.804
80	.580	.599	.612	.628	.642	.660
90	.484	.500	.511	.521	.536	.544
100	.412	.425	.435	.442	.453	.462
110	.362	.372	.381	.386	.396	.404
120	.324	.332	.341	.345	.352	.361
130	.298	.304	.310	.316	.321	.329
140	.275	.280	.287	.293	.297	.304
150	.255	.260	.264	.271	.276	.282
160	.236	.243	.247	.253	.259	.264
170	.222	.227	.232	.238	.244	.246
180	.207	.212	.218	.223	.229	.233
190	.195	.201	.205	.210	.216	.220
200	.184	.189	.193	.198	.202	.207
210	.172	.176	.181	.185	.189	.194

[a] Viscosity expressed in centipoises.

TABLE II

VISCOSITY OF ETHYLENEDIAMINE HYDRATE

Temp., °C.	Bubble point	Pressure, atmospheres 50	100	150	200	250
30	4.920[a]	5.000	5.100	5.170	5.350	5.460
40	3.320	3.400	3.450	3.500	3.550	3.650
50	2.410	2.440	2.460	2.510	2.550	2.610
60	1.830	1.870	1.900	1.920	1.960	1.985
70	1.440	1.470	1.487	1.510	1.530	1.550
80	1.135	1.160	1.170	1.190	1.210	1.225
90	0.900	0.920	0.930	0.945	0.970	0.980
100	.725	.735	.745	.760	.780	.790
110	.585	.600	.605	.615	.630	.640
120	.480	.490	.495	.505	.515	.525
130	.400	.410	.419	.424	.431	.440
140	.340	.350	.351	.351	.378	.380
150	.299	.310	.312	.313	.322	.330
160	.270	.270	.280	.280	.290	.290
170	.240	.240	.250	.260	.270	.270

[a] Viscosity expressed in centipoises.

TABLE III

VISCOSITY OF HYDRAZINE

Temp., °C.	Bubble point	Pressure, atmospheres 50	100	150	200	250
10	1.240[a]	1.246	1.253	1.265	1.273	1.278
20	1.048	1.058	1.064	1.075	1.090	1.098
30	0.888	0.897	0.906	0.917	0.930	0.937
40	.765	.775	.783	.792	.800	.808
50	.665	.676	.682	.688	.696	.702
60	.582	.591	.598	.602	.611	.617
70	.508	.518	.524	.530	.538	.546
80	.438	.448	.456	.464	.472	.482

[a] Viscosity expressed in centipoises.

(7) R. B. Block, *J. Applied Phys.*, 13, 56 (1942).

(8) R. M. Hubbard and G. G. Brown, *Ind. Eng. Chem., Anal. Ed.*, 15, 212 (1943).

TABLE IV

VISCOSITY OF ISOPROPYLAMINE

Temp., °C.	Bubble point	Pressure, atmospheres 50	100	150	200	250
0	0.4605[a]	0.4794	0.4998	0.5197	0.5412	0.5610
10	.3998	.4126	.4300	.4470	.4625	.4758
20	.3500	.3620	.3761	.3900	.4030	.4140
30	.3082	.3179	.3295	.3400	.3501	.3610
40	.2728	.2802	.2899	.2990	.3075	.3176
50	.2455	.2528	.2603	.2689	.2766	.2849
60	.2249	.2319	.2387	.2464	.2530	.2600
70	.2085	.2144	.2213	.2283	.2340	.2407
80	.1941	.2000	.2068	.2127	.2180	.2241
90	.1826	.1875	.1937	.1992	.2048	.2100
100	.1729	.1768	.1826	.1879	.1931	.1981
110	.1632	.1680	.1730	.1785	.1839	.1886
120	.1551	.1601	.1649	.1706	.1760	.1811
130	.1479	.1537	.1586	.1647	.1702	.1759
140	.1411	.1479	.1530	.1600	.1663	.1722
150	.135	.142	.149	.156	.164	.170
160	.129	.138	.145	.154	.162	.169
170	.124	.133	.143	.152	.161	.166
180	.119	.129	.140	.150	.150	.165

[a] Viscosity expressed in centipoises.

TABLE V

VISCOSITY OF RED FUMING NITRIC ACID, WHITE FUMING NITRIC ACID AND FURFURYL ALCOHOL

Temp., °C.	Red fuming[a] nitric acid	White fuming[b] nitric acid	Furfuryl Alcohol
10	2.040[c]	1.013	...
20	1.635	0.875	...
30	1.350	.758	4.402
40	1.105	.651	3.236
50	0.925	.585	2.568
60	.785	.520	2.009
70	.670	.457	1.631
80	.570	.435	1.348
90	.490	.408	1.121
100	.425	.391	0.950
110	.370	.386	.813
120	.315	.385	.708
130	...	...	.621

[a] Initial composition: weight fraction 0.833 HNO_3; 0.143 NO_2; 0.024 H_2O. [b] Initial composition: weight fraction 0.942 HNO_3; 0.040 NO_2; 0.018 H_2O. [c] Viscosity expressed in centipoises.

Results

The smoothed experimental results for ethylenediamine, ethylenediamine hydrate, hydrazine and isopropylamine are presented in Tables I through IV. The changes in absolute viscosity of these compounds do not exhibit abnormalities with respect to the influence of temperature and pressure. There is appreciable uncertainty in the values of viscosity for isopropylamine at temperatures above 150° because of the relatively short roll times involved. The data are presented at 250 atm. as well as at bubble point. Table V records the viscosities of red and white fuming nitric acid and furfuryl alcohol in the liquid phase as a function of temperature at bubble point. The initial composition of the fuming nitric acid samples is presented in this table. The measurements were made under isochoric conditions with a gas phase

volume approximately $^1/_3$ of the total volume of the system. White fuming nitric acid requires an extended period of time to come to chemical equilibrium at 90°. At temperatures above 90°[9] the extent of the reaction is sufficient to affect the viscosity measurements. Such effects were minimized by making the measurements as rapidly as possible at the elevated temperatures.

Values of the viscosity of four of these compounds at atmospheric pressure are available. Information concerning each of the compounds has been obtained for the following temperature ranges: ethylenediamine[10] 20 to 116°; hydrazine[11,12] 0 to 25°; furfuryl alcohol[13] 25°; and white fuming nitric acid[14] 10 to 40°. In each of the tables the viscosity has been recorded to one more significant figure than is justified by the absolute accuracy of the measurements. This number of significant figures was carried in order not to lose accuracy in interpolation and in the estimation of the derivatives with respect to temperature and pressure.

(9) W. R. Forsythe and W. F. Giauque, *J. Am. Chem. Soc.*, **64**, 48 (1942).

(10) J. N. Friend and W. D. Hargreaves, *Phil. Mag.*, **35**, 57 (1944).

(11) P. Walden and H. Hilgert, *Z. physik. Chem.*, **165A**, 241 (1933).

(12) V. I. Semishin, *J. Gen. Chem.* (*U.S.S.R.*), **8**, 654 (1938).

(13) Bulletin No. 83-A, Quaker Oats Company.

(14) "International Critical Tables," Vol. V, McGraw-Hill Book Co., Inc., New York, N. Y., 1929, pp. 10, 13.

IONIZATION OF FLUOROCARBON GASES BY U-234 α-PARTICLES[1]

BY M. E. STEIDLITZ, F. D. ROSEN, C. H. SHIFLETT AND W. DAVIS, JR.

Carbide and Carbon Chemicals Company, Union Carbide and Carbon Corporation, K-25 Laboratory Division, Oak Ridge, Tennessee

Received March 10, 1952

The range and total ionization of U-234 α-particles in three inorganic and ten fluorocarbon gases have been measured. In all cases the average energy utilization was found to be about 30 e.v. per ion pair. Data on ranges have been used to calculate constants in the Geiger equation. Finally, one constant, δ, has been found that permits calculation of the range of U-234 α-particles in any of the gases in terms of atomic numbers and the initial velocity of the α-particle.

Introduction

In the study of radiation chemistry, the chemical reactions of primary concern are those resulting from the passage of charged particles or ionizing radiation through matter. The initial step in this process must involve the transfer of energy from such a particle or quantum to molecules encountered along its path. This energy may be observed in the form of charged ions or electronically excited molecules.

Previous studies by Geiger[2] have shown definite laws governing the range and total ionization caused by an α-particle. The present investigation has been made in an attempt to expand these relationships and to obtain experimental values for a number of fluorocarbon gases which have just recently become available.

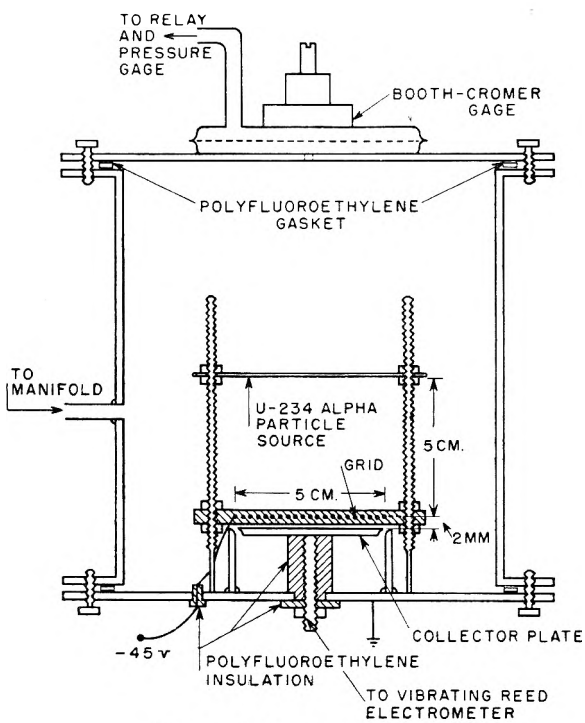

Fig. 1.—Ionization chamber.

Experimental

Apparatus.—The chamber used in these experiments is shown in Fig. 1. It consisted of a nickel shell which enclosed a U-234 α-particle source plated on a 5-cm. diameter disk. This source, not collimated, was mounted about 5 cm. above a collector plate and grid system; the grid was maintained at a −45 v. potential with respect to the plate. As a result of preliminary variations between −30 and −90 v. the value −45 v. was found to be a non-critical optimum, with respect to instrument stability and current reproducibility. A vibrating reed electrometer was used for current amplification. Pressures were relayed through a Booth-Cromer gage[3] to a Wallace and Tiernan gage. The entire system was thermostated at 30 ± 0.5°.

Materials.—All of the gases used, except fluorine, came from standard commercial tanks and were used without further purification. According to specifications the purities of these were in excess of 98%. The fluorine had a purity greater than 95%.

Procedure.—After pumping the system to a vacuum of less than 10^{-4} mm. of mercury and purging with the gas to be studied, the apparatus was filled to a pressure high enough to prevent ionization between the grid and collector plate. The gas was then pumped out in small increments with pressure and current readings being taken after each pumping. This procedure was followed until the gas had been exhausted from the chamber.

(1) This document is based on work performed for the A.E.C. by Carbide and Carbon Chemicals Company at Oak Ridge, Tennessee. Address inquiries concerning this paper to W. Davis, Jr.

(2) H. Geiger, *Proc. Roy. Soc.* (*London*), **A83**, 505 (1910).

(3) S. Cromer, U. S. Atomic Energy Declassified Report, MDDC-803.

Results

In order to compare results of different experiments, the current readings obtained at various pressures were corrected to the reference state of 760 mm. and 0°. Current readings reported are in arbitrary scale units and were corrected by equation (1).

$$i_0 = i_m \times \frac{760}{P} \times \frac{T}{273} \qquad (1)$$

where P is the pressure in mm., T is the temperature in degrees absolute, i_0 is the current reported, and i_m is the current measured.

Similarly, the distance d, in mm., was reduced to S.T.P. conditions by equation (2).

$$d(\text{in mm.}) = d_s \times \frac{P}{760} \times \frac{273}{T} \qquad (2)$$

where d_s is the distance between the source and the grid.

Ionization curves obtained by use of equations (1) and (2) are shown in Figs. 2, 3 and 4. Relative values of total ionization, represented by the areas subtended by the curves, and the range of U-234 α-particles in each of the gases studied are given in Table I. A planimeter was used to measure the subtended areas.

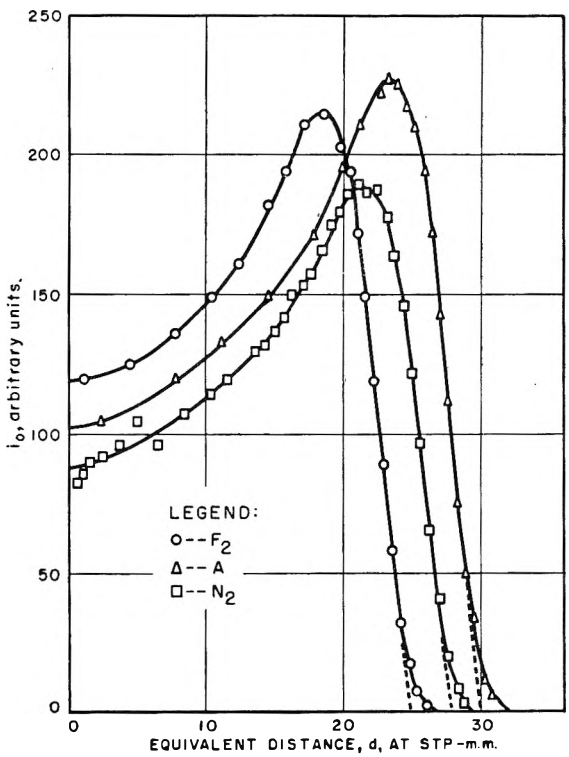

Fig. 2.—Ionization curves of inorganic gases.

Discussion

Experimentally, Geiger[2] has shown the validity of equations (3) and (4) for α-particle ionization.

$$R = k_1 V_0^3 \qquad (3)$$

$$I = k_2 V_0^2 \qquad (4)$$

where R is the range of the α-particle in mm., I is the total number of ion pairs produced by one alpha particle, V_0 is the initial velocity of the alpha particle, and k_1 and k_2 are constants.

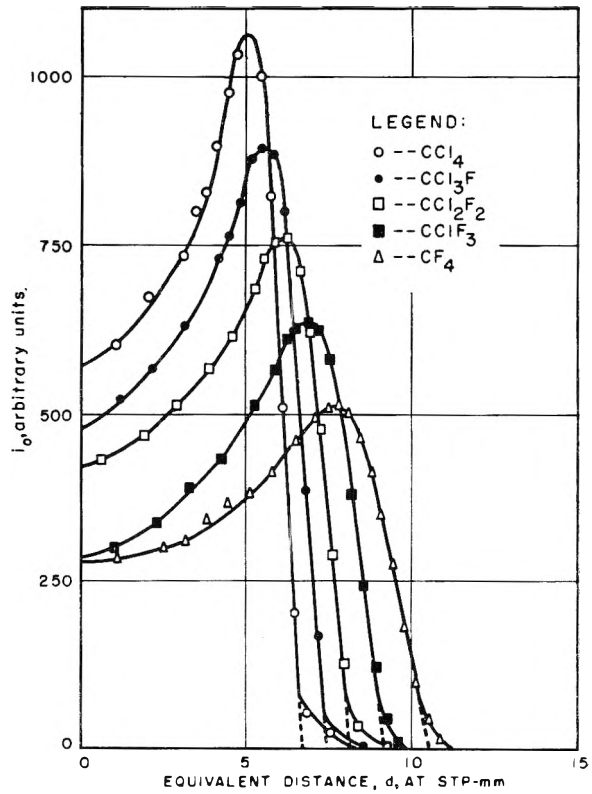

Fig. 3.—Ionization curves of chlorofluoromethanes.

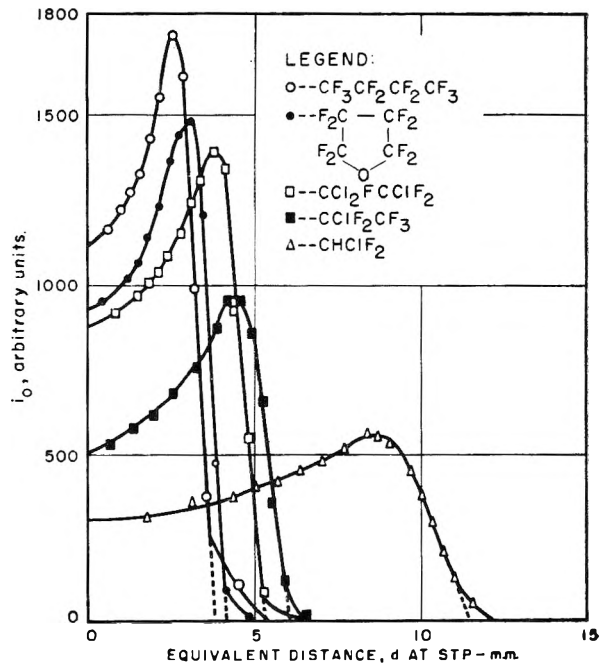

Fig. 4.—Ionization curves of various fluorocarbons.

It has been shown[4] that the range of an α-particle is related to the structure of the molecule by equation (5).

$$\frac{1}{R} = \frac{1}{\delta}\sum_i n_i Z_i^{2/3} \frac{1}{V_0^3} \qquad (5)$$

(4) S. C. Lind, "The Chemical Effects of Alpha Particles and Electrons," Revised ed., American Chemical Society Monograph Series, New York, N. Y., 1928.

TABLE I

RANGE AND IONIZATION VALUES FOR U-234 α-PARTICLES

Compound	Relative ion., arbitrary units	Range, mm. Measd.	Range, mm. Calcd.	Ion pairs/α $\times 10^{-5}$	Average energy utilization, e.v./ion pair	$\sum_i n_i Z_i^{2/3}$	$k_1 \times 10^{27}$, mm. $\times$ (sec./cm.)^3	$\delta \times 10^{28}$ mm. $\times$ (sec./cm.)^3
A	6.91	30.0	30.6	1.73	27.5	6.87	9.64	6.623
N_2	5.26	27.8	28.7	1.32	36.0	7.32	8.93	6.537
F_2	5.52	24.9	24.3	1.38	34.4	8.66	8.00	6.928
$CHClF_2$	6.85	11.4	10.7	1.71	27.8	19.57	3.66	7.163
CF_4	5.74	10.6	10.2	1.44	33.0	20.62	3.41	7.031
$CClF_3$	5.92	9.2	9.2	1.48	32.1	22.90	2.96	6.778
CCl_2F_2	6.70	8.1	8.4	1.68	27.9	25.18	2.60	6.547
CCl_3F	7.22	7.5	7.7	1.81	26.2	27.46	2.41	6.618
CCl_4	7.60	6.7	7.1	1.90	25.0	29.74	2.15	6.394
C_2ClF_5	6.05	6.0	6.0	1.51	31.5	34.86	1.93	6.728
$C_2Cl_3F_3$	6.80	5.3	5.3	1.70	27.9	39.42	1.70	6.701
C_4F_8O	5.82	4.1	4.0	1.46	32.5	51.84	1.32	6.843
C_4F_{10}	6.22	3.8	3.7	1.56	30.4	56.50	1.22	6.893
							Average value	6.753
							95% confidence limits of average	6.753 ± 0.131
							95% confidence limits single value	6.753 ± 0.471

or

$$R = \delta V_0^3 / \sum_i n_i Z_i^{2/3} \qquad (6)$$

where Z_i is the atomic number of an atom of type i in the molecule, n_i is the number of such atoms present and δ is an empirical constant. Combining equations (3) and (6), the value of δ may be determined.

$$\delta = k_1 \sum_i n_i Z_i^{2/3} \qquad (7)$$

Measured values of the range are listed in Table I. Dividing these values by V_0^3, $(1.46 \times 10^9$ cm./sec.$)^3$, for the U-234 α-particle, the value of k_1 is obtained as shown in equation (3); δ is then obtained in each individual measurement by equation (7). It is apparent that the values for δ vary over only a small range for all the gases listed in Table I. On the basis of this constancy of δ the average has been used to obtain, by means of equation (6), "calculated" values of the range of a U-234 α-particle in each gas. These calculated ranges are listed in Table I for comparison with the measured values.

Evaluation of the ionization in terms of total number of ion pairs produced has been made by the use of Bragg's values[4] of ionization, *i.e.*, the total number of ion pairs from a RaC′ α-particle in air, 2.37×10^5, and the ratio of the number of ions produced in nitrogen to the number of ions produced in air, 0.96. Thus, with a RaC′ α-particle traveling at an initial velocity of 1.92×10^9 cm./sec., 2.275×10^5 ion pairs are produced in nitrogen.

From equation (4) it is possible to calculate the number of ion pairs produced in nitrogen using U-234 α-particles with an initial velocity of 1.46×10^9 cm./sec.

$$2.275 \times 10^5 = k_2 \times (1.92 \times 10^9)^2$$
$$k_2 = 6.17 \times 10^{-14}$$
$$I = 6.17 \times 10^{-14} \times (1.46 \times 10^9)^2$$
$$= 1.315 \times 10^5 \text{ ion pairs}/\alpha\text{-particle}$$

From Table I it may be seen that for nitrogen ionization, 5.26 units represent 1.315×10^5 ion pairs, or 1 unit represents 2.50×10^4 ion pairs. Since the scale units are proportional to the number of ion pairs, multiplying the former by the factor 2.50×10^4 yields the total number of ion pairs produced by a U-234 α-particle. Ion pairs per α-particle calculated by this method are shown in Table I.

Ionization energies, calculated by dividing the energy of the α-particle by the number of ion pairs, are shown in Table I. A comparison of these values with ionization potentials of the fluorocarbons would allow an estimation of the fraction of the total α-particle energy that is used in molecular ionization. At the present time ionization potentials have not been determined for fluorocarbons.

Acknowledgments.—The authors wish to express their gratitude to Mr. M. J. Bartkus and Mr. J. H. Lykins of the Laboratory Division for their help in designing and constructing the ionization chamber and current amplifier, and to Drs. S. C. Lind and H. A. Bernhardt for their helpful comments.

SOME PHYSICAL PROPERTIES OF DIACETONE ALCOHOL, MESITYL OXIDE AND METHYL ISOBUTYL KETONE

BY E. T. J. FUGE, S. T. BOWDEN AND W. J. JONES

Department of Chemistry, University College, Cardiff, Wales

Received March 20, 1952

The density, refractive index, vapor pressure and surface tension of diacetone alcohol, mesityl oxide and methyl isobutyl ketone have been measured at various temperatures. Good agreement is found between the experimental values of the molecular refractions, lyoparachors and parachors of the substances and those calculated by the summation of standard atomic and bond constants. The solubility of some of the halides of the alkali and alkaline earth metals has been determined at various temperatures, and the composition of the addition compounds has been ascertained.

Introduction

The present work was undertaken because little is known of the physical properties of the structurally related substances, diacetone alcohol, mesityl oxide, methyl isobutyl ketone, no measurements of the solubilities of salts in these media are recorded, and the only salt solvates described are those of mesityl oxide with platinous chloride, $PtCl_2 \cdot (CH_3)_2C{=}CHCOCH_3$,[1] and with mercuric chloride, $HgCl_2 \cdot (CH_3)_2C{=}CHCOCH_3$.[2]

Standardizations and Controls

The barometer and the thermometers employed in the work had been tested at the National Physical Laboratory, Teddington, the weights were calibrated by the method of Richards,[3] and the volumetric vessels by weighing empty and filled with distilled water. All readings were corrected for known errors. Before the substances were examined by their means, the pycnometer, refractometer, isoteniscope, and apparatus for measuring surface tension were tested with specially purified standard liquids to ensure that they were giving correct and accurate values. The thermostat used in the measurements of density, surface tension and solubility was a bath filled either with water, or, for those above 70°, with castor oil, provided with a motor-driven stirrer and maintained constantly within 0.02° at each temperature by means of a mercury–toluene regulator in circuit with a hot wire vacuum switch relay.

Purification of Substances

Diacetone Alcohol.—The purest obtainable substance was three times fractionally distilled under low pressure. The purified liquid had boiling point, b.p. 61.7° (13 mm.), density at 20°, d^{20}_4 0.9387. Bauer[4] gives b.p. 63–64° (11 mm.).

Mesityl Oxide and Methyl Isobutyl Ketone.—The best commercial products were fractionally distilled several times through a Young column. The purified mesityl oxide had b.p. 129.9° (760 mm.), d^{20}_4 0.8584, $n^{25}D$ 1.4414, and the methyl isobutyl ketone b.p. 116.2° (760 mm.), d^{20}_4 0.8007 and $n^{25}D$ 1.3943. For the former compound Lecat[5] gives b.p. 129.4° (760 mm.), Brühl[6] d^{20}_4 0.8578 and $n^{20}D$ 1.4440, while for the latter Timmermans[7] gives b.p. 116.9° (760 mm.), Varon[8] d^{20}_4 0.801 and $n^{20}D$ 1.396, and Vogel[9] d^{20}_4 0.7978 and $n^{20}D$ 1.39562.

Benzene and Water.—These were used as standard liquids for testing the experimental methods adopted. High quality benzene was purified further by repeated partial freezing and removal of the liquid phase until the freezing point reached 5.5°, after which it was dried with calcium chloride and distilled from sodium wire: it had b.p. 80.2° (760 mm.), d^{20}_4 0.8788, which are almost identical with the values recorded by Young.[10] Water was purified in accordance with the standard procedure with special precautions to ensure the removal of traces of grease and dissolved air.

Density

The densities of mesityl oxide and methyl isobutyl ketone were determined between 20° and the boiling point, but those of diacetone alcohol only up to 120°, because above 130° they were found to decrease with rise of temperature at an accelerated rate, an effect attributable to the thermal instability of that substance, which became evident also in the measurements of its vapor pressure. A glass dilatometer was employed for the density determinations, and correction was made for the thermal expansion of the glass.

The densities determined experimentally are given in grams per cm.^{3} under the heading d in Table I for the corresponding temperature t°, C.

TABLE I

DENSITIES AT VARIOUS TEMPERATURES

Temperature	Diacetone alcohol		Mesityl oxide		Methyl isobutyl ketone	
t°, C.	d	$d_{calcd.}$	d	$d_{calcd.}$	d	$d_{calcd.}$
20.0	0.9387	0.9386	0.8584	0.8582	0.8007	0.8008
40.0	.9207	.9206	.8390	.8390	.7823	.7823
60.0	.9019	.9023	.8194	.8196	.7642	.7636
80.0	.8834	.8838	.7997	.7999	.7442	.7445
100.0	.8652	.8649	.7801	.7801	.7249	.7251
120.0	.8460	.8457	.7602	.7600	..	..

The variation of density with temperature is represented by the equations

Diacetone alcohol

$$d = 0.9562 - 0.000875t - 0.00000038t^2$$

Mesityl oxide

$$d = 0.8772 - 0.000943t - 0.00000028t^2$$

Methyl isobutyl ketone

$$d = 0.8189 - 0.000900t - 0.00000038t^2$$

Densities so calculated are given in Table I under the heading $d_{calcd.}$

Refractive Index

The refractive index of each liquid for the D light of sodium was determined by means of an Abbe refractometer. The temperature of the prisms was maintained at 25.0° by the passage of water from a flask provided with an electric immersion heater in series with a sliding resistance. The accuracy of the refractometer was tested by the use of specimens of water and benzene of known refractive index. In Table II the values of the refractive indices obtained experimentally are given in the first line, and those of the Lorenz–Lorentz molecular refractions, $(n^2 - 1)M/(n^2 + 2)d$ derived from them, the molecular weights M, and the densities d, at 25° given by the equations of the last section are entered in the second line, as R_L found by the authors. The molecular refraction of mesityl oxide derived from the data of Brühl, already quoted in the third section of this paper, and that of methyl isobutyl ketone from the data of Varon, also that found by Vogel, are given in the third line, as R_L found by others, while the molecular refractions calculated by using Eisenlohr's atomic and bond refractions[11] for the keto and enol forms of the substances are given in the last two lines of Table II.

(1) Prandtl and Hofmann, *Ber.*, **33**, 2982 (1900).
(2) Erdmann, *ibid.*, **37**, 4571 (1904).
(3) Richards, *J. Am. Chem. Soc.*, **22**, 144 (1900).
(4) Bauer, *Compt. rend.*, **154**, 1093 (1912).
(5) Lecat, *Ann. Soc. sci. Bruxelles*, **47**, I, 25 (1927).
(6) Brühl, *Ann.*, **235**, 7 (1886).
(7) Timmermans, *Bull. soc. chim. Belg.*, **25**, 300 (1911).
(8) Varon, *Compt. rend.*, **155**, 287 (1912).
(9) Vogel, *J. Chem. Soc.*, **171** (1940); 611 (1948).
(10) Young, *Proc. Roy. Soc. Dublin*, **12**, 431 (1910).
(11) Eisenlohr, *Z. physik. Chem.*, **75**, 585 (1910); **79**, 129 (1912).

TABLE II

REFRACTIVE INDICES AT 25° AND MOLECULAR REFRACTIONS FOR D LIGHT

Property	Diacetone alcohol	Mesityl oxide	Methyl isobutyl ketone
$n^{25}D$	1.4219	1.4414	1.3943
R_L found by the authors	31.58	30.37	30.09
R_L found by others	...	30.37	30.03, 30.15
R_L calcd. for keto form	31.56	29.45	29.92
R_L calcd. for enol form	32.73	30.62	31.08

These substances are of complex structure, being tautomeric, while mesityl oxide has two conjugated double bonds, giving optical exaltation, and diacetone alcohol has been shown by Badger and Bauer[12] to consist partly of molecules containing internal hydrogen bonds.

Vapor Pressure

The isoteniscope described by Smith and Menzies[13] was employed for the determination of the vapor pressures of the liquids. The heating bath consisted of a 5-liter beaker charged with castor oil and controlled at the required temperature by means of a micro bunsen burner, the bath being vigorously agitated by means of a motor-driven stirrer with a slightly bent rod which set up the vibration necessary to agitate the surface of the liquid inside the isoteniscope. The vapor pressure of the liquid was given by the difference in level between the mercury columns in the limbs of the manometer connected to the isoteniscope. After satisfactory checks had been obtained, the temperature of the bath was raised by about 10°, and another set of readings taken. In this way vapor pressure measurements were made between room temperature and the boiling point of the liquid under investigation. To prevent prolonged heating, when the substance was thermally unstable, the isoteniscope was placed in the bath only when conditions had become stabilized. The readings are given in Table III in which $t°$, C. represents the temperature and p the vapor pressure of the liquid in mm.

A plot of log p against $1/(273.1 + t)$ for diacetone alcohol showed, when t exceeded 130°, a sharp divergence from the curve for lower temperatures, with more rapid increase of pressure with rising temperature, thus revealing the incipience of the thermal decomposition of diacetone alcohol into mesityl oxide and water during the course of the measurement, a reaction already shown by Koelichen[14] to occur at 164°

$$(CH_3)_2C(OH)CH_2COCH_3 = (CH_3)_2C{=}CHCOCH_3 + H_2O$$

TABLE III

VAPOR PRESSURES AT VARIOUS TEMPERATURES

Diacetone alcohol			Mesityl oxide			Methyl isobutyl ketone		
$t°$, C.	p	$p_{calcd.}$	$t°$, C.	p	p_{calcd}	$t°$, C.	p	p_{calcd}
28.1	2.2	2.1	14.0	5.7	5.7	21.7	16.5	16.2
41.4	4.5	4.6	23.2	10.0	10.0	32.7	29.5	29.7
51.2	7.9	7.9	31.8	16.0	16.2	41.5	47.0	46.6
61.7	13.0	13.8	44.0	30.2	30.8	50.2	69.5	70.2
71.9	22.5	22.8	56.5	55.5	55.9	60.8	112.5	112.1
81.7	35.7	36.1	65.8	84.5	84.3	70.0	162.0	163.1
91.1	55.5	54.7	79.6	145.5	148.3	80.1	240.0	239.4
102.0	86.0	86.3	94.5	257.5	254.6	90.9	348.0	349.7
114.7	145.0	142.6	103.1	344.0	339.9	116.2	760.0	764.8
...	...	...	129.9	760.0	760.8	...	...	...

The variation of vapor pressure with temperature is represented by the equations

Diacetone alcohol up to 115°

$$\log_{10} p = 8.5552 - 2482.93/(273.1 + t)$$

Mesityl oxide

$$\log_{10} p = 28.7503 - 6.9350 \log_{10} (273.1 + t) - 3144.43/(273.1 + t)$$

Methyl isobutyl ketone

$$\log_{10} p = 31.1616 - 7.7701 \log_{10} (273.1 + t) - 3173.11/(273.1 + t)$$

Values of p calculated from these equations are listed under $p_{calcd.}$ in Table III.

Latent Heat of Vaporization

The latent heats were calculated from the variation of vapor pressure with temperature by means of the Clapeyron–Clausius equation, the latent heat, l, in calories per gram at an absolute temperature T being given by $(CRT - BR \log_e 10)/M$, where M denotes the molecular weight, R the gas constant, and B and C the constants in the vapor pressure equation

$$\log_{10} p = A + B/T + C \log_{10} T$$

of the form given in the preceding section. The latent heat thus calculated for diacetone alcohol between 30 and 110° was 97.8 cal. per g., for mesityl oxide 105.4 at 20° and 90.0 at its boiling point, and for methyl isobutyl ketone 99.8 cal. at 20° and 84.9 at its boiling point.

Table IV gives the result of testing both the constancy, with variation of temperature between 20° and the boiling point of the normal lyoparachor, $[L]$, defined by the equation

$$\frac{Ml^{1/4}}{D - d} = [L]$$

and its additivity[15]; in this expression D and d denote the densities of the liquid and its saturated vapor, respectively, at the temperature for which the value of l is given, while the additive atomic and bond constants are C, −1193.6; H, 844.8; O in ketone, 2092.1; a double bond between two carbon atoms in a chain 1470, and a branch in a carbon chain, −132.7. The expression holds true only for substances that are not molecularly associated, and that have their boiling points between −100 and 200°. Since it is not applicable to alcohols, the data for diacetone alcohol are not included in Table IV.

TABLE IV

LYOPARACHORS AND MOLAR ENTROPIES OF VAPORIZATION

Property	Mesityl oxide	Methyl isobutyl ketone
M	98.14	100.16
D at boiling point	0.7500	0.7092
d at boiling point	0.0030	0.0031
l at boiling point	90.0	84.9
$[L]$ at boiling point	4810	4950
D at 20°	0.8584	0.8007
d at 20°	0.0000	0.0001
l at 20°	105.4	99.8
$[L]$ at 20°	4750	4970
$[L]$ calculated from constants	4720	4940
Molar entropy of vaporization, Ml_b/T_b	21.9	21.8

Surface Tension

The surface tension of the freshly distilled liquids was measured at 20° using the modification of Sugden's maximum bubble pressure apparatus described by Bowden and Butler.[16] The apparatus was calibrated by means of benzene of known surface tension, and thermostatic control of the bath to 0.02° was obtained by a mercury–toluene regulator in conjunction with a vacuum switch to operate the electric heater. The values of the surface tensions are given in the first line of Table V, the parachors, $[P] = M\gamma^{1/4}/(D - d)$, derived from them in the third line, the value of the parachor of mesityl oxide given by Doeuvre[17] and of that of methyl isobutyl ketone by Vogel[9] in the fourth line, while in the last line are entered the values calculated from the following atomic and bond constants based on the work of Sugden[18]: C, 4.8; H, 17.1; O, 20.0; double bond, 23.2; OH group correction, −5.0.

(12) Badger and Bauer, *J. Chem. Phys.*, 5, 839 (1937).

(13) Smith and Menzies, *J. Am. Chem. Soc.*, 32, 1412 (1910).

(14) Koelichen, *Z. physik. Chem.*, 33, 136 (1900).

(15) Bowden and Jones, *Phil. Mag.*, [7] 37, 485 (1946); 39, 155 (1948).

(16) Bowden and Butler, *J. Chem. Soc.*, 75 (1939).

(17) Doeuvre, *Bull. soc. chim.*, [4] 39, 1594 (1926).

(18) Sugden, *J. Chem. Soc.*, 125, 27, 1177 (1924). "The Parachor and Valency," Routledge, London, 1930. "Thorpe's Dictionary of Chemistry," Vol. 9, Longmans, London, 1949, p. 225.

TABLE V

SURFACE TENSIONS AND PARACHORS

Property	Diacetone alcohol	Mesityl oxide	Methyl isobutyl ketone
γ at 20°	31.0	28.4	23.9
$(D - d)$ at 20°	0.9387	0.8584	0.8006
$[P]$	292.0	263.9	276.6
$[P]$ found by others	...	261.7	276.5
$[P]$ calcd. for keto form	292.4	266.2	273.8

In view of the presence of the hydroxyl group, diacetone alcohol might be expected to exhibit association in the liquid state but, in this connection, Badger and Bauer[12] have found that while the substance may consist extensively of molecules containing internal hydrogen bonds, there is no evidence of hydrogen bonding between the separate molecules. From the present work it is evident that there is a close correspondence between the observed parachor and the theoretical value calculated from the atomic and bond constants, but it is not possible to decide unambiguously whether this agreement arises from the balancing of a finite negative anomaly by a positive contribution due to intramolecular hydrogen bonding or from the circumstance that each of these factors is negligible. The value of the surface tension of mesityl oxide is found to be slightly higher than that obtained by Doeuvre,[17] and since the corresponding parachor is closer to the theoretical value, it may be concluded that the system of conjugate double linkages in mesityl oxide does not materially affect the parachor. The parachor of methyl isobutyl ketone has been determined by Vogel,[9] and on the basis of his most recent values for the group constants is computed to be 276.0, which is close to the value obtained in the present work.

Solubility of Salts and Composition of Solid Phases

A survey was made of the solubility of the halides of the alkali and alkaline earth metals in these organic liquids, and the compositions of the addition compounds formed by certain of these salts with the solvents were ascertained.

Drying of Salts.—Several of the salts were extremely hygroscopic, and precautions for the rigorous exclusion of extraneous moisture were taken in the desiccation of the salts and in the solubility determinations. The salts were of high analytical quality, and were dried by heating and shaking the powdered material at 120–130° (15 mm.) for 4–8 hours in a round bottomed flask (provided with a 3-way stopcock) until analysis showed that the removal of water was complete. When the original substance was a hydrate with a transition temperature below 130°, the material was maintained at a temperature about 5° below the transition point for 4 hours before the normal drying procedure was applied. This method served to prevent caking of the solid during the dehydration process.

Solubility Determinations.—Each system was examined in duplicate so that the equilibrium between salt and solution could be established by approaching the bath temperature from above and below the temperature at which the solubility was to be determined. The salt/liquid systems were mechanically agitated in 150-ml. glass-stoppered bottles (protected by plastic caps) in an electrically heated thermostat whose temperature was controlled by a bimetallic thermoregulator. It was found in most cases that equilibration between the solid and liquid phase was established after agitating the system for 2 hours and allowing it to stand in the thermostat for 3 hours to allow for complete settling of the solid phase. Samples of the clear solution were drawn into a glass tube fitted with a small filter cap, the whole being preheated to the bath temperature before insertion into the solution. With several systems the filtration was very slow owing to the high viscosity of the solution. A portion of the filtered solution was weighed and analysed for halide by Volhard's method.

Samples of the solid phase in contact with the solution at the temperature of the experiment were also removed, quickly dried between filter papers, and analyzed in the same way.

Results.—In Table VI and in the following equations the solubility, s, represents the weight of anhydrous salt dissolved at $t°$, in one gram of solvent in the presence of the solid phase indicated. The solubility at these temperatures calculated from the following equations are listed under the heading $s_{calcd.}$

In diacetone alcohol

For lithium chloride,

$$s = 0.06683 - 0.000395t + 0.00001636t^2$$

For lithium bromide,

$$s = 0.11286 - 0.001239t + 0.00006130t^2$$

For calcium bromide,

$$s = 0.03703 - 0.001188t + 0.00004128t^2$$

For strontium bromide,

$$s = 0.05507 - 0.000991t + 0.00007305t^2$$

In mesityl oxide

For lithium bromide,

$$s = 0.31950 + 0.000560t + 0.00002347t^2$$

For strontium iodide,

$$s = 0.43324 - 0.006139t + 0.00013150t^2$$

In methyl isobutyl ketone

For calcium bromide,

$$s = 0.13002 - 0.000717t + 0.00004639t^2$$

For strontium iodide,

$$s = 0.54750 + 0.000505t + 0.00000912t^2$$

TABLE VI

SOLUBILITIES AND SOLID PHASES

t, °C.	s	$s_{calcd.}$	t, °C.	s	$s_{calcd.}$
Lithium chloride in diacetone alcohol: solid phase $LiCl, (CH_3)_2C(OH)CH_2COCH_3$			Lithium bromide in diacetone alcohol: solid phase $LiBr\ 2(CH_3)_2C(OH)CH_2COCH_3$		
20.0	0.0655	0.0655	20.0	0.1126	0.1126
35.0	.0732	.0730	35.0	.1452	.1446
50.0	.0879	.0879	50.0	.2039	.2042
65.0	.1103	.1103	65.0	.2916	.2914
Calcium bromide in diacetone alcohol: solid phase $CaBr_2, 4(CH_3)_2C(OH)CH_2COCH_3$			Strontium bromide in diacetone alcohol: solid phase $SrBr_2, 4(CH_3)_2C(OH)CH_2COCH_3$		
20.0	0.0290	0.0298	20.0	0.0647	0.0645
35.0	.0484	.0460	35.0	.1092	.1098
50.0	.0784	.0808	50.0	.1888	.1881
65.0	.1350	.1342	65.0	.2990	.2992
Lithium bromide in mesityl oxide: solid phase $LiBr, (CH_3)_2C{=}CHCOCH_3$			Strontium iodide in mesityl oxide: solid phase $SrI_2, 4(CH_3)_2C{=}CHCOCH_3$		
20.0	0.3401	0.3401	20.0	0.3618	0.3631
35.0	.3677	.3684	35.0	.3832	.3795
50.0	.4063	.4062	50.0	.4514	.4550
65.0	.4550	.4551	65.0	.5910	.5898
Calcium bromide in methyl isobutyl ketone: solid phase $CaBr_2, 2(CH_3)_2CHCH_2COCH_3$			Strontium iodide in methyl isobutyl ketone: solid phase $SrI_2, 2(CH_3)_2CHCH_2COCH_3$		
20.0	0.1334	0.1342	20.0	0.5610	0.5612
35.0	.1642	.1617	35.0	.5771	.5763
50.0	.2077	.2101	50.0	.5948	.5955
65.0	.2802	.2794	65.0	.6191	.6189

Sodium chloride, potassium chloride and strontium chloride are sparingly soluble, while barium chloride is practically insoluble in diacetone alcohol over the temperature range examined. Iodides

catalyze the decomposition of diacetone alcohol into mesityl oxide and water. In mesityl oxide calcium bromide is very sparingly soluble (s being of the order of 0.0001 at 65°) but the salt swells, with liberation of heat and formation of needle-shaped crystals of the addition compound, $CaBr_2$, $3(CH_3)_2C{=}CHCOCH_3$. Strontium bromide behaves similarly and forms the compound $SrBr_2$, $2(CH_3)_2C{=}CHCOCH_3$. The bromides of sodium, potassium and barium are practically insoluble in mesityl oxide. The chlorides of lithium, sodium and potassium are very sparingly soluble in methyl isobutyl ketone, while those of calcium and barium are practically insoluble.

BINARY FREEZING-POINT DIAGRAMS FOR ACETAMIDE WITH OLEIC AND ELAIDIC ACIDS

BY ROBERT R. MOD AND EVALD L. SKAU

Southern Regional Research Laboratory,[1] *New Orleans, Louisiana*

Received March 24, 1952

Complete binary freezing-point data have been obtained for the stable and unstable forms of acetamide with elaidic acid and with the stable and unstable forms of oleic acid. The freezing-point diagrams show conclusively that acetamide forms a molecular compound with both elaidic (*trans*) and oleic (*cis*) acid. Each of these compounds exhibits two incongruent melting points, the one stable and the other metastable. It can also be concluded from the diagrams that the oleic acid compound tends to dissociate to a lesser degree than the elaidic acid compound.

It has recently been demonstrated by means of binary freezing-point determinations that acetamide forms molecular compounds with various long-chain saturated fatty acids.[2] The present report shows that acetamide forms similar compounds with oleic and elaidic acids, *i.e.*, with both the *cis* and the *trans* forms of $\Delta^{9,10}$-octadecenoic acid.

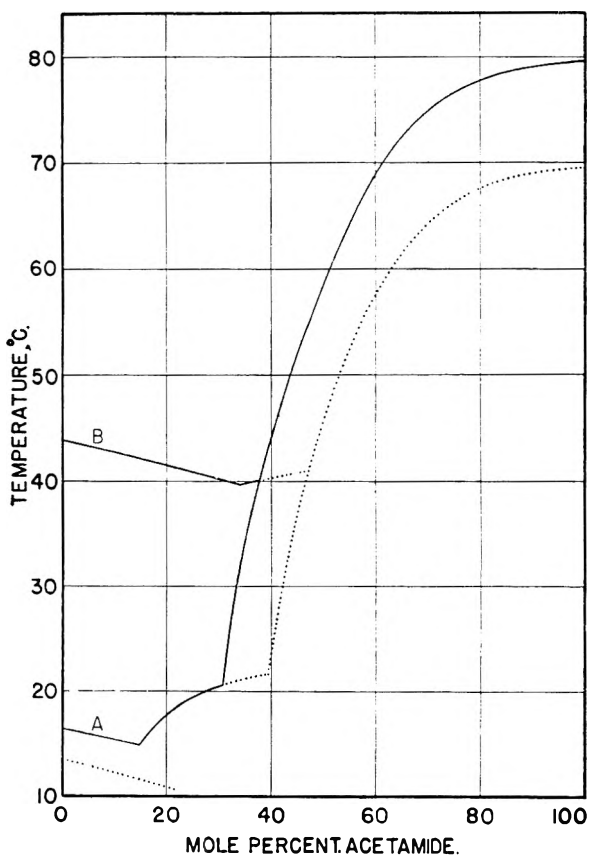

Fig. 1.—Binary freezing-point diagrams for acetamide with: A, oleic acid; B, elaidic acid. Dotted curves represent metastable equilibria.

Experimental

Binary freezing-point data were obtained for acetamide with oleic and with elaidic acid. The oleic acid was purified by vacuum fractional distillation of its methyl ester followed by fractional low-temperature crystallization of the acid from acetone, f.p. of stable form 16.3°, f.p. of unstable form 13.5°. The elaidic acid was obtained by elaidinization of oleic acid followed by fractional crystallization from acetone, f.p. 43.8°. The acetamide was the best grade of Eastman Kodak product.[3] All sample material was dried in vacuum over phosphorus pentoxide. The freezing points were determined by the sealed tube (static) method previously described,[2] which gives the true equilibrium temperature between the crystals and the liquid mixture of the given composition, with an accuracy of ±0.2° after correction for thermometer calibration and emergent stem.

Results and Discussion

The data obtained are given in Table I and are plotted in Fig. 1. As can be seen from the diagram it was possible to obtain the freezing-point curves for both the stable (solid curves) and the unstable (dotted curves) forms of acetamide and also of oleic acid. It is apparent that both oleic and elaidic acids form a crystalline molecular compound with acetamide and that each of these molecular compounds exhibits two incongruent melting points, the one stable and the other metastable.

For the acetamide side of the diagram the stable or unstable forms could be obtained at will by proper manipulation of the temperature. The higher freezing point was always obtained on the initial melting of the samples, as would be expected since they contained the stable modification. After the samples had been heated some degrees above this temperature, however, the freezing points invariably fell on the lower (dotted) curves and in order to obtain the higher freezing point again it was necessary to shock-chill the molten sample to −78° in in a Dry Ice–alcohol mixture. Subsequent heating of the solid resulted in momentary local melting

(1) One of the laboratories of the Bureau of Agricultural and Industrial Chemistry, Agricultural Research Administration, U. S. Department of Agriculture. Article not copyrighted.

(2) F. C. Magne and E. L. Skau, *J. Am. Chem. Soc.*, **74**, 2628 (1952).

(3) The mention of names of firms or trade products does not imply that they are endorsed or recommended by the Department of Agriculture over other firms or similar products not mentioned.

near the surface followed by rapid transformation to the higher melting form.

TABLE I

BINARY FREEZING-POINT DATA[a]

Acetamide–oleic acid system			Acetamide–elaidic acid system		
	Freezing point, °C			Freezing point, °C	
Mole % acetamide	Stable	Meta-stable	Mole % acetamide	Stable	Meta-stable
0.00	16.3	13.5	0.00	43.8	
4.42	15.9		10.31	42.5	
9.37		12.2	19.47	41.5	
12.60	15.1		29.87	40.2	
(15.0)[b]	(14.8)[b]		(34.2)[b]	(39.6)[b]	
17.20	16.3	11.4	36.01	39.9	
21.54	18.4	10.7	(37.8)[c]	(40.0)[c]	
21.75	18.3		40.08	45.1	40.3
24.65	19.1		44.96	51.6	40.7
30.55	20.5		46.08	53.6	40.8
(30.8)[c]	(20.6)[c]		(47.2)[d]		(40.9)[d]
34.14	31.6	20.7	50.59	59.9	47.1
36.73	37.7	21.3	60.26	69.7	58.4
(39.2)[d]		(21.6	70.21	75.1	64.6
39.34	42.3	21.8	79.75	78.1	67.9
44.40		35.6)[d]	90.06	79.4	69.0
48.54	56.0	43.0	100.00	79.7	69.5
70.61	75.2	64.3			
82.17	78.0	67.8			
100.00	79.7	69.5			

[a] The values in parentheses were obtained by graphical extrapolation. [b] Eutectic. [c] Incongruent melting point (stable). [d] Incongruent melting point (metastable).

In contrast, the unstable (low-melting) form of oleic acid tended to transform to the stable form much more readily. On cooling the mixtures rich in oleic acid to about 8 to 10° the samples suddenly became essentially solid; and, on heating in the constant temperature bath, melted so that relatively few crystals remained at the temperatures indicated by the dotted line. At this stage, or sometimes before, the sample again became essentially solid because of the formation of the higher-melting crystalline modification of oleic acid, or of the molecular compound when the acetamide concentration was between 15 and 22 mole %. The sample then showed a melting point corresponding to the upper solid curve. Because of this behavior the freezing points involving the unstable modification of oleic acid could not be obtained with the same assured accuracy.

The acetamide branches of the diagrams for these two *cis–trans* isomeric acids almost coincide. It will be noted, however, that the freezing points for the elaidic acid system tend to fall above the curves as drawn and those for the oleic acid fall below. This is in harmony with the idea that the molecular compound between acetamide and oleic acid is less dissociated than that between acetamide and elaidic acid, which is indicated by the fact that the freezing-point curve for the oleic acid compound is steeper.

THE THEORY OF MEMBRANE POTENTIAL

BY MITSURU NAGASAWA[1] AND YONOSUKE KOBATAKE

Tokyo Institute of Technology, Okayama, Meguro, Tokyo, Japan

Received March 27, 1952

The membrane potentials of organic membranes and glass membranes were discussed on the basis of Eyring's theory of rate processes. It was assumed that these membranes have the rigid mosaic structure and the two ions should permeate with equal velocity through the pore of the membrane. The ionic concentration in the membrane was computed by the Poisson–Boltzmann equation. The experimental data of some investigators and of the present authors were found to be in good agreement with the theory. Asymmetric potential of the glass electrode was explained by assuming it to be caused by the difference of the diffusion of ions of one side of the membrane from that of the other side at the stationary state.

1. Introduction

Various membranes, *i.e.*, collodion, cellophane, parchment paper, glass membrane, etc., have rigid structure due to the strong interaction between their segments, therefore the permeation of electrolyte across the membrane should be considered to be carried out by the diffusion in the pore of the membrane as in the case of gas permeation.[2] The well-known theories of Meyer and Sievers,[3] and Teorell[4] on the membrane potential have been widely criticized on account of their negligence of this rigid structure.[5,6] Moreover, these theories have much to be examined in many other respects, namely, first, according to the classical electrostatistics[7] the occurrence of reversible electrode potentials in general should not be accompanied by any electric current, passing through the boundary layer, and therefore the total number of anions and cations permeating across the membrane should be equal. This is not, however, to be expected from their theories. Second, Meyer and Sievers' selectivity constant should vary from one salt to another because of the mosaic structure of the membrane. The mechanical restraint on the ions by the pores of the membrane should not affect the mobilities of ions in the membrane, but should determine the number of ions in the membrane. The mobilities of ions may chiefly be determined by the viscosity of solvent and secondarily affected by the ionic atmosphere. The viscosity of water in the pore of a membrane is equal to that of the external solution, and it is also well known that the

(1) Department of Applied Chemistry, Faculty of Engineering, Nagoya University, Chigusaku, Nagoya, Japan.

(2) P. Doty, *J. Chem. Phys.*, **14**, 244 (1946).

(3) K. H. Meyer and J. F. Sievers, *Helv. Chim. Acta*, **19**, 649, 665, 987 (1936); H. Mark and K. H. Meyer, *Hochpolymer Chemie Bd.* **2**, (1940).

(4) T. Teorell, *Proc. Soc. Exp. Biol.*, **33**, 282 (1935)

(5) E. S. Fetcher, THIS JOURNAL, **46**, 570 (1942).

(6) K. Sollner, *ibid.*, **49**, 47, 171, 265 (1945).

(7) S. Glasstone, K. J. Laidler and H. Eyring, "The Theory of Rate Process," John Wiley and Sons, Inc., New York, N. Y., 1941.

mobilities of ions may be unaffected by the charged wall if the concentration of electrolyte is considerably high. Therefore, it seems reasonable to assume that the mobilities of ions in the pore are equal to those in the external solution as the first approximation.

In the case of the glass membrane this membrane potential has not fully been explained even on the qualitative aspect, and moreover most of previous hypotheses cannot be said to be fully confirmed experimentally. Accordingly, there are many arguments as to the mechanism of the glass electrode. Now, as the electric conduction of the glass is carried out by ion and not by electron and the glass should be considered to have most compact mosaic structure, it seems reasonable to assume that the glass electrode is one of the most compact membrane electrodes, its potential difference is a diffusion potential, and only the hydrogen ion can enter into pores of the glass and hence the membrane potential for the glass membrane is reversible only against H^+ because of the smallest dimension of H^+ of all ions.

It is the purpose of this report to consistently discuss various membrane potentials from the scope of diffusion potential, assuming that the membranes are of the porous mosaic structure and the rate-determining step of the ionic permeation across the membrane is the diffusion in the membrane.

2. The Fundamental Equation of Membrane Potential

The number of permeating ions in unit time is equal to the number of ions in the membrane multiplied by the frequency of crossing the membrane and hence given by[7]

$$\text{rate of permeation} = KN\bar{C}^{\pm}\frac{\nu}{\delta} = KN\bar{C}^{\pm}\frac{l}{\delta}\frac{kT}{\epsilon} \quad (1)$$

where $\bar{C}^{\pm}$ is the average ionic concentration, ν the mean velocity of ions diffusing, l the mean mobility of ions, in the membrane, δ the effective length of pores in the membrane, k the Boltzmann constant, N the Avogadro number and T is the absolute temperature. In general, the rate of permeation is proportional to the number of ions. However, in the case of a charged membrane there is no such proportionality, due to the interaction between the membrane and ions, and therefore the permeation constant becomes a function of the ionic concentration. Assuming the rate of permeation to be the quasi first-order, it may be written in terms of the permeation coefficient

$$\text{rate of permeation} = KPNC \quad (2)$$

Equating (1) and (2) gives

$$P = \frac{\bar{C}^{\pm}lkT}{C\delta\epsilon} \quad (3)$$

Suppose an electric field is now applied, so that there is a potential gradient which facilitates the movement of the ion from left to right (Fig. 1), then the free energy changes are now indicated by the dotted curve. The free energy in the initial state may be regarded as being increased by an amount αw, where w is the work done in moving the ion from one side of membrane to the other and α is the fraction operative between the initial and activated states. Similarly, the free energy of initial state is diminished by $(1-\alpha)w$, as shown in Fig. 1. The number of ions crossing the membrane in the unit time in the forward direction, *i.e.*, in the direction of the applied field, is given by

$$\text{rate in forward direction} = KN\delta CPe^{\frac{\alpha w}{kT}} \quad (4)$$

Similarly

$$\text{rate in backward direction} = KN\delta\left(C+\delta\frac{dC}{dx}\right)Pe^{-\frac{(1-\alpha)w}{kT}} \quad (5)$$

Combination of eq. (4) and (5) then gives for the net rate of movement from left to right

$$\text{net rate} = KN\delta C\frac{\bar{C}^{\pm}}{C}\frac{l}{\delta}\frac{kT}{\epsilon}e^{\frac{\alpha w}{kT}} - KN\delta\left(C+\delta\frac{dC}{dx}\right)\frac{\bar{C}^{\pm}}{C}\frac{l}{\delta}\frac{kT}{\epsilon}e^{-\frac{(1-\alpha)w}{kT}} \quad (6)$$

Since $kT \gg w$ as a general rule

$$\text{net rate} = KN\delta C\frac{\bar{C}^{\pm}}{C}\frac{l}{\delta}\frac{kT}{\epsilon}\left(1+\frac{\alpha w}{kT}\right) - N\delta\left(C+\delta\frac{dC}{dx}\right)\frac{\bar{C}^{\pm}}{C}\frac{l}{\delta}\frac{kT}{\epsilon}\left[1-\frac{(1-\alpha)w}{kT}\right] \doteqdot KN\delta\bar{C}^{\pm}\frac{l}{\delta}\frac{kT}{\epsilon}\frac{w}{kT} - KN\delta l\frac{\bar{C}^{\pm}}{C}\frac{kT}{\epsilon}\frac{dC}{dx} \quad (7)$$

If the potential gradient of the electrical field is ϕ and the charge of the ion $z\epsilon$, w is given by

$$w = \delta\phi z\epsilon$$

Inserting this relation in eq. (7), we obtain

$$\text{net rate} = KN\delta z\bar{C}^{\pm}l\phi - KN\delta e\frac{kT}{\epsilon}\frac{\bar{C}^{\pm}}{C}\frac{dC}{dx} \quad (8)$$

Since at the stationary state the two ions must permeate with the same rate, we obtain

$$KNl_+z_+\delta\left(-\bar{C}_+^{\pm}\phi - \frac{RT}{z_+F}\frac{\bar{C}_+^{\pm}}{C_+}\frac{dC_+}{dx}\right) = KNl_-z_-\delta\left(\bar{C}_-^{\pm}\phi - \frac{RT}{z_-F}\frac{\bar{C}_-^{\pm}}{C_-}\frac{dC_-}{dx}\right) \quad (9)$$

where it is assumed that the field is applied to facilitate the movement of the negative ion. In the simplest case, *i.e.*, for a uni-univalent electrolyte

$$C_+ = C_- = C \qquad \frac{dC_+}{dx} = \frac{dC_-}{dx} = \frac{dC}{dx}$$

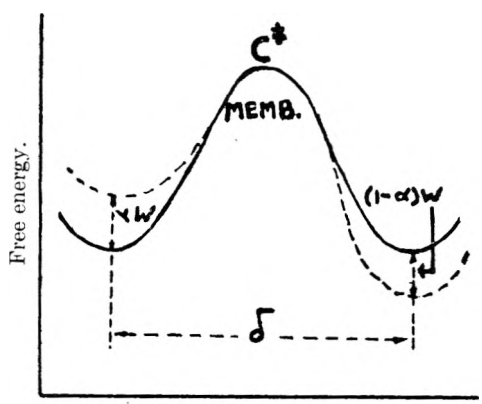

Direction of field→.

Fig. 1.

and hence

$$KNl_+\delta\left(-\bar{C}_+^{\pm}\phi - \frac{RT}{F}\frac{\bar{C}_+^{\pm}}{C}\frac{dC}{dx}\right) = KNl_+\delta\left(\bar{C}_-^{\pm}\phi - \frac{RT}{F}\frac{\bar{C}_-^{\pm}}{C}\frac{dC}{dx}\right)$$

Then the membrane potential E is given by

$$E = -\int_{C_2}^{C_1}\phi dx = \frac{RT}{F}\int_{C_2}^{C_1}\frac{l_+\bar{C}_+^{\pm} - l_-\bar{C}_-^{\pm}}{l_+\bar{C}_+^{\pm} + l_+\bar{C}_-^{\pm}}\frac{1}{\bar{C}}dC \tag{10}$$

As it is permissible to assume that ϕ should not exert influence on the ionic equilibrium distribution, the ionic concentration in the membrane can be calculated for a uni-univalent electrolyte under the following assumption.

Assumption. (1).—Membranes are porous and rigid, and pores are cylindrical. The distribution of pore diameter of the membrane is expressed by $f(r)$. (2) The charge distribution on the pore surface of the membrane is uniform and its charge density per unit area is given by $-N\epsilon A_0$. Therefore, A_0 is the concentration of fixed negative ions per unit area of the pore surface. (3) The concentration of electrolytes is dilute and the Debye–Hückel approximation is applicable.

The ionic concentration at a certain point in a pore with a radius r is given by the Boltzmann distribution, *i.e.*

$$C_+^{\pm} = Ce^{-\frac{\epsilon\psi}{kT}} \qquad C_-^{\pm} = ce^{\frac{\epsilon\psi}{kT}} \tag{11}$$

Now, ψ can be divided into two portions, *i.e.*, $\psi_0 + \psi_c$ where the potential ψ_0 due to the fixed charges on the pore surface must be independent on the coördinate in the pore and the ionic concentration and ψ_c arising from the movable ions is consequently dependent on them. Expanding $e^{\pm\epsilon\psi_c/kT}$ and retaining only the first two terms

$$C_+^{\pm} = Ce^{-\frac{\epsilon(\psi_0+\psi_c)}{kT}} = Ce^{-\frac{\epsilon\psi_0}{kT}}\left(1 - \frac{\epsilon\psi_c}{kT}\right)$$
$$C_-^{\pm} = Ce^{\frac{\epsilon(\psi_0+\psi_c)}{kT}} = Ce^{\frac{\epsilon\psi_0}{kT}}\left(1 + \frac{\epsilon\psi_c}{kT}\right) \tag{12}$$

The relation between ψ and the charge density q is given by the Poisson equation, which is

$$\nabla^2\psi = -\frac{4\pi}{D}q = -\frac{4\pi}{D}\epsilon(C_+^{\pm} - C_-^{\pm})$$

Therefore

$$\nabla^2(\psi_0 + \psi_c) = -\frac{4\pi\epsilon}{D}C\left[\left(e^{-\frac{\epsilon\psi_0}{kT}} - e^{\frac{\epsilon\psi_c}{kT}}\right) - \frac{\epsilon\psi_c}{kT}\left(e^{-\frac{\epsilon\psi_0}{kT}} + e^{\frac{\epsilon\psi_0}{kT}}\right)\right] \tag{13}$$

This expression is simplified by setting

$$\frac{4\pi\epsilon}{D}C\left(e^{-\frac{\epsilon\psi_0}{kT}} - e^{\frac{\epsilon\psi_0}{kT}}\right) = K_1^2$$
$$\frac{4\pi\epsilon^2}{kT}C\left(e^{-\frac{\epsilon\psi_0}{kT}} + e^{\frac{\epsilon\psi_0}{kT}}\right) = K_2^2 \tag{14}$$

eq. (13) becomes

$$\nabla^2\psi_c = -K_1^2 + K_2^2\psi_c$$

This equation can be integrated to give

$$\psi_c = AJ_0(iK_2\rho) + BY_0(iK_2\rho) + \frac{K_1^2}{K_2^2} \tag{15}$$

where J_0, Y_0 is 0'th order Bessel and Neuman function and $i = \sqrt{-1}$. Of the two constants of integration B must be equal to zero, since as ρ decreases the value of ψ approaches to a constant value and the term $Y_0(iK_2\rho)$ increases infinitively. On the other hand, the constant A will be evaluated as follows; the charge on the pore surfaces may approximately be equal and opposite to the net charge located in the pore, *i.e.*

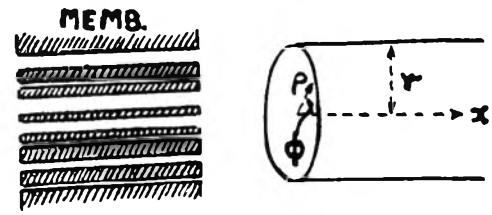

Fig. 2.

$$\int_0^r 2\pi\rho\epsilon(C_+^{\pm} - C_-^{\pm})d\rho = A\frac{DK_2^2r^2}{2}\frac{J_1(iK_2r)}{iK_2r} = 2\pi r\epsilon A_0 \tag{16}$$

Therefore

$$A = \frac{4\pi}{D}\frac{A_0\epsilon}{K_2^2r}\frac{iK_2r}{J_1(iK_2r)} \tag{17}$$

Substituting this value of A in Eq. (15), we obtain

$$\psi_c = \frac{4\pi}{D}\frac{A_0\epsilon}{K_2^2r}\frac{iK_2r}{J_1(iK_2r)}J_0(iK_2\rho) + \frac{K_1^2}{K_2^2} \tag{18}$$

Insertion of eq. (18) in eq. (12) gives

$$C_+^{\pm} = Ce^{-\frac{\epsilon\psi_0}{kT}}\left[1 - \frac{\epsilon}{kT}\left(\frac{4\pi}{D}\frac{A_0\epsilon}{K_2^2r}\frac{iK_2r}{J_1(iK_2r)}J_0(iK_2\rho) + \frac{K_1^2}{K_2^2}\right)\right] \tag{19}$$
$$C_-^{\pm} = Ce^{\frac{\epsilon\psi_0}{kT}}\left[1 + \frac{\epsilon}{kT}\left(\frac{4\pi}{D}\frac{A_0\epsilon}{K_2^2r}\frac{iK_2r}{J_1(iK_2r)}J_0(iK_2\rho) + \frac{K_1^2}{K_2^2}\right)\right]$$

Then the mean ionic concentration in the membrane is given by

$$\bar{C}^{\pm} = \frac{\int_R^{\infty}\int_0^r (C^{\pm}2\pi\rho/d\rho)f(r)dr}{\int_0^{\infty}\pi r^2f(r)dr} \tag{20}$$

where R is the least radius of pores through which the ions may permeate. If $f(r)$ is normalized to be

$$\int_R^{\infty}\pi r^2f(r)dr = 1$$

in order to simplify the later discussion it follows from eq. (19), (20) and (14) that

$$\bar{C}_-^{\pm} = C\left[\int_R^{\infty}\pi r^2 \times e^{\frac{\epsilon\psi_0}{kT}}f(r)dr + \int_R^{\infty}\pi r^2 \times e^{\frac{\epsilon\psi_0}{kT}}\left(1 - e^{\frac{2\epsilon\psi_0}{kT}}\right)^2 f(r)dr\right] + \left[2\pi A_0\int_R^{\infty}e^{\frac{2\epsilon\psi_0}{kT}}\left(1 - e^{-\frac{2\epsilon\psi_0}{kT}}\right)rf(r)dr\right] \tag{21}$$

$\bar{C}_+^{\pm}$ may also be given by a similar equation. Alternatively, it will be easily shown from eq. (16) that

$$\bar{C}_-^{\pm} = \bar{C}_-^{\pm} + 2\pi A_0\int_R^{\infty}rf(r)dr \tag{22}$$

Therefore $\bar{C}_+^{\pm}$, $\bar{C}_-^{\pm}$ may be expressed as

$$\bar{C}_+^{\pm} = k_1C + k_2 + k_3$$
$$\bar{C}_-^{\pm} = k_1C + k_2 \tag{23}$$

where k_1, k_2 etc., is defined by

$$k_1 = \left[\int_R^\infty \pi r^2 e^{\frac{\epsilon\psi_0}{kT}} f(r)dr + \int_R^\infty \pi r^2 e^{\frac{\epsilon\psi_0}{kT}}\left(1 - e^{\frac{2\epsilon\psi_0}{kT}}\right)^2 f(r)dr\right]$$

$$k_2 = \left[2\pi A_0 \int_R^\infty e^{\frac{2\epsilon\psi_0}{kT}}\left(1 - e^{\frac{2\epsilon\psi_0}{kT}}\right) r f(r)dr\right] \quad (24)$$

$$k_3 = \left[2\pi A_0 \int_R^\infty r^2(r)dr\right]$$

It is expected from the qualitative consideration that $\bar{C}_+^{\pm}$ and $\bar{C}_-^{\pm}$ reduces to k_3 and zero, respectively, as ψ_0 increases, and that both $\bar{C}_+^{\pm}$ and $\bar{C}_-^{\pm}$ become C when ψ_0 decreases to zero. This can be obviously shown from eq. (23). But in spite of such an anticipation that the concentration of the neutral salt in the membrane must become zero ($k_2 = 0$) as C goes to zero, this cannot be expected from Eq. (23). The discrepancy will be attributed to the failure of the approximation of eq. (16) in such a limiting case. Although such assumption may be impermissible that the above neutral condition is satisfied even when C goes to zero, the validity of this theory is never spoiled by the discrepancy in the limiting case, since C remains at a finite magnitude in practical cases. Moreover, appropriateness of these approximations is proved experimentally by the fact that k_2 can be ignored in actual cases.

The theoretical equation of the membrane potential can now be obtained from equations (10) and (23) as

$$E = \frac{RT}{F}\int_{C_2}^{C_1} \frac{k_1(l_+ - l_-)C + k_2(l_+ - l_-) + k_3 l_-}{k_1(l_+ + l_-)C + k_2(l_+ + l_-) + k_3 l_+}\frac{1}{\bar{C}}dC = \frac{RT}{F}\left[\frac{k_2(l_+ - l_-) + k_3 l_+}{k_2(l_+ + l_-) + k_3 l_+}\ln\left(\frac{C_1}{C_2}\right) - \frac{k_2(l_+ - l_-) + k_3 l_+}{k_2(l_+ + l_-) + k_3 l_+}\ln\left(\frac{k_1(l_+ + l_-)C_1 + k_2(l_+ + l_-) + k_3 l_+}{k_1(l_+ + l_-)C_2 + k_2(l_+ + l_-) + k_3 l_+}\right) + \left(\frac{l_+ - l_-}{l_+ + l_-}\right)\ln\left(\frac{k_1(l_+ + l_-)C_1 + k_2(l_+ + l_-) + k_3 l_+}{k_1(l_+ + l_-)C_2 + k_2(l_+ + l_-) + k_3 l_+}\right)\right] \quad (25)$$

Upon introducing

$$\alpha = \frac{k_2(l_+ - l_-) + k_3 l_+}{k_2(l_+ + l_-) + k_3 l_+} \text{ and } \beta = \frac{k_2(l_+ + l_-) + k_3 l_+}{k_1(l_+ + l_-)}$$

eq. (25) reduces to

$$E = \frac{RT}{F}\left[\alpha\ln\left(\frac{C_1}{C_2}\right) - \alpha\ln\left(\frac{C_1 + \beta}{C_2 + \beta}\right) + \left(\frac{l_+ - l_-}{l_+ + l_-}\right)\ln\left(\frac{C_1 + \beta}{C_2 + \beta}\right)\right] \quad (26)$$

This equation can be shown to be reduced to the Nernst equation of the diffusion potential in the extremely concentrated solution or in the neutral membrane, *i.e.*

$$E = \frac{RT}{F}\left(\frac{l_+ - l_-}{l_+ + l_-}\right)\ln\left(\frac{C_1}{C_2}\right)$$

In the dilute solution or in much compact membrane β is negligibly small and eq. (26) reduces to

$$E = \alpha\frac{RT}{F}\ln\left(\frac{C_1}{C_2}\right)$$

which is the equation adaptable to the ideal permselective membrane and the glass electrode.

Equation (26) will be discussed for the next three special cases.

3. For the Porous Membrane, *i.e.*, Cellophane, Parchment Paper, Porous Collodion, etc.

In this simple case, it may be assumed that $\psi_0 \fallingdotseq 0$, $e^{-\frac{\epsilon\psi_0}{kT}} \fallingdotseq e^{\frac{\epsilon\psi_0}{kT}} \fallingdotseq 1$, and hence k_2 is negligible compared with k_1 and k_3. Upon making this approximation eq. (26) reduces to

$$E = \frac{RT}{F}\left[\ln\left(\frac{C_1}{C_2}\right) - \ln\left(\frac{C_1 + \beta}{C_2 + \beta}\right) + \left(\frac{l_+ - l_-}{l_+ + l_-}\right)\ln\left(\frac{C_1 + \beta}{C_2 + \beta}\right)\right] \quad (27)$$

where

$$\beta = \frac{l_+}{l_+ + l_-}\frac{k_3}{k_1} = \frac{l_+}{l_+ + l_-}\cdot 2A_0\cdot\frac{\int_R^\infty r f(r)dr}{\int_R^\infty r^2 f(r)dr}$$

Equation (27) can also be easily derived under the assumption that the concentration of the electrolyte in the membrane is determined by the Donnan equilibrium, as has been done by Meyer and Sievers.[3] While the third term corresponding to the Henderson's diffusion potential is the same as that of Meyer and Sievers, the first and second terms differ from their values.

According to S. Oka[8] the relation between the apparent transport number of anion calculated by the Nernst diffusion potential theory and the ionic concentration is given by the formula

$$\frac{1}{n_A} = \frac{l_+ + l_-}{l_-} + \frac{b}{C} \quad (28)$$

where n_A is the apparent transport number of anion, C the concentration of the electrolyte and b is a constant characteristic of the membrane, the electrolyte and of the ratio of the concentration.

This relation can also be derived from equating the Nernst equation and eq. (27). That is

$$\frac{RT}{F}\left[\ln\left(\frac{C_1}{C_2}\right) - \ln\left(\frac{C_1 + \beta}{C_2 + \beta}\right) + \left(\frac{l_+ - l_-}{l_+ + l_-}\right)\ln\left(\frac{C_1 + \beta}{C_2 + \beta}\right)\right] = (1 - 2n_A)\frac{RT}{F}\ln\left(\frac{C_1}{C_2}\right) \quad (29)$$

When $\beta \ll C$, it is permissible to drop all terms beyond the first term of $1/C$ in expanding the "ln" terms, and then eq. (29) becomes

$$\frac{1}{n_A} = \frac{l_+ + l_-}{l^-} + \frac{l_+ + l_-}{l_-}\frac{\beta}{\ln(C_1/C_2)}\left(\frac{1}{C_1} - \frac{1}{C_2}\right)$$

Introducing $\gamma = C_1/C_2$, we obtain

$$\frac{1}{n_A} = \frac{l_+ + l_-}{l_-} + \frac{l_+ + l_-}{l_-}\frac{\gamma - 1}{\ln\gamma}\beta\frac{1}{C_1} \quad (30)$$

Equation (30) is identical in form with eq. (28) derived by S. Oka,[8] which is found to be in good agreement with the experimental values. Then the value of β in eq. (27) is obtained from the slope of the $1/n_A - 1/C_1$ curve. However, if β is of the same order of magnitude as C, the approximation to the form of eq. (30) becomes not admissible, and therefore, since

$$n_A = \frac{l_-}{l_+ + l_-} - \frac{l_-}{l_+ + l_-}\frac{\gamma - 1}{\ln\gamma}\beta\frac{1}{C_1} + \frac{1}{2}\frac{l_-}{l_+ + l_-}\frac{\gamma^2 - 1}{\ln\gamma}\beta^2\frac{1}{C_1^2} - \cdots \quad (31)$$

(8) S. Oka, *J. Ind. Chem. Japan*, **36**, 236, 336 (1933).

β is more reasonably obtained from the tangent of the n_A–$1/C_1$ curve on the origin. Insertion of these values in eq. (27) gives the equation of the membrane potential for a porous membrane.

Experimental Verification.—Most of the works by the previous investigators have been performed for pursuing the electrical properties of the membrane, and therefore only the so-called characteristic membrane potentials for the 0.1 ~ 0.01 *N* potassium chloride solution have been given. Accordingly these data are not taken into account by the present discussion. The data available for the present purpose are those of the measurement of the potential for the solutions of the electrolyte of the symmetrical valence type in which the concentration of one of the solution is progressively increased, the ratio of the activities of the two solutions being kept constant. Most of these data will be taken into account for the comparison with the theory.

In the following calculation the thermodynamic concentration fC, in which f is the activity coefficient, is always used in place of the analytical concentration C.

It is shown in Tables I–III that the calculated values by eq. (27) fairly fit the experimental values. Particularly, it is seen in Table II and III that the experimental values obtained for $C_1/C_2 = 10$ are in satisfactory agreement with the calculated values, using the values of β obtained from the experiments in which $C_1/C_2 = 2$, and the membrane potential approaches to its maximum value, that is, the membrane potential of the ideal permselective membrane, with increasing the value of β.

TABLE I

Calcd. using the data by Oka[8]: memb., parchment paper; electrolyte, KCl; temp., 25.0°; ratio of concentration, 2:1; $\beta = 0.0089$ (calculated from the experiments in which $C_1/C_2 = 2$).

C_1/C_2 (N.)	1/5	1/10/20	1/20/40	1/50/100	1/100/200	1/150/300	1/200/400
n	0.464	0.426	0.375	0.260	0.139	0.113	0.091
$E_{calc.}$ mv.	1.4	2.0	4.0	7.7	9.8	11.5	12.7
$E_{obsd.}$ mv.	1.17	2.39	4.39	8.01	11.60	13.30	14.15

4. For Permselective Organic Membranes, *i.e.*, Dried Collodion, etc.

In this case, the approximation $\psi_0 \doteqdot 0$ cannot be assumed and k_2 is not negligible. Accordingly, eq. (26) reduces to

$$E = \frac{RT}{F}\left[\alpha \ln\left(\frac{C_1}{C_2}\right) - \left\{\alpha - \left(\frac{l_+ - l_-}{l_+ + l_-}\right)\right\}\frac{1}{\beta}(C_1 - C_2) + \cdots\right] \tag{32}$$

when $C/\beta < 1$

Experimental Verification.—The plots of the potential difference for the permselective membrane obtained by some investigators against the concentration of electrolyte are found to give a straight line, as can be expected from eq. (32) (Figs. 3, 4). But toward higher concentrations the deviation makes its appearance. Insertion of α and β, obtained from these figures, into eq. (26) gives the complete equation for the permselective membrane. The comparison of the calculated value with that of the observed is given in Tables IV and V.

Here, values of the potential differences are all used as −mv. Other data by Sollner and Gregor (Memb. Hum58-Shr58, Hum58) are also found to be in good agreement with the calculated values.

5. For the Glass Electrode

In this case, it is supposed that ψ_0 has the very large negative value, and hence $k_2 \doteqdot 0$ and k_1 is very small. Therefore, β becomes much larger and eq. (26) reduces to

$$E = \alpha\frac{RT}{F}\ln\left(\frac{c_1}{c_2}\right) \tag{33}$$

and then α becomes nearly equal to unity. The glass membrane is so compact as to permit the permeation only of hydrogen ion across the membrane. That is why the glass electrode affords the most effective means in measuring *p*H. Equation (33) is usually called the equation of the glass electrode.

As the concentration becomes larger, E deviates further from eq. (33). This deviation, ΔE, is usually called the error of the glass electrode in the acidic and alkaline solution. When the concentration C_2 remains constant, ΔE is given by

$$\Delta E = \frac{RT}{F}\left(\alpha - \frac{l_+ - l_-}{l_+ + l_-}\right)\ln\left(\frac{C_1}{\beta} + 1\right) \tag{34}$$

In the acidic solution eq. (34) becomes

$$\log\left[e^{\frac{F}{RT}\left(\alpha - \frac{l_+ - l_-}{l_+ + l_-}\right)^{-1}\Delta E} - 1\right] = \log \beta^{-1} - p\mathrm{H} \tag{35}$$

In the alkaline solution eq. (34) becomes

$$\log\left[e^{\frac{F}{RT}\left(\alpha - \frac{l_+ - l_-}{l_+ + l_-}\right)^{-1}\Delta E} - 1\right] = \log (\beta^{-1}Kw + p\mathrm{H} \tag{36}$$

TABLE II

Calcd. using the data by Oka[8]: electrolyte, KCl; temp., 25.0°; ratio of concn., 10:1; β was calculated from the results of his experiments in which $C_1/C_2 = 2$; here, E_1, E_2 and E_3 denote the first, second and third term of eq. (27), respectively.

Memb.		Cellophane	Hard filter paper	Congo red parchment	Collodion 2	Collodion 4	Hemoglobin Collodion	Chrom-gelatin	Parchment paper
β		0.0093	0.0034	0.0183	0.0035	0.0099	0.0075	0.00069	0.0089
$E_{calcd.}$ mv.,	E_1	55.1	55.1	55.1	55.1	55.1	55.1	55.1	55.1
	E_2	39.8	49.0	24.5	47.9	39.3	41.9	50.1	40.3
	E_3	0.4	0.5	0.3	0.4	0.4	0.4	0.5	0.4
	E	14.9	5.6	30.3	6.7	15.4	12.6	4.5	14.4
$E_{obsd.}$	(mv.)	15.94	2.73	27.63	4.33	18.54	12.63	2.43	13.37

TABLE III

Calcd. using the data by Oka[8]: elect., KOH; temp., 25.0°; ratio of concn., 10:1; β are calculated from the results of his experiments in which $C_1/C_2 = 2$.

Memb.	Parchment paper	Cellophane	Chrom-gelatin
β	0.019	0.016	0.046
$E_{calc.}$, mv.	8.6	7.0	25.0
$E_{obs.}$, mv.	4.62	4.62	25.20

$E_{obsd.}$ in Table I–III are the mean values of the membrane potentials reported by Oka, their reproducibilities are found in the range of the potential below 0.1 mv.

TABLE IV

Calcd. using the data by Sollner and Gregor[9]: memb., protamine collodion memb. (Hum 20-Shr 20); ratio of concn., 2:1; temp., 25.0°; α and β are obtained from Fig. 3.

Electrolyte	α	β	C_1/C_2	0.002/0.001	0.004/0.002	0.01/0.005	0.02/0.01	0.04/0.02	0.1/0.05	0.2/0.1	0.4/0.2
KCl	0.937	0.927	E_{calcd}	16.4	16.2	16.0	15.7	15.2	14.4	13.7	12.4
			E_{obsd}	16.4	16.5	16.2	16.2	15.9	15.2	14.5	13.2
KI	0.927	0.280	E_{calcd}	16.2	16.0	15.3	14.8	13.8	11.4	9.0	
			E_{obsd}	16.2	16.2	16.1	16.0	14.9	12.4	10.2	
LiCl	0.944	4.60	E_{calcd}	16.5	16.3	16.1	15.9	15.7	15.6	15.6	15.3
			E_{obsd}	16.6	16.5	16.6	16.4	16.4	16.1	16.2	16.1

TABLE V

Calcd. using the data by Masaki[10]: memb., collodion; ratio of concn., 10:1; temp., 25.0°; α and β are obtained from Fig. 4. The reproducibility of these experiments are found to be in the range of the potential below 0.3 mv.

Electrolyte	α	β	C_1/C_2 (N.)	0.05/0.005	0.1/0.01	0.5/0.05	1.5/0.15
KCl	0.919	0.984	$E_{calc.}$ (mv.)	53.9	52.8	46.7	39.6
			$E_{obs.}$ (mv.)	53.82	52.31	47.61	39.53
KBr	0.920	1.018	$E_{calc.}$ (mv.)	53.4	49.4	43.7	36.6
			$E_{obs.}$ (mv.)	52.68	52.53	46.93	38.18
KI	0.903	1.100	$E_{calc.}$ (mv.)	49.3	48.0	45.6	37.3
			$E_{obs.}$ (mv.)	52.43	52.21	47.16	39.56
KNO_3	0.947	0.148	$E_{calc.}$ (mv.)	46.9	43.0	28.8	18.1
			$E_{obs.}$ (mv.)	50.07	45.87	29.82	15.05

where Kw is the dissociation constant of the water. Strictly speaking α is the function of the charge of the membrane (*i.e.*, ψ_0) and of the ionic mobility in the membrane (l_+, l_-). Therefore α cannot be constant and is by no means theoretically determined in general. However, only in the alkaline solution, where the glass electrode is usually used only in the range of lower concentration, α can be assumed to be nearly constant. Even in the acidic solution it may remain equal to unity for the ideal glass membrane. Then we obtain

$$\log\left(e^{\frac{F}{RT}\frac{l_+ + l_-}{2l_-}\Delta E} - 1\right) = \log \beta^{-1} - p\mathrm{H} \quad (37)$$

Therefore the plot of $\log\left(e^{\frac{F}{RT}\frac{l_+ + l_-}{2l_-}\Delta E} - 1\right)$ or $\log\left[e^{\frac{F}{RT}\left(\alpha - \frac{l_+ - l_-}{l_+ + l_-}\right)^{-1}\Delta E} - 1\right]$ against pH should give a straight line of the slope -1 or $+1$ in the acidic and alkaline solution, respectively.

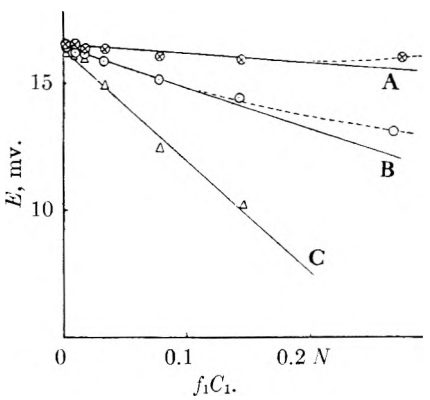

Fig. 3.—The relation between E–f_1C_1 (using the data by Sollner and Gregor,[9] Hum20–Shr20): protamine collodion memb., C_1/C_2 = 2: A, LiCl; B, KCl; C, KI.

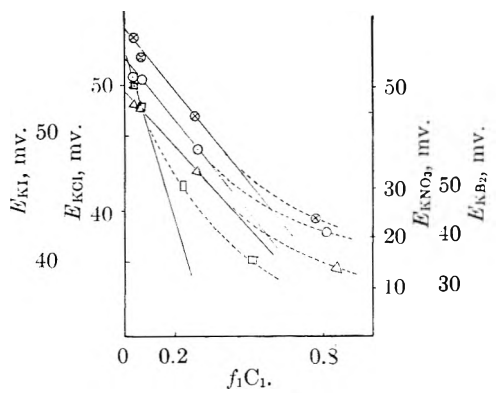

Fig. 4.—The relation between E–f_1C_1 (using the data of Masaki[10]); memb. collodion, C_1/C_2 = 10.

(9) K. Sollner and H. P. Gregor, THIS JOURNAL, **54**, 330 (1930).
(10) K. Masaki, *Mit. med. Akad. Kioto (Japan)*, **5**, 35 (1931).

Experimental Verification.—It is desirable to measure the deviation of the membrane potential from the potential of the hydrogen electrode. The essential parts of the apparatus are shown in Fig. 5. The vessel A contains the solution into which are inserted the glass electrode G (Haber type) and the hydrogen electrode H. The pH of this solution may be changed by the addition of acid or alkali from the buret B. A stream of hydrogen gas, which is purified by Pt-asbest, bubbles through the solution from the tube H_2. A junction between the solution in A and the calomel electrode is made by a satd. KCl bridge. All cells are placed in a thermostat kept at 25°.

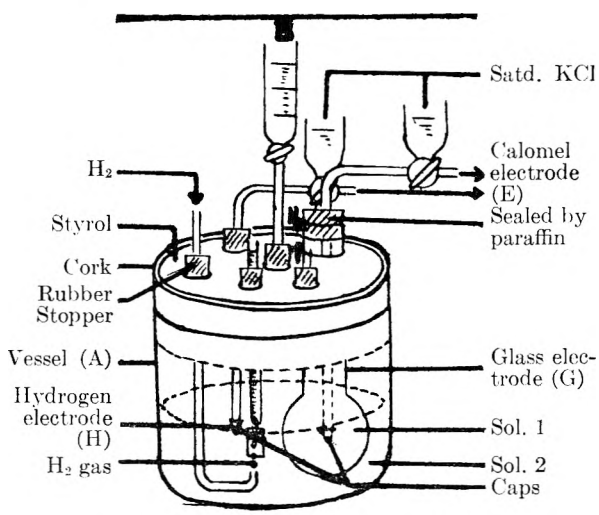

Fig. 5.—The measuring apparatus.

The apparatus for measuring the potentials is of a Du-Bridge type. Glass membranes used in this investigation are those of hard glass and MacInnes glass.

The deviation of the potential of the glass electrode from the potential of the hydrogen electrode is estimated by determining the potential between G and H. Such measurements yield potentials of the cell

$$\mathrm{Pt}H_2 \mid \text{sol. 1} \parallel \text{glass} \parallel \text{sol. 2} \mid \text{satd. KCl HgCl Hg} \quad (A)$$

in which sol. 1 is the liquid in vessel A and sol. 2 in the glass electrode. The pH values are found from the potential difference between E and H. The measurement gives the potential of the cell

$$\text{Hg HgCl satd. KCl} \mid \text{sol. 1} \mid \text{H}_2\text{Pt} \qquad \text{(B)}$$

Cell (A) has at all pH of solution 1 the same potentials as long as the glass electrode acts as a perfect hydrogen electrode. This value depends only on the concentration of sol. 2 inside the glass electrode, the state of the inside surface of the glass membrane and on the pressure of the hydrogen gas. In real cases, as will be shown by the experiments described below, the potential varies slowly with pH (Figs. 6, 7). It is obvious from eq. (33) that this property is due to the essential feature of the glass electrode.

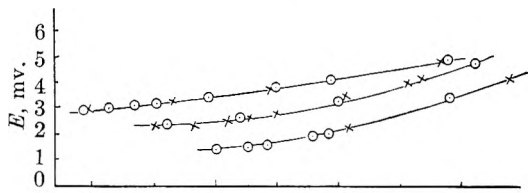

Fig. 6.—Variation of α in the acidic solution; memb., hard glass (memb. 11); ⊙, electrolyte of sol. 2 is the same as that of sol. 1; ×, sol. 2 is a buffer.

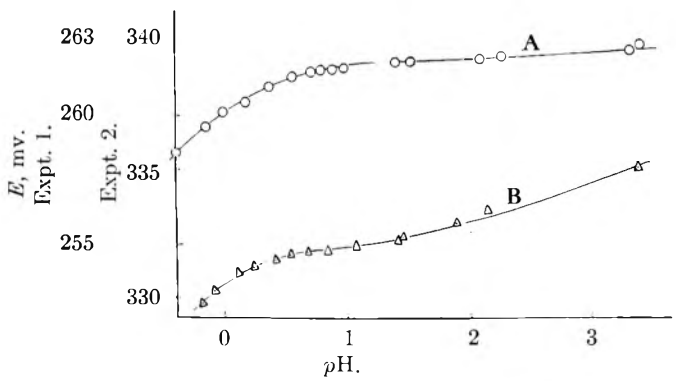

Fig. 7.—Error of glass electrode in the acidic solution; memb., hard glass (memb. 10) and MacInnes glass (memb. 7); electrolyte, HCl: A, expt. 1 (memb. 10); B, expt. 2 (memb. 7).

Moreover, α in the acidic solution varies with the change of pH, because α is the function of the values both ψ_0 and $l_\pm$ which vary also with pH. Accordingly, the deviation ΔE of the potential of cell (A) from the constant value or actually from the extrapolation of eq. (33), which is usually called the error of glass electrode, cannot in general be estimated (Figs. 7, 8). However, in the ideal case when $\alpha \fallingdotseq 1$, *i.e.*, in expt. (1) of Figs. 7 and 8 this estimation is possible and ΔE thus obtained agrees well with eq. (37) as shown in expt. (1) of Fig. 9. And

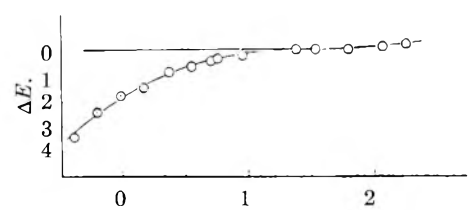

Fig. 8.—Error of glass electrode in the acidic solution, expt. 1, memb. hard glass (memb. 10), HCl: straight line, $E = RT/F$ (pH) + const.; $\alpha = 1$;

$$\beta = \frac{l_+}{l_+ + l_-} \times \frac{k_3}{k_1} = \frac{l_+}{l_+ + l_-} \times 4.32_5.$$

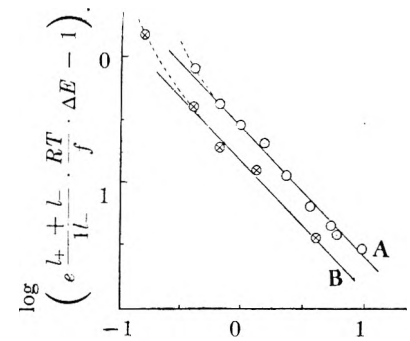

Fig. 9.—Plot of $\log e^{\frac{l_+ + l_-}{l_-} \times \frac{f}{RT} \Delta E - 1}$ against pH, HCl: A, expt. 1 (memb. 10): B, MacInnes and Belcher.

also in the alkaline solution, where the glass electrode is usually used only in the range of lower concentration, ψ_0 remains nearly constant and α can be assumed to be constant (Fig. 11). Accordingly, ΔE can be clearly obtained. ΔE, thus obtained, is found to be in good agreement with eq. (36) as shown in Fig. 12.

Most of the data reported by previous investigators have been obtained by using various buffer solutions. Therefore, they are not adequate for the comparison with the present theory. The only adequate one of them, reported by MacInnes and Belcher,[11] is given in Fig. 9. As seen from the curve, observed data fit fairly well with the theoretical results. It may be due to the impossibility of expanding the exponential term of eq. (12) that the experimental results do not fairly fit the theory at higher concentrated solution in each experiment.

Here, l_+ and l_- in the pore were assumed to be equal to the mobility in the solution and sometimes to be obtained by extrapolating to higher concentration, as were considered in the previous section.

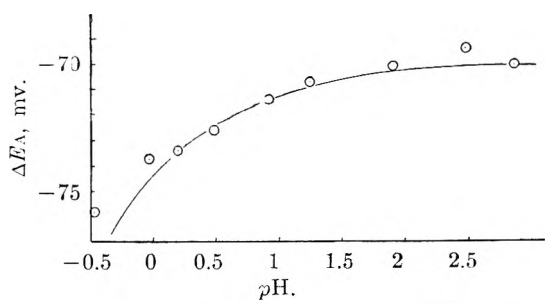

Fig. 10.—Asymmetric potential in the acidic solution; memb., hard glass (memb. 10), HCl: $\alpha = 1$; $\beta_1 = \frac{l_+}{l_+ + l_-} \times \frac{k_3}{k_1} = \frac{l_+}{l_+ + l_-} \times 4.32_5$; $\beta_2 = \frac{l_+}{l_+ + l_-} \times 20.0$; $K = -84.03$.

(11) D. A. MacInnes and D. Belcher, *J. Am. Chem. Soc.*, **53**, 3315 (1931).

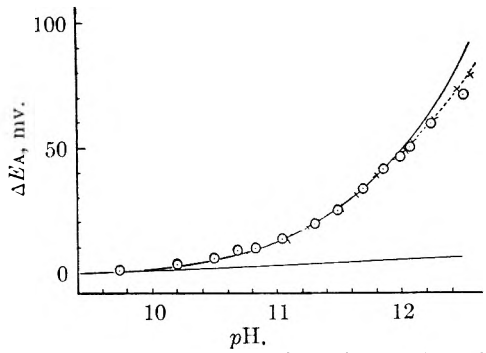

Fig. 11.—Error of glass electrode in the alkaline solution; memb., hard glass (memb. 11), KOH: straight line, $E = \alpha \frac{RT}{F}$ pH + const.; $\alpha = 0.970$; $\beta = \frac{l_+}{l_+ + l_-} \times \frac{k_3}{k_1}$ ($k_2 \fallingdotseq 0$ being assumed) $= \frac{l_+}{l_+ + l_-} \times 0.0162_7$.

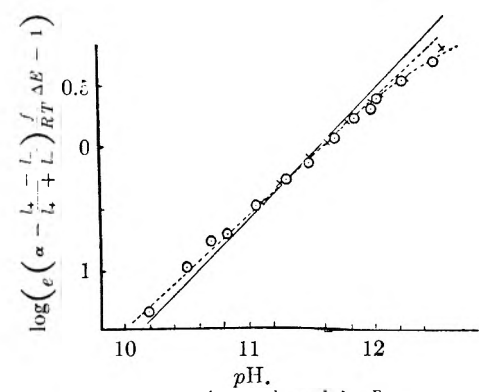

Fig. 12.—Plot of $\log\left(e^{\alpha - \frac{l_+ - l_-}{l_+ + l_-}\frac{F}{RT}\Delta E} - 1\right)$ against pH; memb., hard glass (memb. 11), KOH.

6. Asymmetric Potential

Although asymmetric potential, that is, the potential difference of cell (C) has hitherto been qualitatively attributed to the crystalline state or composition of glass of the inner and outer surface of membrane, it is thermodynamically impossible that cell (C) has any potential difference at the true equilibrium state.

Hg HgCl satd. KCl | Sol. || Glass || Sol. | satd. KCl HgCl Hg (C)

As the ionic diffusion across the glass membrane is supposed to be very much slower owing to its compactness, the stationary state at which ions diffuse into the membrane from both sides of it may reasonably be assumed. This fact will be understood from the experiments that α in eq. (33) is independent of the concentration of the solution inside of the glass membrane. Therefore if the distribution function of the pore diameter on one surface of the membrane differs from that on the other, the diffusion potential at one side of the membrane may not be equal to that at another, so that the asymmetric potential difference is observed. Assuming the concentration in the middle of the membrane to be C_0, asymmetric potential ΔE_A is therefore given by

$$\Delta E_A = \frac{RT}{F}\left[\alpha_1 \ln\left(\frac{C_0}{C_0}\right) - \alpha_1 \ln\left(\frac{C+\beta_1}{C_0+\beta_1}\right) + \left(\frac{l_+ - l_-}{l_+ + l_-}\right) \ln\left(\frac{C+\beta_1}{C_0+\beta_1}\right)\right] + \frac{RT}{F}\left[\alpha_2 \ln\left(\frac{C_0}{C}\right) - \alpha_2 \ln\left(\frac{C_0+\beta_2}{C+\beta_2}\right) + \left(\frac{l_+ - l_-}{l_+ + l_-}\right) \ln\left(\frac{C_0+\beta_2}{C+\beta_2}\right)\right] =$$

$$\frac{RT}{F}\left[(\alpha_1 - \alpha_2)\ln C - \left\{\alpha_1 - \left(\frac{l_+ - l_-}{l_+ + l_-}\right)\right\} \ln(C+\beta_1) + \left\{\alpha_2 - \left(\frac{l_+ - l_-}{l_+ + l_-}\right)\right\} \ln(C+\beta_2)\right] + \mathrm{K} \quad (38)$$

where K is independent of C and is dependent on C_0, l_+, l_-, α_1, etc.

If $\alpha_1 = \alpha_2 = 1$, we obtain

$$\Delta E_A = \frac{RT}{F}\left[-\frac{2l_-}{l_+ + l_-} \ln\left(\frac{C+\beta_1}{C+\beta_2}\right)\right] + \mathrm{K} \quad (39)$$

The experimental results of the asymmetric potential are given in Figs. 10, 13, 14. It is obvious from eq. (38) or (39) that the asymmetric potential has nearly a constant value and happens to deviate from its constant value at the same concentration as the error of the glass electrode, as indicated in Fig. 14.

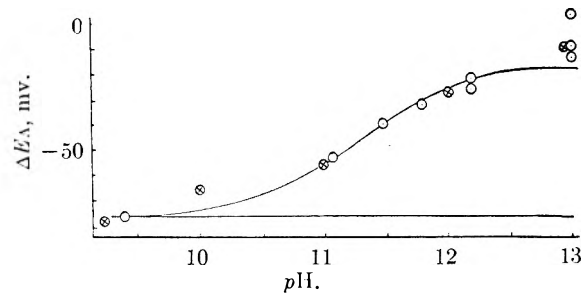

Fig. 13.—Asymmetric potential of glass electrode in the alkaline solution; memb., hard glass (memb. 11), KOH: $\alpha = 0.970$; $\beta_1 = \frac{l_+}{l_+ + l_-} \times \frac{k_3}{k_1}$ ($k_2 \fallingdotseq 0$ being assumed) $= \frac{l_+}{l_+ + l_-} \times 0.0162_7$; $\beta_2 = \frac{l_+}{l_+ + l_-} \times 0.00305_7$; $K = -13.9$.

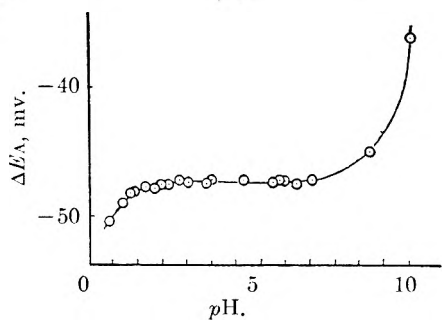

Fig. 14.—Asymmetric potential of glass electrode; memb., hard glass (memb. 10), HCl and NaOH.

The full line in Fig. 8–13 denotes the calculated values, of β_1, β_2, K being assumed. They are seen to be in quite satisfactory agreement with the experimental values of the error of glass electrode and of the asymmetric potential, respectively. Here, it is remarkable that both the asymmetric potential and the error of the glass electrode are fully explained by using the same value of β_1. It may probably be due to the freedom of the empirical constant that this agreement is fairly good up to higher ionic concentration than in the Debye-Hückel theory for the dilute solution of electrolyte.

The authors wish to thank Prof. K. Kanamaru and Assist. Prof. T. Hata and others at the Laboratory of High Polymers in the Tokyo Institute of Technology for their help and encouragement in carrying out this work.